Environmentally benign reactions on biomass-derived furans as an emerging strategy for the synthesis of complex value-added materials.

Franklin Chacón Huete

A Thesis
in
The Department
of
Chemistry and Biochemistry

Presented in Partial Fulfillment of the Requirements
for the Degree of Doctor of Philosophy (Chemistry) at
Concordia University
Montréal, Québec, Canada

October 2019

CONCORDIA UNIVERSITY
School of Graduate Studies

This is to certify that the thesis prepared

By: **Franklin Chacón Huete**

Entitled: **Environmentally benign reactions on biomass-derived furans as an emerging strategy for the synthesis of complex value-added materials.**

and submitted in partial fulfillment of the requirements for the degree of

DOCTOR OF PHILOSOPHY (Chemistry)

complies with the regulations of the University and meets the accepted standards with respect to originality and quality.

Signed by the final examining committee:

_____ Chair
Dr. Michael Sacher

_____ External Examiner
Dr. Alexandre Gagnon

_____ External to the Program
Dr. David Kwan

_____ Examiner
Dr. Louis Cuccia

_____ Examiner
Dr. Brandon Findlay

_____Supervisor
Dr. Pat Forgione

Approved by _____
Dr. Yves Gélinas, Graduate Program Director

November 14th, 2019 _____
Dr. André G. Roy, Dean of the Faculty of Arts and Science

ABSTRACT

Environmentally benign reaction on biomass-derived furans as an emerging strategy for the synthesis of complex valued-added materials

Franklin Chacón Huete, Ph.D.

Concordia University, 2019.

The high demand and uncontrolled use of petroleum feedstocks has had a tremendous negative impact on the environment. Nowadays, much attention is being paid to biomass as a source of organic starting materials, and the U.S. Department of Energy has highlighted furans derived from hemicellulose as potential building blocks for chemical synthesis, such as 5-hydroxymethyl furfural (HMF **3**) and 2,5-furandicarboxylic acid (FDCA **6**). The development of new tools that allow the use of these readily available compounds as starting materials in the construction of complex molecules is necessary for the transition of industrially scaled productions from a petroleum-based chemistry to a biomass-based alternative. The synthesis of high-value biomass derived 2,5-diaryl furans (**190**) has been achieved successfully from good to excellent yields with a wide scope of coupling partners of aryl halides and FDCA (**6**). Keeping in mind that FDCA comes from the direct oxidation of HMF (**3**), a route to access 2,5-non symmetric furans (**30**) was achieved utilizing the latter molecule as starting material. Selective oxidation of the aldehyde moiety has not been reported under mild and accessible conditions, therefore, a solvent-free mechanochemical assisted selective oxidation was studied to synthesize the required 5-hydroxymethyl-2-furoic acid (HMFA **4**) and 2,5-dihydroxymethyl furan (**5**), in a base-promoted disproportionation, reducing the reaction times to only 5 min and with an E_{factor} of only 0.5. Decarboxylative cross-coupling and oxidation of the alcohol moiety allowed access to an

alternative substrate for the decarboxylative cross-coupling, achieving the convenient synthesis of 2,5-diaryl non-symmetric furans (**30**). Additionally, the versatile intermediate 5-hydroxymethyl-2-aryl furan (**216**) was utilized to synthesize bis(5-arylfuran-2-yl)methane (**223**) scaffolds in good to excellent yields. Future work includes efforts to use decarboxylative cross-coupling reactions between FDCA (**6**) and dihalide aryl systems (**235**) to produce conjugated furan co-polymers (**236**).

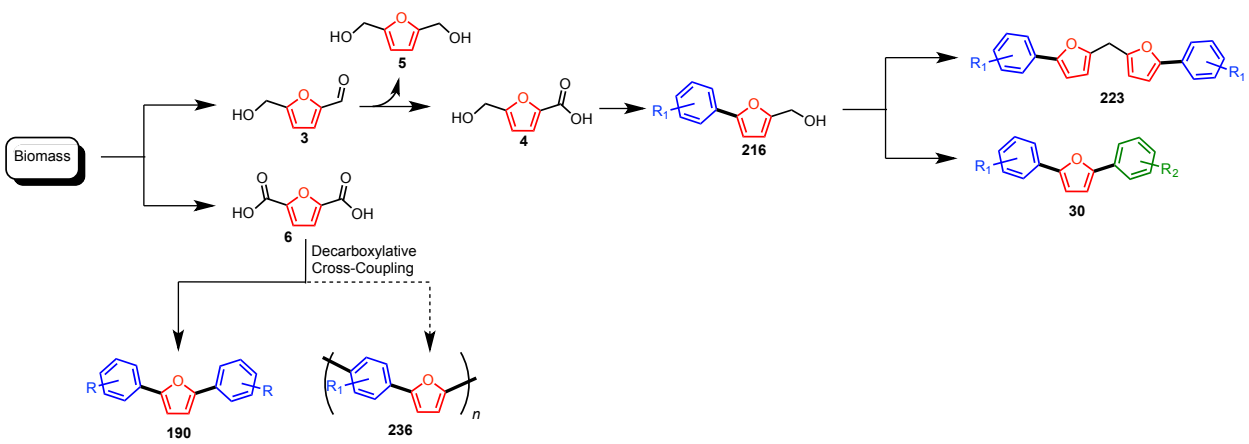

ACKNOWLEDGEMENTS

First, I would like to thank my supervisor Dr. Pat Forgione, who welcomed me into his research group on 2015 and has given me the support constantly all these years. As someone who has worked with various researchers, I believe that Pat really goes far beyond the expectations that anyone could have for a supervisor. Research-wise, he has taken the time to accept my ideas, and discuss them in a constructive way for research to be pleasant. Since the beginning, Pat took the time to guide me on not only the technical skills on what a good researcher is, but also, he cared for my personal well-being. Pat, thanks for every group meeting, every conference you sent me to, every one-on-one research discussion, every time we took to celebrate in PJ's and the BBQs at your house. You definitely made my stay at Concordia to be an experience that not only made me a better scientist, but also prepared me for the next steps in my career after graduate school.

I would also like to thank the committee members I have had during these years in Concordia, Dr. Louis Cuccia, Dr. Brandon Findlay and Dr. Xavier Ottenwaelder. All the valuable discussion that we had during the committee meetings (and also many times outside of them) helped me in understanding better my own research and taught me sometimes that by looking at the big picture, we can see the details better. I am grateful to Dr. David H. Kwan and Dr. Alexandre Gagnon for agreeing to be external readers of this thesis.

I am very thankful to the administrative and technical personnel of the Department of Chemistry and Biochemistry, the labour that you do every day, facilitates the research that we do in the labs. Members of the fORGione group, you have been the support through many days and nights. Fei, Cindy, Cynthia, Fadil, Daniel, Peter, Alex, Rafael, David, you have been incredible fellow graduate students, and I would like to thank you for all your support. All the undergrads I had the pleasure to work with, Maythem, Anthony, Paul, Juan David, Liana, Jason, Luis and

Thiago, I am very happy to have contributed a little bit in your professional development, and I am very proud of all the work that you are doing now that all of you finished your degrees. I was lucky to meet some amazing fellow grad students that went from co-workers to become an essential part in my every day Chris, Javier, Laura, Mike, Nicholas, Felipe, William, Florence, Alicia, Paola, Gaurav, Alan, Farshid and everyone that made my days in Concordia full of warmth and positive energy. Thank you, Diana and Ana, your friendship since the beginning of my Ph.D., has been an essential part in this journey.

My biggest thanks definitely go to my family. Even when we have been apart for thousands of kilometers, there has not been a single day I have not had you present in my mind. A mi madre y a mi padre, gracias por enseñarme a luchar por lo que se quiere. Este logro no es solo mío, sino también de ustedes, ya que en cada una de las batallas que he tenido en mi vida, ustedes siempre han estado apoyándome, dándome ánimos y esperándome siempre en la meta al final de la carrera. A Valerie, mi hermana, una compañera que ha estado conmigo desde el día que nací, y que, aunque la distancia nos separe, nunca me ha dejado solo y sé que siempre estará conmigo en cada nuevo reto que decida tomar.

The research outlined in this thesis was kindly funded by the Natural Sciences and Engineering Research Council (NSERC) of Canada and Le Fonds de Recherche du Québec, Nature et Technologies (FQRNT). Support was also provided by Concordia University and the Centre in Green Chemistry and Catalysis.

Table of Contents

List of figures

List of tables

List of abbreviations

δ	chemical shift in ppm
μw	microwave heating
Δ	conventional heating (hot plate)
i	iso
*i*Pr	2-propyl
o	ortho
p	para
m	meta
J	coupling constant in Hz
*t*Bu	2,2-dimethylpropyl
Ar	aryl
dba	dibenzylideneacetone
DMA	*N,N*-dimethylacetamide
DMF	*N,N*-dimethylformamide
equiv.	equivalents
Et	ethyl
EtOAc	ethyl acetate
JohnPhos	(2-biphenyl)di-*tert*-butylphosphine

MePhos	2-dicyclohexylphosphino-2′-methylbiphenyl
GC-MS	gas chromatography with mass spectrometry detector
MALDI	matrix assisted laser desorption ionization
HPLC	high performance liquid chromatography
NMR	nuclear magnetic resonance
OMe	methoxy
OTf - triflate	trifluoromethane sulfonate
OTs - tosylate	*p*-tolyl-sulfonate
NMP	*N*-methyl-2-pyrrolidone
BINAP	2,2′-bis(diphenylphosphino)-1,1′-binaphthyl

Chapter 1. General Introduction

1.1. Overexploitation of petroleum feedstocks and its impact on the environmental equilibrium

Since 1850, thousands of stations around the world have gathered millions of data points regarding the world's average temperatures. While there has been some fluctuation, undoubtedly, a steady increase of the overall average world temperature can be observed within the last 100 years, as shown in Figure 1. The warming of the world can be quantified at about 0.8-0.9 °C on average since the beginning of the 20th century. This increase is becoming more drastic with the passage of time, as each of the last three decades have shown an even larger growth rate than the preceding decades (before 1950). The northern hemisphere, in the last 30 years, is the warmest it has been relative to reconstructed data from paleoclimatic information of the last 1400 years.

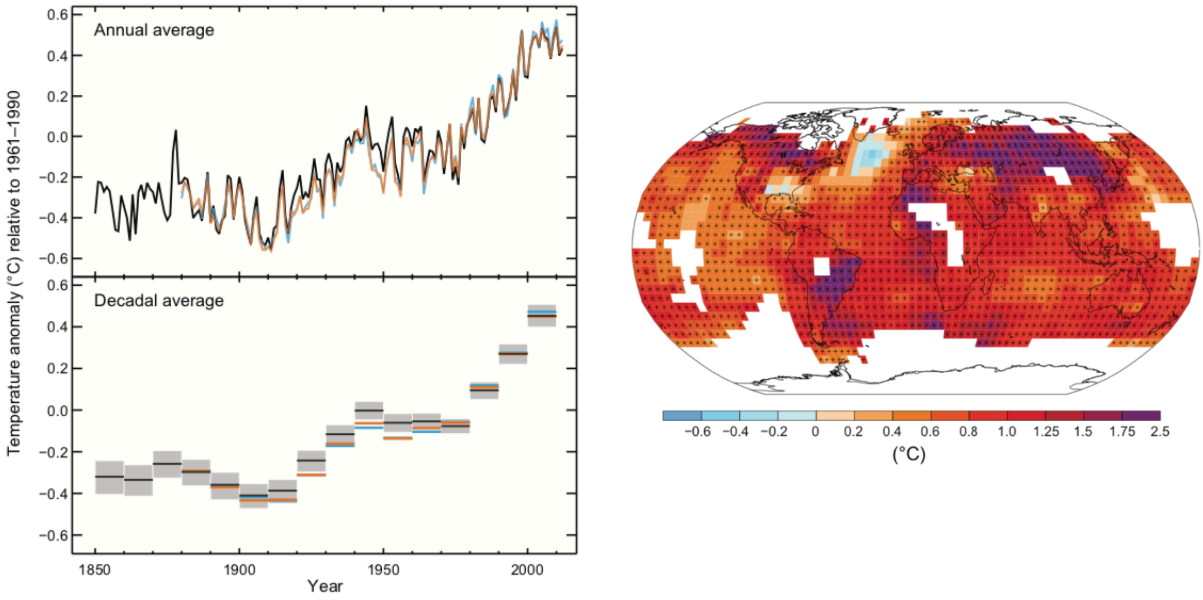

Figure 1. Observed globally averaged combined land and ocean surface temperature[1].

The warming of the climate system is unequivocal – a conclusion that has been made by a consensus of scientists and environmental advocates during the last 5 decades. Climate change is a term that was coined by the Intergovernmental Panel on Climate Change (IPCC), and its

definition has shifted since the 1970's to focus on anthropogenic causes, as it has become clear that human activities have a potential to drastically alter the climate.[1]

Since at least 1859, scientists have known of the greenhouse effect of gases such as CO_2, CH_4, NO_x, among others, when British physicist John Tyndall initiated experiments on the absorption of infrared by different small molecules, leading to the discovery that CO_2 in the atmosphere absorbs the sun's heat, which was not observed for other abundant gases such as oxygen and nitrogen.[2] In 1938, engineer Guy S. Callendar published an influential study suggesting increased atmospheric CO_2 from fossil fuel combustion was causing a rise in global temperatures.[3] Later, in 1958, US climate scientist Charles Keeling began measuring atmospheric CO_2 at the Mauna Loa observatory for use in climate modeling. Using these measurements, Keeling became the first scientist to confirm that atmospheric CO_2 levels were rising rather than being fully absorbed by forests and oceans – global carbon sinks that were previously thought to provide atmospheric adjustments. When Keeling began his measurements, atmospheric CO_2 levels stood at 315 ppm, but currently, these levels have gone as high as 370 ppm, which signifies a 30% increase. Nowadays, levels are at the higher than they have been in the past 800,000 years.[4] In 1977, the US National Academy of Sciences issued the report "*Energy and Climate,*" concluding that the burning of fossil fuels was increasing atmospheric CO_2, and that increased CO_2 was associated with a rise in global temperatures.[5]

There have been multiple reports both from academic and governmental sources predicting the possible consequences of maintaining current CO_2 emission levels, and in the last decades, these possible effects have become a palpable reality. Glaciers have shrunk, seasonal ice on rivers and lakes are melting earlier in the year than ever before, plant and animal ranges have shifted, and trees are flowering earlier. The net increase in the average temperature might seem like a small amount, but it is an unprecedented event in our planet's recent history for it to happen so quickly - the climate record of the Earth preserved in a vegetation equilibrium, ice cores and coral reefs, shows that the global temperatures, while geologically in flux, are stable over very long periods of time. It follows that even small changes in a short timeframe can have enormous environmental impact.[6]

1.2. International Agreements that address the fight against Climate Change

Over 100 years has passed since the first scientific report that correlated the increase in atmospheric CO_2 with an elevation in the planet's temperature; and over 40 years since the first communication from the US government ratifying all the possible catastrophic consequences of the climate change due to the greenhouse effect. Historically, it has become apparent that the fight against climate change has been held back by the economic interest of big petroleum companies and multimillionaire investors, who argue that human endeavors cannot influence the climate. However, some historical instances clearly demonstrate the impact of human intervention, and the potential for course correction to remedy harm caused to the planet. For example, in 1985 the Vienna Convention presented the first multilateral agreement that provided frameworks towards the reduction of chlorofluorocarbons with the aim of diminishing the detrimental damage that had been done to the ozone layer by these chemicals.[7] Since then, a significant trend toward the replenishment of the ozone layer has been reported.

Many international agreements have since emerged with strategic plans to mitigate the advancement of climate change and adapt global economies to address the current situation.[7] In 1987, the Montreal Protocol outlined the plans and endeavors of the signing members to protect the ozone layer by phasing out the production of numerous substances responsible for its depletion. Since then, this protocol has been updated with nine revisions, and has suffered changes with respect to the initial signing members.[8] Arguably, the most impactful of the last three decades is the Kyoto Protocol of 1992. This was the first international convention that included detailed objectives, encompassed in a framework addressing the majority of factors that are key aspects towards fighting climate change, such as ratifications towards the reduction of emission of greenhouse gases.[9] The Kyoto protocol is still in effect, and is set to end in 2020, when it will be replaced completely by the Paris accord of 2015, which was signed by 175 countries. This agreement can be simplified into three major objectives; firstly, it is of paramount importance that the world's average temperature increase is maintained well below 2 °C, and great efforts must be done to hold it below 1.5 °C. Its second objective deals with protocols developed to assist nations with the current devastating effects of climate change and facilitate economic transition to low greenhouse gas emission production, in a manner that does not threaten food production. The third

objective addresses the financial flows necessary to set the world on a pathway towards low greenhouse emissions and climate-resilient development.[10]

From a scientific point of view, the commitments that must be addressed are related to the development and employment of new or replacing technologies that facilitate the transition concerning the mitigation of climate change, and with this, a whole innovative field has been established as the gold standard for research and industrial chemical processes, Green Chemistry.

1.3. Green Chemistry

Green (or Sustainable) Chemistry can be defined as the design of chemical products and processes that reduce or eliminate the use or generation of substances hazardous to humans, animals, plants, and the environment.[11] This field emerged from a variety of existing ideas and research in the late 1980s, within the context of increasing global issues pertaining to chemical pollution and resource depletion. In the northern hemisphere, this discipline arose from the shift in environmental problem-solving strategies – evolving from authoritative regulations mandating the reduction of industrial emissions at the end of the production chain, to a more proactive approach to the prevention of pollution, through the innovative design of environmentally-friendly technologies.

Undoubtedly, John Warner and Paul Anastas are the fathers of the modern Green Chemistry with the publication of "*Green Chemistry: Theory and Practice*" in 1998. In this book, Anastas and Warner discuss the theoretical aspects of improving chemical practices towards minimizing health and environmental impacts.[12] Various metrics and terms to evaluate these efforts have been introduced, but the overarching goal is to seek inspiration from nature's facility for sustainable synthesis and catalysis, while at the same time reducing the environmental impact of existing processes. The tenets supporting this direction have been summarized in the 12 principles of green chemistry:

1. It is better to prevent waste than to treat or clean up waste after it is formed.
2. Synthetic methods should be designed to maximize the incorporation of all materials used in the process into the final product.
3. Wherever practicable, synthetic methodologies should be designed to use and generate substances that possess little or no toxicity to human health and the environment.

4. Chemical products should be designed to preserve efficacy of function while reducing toxicity.
5. The use of auxiliary substances (e.g. solvents, separation agents, etc.) should be made unnecessary wherever possible and innocuous when used.
6. Energy requirements should be recognized for their environmental and economic impacts and should be minimized. Synthetic methods should be conducted at ambient temperature and pressure.
7. A raw material or feedstock should be renewable rather than depleting wherever technically and economically practicable.
8. Reduce derivatives - Unnecessary derivatization (blocking group, protection/ deprotection, temporary modification) should be avoided whenever possible.
9. Catalytic reagents (as selective as possible) are superior to stoichiometric reagents.
10. Chemical products should be designed so that at the end of their function they do not persist in the environment and break down into innocuous degradation products.
11. Analytical methodologies need to be further developed to allow for real-time, in-process monitoring and control prior to the formation of hazardous substances.
12. Substances and the form of a substance used in a chemical process should be chosen to minimize potential for chemical accidents, including releases, explosions, and fires.

In regard to the work presented in this thesis, some of these principles have been directly employed in the development of this research. The use of renewable feedstocks, principle 7, is the biggest objective tackled in the following projects.

1.4. Petroleum Feedstocks vs Renewable Energies

The use of petroleum feedstock-based products has increased exponentially since the late 18th century with the peaking the industrial revolution. Fossil feedstocks constitute the primary source of energy, accounting for more than 75% of the world's energy supply. Additionally, the refining of crude oil generates fuels and a wide variety of products used in multiple applications.[13] Thus petroleum industries have a large amount of control over the economies of not only oil-producing countries, but also of the entire world that utilizes their resources for transportation, energy, etc. Affiliated with this economic dependence, the negative impact of the overexploitation of petroleum feedstocks, and their misuse and mismanagement, on the environment, has propelled

academic and industrial research on petroleum alternatives for the production of energy. A feedstock refers to any unprocessed material used to supply a manufacturing process. When one refers to a renewable feedstock, it refers to material that can be replenished within human timescale.[14]

In recent decades, incredible advances have been made in the development of technologies that derive power from renewable resources, such as wind, solar, geothermal, and ocean energy, as well as burning of biomass. Some countries, such as Costa Rica, have been so successful in the advancements of these industries that more than 99% of their electric household consumption comes entirely from renewable sources.[15] The advent of alternative sources of energy has also led scientists to explore possibilities to substitute other dependencies from the petroleum feedstocks, a salient example of which are chemical raw materials. In this regard, biomass has been targeted as a raw material with tremendous potential for the extraction and production of small building blocks for the chemical industry.[16]

1.5. Biomass as a renewable feedstock

1.5.1. Potential platform chemicals derived from biomass

The biomass is the mass of living biological organisms in a given area or ecosystem at a given time.[17] For application purposes, biomass can be defined as all plant or animal material used for energy production, heat production, or as raw material for a range of products in various industrial processes.[18] Biomass can be classified in many ways, but from a technical point of view, the composition classification is probably the most useful. In this regard, this material can be classified as polysaccharides, lignin, triglycerides and proteins. Whereas a great portion of these materials are currently considered waste, scientists have begun to explore the possible products that can be derived from the treatment of these raw materials.[19]

Utilization of waste biomass as a feedstock for energy production was unimaginable 50 years ago, but nowadays, there is a whole industry dedicated to the exploitation of useful waste materials worldwide.[19] Alongside this, political efforts have made possible for the scientific community to investigate the substitution of petroleum-based chemical feedstocks for biomass-based feedstocks. In this regard, polysaccharides have been drawing much attention for their ease

of breakdown, meaning that the transformations into smaller useful building blocks is readily accomplished. Polysaccharides are readily found in any source of lignocellulosic biomass, which is the most abundant raw material on earth, with an estimated $77x10^9$ tons of renewable carbon fixed annually.

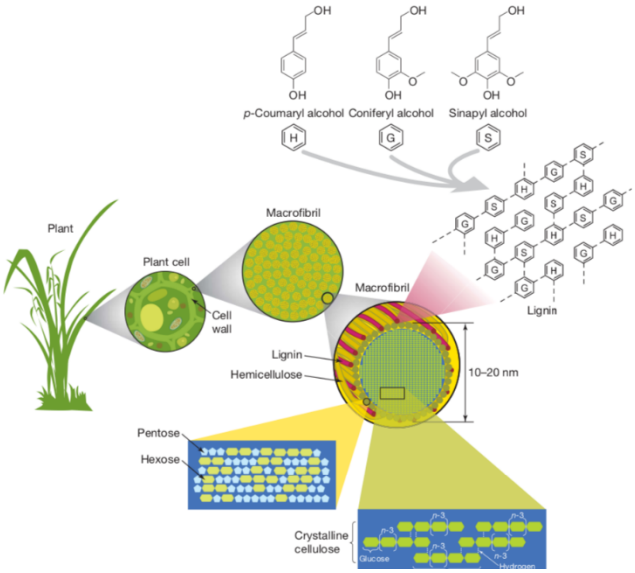

Figure 2. Structure of Lignocellulose (taken from [21]).

Lignocellulosic biomass can be broadly classified into virgin biomass, waste biomass and energy crops. Virgin biomass includes all naturally occurring terrestrial plants such as trees, bushes and grass. Waste biomass is a low value by-product of various industrial sectors, such as agriculture (corn stover, sugarcane bagasse, rice husk, etc.) and forestry (saw mill and paper mill discards). Energy crops are crops with high yield of lignocellulosic biomass produced to serve as raw material for the production of second-generation biofuel. Examples include switch grass (*Panicum virgatum*) and elephant grass (*Miscanthus giganteus*).[20]

Three main components are derived from lignocellulosic biomass: cellulose, hemicellulose and lignin. The ratios of each vary from species to species, with cellulose generally being the most abundant, and lignin the minor component (Figure 2).[21]

Cellulose is a polysaccharide composed of D-glucose monomers linked by β-1,4 glycosidic bonds. It is considered the most abundant organic polymer on earth, and it can easily be derivatized into glucose with developed catalytic treatments.[22] Hemicellulose is the second most abundant polysaccharide composed of a mixture of pentoses (mainly xylose and arabinose) and hexoses

(mainly glucose, mannose, galactose and rhamnose).[23] Lignin is an aromatic polymer that lacks a primary defined structure, and is primarily composed of phenylpropane derivative units. As expected, the breakdown of lignin to small useful building blocks represents a bigger challenge, due to the nature of the bonds present in the biopolymer.

Several scientific reports have been made of the most important (and abundant) components that can be derivatize from polysaccharides, and according to their potential, some of them have been classified as major targets for the future of the synthetic organic industry.[16,24–28] In 2004, the United States Department of Energy Efficiency and Renewable Energy reported a list of the top value-added chemicals from biomass – specifically those derived from sugars. These building blocks were selected through rigorous standards, in which factors such as the ease of obtaining the material and the impact of their potential uses, were considered. These selected building blocks are 1,4-diacids (succinic, fumaric and malic), 2,5-furandicarboxylic acid, 3-hydroxy propionic acid, aspartic acid, glucaric acid, glutamic acid, itaconic acid, levulinic acid, 3-hydroxybutyrolactone, glycerol, sorbitol and xylitol (Figure 3).

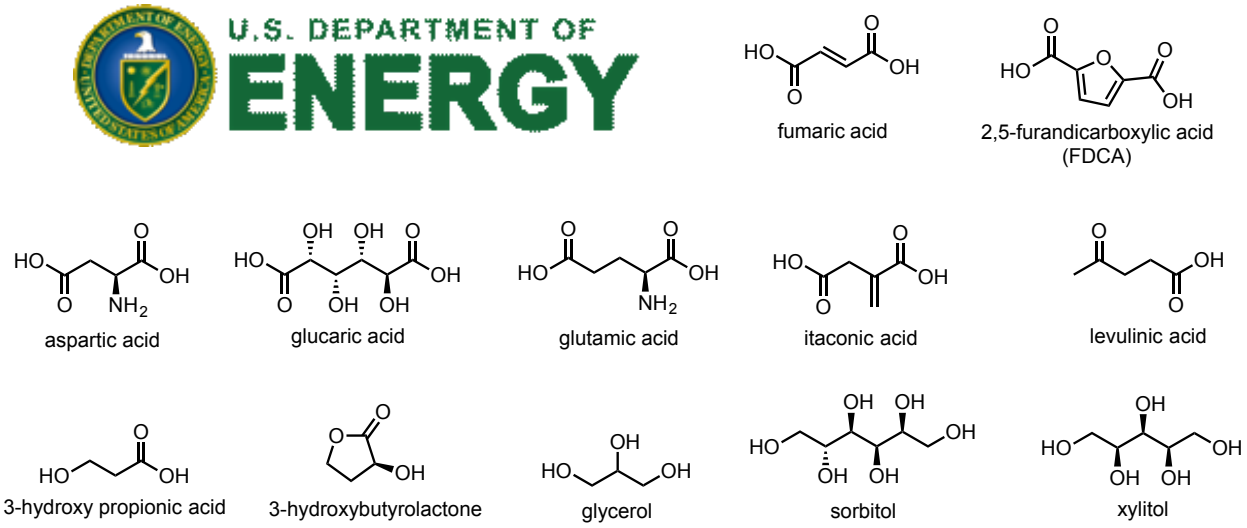

Figure 3. Top 12 Value-Added Chemicals from Biomass.

1.5.2. Reported synthesis and processes for the production of furans derived from hemicellulose and cellulose

From all the different kind of chemicals derived from biomass (carbohydrates, amino acids, lipids, etc.), furans such as HMF (**3**) and FDCA (**6**) are projected to have the most potential as

important building blocks in organic synthesis. The synthesis of furan compounds from biomass follows a pathway (Figure 4) that starts with the enzymatic degradation of complex carbohydrates (cellulose and hemicellulose **1**) into simple carbohydrates (**2**),[22] and a subsequent acid-catalyzed dehydration to achieve furfurals. HMF (**3**) is one of the abundant furfural products, with many methodologies developed for its derivation from biomass.[29–32] A procedure reported recently by Dumesic *et al.*[33,34], addresses the problems of synthesis and separation of these product with a biphasic system, employing $AlCl_3$/HCl aqueous media dehydration of hexoses to 5-hydroxymethyl furfural (HMF **3**) that is transferred to the organic layer. Under the same system, this HMF can be the platform to obtain multiple derivatives such as δ-valerolactone, dimethyl furan, levulinic acid and even formic acid.

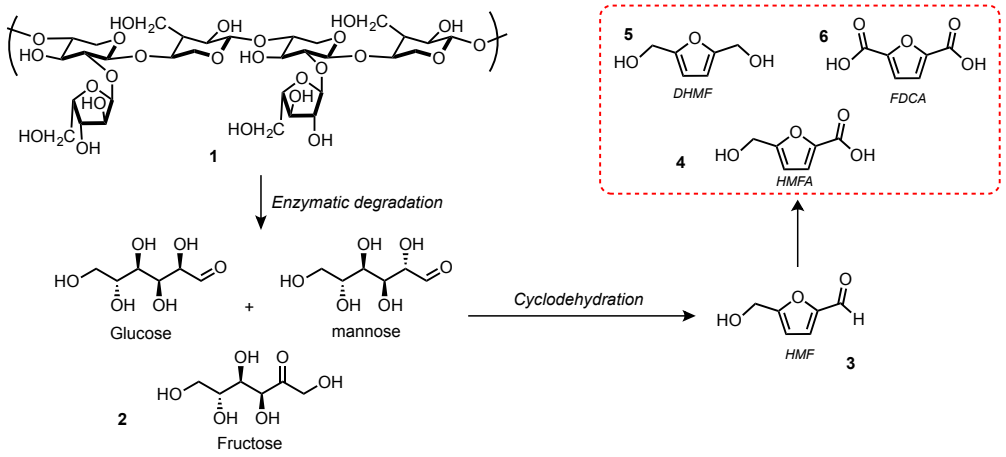

Figure 4. Synthetic pathway towards the production of furan derivatives from biomass.

Furthermore, HMF can be oxidized to FDCA, with this reaction being widely developed in the last decade in many research groups,[35–38] employing various supported transition metal heterogeneous catalysts like PtBi/C[39], Pd/PVP[40], Au/HT[41] and Ru/C[42]. Electrochemical methodologies[43] have also been investigated. Partial oxidation of HMF into other furan derivatives, such as 5-hydroxymethyl furoic acid (HMFA) and 2,5-diformyl furan (DFF), has been scarcely reported due to the challenges involved in the prevention of obtaining the fully oxidized derivative, FDCA. Biochemical approaches have been reported by the groups of Domínguez de María[44] and Li[45], in which HMFA and DFF were obtained employing lipases and alcohol oxidases. Even though the enzyme-catalyzed approach to the synthesis of these compounds gives excellent results, some challenges still need to be addressed, such as the long reaction times, as well as the meticulous manipulation of enzymes and their extraction.

Pentoses have also been used also for the synthesis of FDCA, through a less diversified route. Thiyagarayan *et al.*[46] reported an industrial approach (Figure 5) to the synthesis of FDCA that begins with a dehydration of these carbohydrates to produce furfuraldehyde **7**, which is subsequently oxidized to the potassium furoate (**8**). This salt is then heated to 260 °C with CdI_2 or $ZnCl_2$ as catalyst, and it disproportionates to produce furan and FDCA (**6**, **9** and **10)** (with selectivity towards the 2,5 isomer **6**)

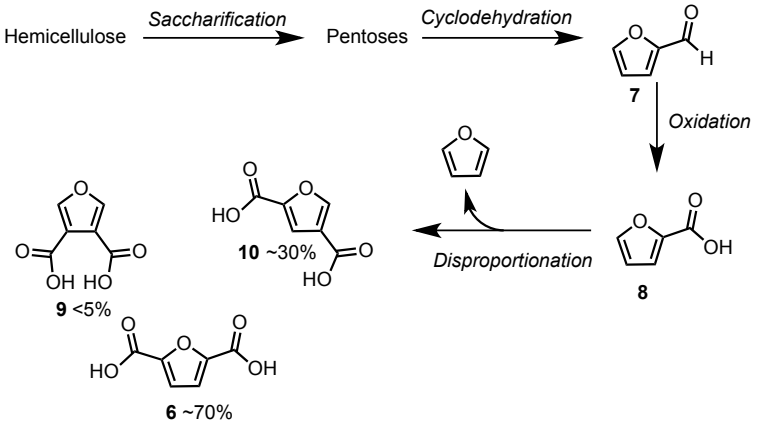

Figure 5. Synthesis of FDCA from hemicellulose through the disproportionation of Furoic Acid.

The production of biochemicals at industrial levels has various challenges, including the divergence of the overall process. To understand this concept, one must analyze a complementary process, such as the production of biofuels. The latter is produced at industrial scales and is considered a convergent process, meaning that multiple technologies (chemical processes) will arrive to a common product, i.e. biofuels. On the other hand, when this rationalization is applied to the synthesis of bio-based chemicals, a single technology, like reduction or oxidation, could have several products (Figure 6), which complicates its economic analysis. This also implies additional separation steps in the overall process, and it follows that for many years this facet disincentivized investment. Nevertheless, in recent decades, advances in the chemistry of biomass conversion have created novel solutions with high efficiencies.[47]

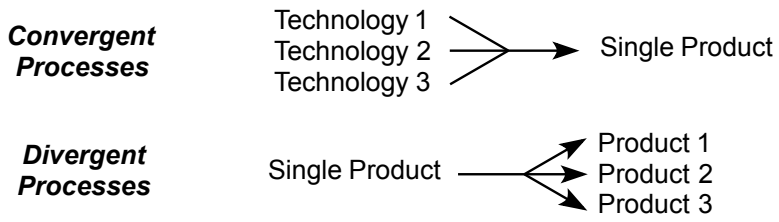

Figure 6. Research approaches for biobased fuels and chemicals (adapted from[47])

The importance of these materials has surpassed the academic environment, and some industries have initiated their production in pilot plants. BASF and Avantium created a joint venture to produce FDCA and bioplastics derived from it in a new plant called Synvina, with an approximated capacity of 50000 tons per year.[48] In 2016, ADM and DuPont announced the opening of a plant that will produce 2,5-furan dicarboxylic methyl ester, derived from biomass. This joint plant will start the production of polytrimethylene furandicarboxylate (PTF), a bioplastic that results in the polycondensation of FDCA and 1,3-propanediol.[49]

The latest big company to join this new era of chemical production is MetGen. They invented a revolutionary chemo-enzymatic pathway that enables streamlined processes towards platform chemicals, for example FDCA.[50] MetGen's ENZINE® Technology Platform allows the design and production of necessary enzymes for full bioconversion of glucose. The advantage of this enzymatic reaction stems from the complete conversion of glucose. In the conventional fructose-based process, the interconversion between glucose and fructose reaches an equilibrium at less than 50% fructose, therefore requiring an additional and inefficient separation step. It is noteworthy in the case of MetGen's approach that no additional chemicals or co-factors are needed in order to perform the bioconversion.[50] Furthermore, MetGen has filed a patent for the chemical route to convert the resulting sugars to oxidized forms of HMF. In that respect, the dehydration of the MetGen's bioconversion product is considered to be much more efficient than the dehydration of fructose: This form of sugar is known to have above 90% conversion yields, whereas fructose dehydration has only around 60% yield.

1.5.3. Current applications of Biomass-derived furans

Hydroxymethyl furfural has been called the *"sleeping giant"*[51] of the organic synthetic industry, for its potential, not only for use directly in many synthetic transformations, but also as

a platform chemical from which many other compounds can be derivatized. Even though industrial level production of such bio-based furans has been developed, Bozell and co-workers highlighted in their 2010 review[47] that furans like HMF and FDCA have been reported extensively in the recent literature and somewhat high volume production, they still rank very poorly in terms of product applicability, direct substitution, and the commercial biobased products available. These criteria objectively refer to the lack of chemical tools available to utilize such starting materials in the fabrication of commercially useful products.

Fundamental efficient transformations of HMF have been reported recently with the aim of increasing the interest of industries in incorporating these chemicals into their production. Chemical transformations of the formyl group of HMF have been reported, such as reductive amination[52], which led to patented indolopyrrolocarbazole derivatives from Kojiri *et al.*, novel discoveries that have antitumor properties.[53] Other transformations that have been reported towards the derivatization of biomass derived HMF include Wittig-type reactions[54], Horner-Wadsworth-Emmons[55], Baylis-Hillman reaction[56,57], acetal chemistry[58], and aldol condensations[59], among others[51].

Given the large potential volumetric production of these furans from biomass sources, increased research interest has been initiated into their transformation into other commodity chemicals (Figure 7). The group of Dauenhauer reported the use of biomass-derived 2,5-dimethylfuran as a platform to produce *p*-xylene, a compound widely used as a solvent in organic synthesis.[60] Lobo and co-workers explored the Diels-Alder/dehydration of biomass-derived furan and acrylic acid for the synthesis of benzoic acid, a compound used as a reagent in organic synthesis and also as a food additive.[61] Methyl furan has been used also as a reagent in Diels-Alder chemistry to synthesize xylenes, when reacted with propylene on zeolite heterogeneous catalysis.[62] Moreover, the Gordon group of the University of Guelph has reported synthetic strategies in which biomass-derived furans could be used as a feedstock for the production of different length alkanes, which are useful in organic synthesis and have tremendous potential as fuel alternatives.[63]

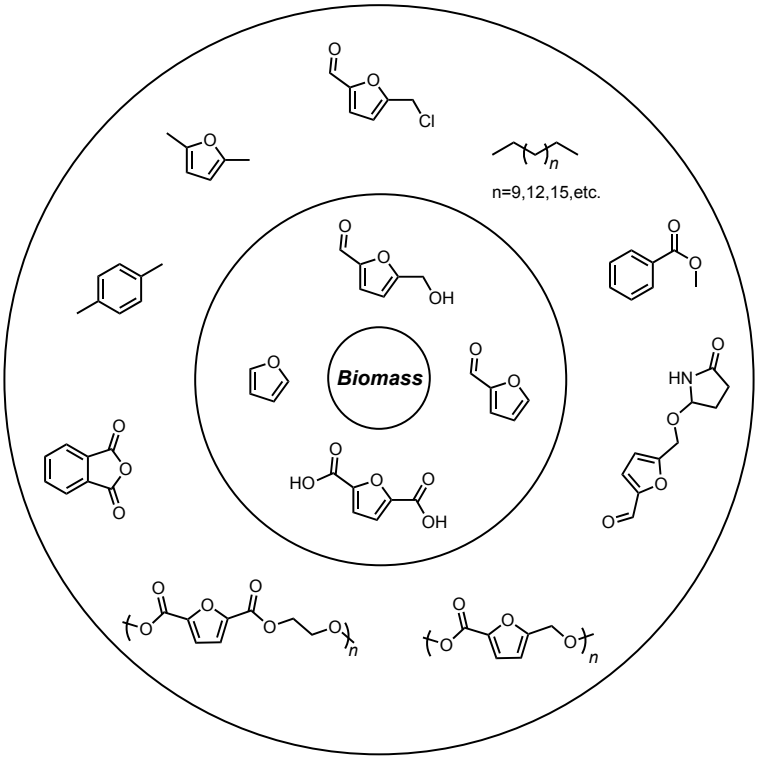

Figure 7. Production of useful molecules from bio-based starting materials derived from carbohydrates.

In terms of synthetic strategies, furans derived from biomass have been investigated mainly as potential replacements in the production of certain polyesters. Being an important base monomer, 2,5-furandicarboxylic acid (FDCA) has been identified by the United States Department of Energy as one of the 12 priority chemicals derived from biomass predominantly for its potential as replacement for petroleum terephthalic acid in polymer applications. Synthesis of the most common furan-based polyester, polyethylene 2,5-furandicarboxylate (PEF), can be carried out directly from FDCA and ethylene glycol utilizing a standard polycondensation procedure with antimony glycolate as catalyst.[64]

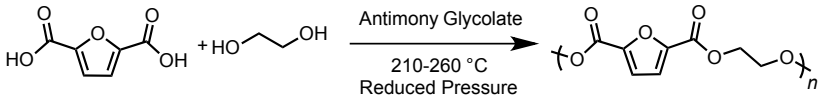

Figure 8. Synthesis of polyethylene furanoate by Furanix Technologies[62].

Other modifications have also been investigated on related polymers based on the mixture of itaconic acid (IA), FDCA, succinic acid (SA) and trimethylene glycol (PD), yielding a structure capable of forming cross-linked networks, and cured biopolymers thermally stable up to 330 °C.[65]

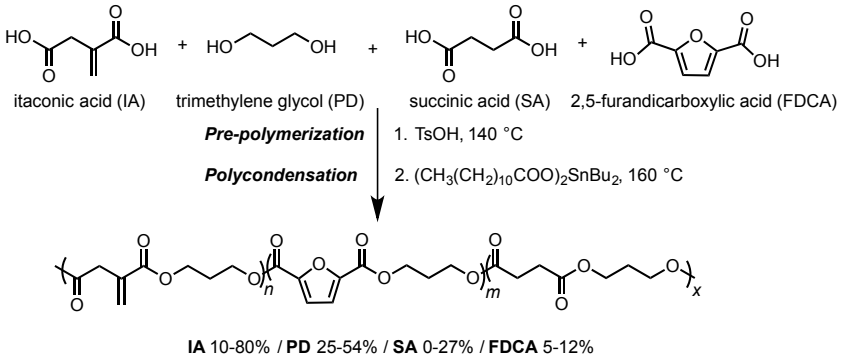

Figure 9. Synthesis of Bioderived Unsaturated Polyesters Based on FDCA.[65]

Furanic polyesters have also demonstrated a considerable number of useful properties. PEF synthesized with conventional melt polycondensation under high vacuum was successfully utilized as a source material for 3D-printing,[66] and its longer congener, trimethylene furandicarboxylate (PTF), was used in the fabrication of a gas separation membrane.[67] As these polymers exhibit substantial barrier properties, the development of new gas-impermeable materials is currently under way.[68] Also, FDCA has been reacted with eugenol to produce a resin that after treatment with methyl hexahydrophtalic anhydride (MHHPA), exhibits a glass transition temperature of 153 °C (Figure 10), around 40 °C higher than regular polystyrene or poly(methyl methacrylate).[69]

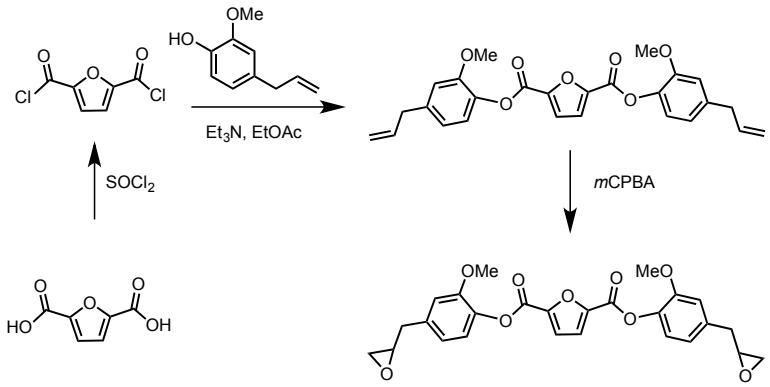

Figure 10. Synthesis of source material for epoxy resin starting from FDCA and Eugenol.

The most recent use of these biomass derived furans is the preparation of Metal-Organic Frameworks (MOF)s by the group of Yang, with metals such as Cr, Cu, Al, Fe and Zr. These materials have achieved thermal stabilities to other analog MOFs and so have raised curiosity of the applications they could be used for.[70] Incorporation of Eu and Tb in these MOFs products materials with strong photoluminescence and excellent fluorescence sensing for small molecules.

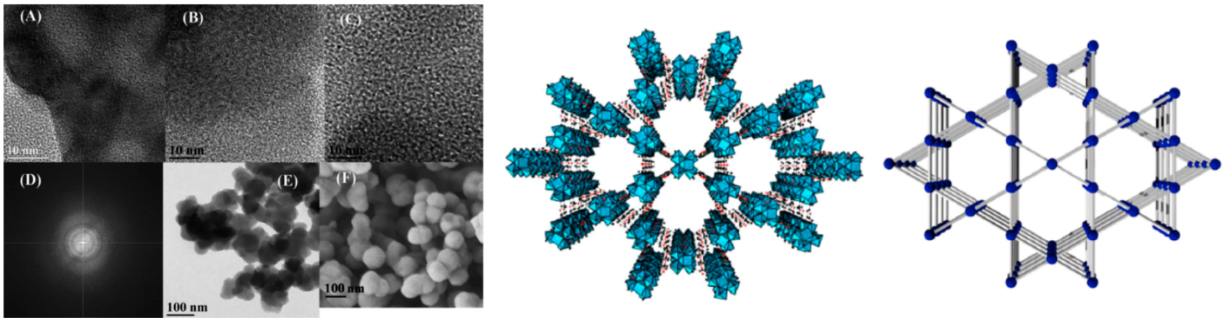

Figure 11. LEFT: HR-TEM images of (A)ZrO_2 and (B) Zr-FDCA, (C) TEM diffraction pattern of Zr-FDCA, (D) TEM image of Zr-FDCA, (E) SEM image of Zr-FDCA. Taken from [70]. RIGHT: Framework structure of Zr-FDCA (Zr-CAU-28) and the underlying kagome topology.

Only a handful of reports have used biomass-derived furans as starting materials for the total synthesis of attractive medicinal compounds. One remarkable example is the synthesis of anti-inflammatory furan fatty acids from biomass derived 5-(chloromethyl)furfural.[71] The group of Kalaus utilized HMF as a starting material for the synthesis of Sessiline, an alkaloid which was isolated from *Acanthopanax sessiliflorus*.[72]

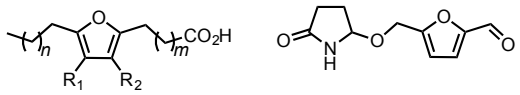

Figure 12. Example of compounds synthesized utilizing biomass-derived HMF as starting material: (right) sessiline, (left) furan-derived fatty acids.

1.6. Importance of the Furan-Aryl moiety in different fields

Even though biomass-derived furans have not been used extensively for the synthesis of value-added compounds or materials, the appearance of aryl substituted furans is ubiquitous in many fields. The furan moiety is found recurrently in compounds with interesting biological activities, and specifically, aryl substituted furans have been reported as the main core of different

drug-like compounds (Figure 13). For example, Kumar and co-workers reported a series on chalcones (**22**) with antibacterial activity bearing the aryl furan moiety against gram positive and gram negative bacterial strains.[73] Haddach *et al.* reported the discovery of CX-6258 (**23**) , a potent, selective and orally efficacious pan-Pim Kinase inhibitor with 2-aryl furan moiety in its core structure.[74] Katritzky and collaborators utilized computational docking studies to design a library of 2-aryl substituted furans (**24**) as HIV-1 fusion inhibitors, with effective inhibition for the infection.[75]

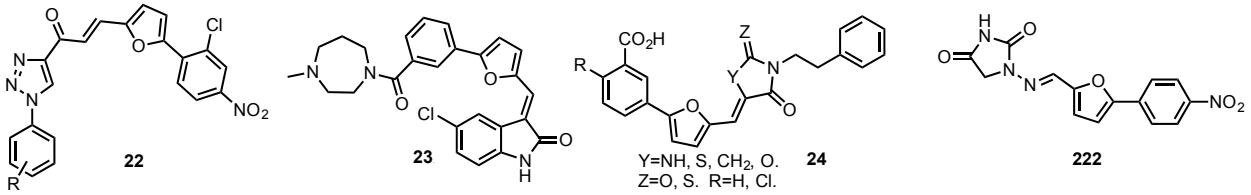

Figure 13. Examples of molecules bearing the Aryl-furan moiety with relevant biological activity.

This motif can also be encountered in approved drugs, such as the example of Dantrolene® (**222**), the chief drug in the prevention and treatment of malignant hyperthermia. In this molecule, a 2-*p*-nitrophenyl furan moiety is found in conjugation with an hydantoin.[76]

The furan aryl moiety is also present in materials chemistry. The research group of Michael Krayushkin utilized the furan moiety as a non-reversible template for the photoisomerization of cyclopentane-based β-(2-furanyl)enones (Figure 14) for application in fluorescent switches with optical memory recording.[77]

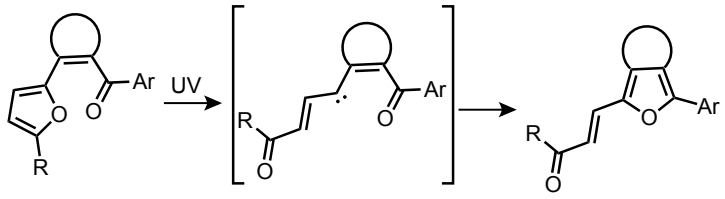

Figure 14. Photoisomerization of β-(2-furanyl)enones.

A novel application for the 2,5-diaryl substituted furans was also reported by S. Thomas and collaborators, which involves the incorporation of these motif as non-conjugated pendants in the backbone of conjugated polymers, as probes to sense singlet oxygen ($^1O_2$). The rapid rate of

reaction between $^1O_2$ and diarylfurans enabled a fast fluorescence quenching response of these polymers, with tunability allowed by the substitution on the aryl rings (Figure 15).

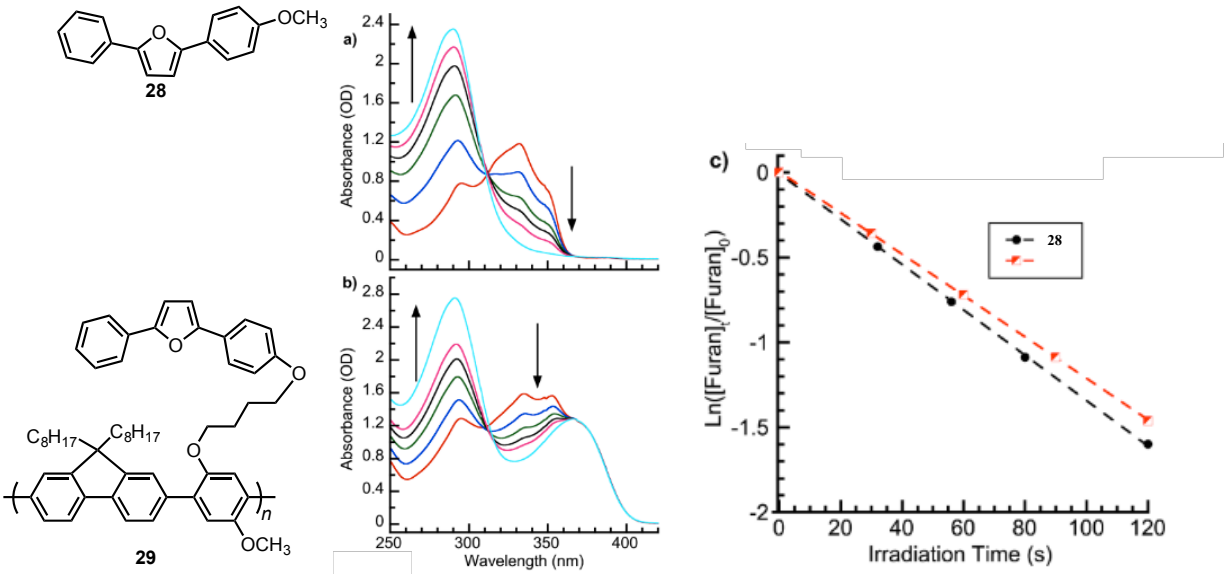

Figure 15. Structure of the singlet oxygen responsive polymer **29** and its building block **28**. Response UV-vis spectrum of **28** (a) and **29** (b), and pseudo-first order kinetics of furan disappearance in **28** and **29**.

1.7. Reported Synthetic Methodologies

The 2,5-diaryl furan scaffold is often found in molecules with interesting biological activities, and as a building block for both heterocyclic and acyclic compounds. Hence, the synthesis of this moiety is of great interest and various methodologies have been previously reported. Kel'in and Gevoryan reported the synthesis of 2,5-disubstituted furans from the cycloisomerization of substituted alkynes (**32** and **33**) and alkynyl ketones (**31**) catalyzed by CuI (Figure 16)[78], and later reported the transformation of haloallenyl ketones (**34**) to furans catalyzed by $AuCl_3$.[79] The group of M. Krische reported the use of γ-acyloxy butynoates in the presence of triphenylphosphine as a strategy to synthesize furans in very high yields and under mild conditions.[80] The group of Gevoryan continued to explore the possibility of using coinage metals for the cyclization of tethered nucleophiles, and employed a 1,2-migration of acetate groups from alkynyl ketones (**35**) to finally synthesize substituted furans, this time catalyzed by $AgBF_4$.[81]

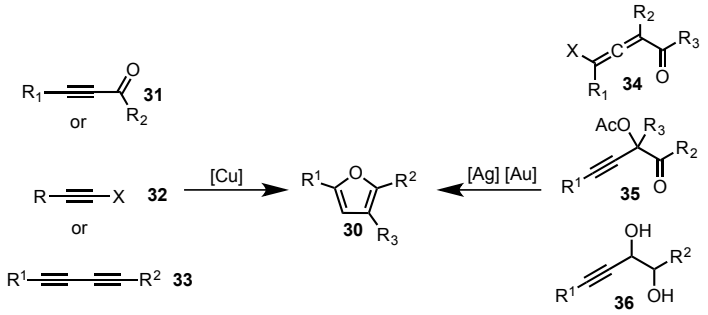

Figure 16. Synthesis of 2,5-substituted furans employing coinage metals as catalysts.

Other important catalytic methods have been reported that utilize transition metals (Figure 17) for the synthesis of 2,5-disubstituted furan. Rhodium catalysis was employed by the group of Mortreaux, in which they used a carbonylative addition of arylboronic acids (**37**) to propargylic alcohols (**38**) as a modular approach to the cyclisation reaction to obtain substituted furans.[82] In 2009, Zhang *et al.*, utilized a similar approach employing the Ruthenium-catalyzed head-to-head dimerization of alkynes (**43**) leading to a bis(carbene)-ruthenium intermediate, which subsequently formed a 1,3-dienyl ether after the addition of alcohols. This useful intermediate was submitted to a Cu^{2+} induced cyclization.[83] Yin *et al.*, reported the $SnCl_2$-induced cyclization of 1,4-diaryl-2-butene-1,4-dione (**40**), as an excellent strategy for the synthesis of thioether substituted 2,5-diaryl furans, in moderate to good yields.[84] Palladium has also been employed in a related transformation, such as the microwave-assisted transformations of 2-butene-1,4-diones and 2-butyne-1,4-diones (**39**) to furans, with a Pd//PEG-200 medium.[85]

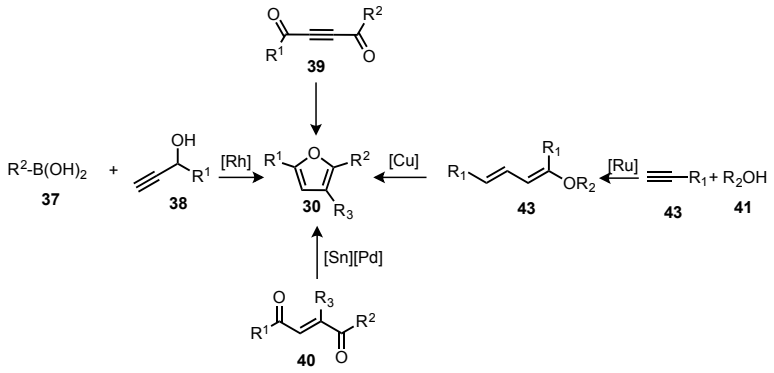

Figure 17. Synthesis of 2,5-substituted furans employing other metals as catalysts.

The main limitation of the previously mentioned methodologies is the preparation of the alkenes or alkynes necessary for the cyclization-aromatization to proceed. Very often, the synthesis of precursors requires the use of organometallic synthetic intermediates with high reactivity, which prevents their use on industrial scale. The research conducted in this thesis intends to develop new synthetic methodologies that complement the existing routes, with the advantage of employing biomass-derived furans as starting materials, which are classified as renewable resources.

1.8. Palladium-catalyzed cross-coupling reactions

1.8.1. Classical reactions (organometallic/organometalloid)

1.8.1.1. General Mechanism

In general terms, the classical palladium-catalyzed cross-coupling reactions have three major components; the nucleophilic coupling partner (usually an organometallic/organometalloid species) (**47**), the electrophilic coupling partner (usually an aryl halide or pseudohalide) (**45**) and the catalyst (**44**). There have been extensive reports in the literature of different reaction conditions and catalytic systems employed to perform cross-coupling reactions, of which tetrakis(trphenylphosphine)-palladium(0) [$Pd(PPh_3)_4$] catalyzed reactions are the most common.[86,87] Pd^0L_4 complexes are neutral, tetrahedral and have a 18 electron count, but due to the size of the phosphine ligands (L), these exist in equilibrium a variation of the complex with open coordination positions, where one, two or three ligands dissociate to form more reactive 16, 14 and even 12 electron species. Generally, a PdL_2 is accepted as the active catalytic species necessary for the catalytic cycle to begin.[88] Another alternative is to start the reaction from a Pd(II) species, which is more stable towards oxidation than the Pd(0) homologues. It is believed that the reduction process from Pd(II) to Pd(0) is mediated by either an excess of the phosphine ligands, by any heteroatom with an electron lone-pair or a carbon-carbon double bond present in the solvent, or *via* a reductive reagent in solution. This reduction process is sometimes confusingly described as thermal reduction, due to the often high reaction temperatures necessary and with no exact identification of the reductant.[87] Any or all of these processes can produce the catalytic species required for the reaction cycle, which is described is Figure 18.

The active catalyst first undergoes an oxidative addition into the C_{sp2}-X bond of the aryl halide (or pseudohalide) coupling partner. The overall net effect of this process is the formation of two new bonds (Pd-C_{sp2} and Pd-X) and the oxidation state of the Pd from 0 to +2. Pd(II) complexes are described as square planar, with an ideal bonding angle of 90° between the ligands. At this point, in most classic cross-coupling reactions, the complex (**46**) undergoes a transmetallation with the nucleophilic cross-coupling partner, that leads to the formation of a bisarylated palladium complex (**48**) and a metal salt as by-product (a notable exception is the Mizoroki-Heck reaction, which will be discussed in the upcoming sections). It is important to know that after the transmetallation step, the square planar complex has a *trans* orientation of the aryl ligands, and therefore undergoes an isomerization to locate the aryl ligands in a *cis* geometry (**49**). To complete the catalytic cycle, the Pd(II)-*cis*-bisarylated complex undergoes a reductive elimination that results in the re-formation of the Pd^0L_2 active catalytic species (**44**) and the synthesis of the corresponding biaryl (**50**).[87,89]

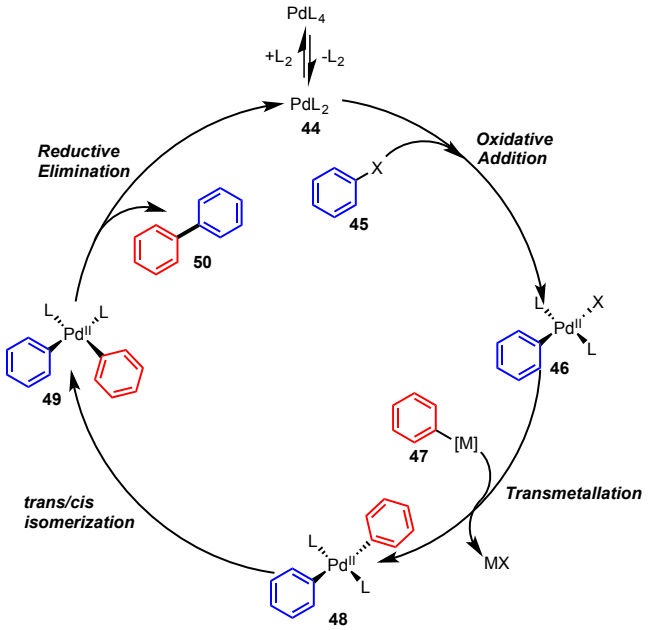

Figure 18. General mechanism for most Palladium-catalyzed cross-coupling reactions.

The following section will explore pivotal research in the development of Pd-catalyzed cross-coupling reactions. These are generally referred to as the "classical" transitional metal catalyzed C-C bond formations developed in the 1970-1980s, and include the works of Mizoroki-Heck, Kumada-Corriu, Sonogoshira, Negishi, Stille and Suzuki-Miyura, among others.[90]

1.8.1.2. Mizoroki-Heck

Richard Heck reported a series of palladium mediated cross-coupling reactions between organomercury compounds and olefins in 1968.[91] The first reports used stoichiometric amounts of palladium(II) salts (mainly $Pd(OAc)_2$) and generated Pd(0) as final product, but later this was circumvented by the use of stoichiometric amounts of $CuCl_2$ (with catalytic amounts of Pd) for reoxidation to Pd(II) (see Figure 19). Fitton and McKeon substituted the organomercury compounds, demonstrating that palladium(0) can undergo oxidative addition with vinyl chlorides to form arylpalladium(II) compounds.[92] This important discovery was independently built upon by Mizoroki who introduced a cross-coupling reaction without a transmetallation step in 1971, including an oxidative addition.[93] Shortly thereafter, Heck and Nolley[94] demonstrated their palladium-catalyzed cross-coupling reactions for the first time without an organometallic reagent in 1972 (Figure 19). This reaction has become a powerful tool for the formation of new C-C bonds on olefins with at least one hydrogen necessary for a β-hydride elimination to occur, which is the key step in the mechanism of the Mizoroki-Heck reaction.

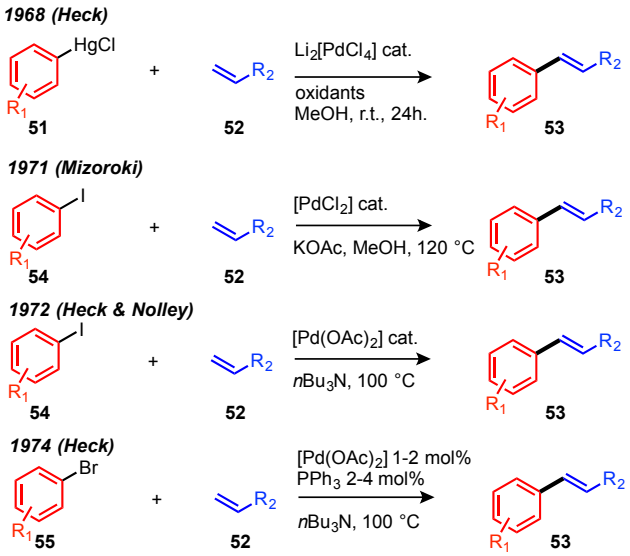

Figure 19. Palladium-catalyzed cross-coupling reaction of aryl halides (and organozincates) and alkenes.

Generally speaking, this reaction follows a different mechanistic pathway than the others Pd-catalyzed cross-coupling reactions. After oxidative addition, the palladium(II)-complex reacts with the double bond in a *syn*-migratory insertion. Then a rotation of the bond is needed to position a hydrogen in the β-position *syn* to the palladium, so that a β-hydride elimination can occur. This

regenerates the double bond, and in the process forms a palladium(II)-hydride complex, that proceeds to reductively eliminate HX.

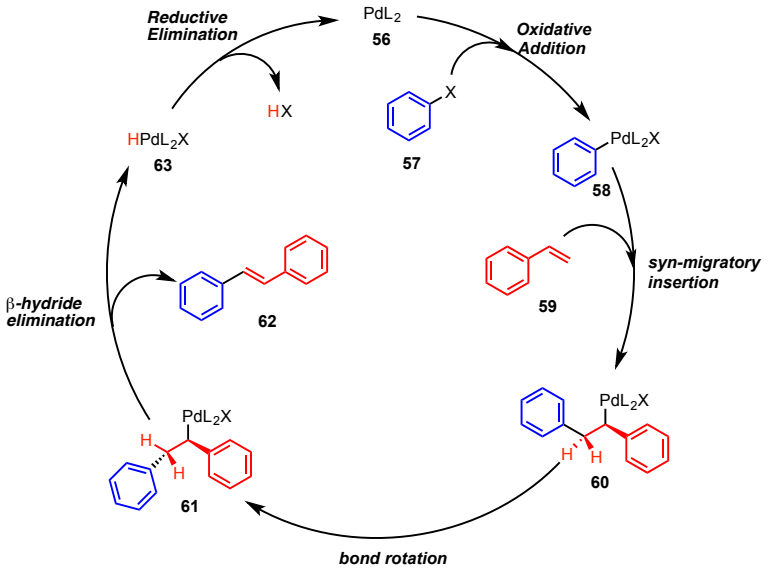

Figure 20. Mechanism of the Mizoroki-Heck reaction.

The Mizoroki-Heck reaction has the advantage over other classic addition reactions to double bonds of maintaining the oxidation state and hybridization of the substrate in the product, as retaining the double bond as a functional group allows for further transformations. Usually, the anti-Markovnikov product and *E*-alkene are produced due to a migratory insertion occurring in a fashion that adds the R group to the more accessible sp^2-carbon for the obligatory syn β-hydride elimination, which requires a rotation after the syn-addition and favors the energetically more stable conformer.[95] Heck also demonstrated in his early papers that the combination of this reaction with carbon monoxide results in the production of ketones and esters (Figure 21)[96].

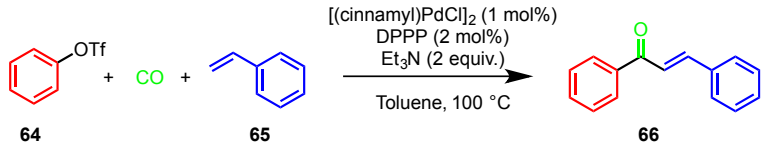

Figure 21. Carbonylative Heck-type cross-coupling reaction of Aryl triflates and olefins**.**

1.8.1.3. Kumada-Corriu

Independently, Kumada[97] and Corriu[98] discovered nickel catalyzed cross-couplings of Grignard reagents and aryl halides in 1972, work which was based on the research by Job[99] and Kharasch[100](Figure 22). This advancement in transition metal-catalyzed cross-coupling reactions greatly increased scope, and allowed for a larger functional group tolerance than the early processes (baring functional groups that are electrophilic enough towards Grignards reagents). The group of Kumada is considered the first to introduce the modulation of the metal catalyst in C-C bond formation with the employment of phosphines as ligands.[97] The reaction became increasingly robust and reproducible when palladium was introduced as the catalyst, as it allowed for a lower rate of homo-coupling by-product formation. Palladium catalysts are also more easily prepared than their nickel counterparts, less sensitive to air and moisture, and overall more tolerant of reagent functional groups.[101] Additionally, employing a highly nucleophilic organometallic reagent (Grignard) in a Pd-mediated coupling highlighted the efficiency of the transmetallation step in the overall general cross-coupling mechanism, while demonstrating palladium's robustness as a catalyst. This facet served as inspiration for continuing research into transition-metal catalyzes C-C bond formations, in order to further identify organometallic reagents that were more stable and more functional group-tolerant than the previously employed Grignards and organolithium compounds. Recent efforts are re-exploring the use of nickel as the transition metal catalyst, as the price and availability of palladium could become problematic. A variety of modern nickel-catalyzed reactions currently exist, and the economically friendly iron has also demonstrated its usefulness as a catalyst for related transformations.[102]

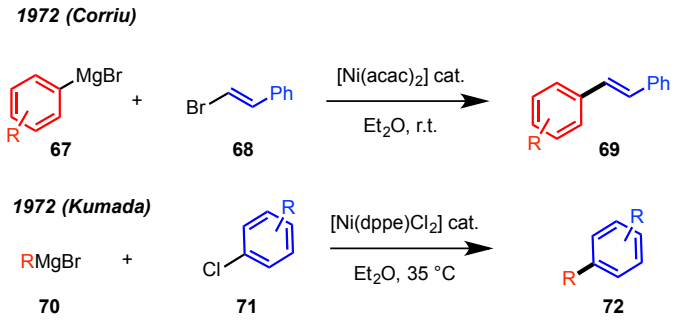

Figure 22. Initial reports on Nickel-catalyzed cross-coupling reactions of Grignard reagents.

1.8.1.4. Sonogashira

Copper had been used in coupling processes many times in the formation of C-C bonds (sp–sp and sp–sp^2),[103–107] yet in 1975, Sonogashira was the first to report the Pd-catalyzed cross-coupling of aryl iodides and terminal acetylenes, improving on the earlier protocols.[108] His methodology became the prevalent method for this type of coupling, as it can be done at room temperature and is mediated by the use of copper co-catalyst (Figure 23).

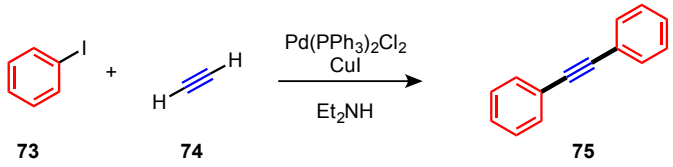

Figure 23. First report by Sonogashira of the coupling of acetylene with Cu-activated phenyl iodide.

In the presence of a base, the copper(I) salt activates the terminal proton of the alkyne for deprotonation and leads to formation of a copper acetylide which can enter the general mechanism (see figure X) as the organometallic compound. The transmetallation would regenerate the copper(I) salt to continue the catalytic *in situ* formation of copper acetylides and yield the arylated and alkynylated palladium species for subsequent reductive elimination and cross-coupling. The Sonogashira coupling has gained seminal importance as the standard, mild method for sp–sp^2 bond and the advancement in palladium catalysts has also led to mild variants that do not require the added copper[109] (Figure 24).

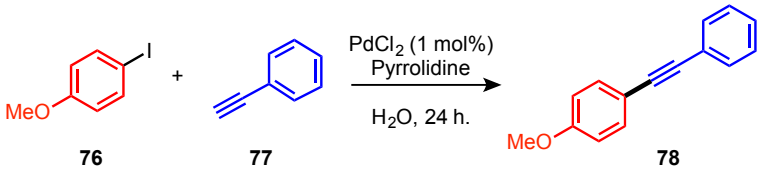

Figure 24. Copper-free Sonogashira reported in 2004 by the Yang group.

1.8.1.5. Negishi

The Negishi group[110] and Jutand[111] developed similar methods in parallel for the transition metal-catalyzed cross-coupling organozinc compounds with arly halides, but over time the Negishi reaction conditions reaction have become more widespread. Negishi *et al.* successfully demonstrated that less reactive organometallic species than the previously employed Grignard

reagents could undergo transmetallation and participate in palladium and nickel catalyzed coupling reactions. The Negishi cross-coupling allows for a wide range of substrates and bisorganozincates as well as organozinc salts to be employed (Figure 25 *top*).[103] Depending on the equilibrium between organozincates, organozinc salts and zinc halides, different transmetallations can occur, and this influences the success of the reaction and the side product formation. Transmetallation with organozincates happens more rapidly, but the *trans*-palladium complex is formed, and isomerization is required before reductive elimination can form the desired product. Organozinc salts, on the other hand, directly form the *cis*-complex during transmetallation and therefore undergo reductive elimination more rapidly, decreasing side-product formation.[112] In general, the Negishi protocols have been used extensively as a complementing methodology in the Pd-mediated C-C bond formation reactions for total synthesis (Figure 25 *bottom*).

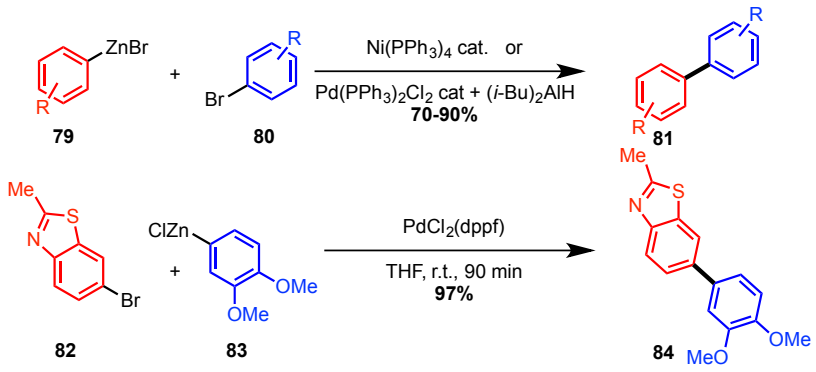

Figure 25. First report of cross-coupling of Organozinc reagents (top) and new reported conditions (bottom).

1.8.1.6. Stille

Milstein and Stille[113] first disclosed the Pd-catalyzed coupling of an acyl chloride with tetramethylstannane, and subsequently developed these conditions for a more versatile and robust reaction, due to the small electronegativity difference between carbon and tin (Figure 26). Stannanes proved to be robust organometallic reagents that were readily available and had less stability issues than other nucleophilic coupling partners.

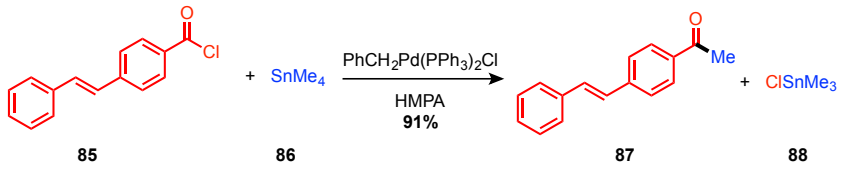

Figure 26. Initial report by Stille of the cross-coupling of acid chlorides and organotin compounds.

Stannanes are thus uniquely suited for complex reactions and synthetic problems that can be encountered in the total synthesis of natural products. The application of the Stille reaction in non-trivial total syntheses by the groups of Kuwahara[114] and Panek[115] (Figure 27) not only made this particular cross-coupling reaction popular, but was a service to all palladium catalyzed C–C coupling reactions and helped to popularize carbon-carbon bond formation. Although the toxicity of stannanes has always been the critical issue of this coupling, this has yet to prevent the favorability of the reaction within industrial and pharmaceutical applications.

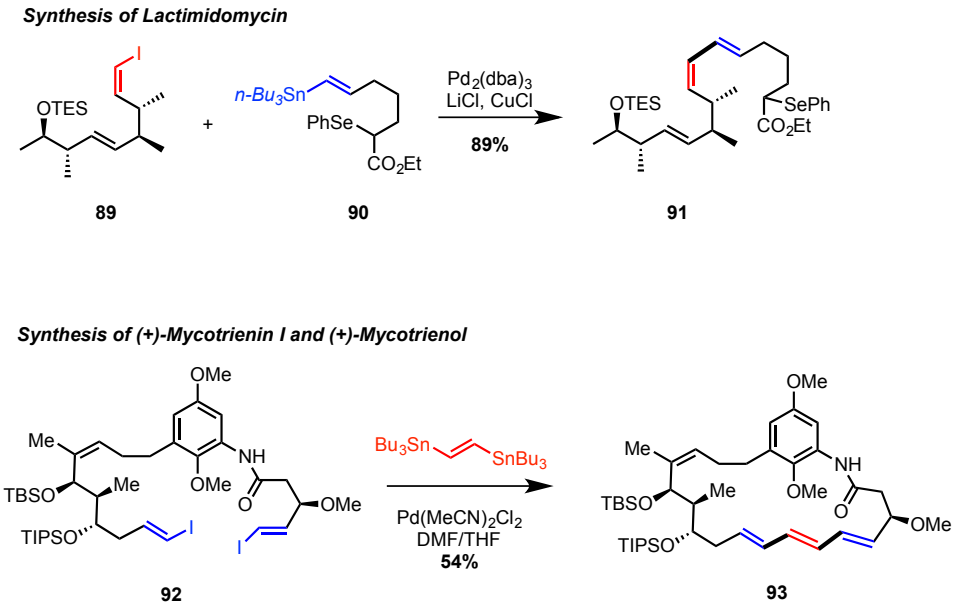

Figure 27. Examples of the utilization of the Stille cross-coupling in the synthesis of natural products.

1.8.1.7. Suzuki-Miyaura

The number of applications of the Stille reaction has only been surpassed by the Suzuki-Miyaura reaction, developed by Akira Suzuki (Figure 28)[116], which utilizes organoboranes as the nucleophilic coupling partner in cros-coupling reactions. This work was built on research previously conducted by Negishi, who first identified that boron, along with tin and zinc could be

utilized in cross-coupling reactions. The Suzuki-Miyaura reaction surpassed the Stille reaction in popularity as there was a parallel development of methods for the preparation of various organoboronates and boronic acids, which are considered the most stable and easy to handle nucleophilic coupling partners of the described organometallic reagents. The reaction possesses a high tolerance for functional groups and a wide applicability, which led to its dissemination into all areas of chemistry and thus becoming the gold standard. As reported in a study by Roughley and Jordan[117], about 80% of the palladium-catalyzed transformations used in the pharmaceutical industry were Suzuki-Miyaura reactions.

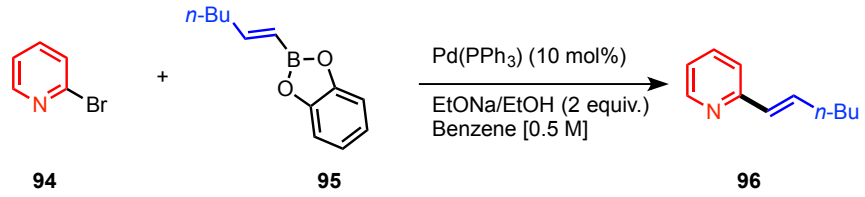

Figure 28. Initial report by Miyaura and Suzuki of the cross-coupling of alkenyl boranes and aryl halides.

The Suzuki-Miyaura coupling follows the general mechanism in Figure 29, with the additional requirement of a base. The base is necessary to activate the boronic acid or ester (**101**) by adding to the boron atom and forming the boronate anion (**102**), which increases its nucleophilicity necessary for transmetallation (Figure 29). Additionally, the base also substitutes a labile halide ligand on the palladium after oxidative addition (**99** to **100**), which helps the transmetallation as it increases the stability of the borate (or boronate) formed as by-product. The requirement for the presence of a base in the reaction, and the relative stability of boronic acids and their derivatives, allows these reactions to proceed in water and with milder conditions than required by the other organometallic reagent coupling partners.

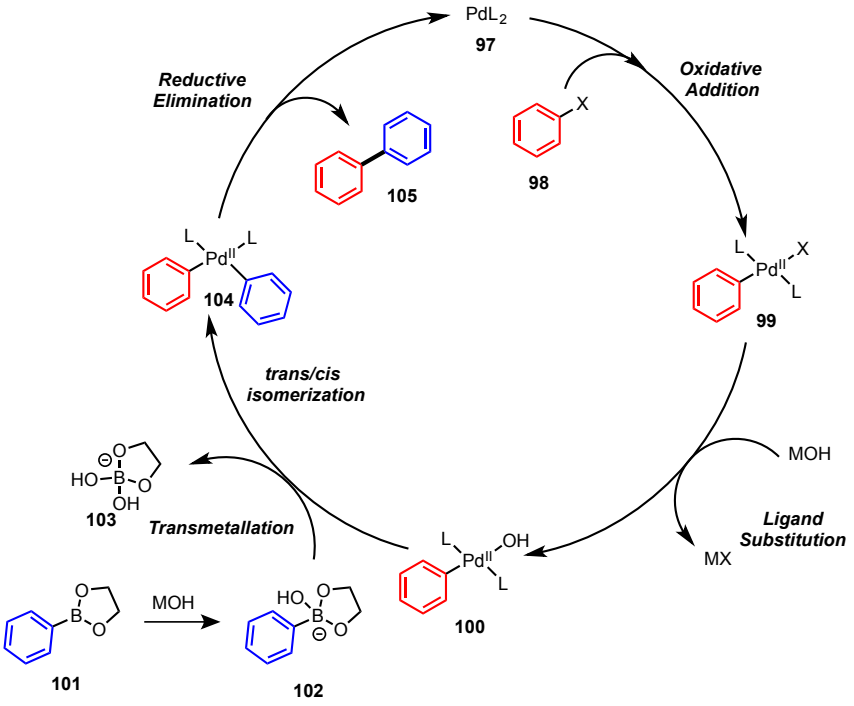

Figure 29. Mechanism of the Suzuki-Miyaura cross-coupling reaction: Role of the base.

1.8.2. Modern Pd-Catalyzed C-C bonding reactions

Classical palladium-catalyzed cross-coupling reactions are well established methodologies with a wide range of applications that has increased their importance and impact in the way we synthesize organic compounds. Even though these reactions are robust, some challenges remain to be solved for their use in modern organic chemistry, especially at the industrial level. The environmental impact of reactions employed on large industrial scales are of great consideration, and this aspect is one of the main drawbacks for using transition metal catalyzed cross-coupling reactions in industry. Additionally, some of the organometallic nucleophilic partners described herein are highly reactive and sensitive to air and moisture, which complicates their manipulation, and inert atmosphere techniques must be used in order to obtain high yeilds (examples are the organomagnesium and organozincates). In terms of green chemistry, some of the organometallic coupling partners are not very atom-economic, especially the larger tin reagents, and therefore produce large amounts of metal salts and other by-products, sometimes not very easily removed from the desired product. Typically, multiple functionalization steps are also needed to access the organometallic reagents, producing more waste and requiring more energy. It is for these reasons that researchers have continued to optimize the above-mentioned cross-couplings, and also have

been investigating new transformations that avoid the stoichiometric amounts of organometallic reagents for C-C bond formation.

1.8.2.1. C-H activation

Ideally, no pre-functionalization of the starting materials for a cross-coupling reaction should be required, and a C–C bond could be formed directly by activating a C–H bond on the starting material for reaction with the electrophilic coupling partner.[118] This would only produce HX in direct arylation reactions with aryl halides[86,119,120] and formally H_2 in oxidative coupling processes that involve the activation of two carbon-hydrogen bonds[121,122]. Several examples of such reactivity have been reported through the decades. Dubeck[123] and Chatt and Davidson[124], reported in the earlier 60's that some transition metals complexes were able to react with C-H arylic bonds, forming a metal-carbon bond and a metal hydride bond, but this research was not exploited until the advent of late transition metal catalyzed cross-couplings, in which those organometallic species could be incorporated in catalytic cycles. Mechanistically, C-H activations can be classified into three different categories; oxidative addition, electrophilic activation and sigma-bond metathesis. The three mechanisms are theorized to be different, but the net effect is the same with respect to the products formed.

The first carbon-carbon bond formation *via* C–H activation employed stoichiometric amounts of palladium(II) and was a homo-coupling reaction of benzene and substituted derivatives (see Figure 30)[125]. The stoichiometric metal is necessary due to the oxidant required in double C–H activations, and the reaction demonstrates the necessity for the presence of a base. An early example of a cross-coupling reaction involving C–H activation was disclosed by Fujiwara *et al*.[126] shortly after Heck's initial report, replacing the arylmercury salt with a non-functionalized benzene. It is otherwise very similar and can also be transformed into a catalytic process by the addition of an oxidant.

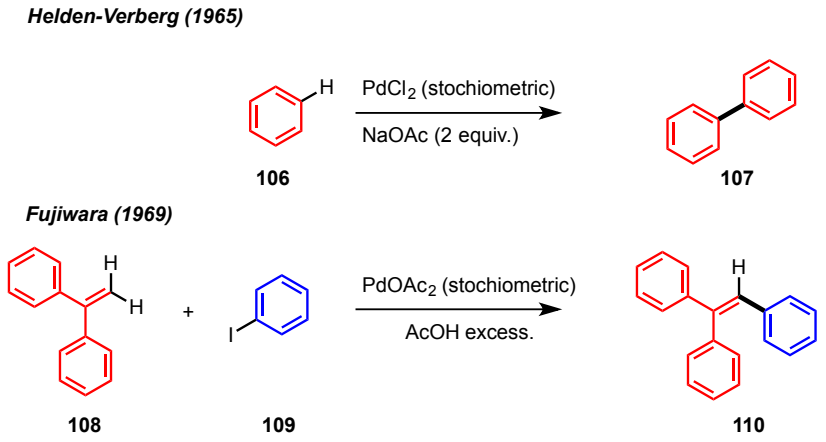

Figure 30. Early reports of Pd-mediated C-H arylations.

During the early 2000's, different groups reported the use of Pd complexes and oxidants for the arylation of relatively unreactive C-H bonds, including reports from Sandford[127,128], Daugulis[129] and Doucet[130] (Figure 31).

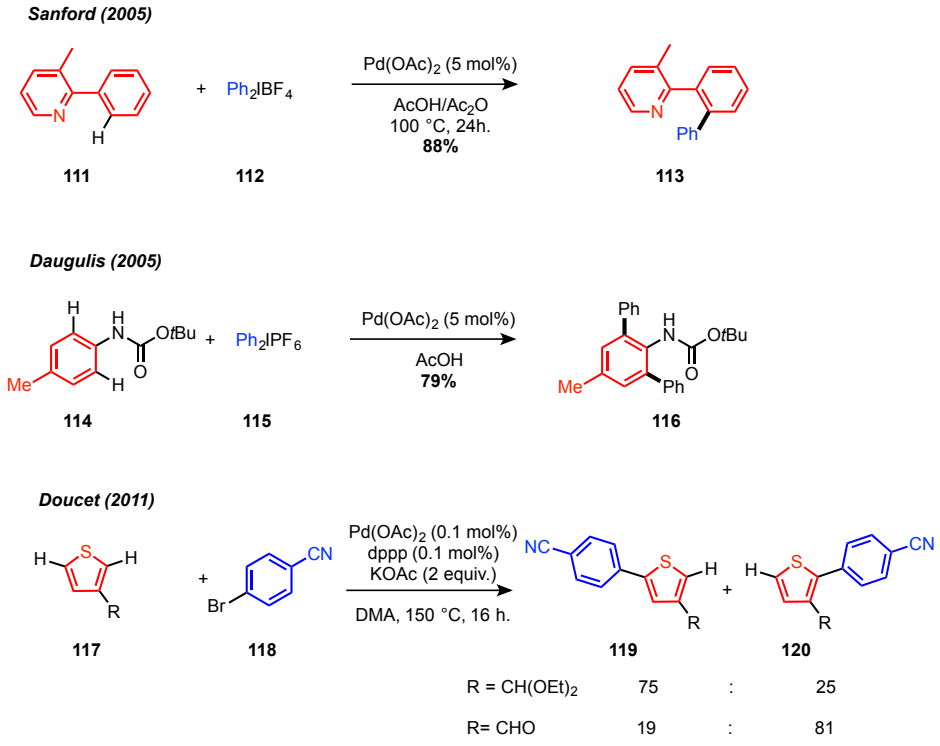

Figure 31. Examples of recently reported C-H arylations.

Given the abundance of similarly reactive C-H bonds in a single molecule, the main drawback from these methodologies are the regioselectivity of the reaction, and this is why recent efforts have focused on the directed C-H bonds through directed pre-complexation of the active catalyst. These so-called directing groups have been reported extensively in the literature, with both permanent and transient groups that influence both regiochemistry and stereochemistry of the products. Strongly coordinating nitrogen distal groups pioneered the directed C-H modifications, as these undergo cyclometallation readily by many transition metals.[131–133]

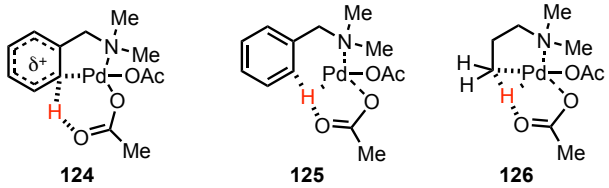

Figure 32. Examples of distal *N,N*-dimethylamino groups directing C-H functionalizations.

Murai reported various weakly coordinating groups that directed the formation of C-C bonds in *ortho* positions utilizing ruthenium catalysis.[134] One very important application of these reactions is the borylation reactions developed by the Hartwig group.[135] The aforementioned reaction reported high regioselectivity in arene and alkane borylation catalyzed by rhodium. This reaction is especially important because it allows the synthesis of otherwise challenging coupling partners for Suzuki-Miyaura cross-coupling reactions.

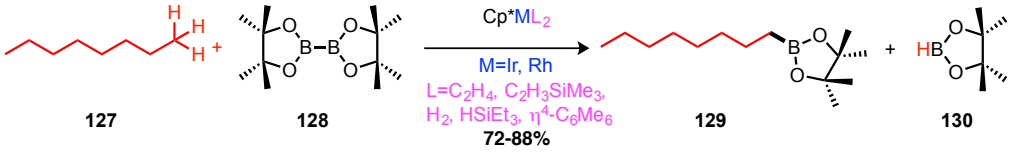

Figure 33. Highly regioselective borylation of alkanes reported by the Hartwig group.

Other groups have modified reaction conditions in order to manipulate the regioselectivity of C-H arylation on some substrates, rather than modifying the substrate itself. One example of this was presented by researchers at GlaxoSmithKline, in which they submitted ester substituted thiophenes and furans at the C3 position to different C-H arylation conditions and obtained selectivity C2 or C5 arylation depending on the catalytic system employed.[136]

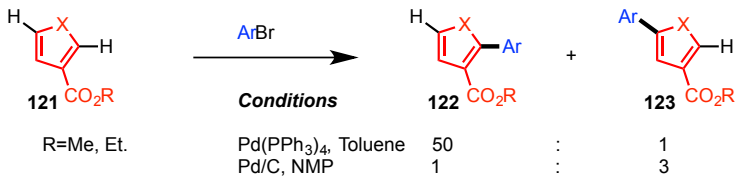

Figure 34. Regioselectivity of C-H arylation on substituted Furans and Thiophenes achieved by tuning the reaction conditions.

1.8.2.2. Decarboxylative cross-coupling reactions

Another methodology recently developed to circumvent the use of organometallic coupling partners is the decarboxylative cross-coupling reactions. This methodology utilizes carboxylic acids as the nucleophilic partners, with aryl halides in cross-coupling reactions, and therefore eliminates the regioselectivity issue presented by the C-H activation methodologies, while negating the need for organometallic reagents.

Over the last century, decarboxylation has been shown in the case of activated acids like β-ketoacids and malonic esters[137–139], as well as in several metal-assisted decarboxylations on non-activated acids at elevated temperatures. Depending on the catalyst, carboxylic acids can serve as synthetic equivalents of acyl, aryl, or alkyl halides, or organometallic reagents.

In 1966, Nilson *et al*. performed a trapping experiment employing excess aryl iodide with aryl-copper intermediates (generated from decarboxylative metalation from copper benzoates) which resulted in the detection of unsymmetrical biaryls.[140] The development of a methodology based on these conditions was achieved by combining the decarboxylative catalyst with a two-electron catalyst capable of promoting the cross-coupling of the organocopper species with aryl electrophiles. These reactions remained unstudied for about three decades until Steglich and coworkers reported an intramolecular decarboxylative coupling in their total synthesis of the Lamellarin G (1997)[141] and L (2000, Figure 35)[142]. To avoid the use of an extra metal co-catalyst, a stoichiometric amount of palladium was employed.

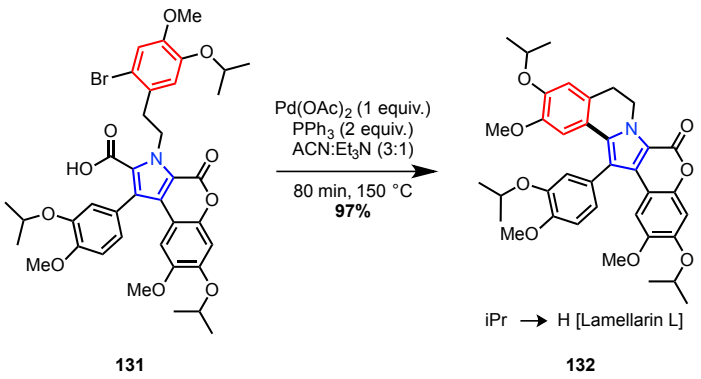

Figure 35. Decarboxylative cross-coupling reported in the synthesis of Lamellarin L by Steglich and co-workers.

Following that, Myers *et al*. reported a palladium-catalyzed decarboxylative Heck-type reaction in 2002[143] between *ortho*-substituted carboxylic acids and acryl derivatives and styrenes employing stoichiometric amounts of Ag_2CO_3 that served both as an oxidant and base. Heteroaromatic and electron-poor and -rich aromatic acids were tolerated in this reaction. The olefin scope was enlarged in 2004[144] to 5,6 and 7 membered cyclic α,β-unsaturated ketones and *ortho*-substituted benzoic acids that have been challenging to utilize in traditional Heck-coupling reactions.[144]

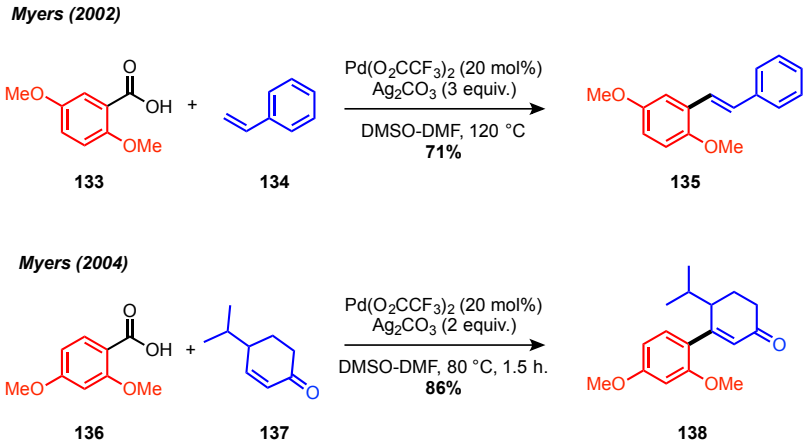

Figure 36. Decarboxylative of electron-rich carboxylic acids with styrene-derivatives and α,β-unsaturated ketones.

Following this work, there have been several successful protocols developed for decarboxylative cross-couplings, differing in substrate scope and in their utilization of either mono- or bimetallic catalytic systems. In his initial report, Goossen *et al.*, describe the cross-coupling of 2-nitrobenzoic acids and aryl bromides using NMP as solvent. The reactions are stirred

for several hours at 120 °C in the presence of stoichiometric amounts of basic copper carbonate and potassium fluoride, an excess of ground molecular sieves and 2 mol% of a $Pd(acac)_2/P(iPr)Ph_2$ catalyst. This way, the arylcopper species can be coupled with various aryl bromides by the palladium co-catalyst (Figure 37).[145]

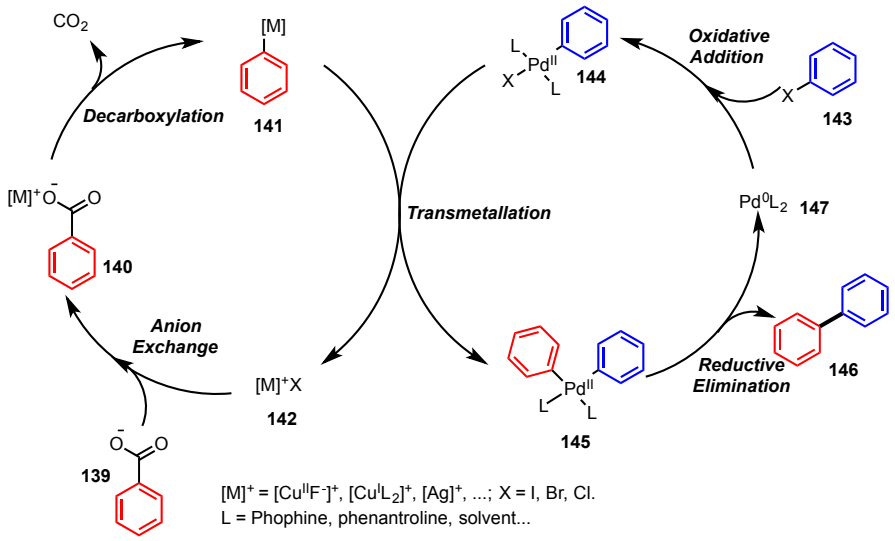

Figure 37. General mechanism for the formation of biaryls via decarboxylative cross-coupling under bimetallic systems.

The reaction starts with the extrusion of CO_2 from a metal carboxylate, generated from the treatment of the carboxylic acid with the metal base, or an appropriate base and the metal salt. The resulting aryl-metal undergoes transmetallation with an arylpalladium(II) complex, generated by oxidative addition of the palladium co-catalyst into the C_{sp2}-X (X=Halide) bond of the aryl halide cross-coupling partner, giving rise to biarylpalladium(II) species. The catalytic cycle for the palladium is closed by a reductive elimination of the biaryl, thus regenerating the initial palladium(0) species. The efficiency of the palladium catalysts was improved by the addition of the sterically demanding, electron-rich Büchwald-type phoshines[146], like bis(*t*-butyl)biphenylphosphine, allowing for a wider range of aryl halide coupling partners that cancbe employed.

The decarboxylative metallation is the key step in any cross-coupling reactions employing carboxylic acids. The difficulty connected to this process is that metal salts of simple carboxylates generally require harsh conditions to extrude CO_2, and under such conditions, the resulting

organometallic species are very reactive and can be protonated by the surrounding media, giving the corresponding protonated products before the C-C coupling. Goossen's group also developed modified reaction conditions that employed catalytic amounts of both palladium and copper at high temperatures[145] (Figure 38). The requirement for ortho-substituted benzoic acids substrates still remained the limitation of this method. Further optimization expanded the reaction scope to other aryl coupling partners such as aryl chlorides[147], tosylates[148] and triflates[149]. The employment of aromatic triflates as coupling partners eliminated the need for *ortho*-substitution of the benzoic acids.[149]

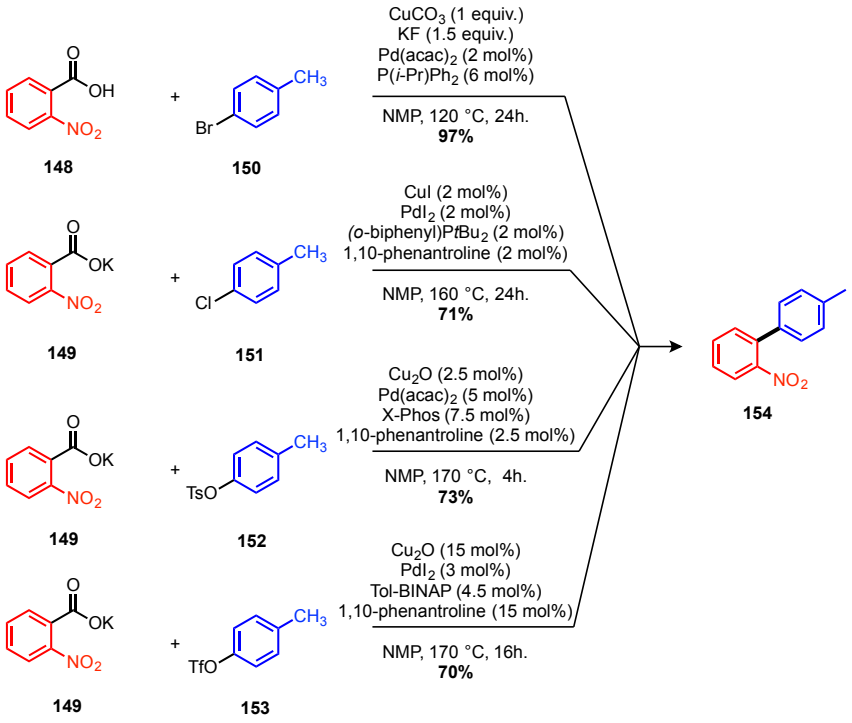

Figure 38. Summary of the reports of Goossen employing a Cu/Pd Bimetallic system on electron poor carboxylic acids/carboxylates.

In 2007, the Becht group reported a Pd-catalyzed decarboxylative cross-coupling protocol for the cross-coupling of electron-rich aromatic carboxylic acids and aryl iodides[150] or diaryliodonium salts[151]. Similar to Goossen's original work, this method also requires the use of stoichiometric amounts of silver carbonate. This work proposed that the silver salt serves as both base and possibly co-catalyst with coordination of the carboxylate (Figure 39). Similar reactions were developed by Wu *et al*. with the use of a $PdCl_2$/BINAP catalytic complex.[152]

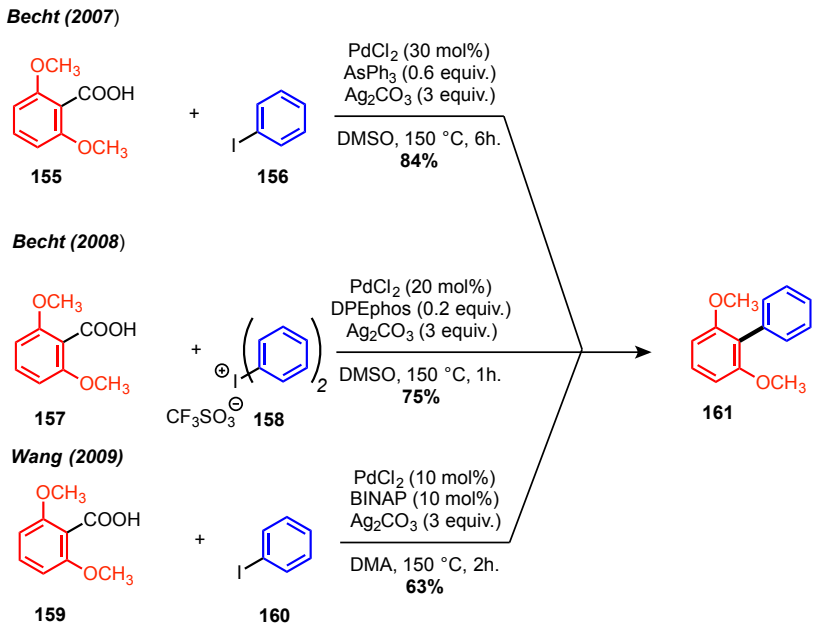

Figure 39. Bimetallic Ag/Pd systems reported for decarboxylative cross-coupling reactions.

In 2006, Forgione *et al*. reported a Pd-catalyzed decarboxylative cross-coupling of aryl bromides and heteroaromatics as an unexpected result while attempting direct arylations of heterocycles with the C2 position blocked with a carboxylic acid.[153] The reaction differs from previous decarboxylative cross-couplings in several aspects; only palladium was employed as the catalyst and tetrabutylammonium chloride was used -presumably- to help in the solubilization of the base. One great advantage of this methodology involved the short reaction time (8 minutes) through microwave irradiation (Figure 41). Subsequent studies by the same group, expanded the substrate scope to aryl chlorides, iodides and triflates.[154]

The plausible mechanism (Figure 40) begins with an oxidative addition of the palladium(0) complex (**162**) into an aryl halide to provide aryl palladium(II) intermediate (**163**). The carboxylate anion (**164**) undergoes a ligand exchange with the halide to form intermediate (**165**). From here, three different mechanistic pathways were proposed for the decarboxylation step. Path A goes through a direct decarboxylation and extrusion of CO_2 resulting in the generation of a C2 palladated species (**166**). This intermediate undergoes reductive elimination to form the desired heteroaryl product (**167**) and reform the active catalytic species (**162**), but since benzoic acids and heteroaromatic-3-carboxylic acids failed to react under these conditions, path A is the least probable of the three. For path B, the electron richness of the heteroaromatic, and the carboxylate

as the directing group, assists the electrophilic palladation of the heteroaromatic to form intermediate (**168**). CO_2 extrusion occurs to provide bisarylated palladium species (**166**) (recovering the aromaticity on the ring), which can undergo reductive elimination to form the desired product (**167**). The formation of trace amounts of C3 palladation by-product in those cases where C3 of the heteroaromatic is hydrogen, suggested path C. In this case the π-nucleophilicity of the heteroaromatic forms intermediate (**169**) with a C3 palladation. A C3 to C2 migration is possible to form the more stable intermediate (**168**) that goes through the same CO_2 extrusion and reductive elimination such as path A, but in those cases where R is a hydrogen, deprotonation at C3 provides the re-aromatized complex (**170**), that undergoes reductive elimination to generate (**171**). This intermediate can re-renter the catalytic cycle to form the 2,3-biarylated compound.

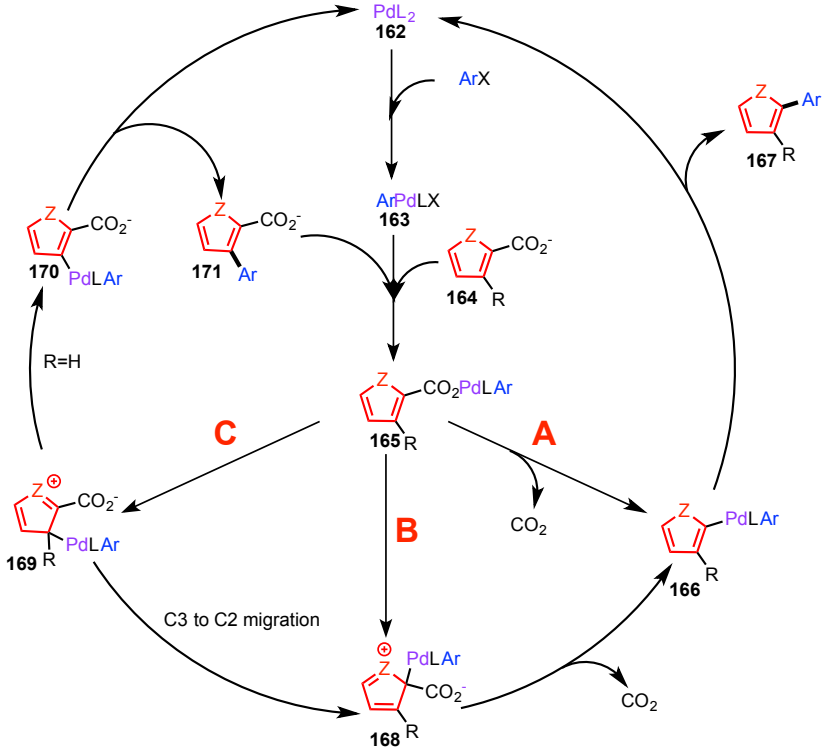

Figure 40. Proposed mechanism for the decarboxylative cross-coupling of 5-membered heteroaromatic-2-carboxylic acids and aryl halides.

Since the initial report in 2006, the Forgione group has become a leading research group on decarboxylative cross-coupling on 5-membered heteroaromatic carboxylic acids (Figure 41), with multiple reports on the adaptation of decarboxylative cross-coupling for application towards

thiophene materials, drug-like targets[155,156] and biomass-derived furans (central topic of this thesis).

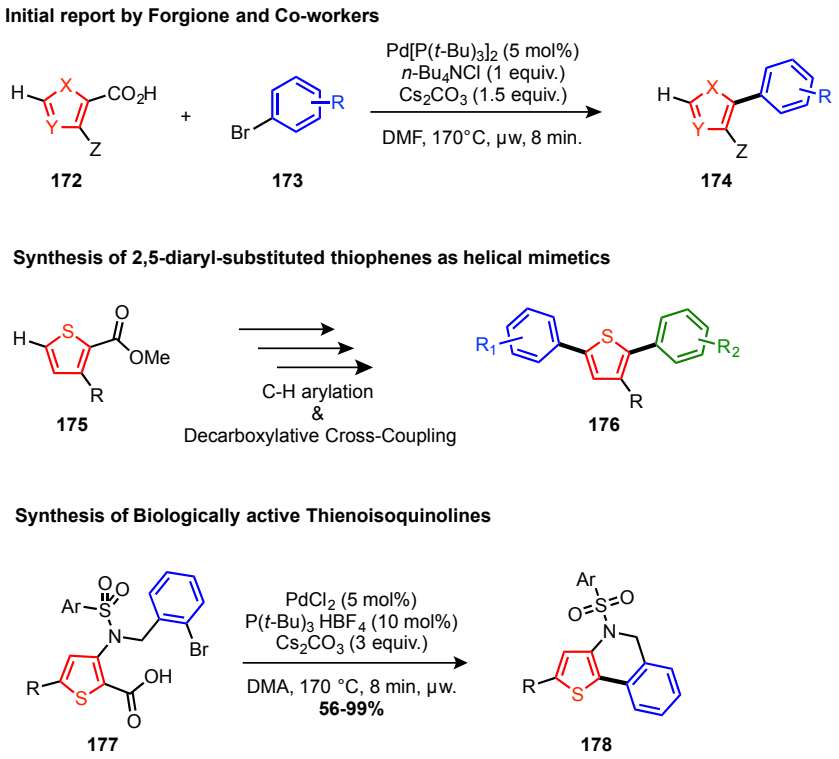

Figure 41. Initial report of Forgione and co-workers on the decarboxylative cross-coupling of 5-membered heteroaromatic-2-carboxylic acids and aryl bromides, and the utilization of this methodology in the synthesis of interesting bioactive molecular targets.

1.9. Research goals and thesis organization

The research outlined in this document has as a main objective to develop new reactions that tackle the problem of using of renewable starting materials (specifically furans derived from polysaccharides) for the synthesis of complex value-added molecules. The employment of green reaction conditions was essential in the development of this research, where possible. Chapter 1 introduced the reader to the problematic of overexploitation of petroleum resources, and the consequences it has had and could potentially have in the environment and life in general. Following this, the emerging of green chemistry as a field and the consolidation of specific goals towards the improvement of chemical procedures to alleviate the dependence on petrochemicals is discussed. Biomass was introduced as a raw material that functions as a bio-renewable sources of chemicals and the furans derived from this material are discussed. The importance of the aryl

furan moiety and its reported synthesis was discussed, and the common cross-coupling methodologies to perform these transformations are outlined.

Chapter 2 discusses the double decarboxyative cross-coupling of FDCA and aryl halides, to obtain the valuable 2,5-diaryl furans in a one pot microwave assisted reaction. Initial screening for the conditions were done by Daniel Mangel and Maythem Ali. Optimization of the reaction conditions and scope was done by the author of this thesis. Anthony Sudano contributed with the isolation of several of these compounds as part of his bachelor degree thesis. This work was disclosed to the public as an article in the journal ACS Sustainable Chemistry and Engineering (DOI: 10.1021/acssuschemeng.7b01277).

Chapter 3 is divided into 2 main sections. Section 3.1 discusses the base-promoted solvent-free disproportionation of HMF into DHMF and HMFA. The work outlined was done mostly by the author of this thesis. Contributions of Cynthia Messina were done in the scale up experiments and Fei Chen in the screening of sacrificial reagents for the selective reactions. This work was published in the journal Green Chemistry (DOI: 10.1039/C8GC02481B). Section 3.2 discusses the synthesis of 2,5-diaryl non-symmetric furans from HMF. Optimization of the reaction conditions was done in collaboration with Juan David Lasso and Paul Szavay contributed with the initial reaction including the silyl protected HMFA. Contributions were also done by Jason Covone in the characterization of several compounds of the scope. Optimization of the decarboxylative cross-coupling, oxidation of the alcohol and aldehyde moiety and the final scope of the second decarboxylative cross-coupling was done by the author of this thesis, including the work on the formal synthesis of Dantrolene®. This work has been submitted for publication in the journal Advanced Synthesis and Catalysis.

Chapter 4 presents an unsubmitted manuscript that discusses the synthesis of bis(5-arylfuran-2-yl)methane scaffolds, utilizing a defunctionalization approach starting with HMF. The initial screenings for this reaction were done in collaboration with Liana Zaroubi as part of her honours 450 project in her undergraduate degree. Jason Covone contributed with the characterization of some of the finalized compounds and revisions of the manuscript. This manuscript is undergoing final revisions to submitted for publication.

Chapter 5 discusses the general conclusions of all projects and the future directions.

Chapter 2. High Value Biomass-Derived 2,5-Furandicarboxylic Acid Derivatives *via* a Double Decarboxylative Cross-Coupling

2.1. Abstract

A new methodology was developed employing biomass-derived 2,5-furandicarboxylic acid to produce 2,5-diaryl furans in good to excellent yields through palladium-catalyzed double decarboxylative cross-couplings. Various aryl halides were successfully evaluated as coupling partners. The present work contributes to the development of useful methodologies employing biomass-derived starting materials for the chemical synthesis industry.

2.2. Introduction

The ability of the global fine chemical industry to support a growing and developing world population is compromised by its heavy reliance on non-renewable petrochemical feedstocks. As such, there is significant economic, social and scientific interest in biobased, sustainable feedstocks for the production of value-added chemicals[157]. In 2004, the US Department of Energy released a list of compounds derived from biorefining carbohydrates with the purpose of stimulating and focusing research and industrial efforts on processes to convert lignocellulosic biomass into chemical feedstocks[47]. That list included 2,5-furandicarboxylic acid (FDCA) and triggered a significant amount of research concerning the production of FDCA from fructose[158,159], and its subsequent use as a monomer in the production of industrially important condensation polymers[160].

The success of those efforts, which notably includes a BASF/Avantium joint 50,000 MT/year FDCA plant[48], ADM-DuPont platform[49] and the MetGen recent efforts[50], suggests that FDCA will evolve into a widely available, cost-effective raw material. As such, chemical transformations of FDCA to more complex, high-value structures are expected to be of broad interest.

Palladium-catalyzed reactions have proven to be effective for creating C-C bonds, but the classical approach requires pre-functionalization of the starting material, which often are highly reactive organometallic compounds. Modification of heteroaromatic carboxylic acids *via* the highly regioselective decarboxylative cross-coupling reaction[151,154,168–171,155,161–167] and photoredox

systems[172–174], have been reported. These transformations would yield a type of di-substituted furan that are present in a variety of pharmaceutical targets (Figure 42). The decarboxylative cross-coupling of furoic acid have proven to be challenging, in comparison with other heteroaromatic carboxylic acids, as depicted by Forgione *et al.*, in which they reported the decarboxylative cross-coupling reaction between 2-furoic acid and bromobenzene, with a 40% yield[153] (Figure 43). The same reaction using modified conditions was reported by Gooβen *et al.*, with a yield of 38%.[32]

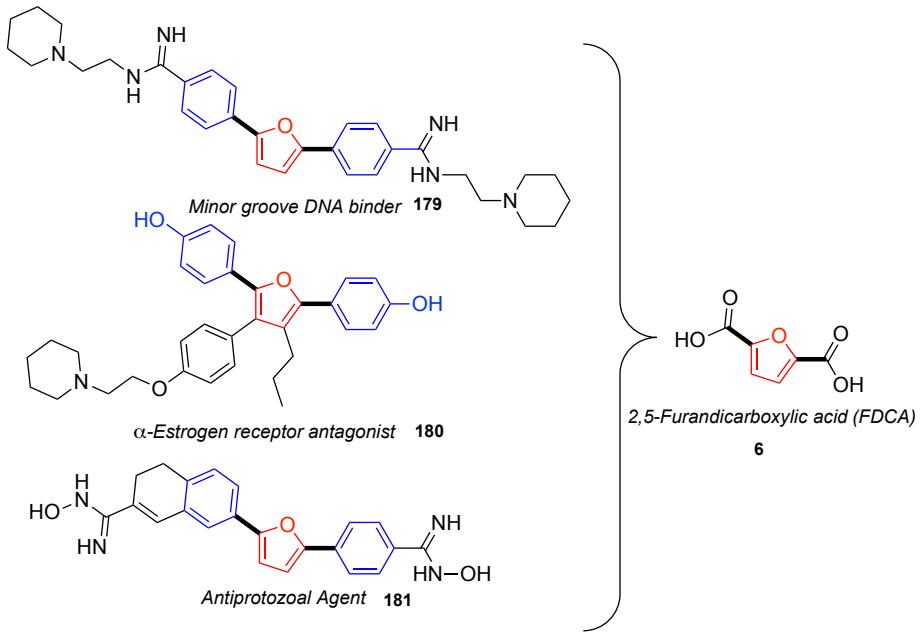

Figure 42. Reported examples of 2,5-disubstituted furans with pharmaceutical applications, Minor groove DNA binder, Estrogen receptor antagonist and antiprotozoal agent.

The only two reports of a decarboxylative cross-coupling of furoic acid (**182**) produced a single arylation (**184**) in moderate yields (Figure 43).[153,32] When these conditions were applied to the double-decarboxylative cross-coupling between FDCA (**6**) and bromobenzene (**185**), no di-arylation product (**186**) formation was observed (Figure 43). A systematic optimization pathway was followed towards a double-decarboxylative cross-coupling arylation of FDCA.

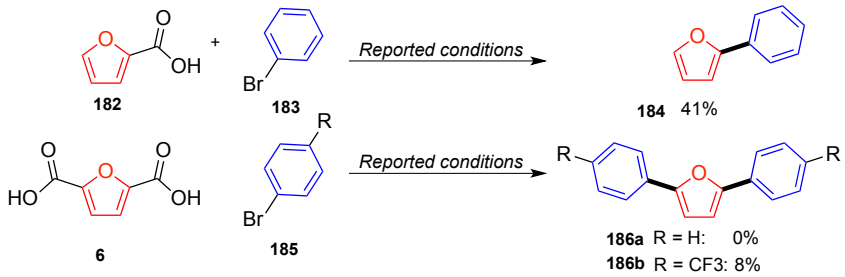

Figure 43. Previously reported decarboxylative cross-coupling of 2-furoic acid, and the first attempt of the double-decarboxylative cross-coupling of FDCA. Reaction conditions (same as reported): 2-furoic acid:bromobenzene, 2:1; FDCA: bromobenzene, 1:1; $Pd[P(t\text{-}Bu)_3]_2$ 5 mol%, Cs_2CO_3 1.5 equiv., *n*-Bu_4NCl 1.0 equiv., DMF [0.2 M], microwave (μw), 170 °C, 8 min.

2.3. Results and Discussion

Decarboxylative cross-coupling conditions previously reported[153] were used as the starting point for the optimization of the di-arylation of FDCA (**6**) with *p*-bromobenzotrifluoride (**187**) as coupling partner. A variety of palladium catalysts were tested for their utility in the double cross-coupling reaction shown in Table 1. No difference was observed when employing Pd^{II} vs Pd^0 sources (entries 1,4,8 vs 2,5,6 in Table 1). An increase in catalyst loading from 5% to 15% improved the product yield substantially (entry 8 vs 9, Table 1). $Pd(dba)_2$ at the higher loading provided the best results among the palladium source screened, and was selected for subsequent optimization of additional parameters.

Table 1. Optimization of Palladium source for the reaction.

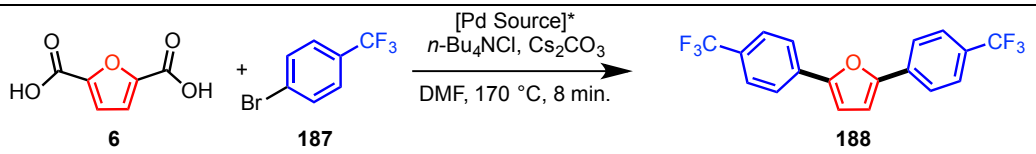

Entry	Pd Source	Pd mol%	Ligand	Ligand mol%	Yield (%)
1	$Pd(PPh_3)_4$	10	-----	0	0
2	$Pd(OAc)_2$	15	JohnPhos	30	14
3	$Pd[P(t\text{-}Bu)_3]_2$	15	-----	0	8
4	$Pd(acac)_2$	15	JohnPhos	30	10
5	PdI_2	15	JohnPhos	30	0
6	$Pd(TFA)_2$	15	JohnPhos	30	17
7	$Pd(dba)_2$	5	JohnPhos	10	9
8	$Pd(dba)_2$	15	JohnPhos	30	20

Reaction Conditions: 1.0 equiv. (0.2 mmol) of FDCA, 2 equiv. of *p*-bromobenzotrifluoride, 1 equiv. of n-Bu_4NCl, 3 equiv. of Cs_2CO_3, 2 mL of DMF. Reaction in μw at 170 °C for 8 min. *for those Pd sources not containing Phosphine Ligands it was added at a 1:2 molar ratio of Pd: JohnPhos.

Multiple solvent systems were studied; high boiling, polar aprotic solvents like DMA and DMF provided the best results with product yields ranging from 20-25%. Other solvents including isopropanol, water, ethanol and dioxane did not yield the desired product. DMA was used for subsequent optimization reactions. In all cases, the major by-product obtained was the homo-coupling of the aryl halide, nonetheless, a mono-arylation was observed in small amounts for some cases (GC-MS), which suggests that the second decarboxylation occurs faster that the first one.

Table 2. Optimization of the base employed in the reaction.

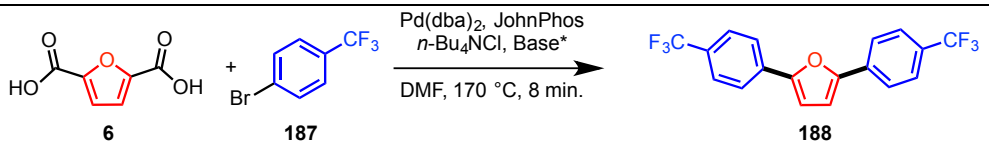

Entry	Base	Additive	Yield (%)
1	KOtBu	*n*-Bu_4NCl	Trace
2	LiOtBu	*n*-Bu_4NCl	Trace
3	N-Et-iPr_2	*n*-Bu_4NCl	0
4	K_2CO_3	*n*-Bu_4NCl	Trace
5	Ag_2CO_3	*n*-Bu_4NCl	30
6	Ag_2CO_3	None	36
7[a]	Ag_2CO_3	None	34
8	Ag_2CO_3:KOH(1:1)	*n*-Bu_4NCl	5
9	$Cu_3(OH)_2CO_3$	*n*-Bu_4NCl	0
10[b]	Ag_2CO_3	None	44

Reaction Conditions: 1 equiv. (0.2 mmol) of FDCA, 2 equiv. of *p*-bromobenzotrifluoride, 1 equiv. of n-Bu_4NCl, 3 equiv. of Base [(a) only 2 equiv. of Ag_2CO_3], 15 mol% of $Pd(dba)_2$, 30 mol% of JohnPhos, 2 mL of DMA. (b) Reaction carried out at 200 °C with 4 equiv. of aryl bromide.

Base optimization (Table 2) was done in the presence of one equivalent of *n*-Bu_4NCl, as suggested by previous reports.[154] Tert-butoxides (entries 1 and 2) yielded only trace amounts of the desired product, as observed by ^{1}H-NMR. An organic tertiary amine (entry 3) gave a complex mixture of products, and none of the desired product. Given the general utility of Cs_2CO_3 in this reaction and previous reports for related reactions[153,156,175], K_2CO_3 was evaluated (entry 4), but no product was observed. With inspiration from the approaches of Goossen[164,176,177] and Becht[151,178], bi-metallic systems were evaluated. A silver containing base, Ag_2CO_3, had a positive impact on the product yield (entry 5), which suggests that the decarboxylation is the rate limiting step[177]. Control experiments were done using Cs_2CO_3 as base and silver salts ($AgBF_4$; AgOTf; AgCl) as additives, but none of them yielded the desired product. In contrast to the results presented here

for FDCA, in which the highest yields occurred at an elevated temperature of 200 °C (entry 10), the reports of Gooßen[32] indicate that silver-mediated systems allow palladium-catalyzed protodecarboxylation to proceed at lower temperatures. However, when this reaction was carried out at 170 °C, only a 16% yield was obtained. Interestingly, decreasing the equivalents of base had no significant impact on the yield (entry 6 and 7). Ag_2CO_3 and a 200 °C reaction temperature were used in subsequent optimization reactions, and the equivalents of aryl halide were increased to four.

In agreement with work reported by others, the screening of different ligands indicated that bulky tri-substituted phosphines provided the highest yields (Table 3)[179]. Two very similar phosphines, MePhos and JohnPhos, were employed in the subsequent optimization reactions.

Table 3. Optimization of the ligand used in the reaction.

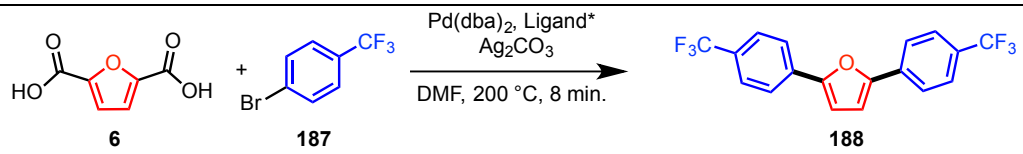

Entry	Ligand	Yield (%)
1	JohnPhos	44
2	$P(Cy)_3$	trace
3	*t*-BuMePhos	40
4	dppf	30
5	MePhos	45
6	PPh_3	14
7	$P(Cy)_3HBF_4$	trace
8	$P(t\text{-Bu})_3$	trace

Reaction Conditions: 1 equiv. (0.2 mmol) of FDCA; 4 equiv. of *p*-bromobenzotrifluoride; 02 equiv. of Ag_2CO_3; 15 mol% of $Pd(dba)_2$; 30 mol% of JohnPhos; 2 mL of DMA.

Given earlier results indicating that reducing the equivalents of silver carbonate did not have a substantial impact on the yield (Table 2, entries 6 and 7), a base and additive loading and ratio optimization was conducted (Table 4). The highest yields were achieved with 1.5 equivalents

of each of these components at a 1:1 ratio that impressively provided the corresponding di-arylated product in 80% yield (entry 3) without the need to employ excess aryl iodide.

Table 4. Optimization of the equivalents of Ag_2CO_3 and *n*-Bu_4NCl used in the reaction.

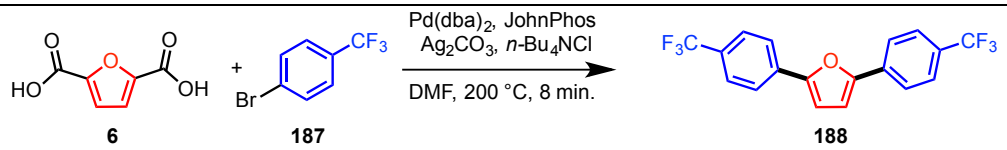

6 **187** **188**

Entry	**Ag_2CO_3(equiv.)**	***n*-Bu_4NCl (equiv.)**	**Yield (%)**
1	3.0	0.0	42
2	2.0	1.0	38
3	1.5	1.5	80
4	1.0	2.0	47
5	3.0	4.0	23

Reaction Conditions: 1 equiv. (0.2 mmol) of FDCA; 4 equiv. of *p*-bromobenzotrifluoride; varying Ag_2CO_3 and *n*-Bu_4NCl; 15 mol% of $Pd(dba)_2$; 30 mol% of JohnPhos; 2 mL of DMA.

With the final optimized conditions, the reaction scope was evaluated employing a range of coupling partners (Table 5).

Table 5. Scope of the reaction under the optimized conditions.

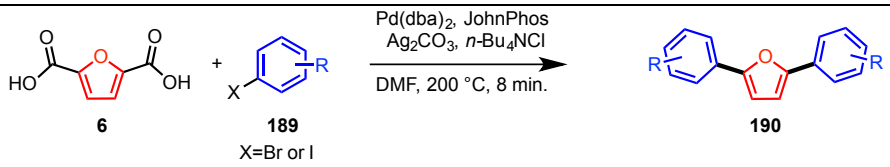

Entry	*R*	*Product*	*Yield (%) X=Br*	*X=I*
1	*p*-CF_3	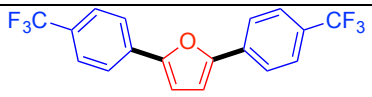 **190a**	80	84
2	*p*-CN	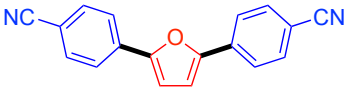 **190b**	93	94
3	*p*-NO_2	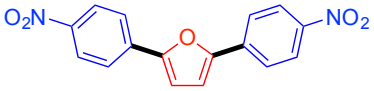 **190c**	90	---
4	*p*-CO_2Et	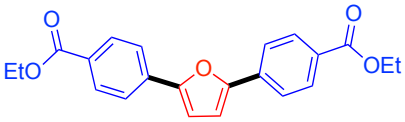 **190d**	70	---
5	*m*-CF_3	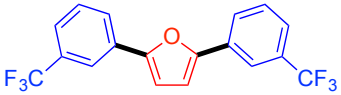 **190e**	66	74
6[a]	*p*-OCH_3	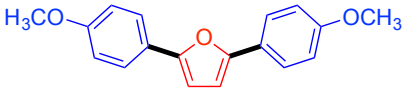 **190f**	70	89
7[a]	*m*-OCH_3	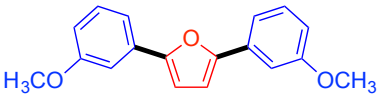 **190g**	70	75
8[a]	*p*-CH_3	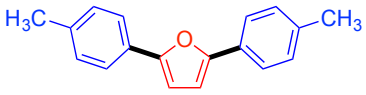 **190h**	71	76
9[a]	*o*-CH_3	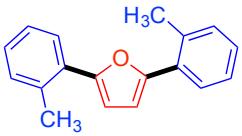 **190i**	57	69
10	H	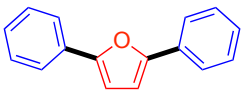 **190j**	44	80

Reaction Conditions: 1 equiv. (0.2 mmol) of FDCA; 4 equiv. of Aryl Halide; 1.5 equiv. of Ag_2CO_3; 1.5 equiv. of *n*-Bu_4NCl; 15 mol% of $Pd(dba)_2$; 30 mol% of JohnPhos (a:using MePhos instead); 2 mL of DMA.

The reaction gave satisfactory to excellent yields for a wide scope of aryl halides. Electron defficient aryl halides provided the highest yields when JohnPhos was employed as the ligand. For the neutral and electron rich coupling partners, the best results were obtained when MePhos is used instead, with the other parameters remaining the same. Lower yields were obtained for ortho- or meta- isomers (entries 1 vs 5, and 8 vs 9) when compared to their para- homologues, which is potentially attributed to the steric effects of the substituents.

When using coupling partners with phenol groups, the reaction did not yield the desired compound. Using tosylates or chlorides as coupling partners, proved to be ineffective for the reaction to occur. As is usually observed in cross-coupling reactions involving aryl halides, the aryl iodides provided higher yields than their bromide analogues, likely due to the more facile oxidative addition of the Pd(0) into the C_{sp2}-I in comparison to the C_{sp2}-Br[180,181].

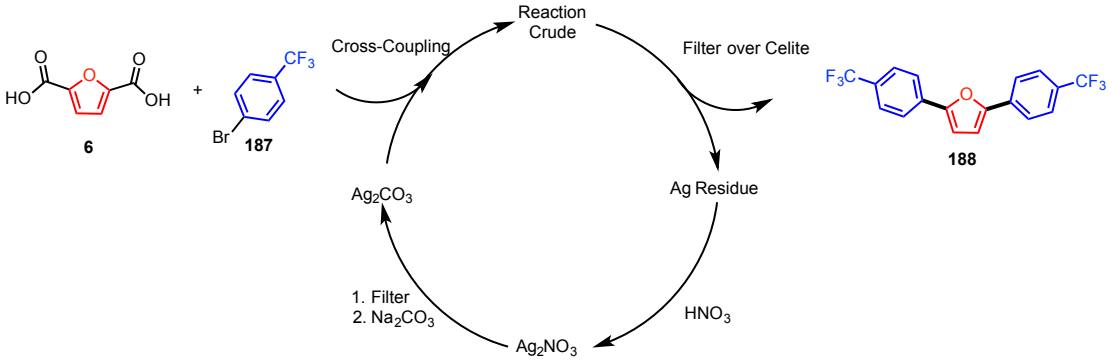

Figure 44. Experimental procedure to recycle the Ag_2CO_3 used in subsequent reaction batches.

In order to increase the utility of this method, the possiblity of recycling the silver carbonate based on a protocol employed by Guangying *et al*[182] was evaluated (Figure 44). Promising results were obtained in small scale experiments, indicating this could be accomplished with little effect on the subsequent cross-coupling yields (Table 6).

Table 6. Effect of recycling the Ag_2CO_3 in subsequent reactions.

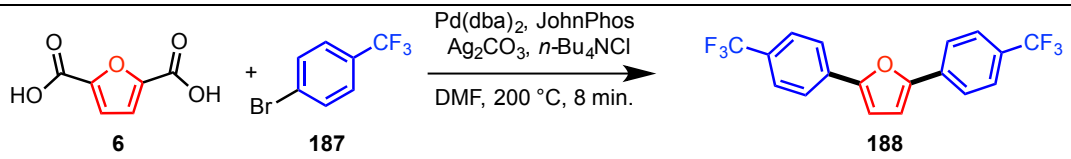

Cycle	Yield (%)	Recovery of Ag_2CO_3 (%)
1	77	84
2	81	84
3	76	81
4	63	80
5	74	79

Reaction Conditions: 1 equiv. (0.2 mmol) of FDCA; 4 equiv. of *p*-bromobenzotrifluoride; 1.5 equiv. Ag_2CO_3, 1.5 equiv. *n*-Bu_4NCl; 15 mol% of $Pd(dba)_2$; 30 mol% of JohnPhos; 2 mL of DMA. [a] Calculated by ^{1}H-NMR, using trimethoxybenzene as internal standard.

2.4. Conclusions

To conclude, a double-decarboxylative cross-coupling reaction for has been developed that employs biomass derived 2,5-furandicarboxylic acid as the starting material. The scope of the reaction proved to be broad, and the yields to form two new carbon-carbon bonds ranged from moderate to excellent. The presented work suggests that the efficient and innovative use of small molecules coming from renewable feedstocks is one of many ways that sustainable chemistry can be developed. The use of biomass as a resource for building blocks rather than biofuels, is an area that needs to be explored, but enourmous efforts are being made towards the advance of sustainable chemistry.

2.5. Experimental Section

General procedure for the preparation of the 2,5-disubstituted furans: 2,5-Furandicarboxylic acid (0.2 mmol), Ag_2CO_3 (0.3 mmol), n-Bu_4NCl (0.3 mmol), $Pd(dba)_2$ (0.03 mmol) and ligand (either JohnPhos or MePhos, as indicated in Table 5) (0.06 mmol) was added to a 2.0 mL conical microwave vial, equipped with a spin-vein. Aryl halide (0.8 mmol), anhydrous DMA (2 mL) were added to the mixture, and the vial was sealed. The mixture was heated in a

microwave at 200 °C for 8 min. The reaction was cooled to 23 °C, the crude was diluted with EtOAc (15 mL) and washed with saturated NaCl (2x20 mL) and saturated $NaHCO_3$ (1x20 mL). The combined organic phases were dried over Na_2SO_4, filtered and the solvent evaporated under reduced pressure. The crude mixture was purified by column chromatography to yield the desired product.

Recycling of Silver Carbonate for subsequent reactions: For the recycling of the silver carbonate, reactions were carried out with the optimized conditions and *p*-bromobenzotrifluoride as a coupling partner (0.2 mmol scale). After the reaction was complete, the reaction mixture was filtered through celite and washed with small portions (2x5 mL) of EtOAc, after this, the celite and silver residues (black powder) were stirred with 10mL of HNO_3 (10% v/v) for 12 hours. After this, the celite was filtered, and the filtrate was then evaporated using the rotatory evaporator to yield a white solid ($AgNO_3$). This solid was dissolved in the smallest volume of water needed and then 7 mL of Na_2CO_3 (10% m/v) were added. After stirring for 2 hours, the yellow solid was filtered and dried under vacuum. Special care must be taken to not expose to light, the recovered Ag_2CO_3 during extended periods of time, since it may decompose.

2.6. Characterization Data

Compound 190a: 2,5-bis-(4-(trifluoromethyl)phenyl)furan

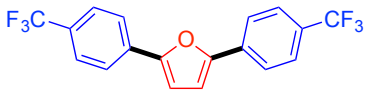

Compound **190a** was prepared following the general procedure for decarboxylative cross coupling on a 0.20 mmol scale. 5-1 was isolated with column chromatography (R_f = 0.30) Hexanes:EtOAc (9:1) as a white solid. **^{1}H NMR** (500 MHz, $CDCl_3$) δ ppm 7.83 (d, J = 8.1 Hz, 4H), 7.66 (d, J = 8.1 Hz, 4H), 6.87 (s, 2H). **^{13}C NMR** (125 MHz, $CDCl_3$) δ ppm 152.8 (2C), 133.4 (2C), 129.4 (q, *J* = 32.7 Hz, 2C), 125.8(q, *J* = 3.8 Hz, 4C), 124.1(q, *J* = 271.9 Hz, 2C), 123.9 (4C), 109.4 (2C). **HRMS (EI)**: Exact mass calculated for $C_{18}H_{10}F_6O$ [$M^{+\cdot}$]: 356.0630 found 356.0626 (-1.1 ppm).

Compound 190b: 4,4'-(furan-2,5-diyl)dibenzonitrile

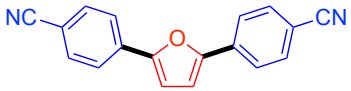

Compound **190b** was prepared following the general procedure for decarboxylative cross coupling on a 0.20 mmol scale. Compound was isolated with column chromatography (R_f = 0.34) Hexanes:DCM:EtOAC (4.5:5:0.5) as a yellow solid. **^{1}H NMR** (500 MHz, $CDCl_3$) δ ppm 7.82 (d, J = 8.8 Hz, 4H), 7.70 (d, J = 8.8 Hz, 4H), 6.95 (s, 2H). **^{13}C NMR** (125 MHz, $CDCl_3$) δ ppm 152.8 (2C), 133.8 (2C), 132.7 (4C), 124.1(4C), 118.7(2C), 111.0 (2C), 110.6 (2C). **HRMS (EI)**: Exact mass calculated for $C_{18}H_{10}N_2O$ [$M^{+\cdot}$]: 270.0788 found 270.0789 (0.5 ppm).

Compound 190c: 2,5-bis(4-nitrophenyl)furan

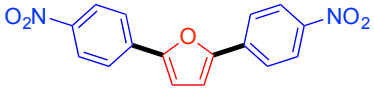

Compound **190c** was prepared following the general procedure for decarboxylative cross coupling on a 0.20 mmol scale. Compound was isolated with column chromatography (R_f = 0.11) Hexanes:Ethyl ether (8:2) as an orange solid. **^{1}H NMR** (500 MHz, $CDCl_3$) δ ppm 8.31 (d, J = 9.0 Hz, 4H), 7.91 (d, J = 9.0 Hz, 4H), 6.95 (s, 2H). **^{13}C NMR** (125 MHz, $CDCl_3$) δ ppm 153.0 (2C), 147.0 (2C), 135.5 (2C), 124.5(4C), 124.3(4C), 111.5 (2C). **HRMS (EI)**: Exact mass calculated for $C_{16}H_{10}N_2O_5$ [$M^{-\cdot}$]: 310.0595 found 310.0596 (0.1 ppm).

Compound 190d: diethyl-4,4'-(furan-2,5-diyl)dibenzoate

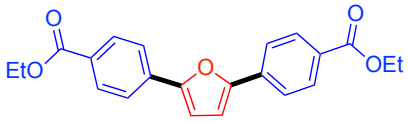

Compound **190d** was prepared following the general procedure for decarboxylative cross coupling on a 0.20 mmol scale. Compound was isolated with column chromatography (R_f = 0.56) Hexanes:DCM:EtOAC (4.5:5:0.5) as a pale yellow solid. **^{1}H NMR** (500 MHz, $CDCl_3$) δ ppm 8.09 (d, J = 8.8 Hz, 4H), 7.80 (d, J = 8.8 Hz, 4H), 6.90 (s, 2H), 4.40 (q, J = 7.1 Hz, 4H), 1.42 (t, 7.1 Hz, 6H). **^{13}C NMR** (125 MHz, $CDCl_3$) δ ppm 166.2 (2C), 153.3 (2C), 134.1 (2C), 130.1 (4C), 129.3

(2C), 123.5 (4C), 109.6 (2C), 61.0 (2C), 14.3 (2C). **HRMS (EI)**: Exact mass calculated for $C_{22}H_{20}O_5$ [$M^{+\cdot}$]: 364.1305 found 364.1303 (-0.7 ppm).

Compound 190e: 2,5-bis(3-(trifluromethyl)phenyl)furan

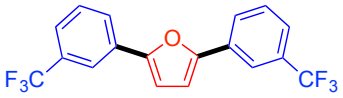

Compound **190e** was prepared following the general procedure for decarboxylative cross coupling on a 0.20 mmol scale. Compound was isolated with column chromatography (R_f = 0.35) Hexanes:EtOAC (9:1) as a white solid. **^{1}H NMR** (500 MHz, $CDCl_3$) δ ppm 7.96 (s, 2H), 7.92 (t, J = 4.3 Hz, 2H), 7.54 (d, J = 4.3, 4H), 6.85 (s, 2H). **^{13}C NMR** (125 MHz, $CDCl_3$) δ ppm 152.6 (2C), 131.3 (q, J = 32.6 Hz, 2C), 131.0 (2C), 129.3 (2C), 126.8 (2C), 124.0 (q, J = 271.9 Hz, 2C), 124.1 (q, J = 3.9 Hz, 2C), 120.5 (q, J = 3.8 Hz, 2C), 108.7 (2C). **HRMS (EI)**: Exact mass calculated for $C_{18}H_{10}F_6O$ [$M^{+\cdot}$]: 356.0630 found 356.0629 (-0.3 ppm).

Compound 190f: 2,5-bis(4-methoxyphenyl)furan

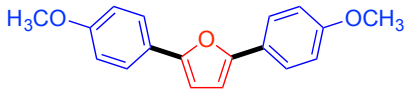

Compound **190f** was prepared following the general procedure for decarboxylative cross coupling on a 0.20 mmol scale. Compound was isolated with column chromatography (R_f = 0.51) Hexanes:DCM (1:1) as a white solid. **^{1}H NMR** (500 MHz, $CDCl_3$) δ ppm 7.66 (d, J = 9.0 Hz, 4H), 6.94 (d, J = 9.0 Hz, 4H), 6.58 (s, 4H), 6.85 (s, 2H), 3.85 (s, 6H). **^{13}C NMR** (125 MHz, $CDCl_3$) δ ppm 158.9 (2C), 152.8 (2C), 125.0 (4C), 124.1 (2C), 114.1 (4C), 105.6 (2C), 55.3 (2C). **(EI)**: Exact mass calculated for $C_{18}H_{16}O_3$ [$M^{+\cdot}$]: 280.1094 found 280.1094 (0.0 ppm).

Compound 190g: 2,5-bis(3-methoxyphenyl)furan

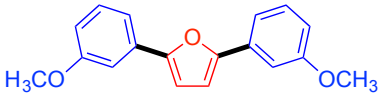

Compound **190g** was prepared following the general procedure for decarboxylative cross coupling on a 0.20 mmol scale. Compound was isolated with column chromatography (R_f = 0.45) DCM:Hexanes (7:3) as a pale yellow oil. **^{1}H NMR** (500 MHz, $CDCl_3$) δ ppm 7.37-7.31 (m, 6H), 6.85 (ddd, J = 7.3, 2.6, 1.8 Hz, 2H), 6.75 (s, 2H), 3.90 (s, 6H). **^{13}C NMR** (125 MHz, $CDCl_3$) δ ppm 159.9 (2C), 153.2 (2C), 132.0 (2C), 129.8 (2C), 116.4 (2C), 112.9 (2C), 109.3 (2C), 107.6 (2C), 55.3 (2C). **HRMS (EI)**: Exact mass calculated for $C_{18}H_{16}O_3$ [$M^{+\cdot}$]: 280.1094 found 280.1094 (0.0 ppm).

Compound 190h: 2,5-di-*p*-tolylfuran

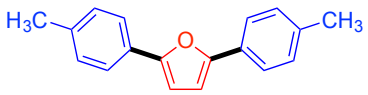

Compound **190h** was prepared following the general procedure for decarboxylative cross coupling on a 0.20 mmol scale. Compound was isolated with column chromatography (R_f = 0.18) DCM:Hexanes (1:19) as a yellow oil. **^{1}H NMR** (500 MHz, $CDCl_3$) δ ppm 7.63 (d, J = 8.0 Hz, 4H), 7.21 (d, J = 8.0 Hz, 4H), 6.66 (s, 2H), 2.38 (s, 6H). **^{13}C NMR** (125 MHz, $CDCl_3$) δ ppm 153.2 (2C), 137.0 (2C), 129.3 (4C), 128.2 (2C), 123.6 (4C), 106.4 (2C), 21.3 (2C). **HRMS (EI)**: Exact mass calculated for $C_{18}H_{16}O$ [$M^{+\cdot}$]: 248.1196 found 248.1195 (-0.4 ppm).

Compound 190i: 2,5-di-*o*-tolylfuran

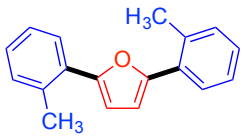

Compound **190i** was prepared following the general procedure for decarboxylative cross coupling on a 0.20 mmol scale. Compound was isolated with column chromatography (R_f = 0.70) DCM:Hexanes:EtOAc (5:4.5:0.5) as a yellow oil.

^{1}H NMR (500 MHz, $CDCl_3$) δ ppm 7.82 (dd, J = 7.7, 1.4 Hz, 2H), 7.31-7.27 (m, 4H), 7.25-7.22 (m, 2H), 6.69 (s, 2H), 2.60 (s, 6H). **^{13}C NMR** (125 MHz, $CDCl_3$) δ ppm 152.7 (2C), 134.4 (2C), 131.2 (2C), 130.1 (2C), 127.4 (2C), 126.9 (2C), 126.1 (2C), 110.5 (2C), 22.5 (2C). **HRMS (EI)**: Exact mass calculated for $C_{18}H_{16}O$ [$M^{+\cdot}$]: 248.1196 found 248.1195 (-0.4 ppm).

Compound 190j: 2,5-diphenylfuran

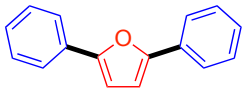

Compound **190j** was prepared following the general procedure for decarboxylative cross coupling on a 0.20 mmol scale. Compound was isolated with column chromatography (R_f = 0.45) DCM:Hexanes (3:7) as a white solid. **^{1}H NMR** (500 MHz, d^6-DMSO) δ ppm 7.80 (d, J = 7.4 Hz, 4H), 7.44 (t, J = 7.4 Hz, 4H), 7.30 (t, J = 7.4 Hz, 2H), 7.07(s, 2H). **^{13}C NMR** (125 MHz, d^6-DMSO) δ ppm 153.0 (2C), 130.5 (2C), 129.4 (4C), 128.0 (2C), 123.9 (4C), 108.6 (2C). **HRMS (EI)**: Exact mass calculated for $C_{16}H_{12}O$ [$M^{+\cdot}$]: 220.0883 found 220.0882 (-0.2 ppm).

2.7. Additional Experiments

2.7.1. Utilization of Silver salts as co-catalysts in the reaction.

With the hypothesis that Silver Carbonate was being employed both as base and co-catalyst in the reaction, we decided to test several silver salts as potential co-catalysts in the reaction (Table 7). The different anions would help in the solubility of the salts in the organic solvent.

As observed in Table 7, the addition of different Silver Salts did not have any positive impact on the yield of the reaction. Even though several reports of the group of Becht and Gooßen propose that silver and copper are responsible for creating an activated nucleophilic coupling partner that is suitable for transmetallation. Becht never disclosed the use of other Silver salts in this type of cross-couplings, which implies that its role is still undetermined. For the subsequent reactions, Silver carbonate was employed as the base, and its recycling was studied to compensate for its stoichiometric use.

Table 7. Screen of different Silver salts as co-catalysts in the decarboxylative cross-coupling.

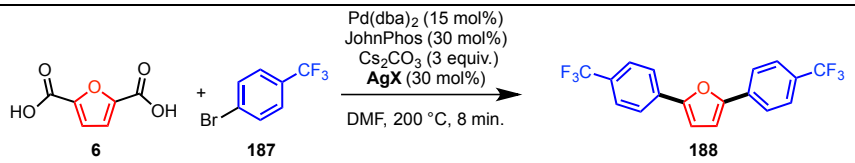

6 187 188

Entry	Silver Salt (30 mol%)	Yield (%)[a]
1	$AgBF_4$	0
2	$AgSbF_6$	0
3	AgCl	0
4	$AgNO_3$	0
5	AgOTf	0
6	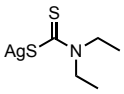	0
7	Ag_2CO_3	45

[a] *Determined by HNMR using TMB as internal standard.*

2.7.2. Utilizing two different Aryl halides in the same reaction

In order to synthesize non-symmetric products to introduce two different aryl moieties on a single furan ring, we decided to add in a competition experiment employing two different aryl halides (2 equivalents of each) into a single reaction. Different electronic and steric situations were evaluated as seen on Table 8.

Table 8. Experiments regarding the use of two different aryl halides simultaneously to achieve non-symmetric furan arylations.

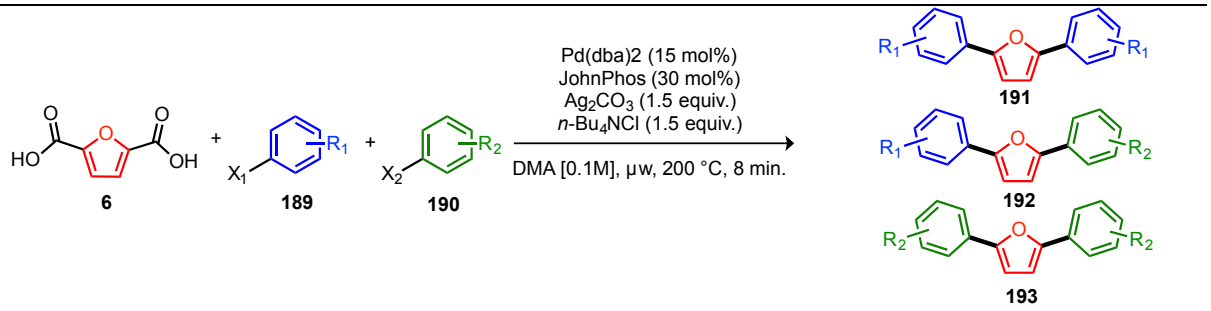

Entry	X_1	R_1	X_2	R_2	Ratio[a] 191:192:193	% Yield[b]
1	Br	4-CF_3	Br	4-CN	40:7:53	28
2	Br	4-CF_3	Br	4-OMe	70:27:3	23
3	Br	4-Me	Br	4-OMe	Mainly 193	17
4	Br	4-CF_3	I	4-CN	1:94:5	21

[a]Estimated using GCMS (FID chromatogram). [b] Determined by HNMR using TMB as internal standard

When employing aryl bromides with opposite electronic situations (Table 8, entries 2 and 3), no selectivity was observed towards the non-symmetric product, and rather the major product was observed to be either of the symmetric side products. Entry 1 was performed as a control competition experiment between two coupling partners with similar electronic situations, and no selectivity was observed towards either of the corresponding products. An interesting result was obtained when using an aryl iodide and aryl bromide that provided high selectivity for the non-symmetric product (entry 4). Even though this is a promising result, the yields obtained in all cases were very poor, and further ^{1}H NMR analysis showed a complicated reaction mixture between the arylated furan products and the homo-coupling or cross-coupling side-products of the aryl halide species, which made it impossible their isolation. Subsequently, we decided to employ HMF as an alternative biomass-derived starting material for the synthesis of 2,5-diaryl non-symmetric furans. This research is discussed in Chapter 3.

Chapter 3. A new route for the synthesis of 2,5-diaryl non-symmetric furans utilizing biomass-derived HMF as starting material

3.1. Solvent-free Mechanochemical Oxidation and Reduction of Biomass Derived 5-Hydroxymethyl Furfural

3.1.1. Abstract

The simultaneous synthesis of 5-hydroxymethyl-2-furoic acid and bis-2,5-hydroxymethylfuran from biomass derived 5-hydroxymethyl furan was developed using a solvent-free mechanochemical approach. The results obtained for the Cannizzaro disproportionation reaction show quantitative conversions of the starting materials with reaction times of only 5 min. Employing solvent-free conditions allows for a more sustainable synthetic approach that is reflected in an Efactor 7 times smaller than the previous reports. Additionally, initial results of the use of a sacrificial reagent, with the same solvent-free mechanochemical approach, for the selective reduction and oxidation of HMF are presented.

3.1.2. Introduction

In the last decades, an uncontrolled overexploitation of fossil resources has led to increasing levels of emissions contributing to global warming, produced during the extraction and the utilization of petrochemistry-based raw materials.[24] As such, new chemical resources, coupled with greener methodologies, have become an attractive new target for academic research for potential industrial application.[157] In addition, the need to find new sustainable resources for energy has been accompanied with a search for new sources of small molecules for the synthetic organic industry.[183] In this context, much attention has been paid to biomass as a potential source for a wide variety of small molecules.[47,184–186] Every year, 170 billion tons of biomass are produced by photosynthesis. Seventy five percent of this material can be classified as carbohydrates, but only less than 4% is used as food and non-food consumables, which leads to a vast accumulation of an untapped raw material.[19,187]

The dehydration of common hexoses has been reported to efficiently produce 5-hydroxymethyl furfural (HMF) as one of the major products. HMF is a versatile small molecule that can serve as a substrate for the production of a multitude of furan derivatives (Figure 45).[188,189] These biomass-derived platform chemicals have potential application in multiple fields of synthetic chemistry.[190]

Previous reports have demonstrated the oxidation of HMF 3 into 2,5-furandicarboxylic acid (FDCA) using various supported transition metal heterogeneous catalysts including PtBi/C[159], Pd/PVP[40], Au/HT[191], Ru/C[42], among others[192–195]; but the partial oxidation into 5-hydroxymethyl furoic acid (HMFA **4**) or even 2,5-diformyl furan (DFF) has been scarcely reported due to the challenge in preventing complete oxidation (FDCA). Domínguez de María[44] and Li[45] reported enzyme-mediated methodologies in which HMFA and DFF were obtained employing lipases and alcohol oxidases with good yields, but long reaction times.

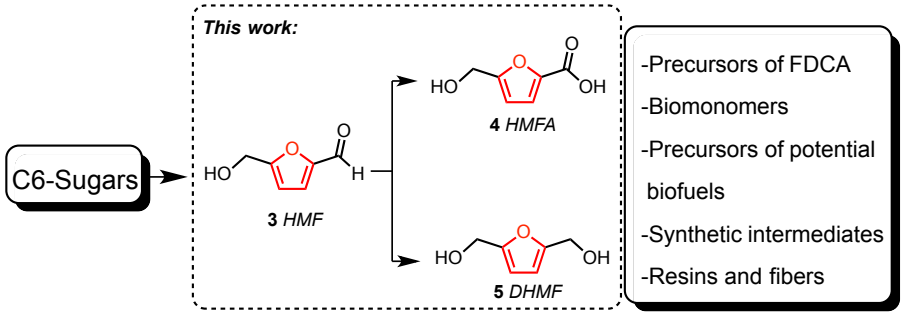

Figure 45. Biomass derived furans with potential use as eco-friendly starting materials.

The conversion of HMF **3** into HMFA **4** and 2,5-dihydroxymethyl furan (DHMF **5**) is an important transformation that has been scarcely reported (Figure 45) when compared to the synthesis of the higher oxidation state derivatives like FDCA[34,42,158,196]. Nonetheless, these molecules have been highlighted as important potential bio-monomers for the synthesis of polymers, such as polyurethane foams[197,198] and polyesters[68].

In 2013, Afonso and co-workers reported the use of a Cannizzaro disproportionation reaction to synthesize both HMFA and DHMF simultaneously from HMF, under basic conditions.[199] The Cannizzaro reaction was originally reported in the 1850's as a facile mode to synthesize benzoic acids.[200–202] One of the most prescient limitations of this reaction is that it

allows for a maximum transformation of only 50% of the starting material into a specific target (either the reduced or oxidized product), which limits the efficiency of the overall reaction. For the modification of HMF, however, employing the Cannizzaro disproportionation takes advantage of this reactivity, since the simultaneous production of both HMFA and DHMF is beneficial due to their potential applications as biomass-derived platform chemicals.[33,202,203] Our goal is to develop conditions that allow for the synthesis of these biomass-based materials with an even smaller impact on the environment through a solvent-free methodology.

Solvents represent an estimated 80 to 90 % by mass of the waste produced in a typical pharmaceutical batch chemical operation.[204] A valuable strategy to circumvent this issue is the use of mechanochemistry, which refers to solvent-free chemical transformations induced by mechanical energy, such as compression, shear, or friction.[205] The environmental benefits in the use of these greener reactions are extended to the work-up (Figure 46) and purification processes, often overlooked sources of chemical waste.[206]

3.1.3. Results and Discussion

With the aim on developing new efficient and innovative methodologies for the production of the potential biomass-derived platform chemicals HMFA and DHMF, Cannizzaro solvent-free conditions were explored. The reaction was performed mechanically assisted with manual grinding, automatic grinding, lysis milling and planetary ball milling.[207]

Initial results derived from the conditions of previous work have satisfactory reproducibility when water was employed as the solvent for the Canizzaro reaction of HMF (Table 9, entry 1), but when the reaction was left for 36 hours at room temperature, decomposition appears to have occurred, as no product was observed by GC-MS and ^{1}HNMR analysis. Even though the reaction proceeds in an acceptable yield, it was valuable to improve towards greener conditions and hence the use of a solvent-free mechanochemical approach was evaluated. Employing a slight excess of NaOH under manual grinding for 5 minutes gave a 64% disproportionation of the starting material that was essentially equivalent in yield to the solution reaction while using no solvent and reducing the reaction time from 24 hours to 5 minutes (entry 3).

Table 9. Optimization for the solvent-free mechanochemical Cannizzaro disproportionation of HMF.

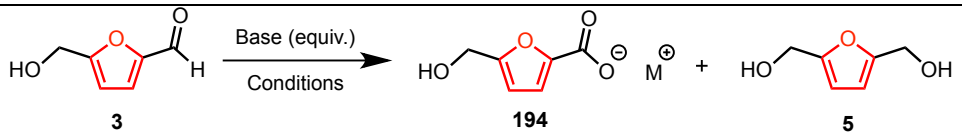

3 194 5

Entry	Base (equiv.)	Conditions	Time	%HMFA	%DHMF
1	NaOH (1.1)	24 °C [0.2 M] in H_2O	24 h	67	67
2	NaOH (1.1)	24 °C [0.2 M] in H_2O	36 h	<5	23
3	NaOH (1.1)	Manual Grind [a]	5 min	64	64
4	KOH (1.1)	Lysis mill [b]	5 min	12	12
5	KOH (1.1)	Auto. Grind [c]	5 min	76	76
6	KOH (2.0)	Manual Grind [a]	5 min	88	88
7	KOH (1.1)	Ball Milling [d]	5 min	66	66
8	KOH (2.0)	Ball Milling [d]	5 min	>99	>99
9	KOH (3.0)	Manual Grind [a]	5 min	87	87

[a]Reaction done under manual grinding with a mortar and pestle. [b]FastPrep24, MP Biodemicals, used with ceramic beads at maximum speed. [c]Automatic mortar and pestle. [d]Planetary Ball Mill at 60 Hz.

New mechanochemical techniques have been developed over the years to automatize solvent-free approaches to physical and chemical transformations. Lysis mill machines have been employed as a mechanochemical tool in synthetic chemistry,[208] and we investigated the use of ceramic beads to perform the disproportionation reaction under solvent-free conditions (entry 4), but only a 12% yield was obtained. When the same reactions conditions were attempted with an automatic grinding apparatus, the yield increased to 76% (entry 5). An increase to 2 equivalents of base achieved an 88% yield, but no further increase was observed with 3 equivalents of the base (entries 5 and 6). Recent publications highlight the efficiency of employing ball milling systems in organic systems, especially in those with solvent-free chemistry.[209,210] When assessing the efficiency of the reaction using a ball milling system, a quantitative conversion was achieved with two equivalents of the base (entry 8) in five minutes without the use of solvents. Identical results were obtained with different alkaline hydroxides.

Table 10. Scale-up for the disproportionation reaction using the planetary Ball Mill apparatus.

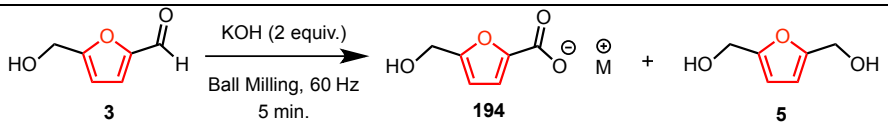

Entry	HMF Scale	%HMFA	%DHMF
1	0.200 g	>99	>99
2	0.400 g	>99	>99
3	0.800 g	>99	>99
4	3.200 g	96	96
5	12.80 g	92	92
6[a]	12.80 g	>99	>99

[a]Reaction time was 7 min instead of 5 min.

Given the potential quantities of DHMF and HMFA that will be needed for industrial applications, we decided to explore the efficiency of our optimized solvent-free methodology in larger reaction scales. Scaling up of the solvent free conditions from 200 mg up to 12.80 g provided the products in excellent yields in all cases (Table 10). When the 12.8 reaction spun for 7 min instead of 5 min, a quantitative yield was obtained (Table 10). These series of experiments suggest the continued efficiency of using a solvent-free approach for the synthesis of these small molecules at an industrial scale, with new machineries that can take tons of material for grinding purposes, highlighting the potential for sizable reductions in industrial chemical waste production.

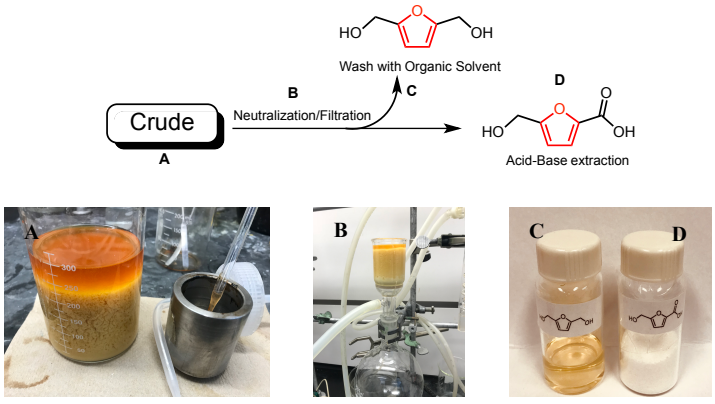

Figure 46. Schematic representation and photographs regarding the large-scale work-up and isolation of the compounds.

It is remarkable to say that the optimized reaction is both efficient in time and in its green chemistry indicators[211], with an E_{factor} of 0.55. Previous reports[199] describe a methodology with an E_{factor} of approximately 3.6, considering a 90% of re-use of the solvent, and 34 when no-solvent is recycled. This new solvent-free approach pushes the limits of this chemical transformation in both simplicity and green efficiency.

Initially this method was developed towards biomass-derived 5-hydroxymethylfurfural, however efforts were undertaken to evaluate the optimized conditions with other substrates for Cannizzaro disproportionation reactions (Table 11).

Table 11. Scope of different aldehydes with the optimized disproportionation reaction conditions.

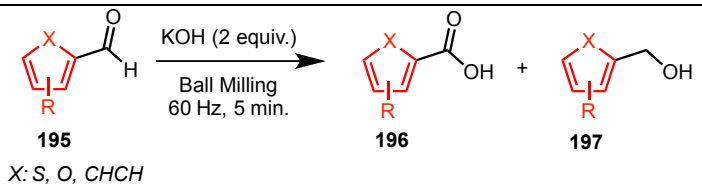

Entry	*Substrate*	*% Acid*	*% Alcohol*
1	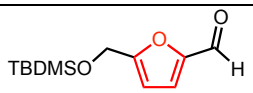	>99	>99
2	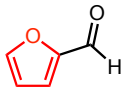	>99	>99
3	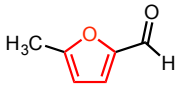	>99	>99
4	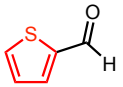	98	98
5	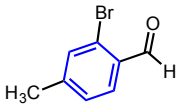	>99	>99
6	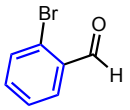	90	91
7	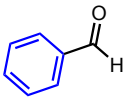	98	98
8	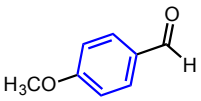	95	94
9	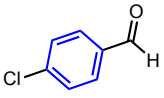	95	95

10	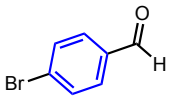	92	92

Disproportionation was found to occur in excellent yields for several aromatic aldehydes (Table 11). Nonetheless, as the reaction is carried out in a highly basic media, the scope is limited to substrates that do not bear any basic-sensitive functionalities. A variety of other biomass derived furanecarboxaldehydes and their derivatives (entries 1-3) gave quantitative yields for this disproportionation. We also evaluated the possibility of employing benzaldehydes as substrates with the optimized conditions, and found that these also exhibited excellent results, with quantitative yields for arenes bearing different functionalities. This reaction represents a great advantage when compared to the classical Canizzaro approach in both time and reagents. For in-solution Canizzaro disproportionation, reported reaction times vary from a few hours to days, but with the solvent-free mechanochemical conditions reported herein are employed, this time is reduced to only 5 minutes or less.

Cannizzaro disproportionation leads to a theoretical maximum of only 50% of the starting material transformed into a primary alcohol and 50% to a carboxylic acid, which limits the quantity of desired material produced. To mitigate this outcome, some groups have studied the use of sacrificial agents in a cross-Cannizzaro reaction[212,213]. For this, a stoichiometric amount of a sacrificial molecule is employed within the reaction that can be fully reduced or oxidized, with the objective of transforming the starting material to the corresponding fully oxidized or reduced moiety, respectively.

Towards this end, we evaluated several sacrificial agents in order to control the production of one of the two possible Cannizzaro products for this reaction.

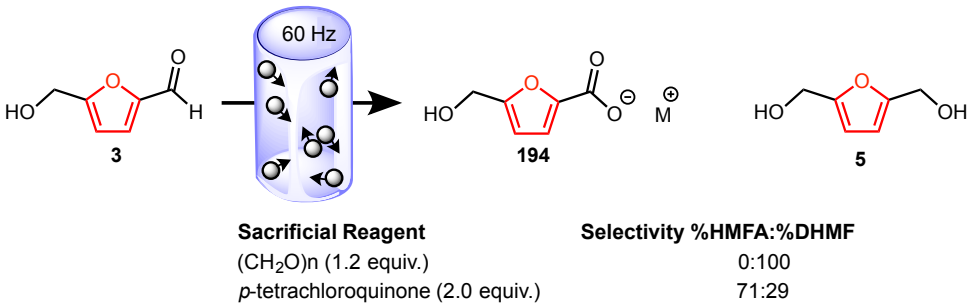

Figure 47. Preliminary results of the selective solvent-free mechanochemical cross-Cannizzaro reaction of HMF employing a sacrificial reagent.

Several sacrificial reagents were employed for the cross-Cannizzaro reaction of HMF, including several readily available aldehydes (Table 12). Benzaldehyde, acetaldehyde and D-glucose did not enhance selectivity for the desired products. Anisaldehyde gave a small selectivity (1.2:1) favouring the synthesis of DHMF, but when paraformaldehyde was employed in a slight excess, the reaction was specific towards the synthesis of DHMF, affording a 90% yield. The oxidation of HMF to HMFA definitely represents a bigger challenge synthetically, since the presence of the primary alcohol creates a wider range of possible oxidation products. Based on the reported mechanism for the cross-Cannizzaro reaction, it is necessary to have first a nucleophilic addition of the hydroxide anion into the aldehyde moiety of HMF, to produce a tetrahedral intermediate that collapses through a hydride transfer to the sacrificial agent, producing a carboxylic acid group. For this reason, we decided to employ *p*-quinones as our sacrificial reagents as these are known to be readily available, excellent hydride acceptors.[214] After evaluating several *p*-quinones, a 7:3 selectivity towards the oxidation of the HMF was obtained, albeit in relatively low yields (Table 12). These preliminary results indicate the solvent-free complete conversion of HMF selectively to HMFA is possible and further studies toward this aim are currently underway.

3.1.4. Conclusions

A new solvent-free, facile protocol was developed for the simultaneous synthesis of 5-hydroxymethylfuroic acid and 2,5-dihydroxymethylfuran through the Cannizzaro disproportionation under mechanochemical assistance with a planetary ball milling apparatus of biomass derived 5-hydroxymethyl furfural, with an E_{factor} of 0.55, (7 times smaller than the previous reports), and a reaction time of 5 min. The optimized conditions proved adaptable to

several aromatic aldehydes, including other biomass derivatives of HMF, affording excellent yields. Also, initial results towards the selective oxidation or reduction of HMF *via* a cross-Cannizzaro reaction under solvent-free conditions are presented, with promising preliminary results that will be expanded in future work.

It is of tremendous importance to develop reactions that allow for the efficient transformation of biomass-derived materials to useful synthetic intermediates. This work highlights the importance of not only the employment of renewable sources, but also synthetic targets that use greener reaction conditions that minimize waste and use of solvents, especially when these reactions are expected to occur at industrial scales in the future.

3.1.5. Experimental Section

General procedure for the disproportionation reaction: To the reaction vessel was added aldehyde (0.8 mmol, 1 equiv.) and finely ground and oven dried KOH (1.6 mmol, 2 equiv.), 7 stainless steel balls (8mm diameter) and then the vessel was closed with a rubber seal equipped lid (stainless steel). The apparatus was set to run for 5 min at a 60 Hz frequency. The reaction mixture is dissolved in water and extracted with EtOAc three times. Organic extracts are combined and dried over Na_2SO_4. After filtration the solvent is evaporated under vacuum to obtain the corresponding primary alcohol. The aqueous portion of the extraction is acidified to pH 2 with concentrated HCl to precipitate the desired carboxylic acid, which is collected through vacuum filtration.

For HMF: Once the reaction is complete (general procedure) the crude was diluted with EtOH and transferred into a beaker, and then pH was brought to 7 with concentrated HCl. The suspension was then filtered through a short Celite pad. Once the solvent is evaporated under vacuum, the solid/oil mixture is washed three times with EtOAc. After evaporating the solvent of the combined EtOAc washes, a pale-yellow oil is obtained (DHMF). For the solid that did not solubilized with the EtOAc washes, a recrystallization in EtOH:EtOAc (2:98) was performed. Additionally, this salt can be converted to the free acid after and acid-base extraction. For a detailed description of the procedure please refer to the supplementary information document.

3.1.6. Characterization Data

Compound 4 : 5-hydroxymethylfuran-2-oic acid

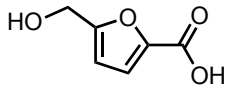

Compound **4** was prepared following the optimized conditions for the Cannizzaro disproportionation of HMF on solvent-free planetary ball milling. It is highly important to use oven dried grinded KOH as humidity could affect the outcome of the reaction greatly. Compound **4** was isolated as described in the experimental section, and converted to the carboxylic with HCl/acid-base extraction treatment, to yield a white solid. This compound has proven to be sensitive to long-term exposure to air and light. So, it was properly stored in an amber vial at 4 °C under inert atmosphere. **^{1}H NMR** (500 MHz, DMSO-d^{6}) δ ppm 12.94 (bs, 1H), 7.15 (d, J = 3.4 Hz, 1H), 6.46 (d, J = 3.4 Hz, 1H), 5.45 (bs, 1H), 4.44 (s, 2H). **^{13}C NMR** (125 MHz, DMSO-d^{6}) δ ppm 160.1 (1C), 159.8 (1C), 144.4 (1C), 119.0 (1C), 109.4 (1C), 56.2 (1C). **HRMS (EI)**: Exact mass calculated for $C_5H_3O_3^-$ $[M-1]^{-\cdot}$: 141.1021 found 141.0196 (-1.6 ppm).

Compound 5 : 2,5-bishydroxymethyl furan

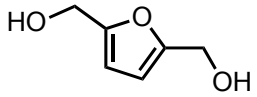

^{1}H NMR (500 MHz, $CDCl_3$) δ ppm 6.19 (s, 2H), 5.18 (bs, 2H), 4.36 (s, 4H). **^{13}C NMR** (125 MHz, $CDCl_3$) δ ppm 155.0 (2C), 107.9 (2C), 56.2 (2C). **HRMS (EI)**: Exact mass calculated for $C_6H_7O_3^-$ $[M-1]^{-\cdot}$: 127.1191 found 127.1186 (3.5 ppm).

Compound 196a : 5-(((*tert*-butyldimethylsilyl)oxy)methyl)furan-2-carboxylic acid

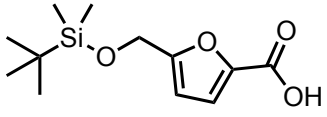

^{1}H NMR (500 MHz, $CDCl_3$) δ ppm 8.88 (bs, 1H), 7.26 (d, J = 3.5 Hz, 1H), 6.40 (d, J = 3.5 Hz, 1H), 4.72 (s, 2H), 0.91 (s, 9H), 0.10 (s, 6H). **^{13}C NMR** (125 MHz, $CDCl_3$) δ ppm 163.4 (1C), 160.3 (1C), 121.0 (1C), 109.1 (2C), 58.6 (1C), 25.8 (3C), 18.3 (1C), -5.4 (2C). **HRMS (EI)**: Exact mass calculated for $C_{12}H_{19}O_4Si^-$ $[M-1]^{-\cdot}$: 255.1059 found 255.1059 (2.4 ppm).

Compound 197a : (5-(((*tert*-butyldimethylsilyl)oxy)methyl)furan-2-yl)methanol

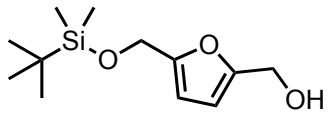

^{1}H NMR (500 MHz, $CDCl_3$) δ ppm 6.20 (d, J = 3.1 Hz, 1H), 6.16 (d, J = 3.1 Hz, 1H), 4.60 (s, 2H), 4.54 (s, 2H), 2.62(bs, 1H), 0.89 (s, 9H), 0.07 (s, 6H). **^{13}C NMR** (125 MHz, $CDCl_3$) δ ppm 154.2 (1C), 153.6 (1C), 108.4 (1C), 108.0 (1C), 58.2 (1C), 57.4 (1C), 25.9 (3C), 18.4 (1C), -5.3 (2C). **HRMS (EI)**: Exact mass calculated for $C_{12}H_{21}O_3Si^-$ $[M-1]^{-\cdot}$: 241.1260 found 241.1267 (2.4 ppm).

Compound 196b: furan-2-carboxylic acid

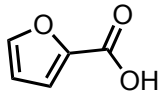

^{1}H NMR (500 MHz, DMSO-d^6) δ ppm 13.06 (bs, 1H), 7.92 (dd, *J* = 1.7, 0.8 Hz, 1H), 7.22 (dd, *J* = 3.5, 0.8 Hz, 1H), 6.66 (dd, *J* = 3.5, 1.7 Hz, 1H). **^{13}C NMR** (125 MHz, DMSO-d^6) δ ppm 159.7 (1C), 147.5 (1C), 145.3 (1C), 118.1 (1C), 112.5 (1C). **HRMS (EI)**: Exact mass calculated for $C_5H_3O_3^-$ $[M-1]^{-\cdot}$: 111.0082found 111.0085 (2.6 ppm).

Compound 197b: furan-2-ylmethanol

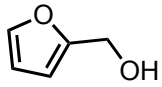

^{1}H NMR (500 MHz, DMSO-d^6) δ ppm 7.57 (dd, *J* = 1.8, 0.8 Hz, 1H), 6.38 (dd, *J* = 3.1, 1.9 Hz, 1H), 6.27 (dd, *J* =3.1, 0.8, 1H), 5.16 (bs, 1H), 4.37 (s, 2H). **HRMS (EI)**: Exact mass calculated for $C_5H_5O_2^-$ $[M-1]^{-\cdot}$: 97.0931 found 97.0927 (3.7 ppm). Spectral data in agreement with reported

data from R. Ambre, C. Y. Yu, S. B. Mane, C. F. Yao and C. H. Hung, *Tetrahedron*, 2011, **67**, 4680–4688.

Compound 196c: 5-methylfuran-2-carboxylic acid

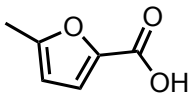

^{1}H NMR (500 MHz, DMSO-d^6) δ ppm 12.77 (bs, 1H), 7.10 (dd, J = 3.3, 0.5 Hz, 1H), 6.28 (dd, J = 3.3, 0.9 Hz, 1H), 2.33 (dd, J = 0.9, 0.5 Hz, 3H). **HRMS (EI)**: Exact mass calculated for $C_6H_6O_3^-$ [M-1]$^{-\cdot}$: 125.0239 found 125.0245 (4.7 ppm). Spectral data in agreement with reported data from E. Grovenstein and P. C. Lu, *J. Org. Chem*., 1982, **47**, 2928–2939.

Compound 197c: (5-methylfuran-2-yl)methanol

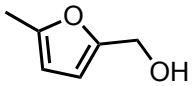

^{1}H NMR (500 MHz, $CDCl_3$) δ ppm 6.16 (d, J = 3.1 Hz, 1H), 5.91 (d, J = 3.1 Hz, 1H), 4.54 (s, 2H), 2.29 (s, 3H). **HRMS (EI)**: Exact mass calculated for $C_6H_7O_2^-$ [M-1]$^{-\cdot}$: 111.1201 found 111.1205 (3.9 ppm). Spectral data in agreement with reported data from B. Martín-Matute, C. Nevado, D. J. Cárdenas and A. M. Echavarren, *J. Am. Chem. Soc*., 2003, **125**, 5757–5766.

Compound 196d: Thiophene-2-carboxylic acid

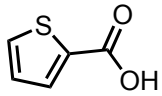

^{1}H NMR (500 MHz, DMSO-d^6) δ ppm 13.02 (bs, 1H), 7.85 (dd, *J* = 5.0, 1.3 Hz, 1H), 7.71 (dd, *J* = 3.7, 1.3 Hz, 1H), 7.16 (dd, *J* = 5.0, 3.7 Hz, 1H). **^{13}C NMR** (125 MHz, DMSO-d^6) δ ppm 163.3 (1C), 135.1 (1C), 133.7 (1C), 133.6 (1C), 128.6 (1C). **HRMS (EI)**: Exact mass calculated for $C_5H_3O_2S^-$ [M-1]$^{-\cdot}$: 126.9853 found 128.9847 (4.4 ppm).

Compound 197d: Thiophene-2-ylmethanol

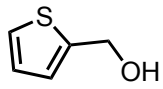

^{1}H NMR (500 MHz, $CDCl_3$) δ ppm 7.28 (dd, *J* = 5.0, 1.3 Hz, 1H), 7.02 (ddt, *J* = 3.5, 1.3, 0.8 Hz, 1H), 6.98 (dd, *J* = 5.0, 3.5 Hz, 1H), 4.83 (s, 2H), 1.85 (bs, 1H). **^{13}C NMR** (125 MHz, $CDCl_3$) δ ppm 143.9 (1C), 126.8 (1C), 125.6 (1C), 125.5 (1C), 60.0 (1C). **HRMS (EI)**: Exact mass calculated for $C_5H_5OS^-$ $[M-1]^{\cdot-}$: 113.0060 found 113.0063 (3.0 ppm).

Compound 196e: 2-bromo-4-methylbenzoic acid

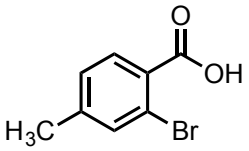

^{1}H NMR (500 MHz, DMSO-d^6) δ ppm 13.18 (bs, 1H), 7.67 (d, *J* = 7.8 Hz, 1H), 7.54 (dd, *J* = 1.7, 0.8 Hz, 1H), 7.25 (ddd, *J* = 7.8, 1.7, 0.8 Hz, 1H), 2.32 (s, 3H). **HRMS (EI):** Exact mass calculated for C8H6O2Br- $[M-1]^{\cdot-}$: 212.9550 found 212.9544 (-2.6ppm). Spectral data in agreement with reported data from T. S. Mei, R. Giri, N. Maugel and J. Q. Yu, *Angew. Chemie - Int. Ed*., 2008, **47**, 5215–5219.

Compound 197e: 2-bromo-4-methylbenzoic acid

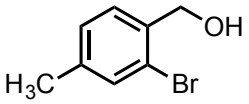

^{1}H NMR (500 MHz,$CDCl_3$) δ ppm 7.33 (m, 2H), 7.10 (d, J = 7.8Hz, 1), 4.68 (s, 2H), 2.31 (s, 3H), 2.24 (bs, 1H). **HRMS (EI)**: Exact mass calculated for $C_8H_8OBr^-$ $[M-1]^{\cdot-}$: 198.9758 found 198.9764 (3.2 ppm). Spectral data in agreement with reported data from Spectral data in agreement with reported data from G. Giorgi, S. Maiti, P. López-Alvarado and J. C. Menéndez, *Org. Biomol. Chem*., 2011, **9**, 2722–2730.

Compound 196f: 2-bromobenzoic acid

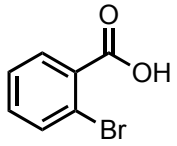

^{1}H NMR (500 MHz, DMSO-d^{6}) δ ppm 13.37 (bs, 1H), 7.70 (ddd, *J* = 12.9, 7.6, 1.7 Hz, 2H), 7.42 (ddd, *J* = 12.9, 7.6, 1.7 Hz, 2H). **^{13}C NMR** (125 MHz, DMSO-d^{6}) δ ppm 167.8 (1C), 134.3 (1C), 134.2 (1C), 132.9 (1C), 131.0 (1C), 128.1 (1C), 120.4 (1C). **HRMS (EI)**: Exact mass calculated for $C_7H_4O_2Br^-$ [M-1]$^{-\cdot}$: 198.9394 found 198.9389 (-2.3 ppm).

Compound 197f: 2-bromobenzyl alcohol

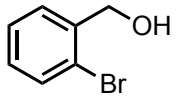

^{1}H NMR (500 MHz, DMSO-d^{6}) δ ppm 7.55 (dd, *J* = 7.6, 1.3 Hz, 2H), 7.40 (td, *J* = 7.6, 1.3 Hz, 1H), 7.20 (td, *J* = 7.5, 1.3 Hz, 1H), 5.41 (bs, 1H), 4.51, (s, 2H). **^{13}C NMR** (125 MHz, DMSO-d^{6}) δ ppm 141.4 (1C), 132.4 (1C), 129.0 (1C), 128.6 (1C), 128.0 (1C), 121.5 (1C), 63.0 (1C). **HRMS (EI)**: Exact mass calculated for $C_7H_6OBr^-$ [M-1]$^{-\cdot}$: 184.9601 found 184.9594 (-3.6 ppm).

Compound 196g: Benzoic acid

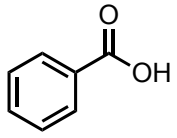

^{1}H NMR (500 MHz, DMSO-d^{6}) δ ppm 12.92 (bs, 1H), 7.92 (m, 2H), 7.60 (m, 1H), 7.48 (m, 2H). **^{13}C NMR** (125 MHz, DMSO-d^{6}) δ ppm 167.7 (1C), 133.3 (1C), 131.2 (1C), 129.7 (2C), 129.0 (2C). **HRMS (EI)**: Exact mass calculated for $C_7H_5O_2^-$ [M-1]$^{-\cdot}$: 121.0290 found 121.0293 (2.9 ppm).

Compound 197g: Benzyl alcohol

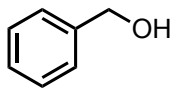

^{1}H NMR (500 MHz, DMSO-d^{6}) δ ppm 7.30 (d, *J* = 4.4 Hz, 4H), 7.21 (m, 1H), 5.14 (m, 1H), 4.49 (d, J = 5.7 Hz, 1H). **^{13}C NMR** (125 MHz, DMSO-d^{6}) δ ppm 143.0 (1C), 128.5 (2C), 127.0 (1C), 126.8 (2C), 63.3 (1C). **HRMS (EI)**: Exact mass calculated for Tropylium $C_7H_7^+$ $[M\text{-}OH]^{+\cdot}$: 91.0542 found 91.0541 (1.4 ppm).

Compound 196h: 4-methoxy benzoic acid

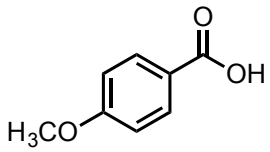

^{1}H NMR (500 MHz, DMSO-d^{6}) δ ppm 12.57 (bs, 1H), 7.87 (d, J = 8.9Hz, 2H), 7.00 (d, J = 8.9Hz, 2H), 3.80 (s, 3H). **^{13}C NMR** (125 MHz, DMSO-d^{6}) δ ppm 167.4 (1C), 163.3 (1C), 131.8 (2C), 123.4 (1C), 114.2 (2C), 55.9 (1C). **HRMS (EI)**: Exact mass calculated for $C_8H_7O_3^-$ $[M\text{-}H]^{-\cdot}$: 151.0395 found 151.0401 (3.9 ppm).

Compound 197h: 4-methoxy benzoic acid

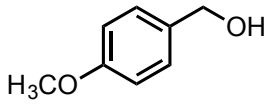

^{1}H NMR (500 MHz, DMSO-d^{6}) δ ppm 7.20 (d, J = 8.5Hz, 2H), 6.86 (d, J = 8.5 Hz, 2H), 5.01 (t, J = 5.7Hz, 1H), 4.40 (d, J = 5.7Hz, 2H), 3.71 (s, 3H). **^{13}C NMR** (125 MHz, DMSO-d^{6}) δ ppm 158.6 (1C), 134.9 (1C), 128.3 (2C), 113.9 (2C), 63.0 (1C), 55.5 (1C). **HRMS (EI)**: Exact mass calculated for $C_8H_9O_2^-$ $[M\text{-}H]^{-\cdot}$: 137.0602 found 137.0606 (3.2 ppm).

Compound 196i: 4-chlorobenzoic acid

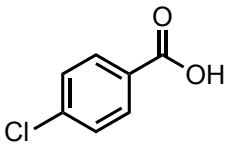

^{1}H NMR (500 MHz, DMSO-d^{6}) δ ppm 13.5 (bs, 1H), 7.93 (d, J = 8.7Hz, 2H), 7.52 (d, J = 8.7Hz, 2H). **^{13}C NMR** (125 MHz, DMSO-d^{6}) δ ppm 166.9 (1C), 138.2 (1C), 131.5 (2C), 130.1 (1C),

129.1 (2C). **HRMS (EI)**: Exact mass calculated for $C_7H_4O_2Cl^-$ $[M-H]^{-\cdot}$: 154.9899 found 154.9903 (2.8 ppm).

Compound 197i: 4-chlorobenzyl alcohol

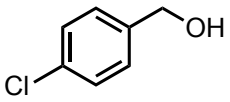

^{1}H NMR (500 MHz, $CDCl_3$) δ ppm 7.26 (d, J = 8.5 Hz, 2H), 7.18 (d, J = 8.5 Hz, 2H), 4.51 (s, 2H), 3.16 (bs, 1H). **^{13}C NMR** (125 MHz, $CDCl_3$) δ ppm 139.2 (1C), 133.2 (1C), 128.6 (2C), 128.2 (2C), 64.2 (1C). **HRMS (EI)**: Exact mass calculated for $C_7H_6OCl^-$ $[M-H]^{-\cdot}$: 141.0206 found 141.0210 (3.1 ppm).

Compound 196j: 4-bromobenzoic acid

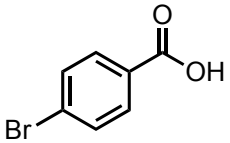

^{1}H NMR (500 MHz, DMSO-d^6) δ ppm 13.14 (bs, 1H), 7.85 (d, J = 8.7 Hz, 2H), 7.66 (d, J = 8.7 Hz, 2H). **^{13}C NMR** (125 MHz, DMSO-d^6) δ ppm 167.0 (1C), 132.0 (2C), 131.7 (2C), 130.4 (1C), 127.8 (1C). **HRMS (EI)**: Exact mass calculated for $C_7H_4O_2Br^-$ $[M-H]^{-\cdot}$: 198.9394 found 198.9399 (2.7 ppm).

Compound 197j: 4-bromobenzyl alcohol

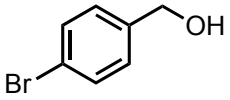

^{1}H NMR (500 MHz, $CDCl_3$) δ ppm 7.45 (d, J = 8.5 Hz, 2H), 7.17 (d, J = 8.5 Hz, 2H), 4.56 (d, J = 3.9Hz, 2H), 2.70 (t, J = 3.9 Hz, 1H). **^{13}C NMR** (125 MHz, $CDCl_3$) δ ppm 139.7 (1C), 131.6 (2C), 128.6 (2C), 121.4 (1C), 64.3 (1C). **HRMS (EI)**: Exact mass calculated for $C_7H_6OBr^-$ $[M-H]^{-\cdot}$: 184.9601 found 184.9596 (-2.5 ppm).

3.1.7. Additional Experiments

A complete table is presented with the chosen sacrificial reagents for the selective cross-Cannizzaro reaction of HMF.

Table 12. Full scope table for the sacrificial agents utilized in the cross-Cannizzaro disproportionation.

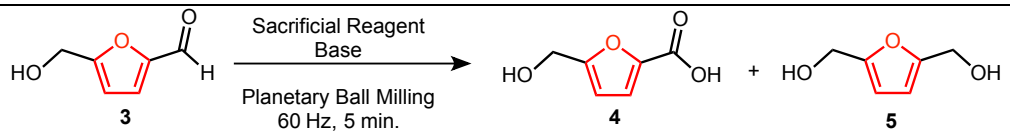

Entry	Sacrifice Reagent (equiv.)		Base (equiv.)	%yield (5:4)
1	$(CH_2O)_n$	1.2 equiv.	KOH (2)	44% (only 5)
2	$(CH_2O)_n$	1.2 equiv.	KOH (4)	90% (only 5)
3	D-Glucose	1.2 equiv.	KOH (4)	95% (1:1)
4	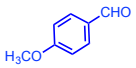	1.2 equiv.	KOH (4)	88% (1.2:1)
5	Benzaldehyde	1.2 equiv.	KOH (4)	93% (1:1)
6		1.2 equiv.	KOH (4)	87% (1:1)
7	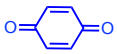	1.2 equiv.	KOH (4)	45% (1:1)
8	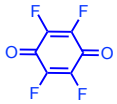	1.2 equiv.	KOH (4)	31% (2:1)
9	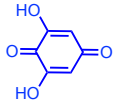	1.2 equiv.	KOH (4)	52% (4:1)
10	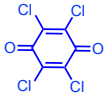	1.2 equiv.	KOH (4)	20% (1:2)
11		1.5 equiv.	KOH (6)	45% (1:2)

12	2.0 equiv.	KOH (4)	20% (1:2.5)
13	2.0 equiv.	KOH (8)	52% (1:2)

In most cases, no selectivity was observed, and this was accompanied by low yields. The utilization of paraformaldehyde gave a satisfactory conversion of HMF **4** to DHMF **5** in high yields, with an excellent selectivity. The selectivity towards HMFA **5** was harder to achieve. Initially, sources were looked for aldehyde groups with a higher electrophilicity towards hydride than HMF **4**. D-Glucose and benzaldehydes did not give satisfactory yields. We decided then to utilize quinones as hydride-acceptors. For our surprise, the utilization of *p*-tetrachlorobenzoquinone gave selectivity towards the synthesis of HMFA **4**. We decided to continue the experiments trying different ratios of this benzoquinone to HMF and base, but even though the selectivity observed was satisfactory, the overall yields remain very low.

3.2. Expedient synthesis of 2,5-non-symmetric furans platform chemicals via catalytic conversion of biomass and the formal synthesis of Dantrolene®.

3.2.1. Abstract

5-Hydroxymethyl furfural was employed as starting material for a new synthetic approach to obtain 2,5-diaryl non-symmetric furans. Decarboxylative cross-couplings were optimized to biomass-derived furans, where it was found that the presence of the methylenehydroxyl handle has an enhancing effect in the yields obtained through palladium-catalyzed decarboxylative cross-coupling reactions for a broad scope of coupling partners. Additionally, this green synthetic strategy was employed for a formal synthesis of the muscle relaxant Dantrolene® in excellent yields.

3.2.2. Introduction

The exponential growth of the demand on organic chemical materials has led to an uncontrolled exploitation of petroleum feedstock sources. Most of the primary starting materials for the chemical synthesis industry are derived directly from the refining of petroleum crude with processes that lead to an environmental concern because of the increase on green-house emissions and land-use change as a result of human activities.[19,51,215] To reduce dependence on petroleum derivatives and mitigate climate change in the chemical sectors, the employment of alternative production systems is required. Towards this end, biomass has been explored as a potential renewable resource for the production of fuels and starting materials for chemical synthesis.[216,217] Academic research is now moving into pilot plants as shown by the recent efforts of the Avantium-BASF[48] joint venture for 50000 MT/year production of biomass derived furans; and the ADM-DuPont[49,50] pilot plant for the production of carbohydrate-derived platform chemicals.

Within biomass, furans derived from carbohydrates have been highlighted as the "sleeping giant"[218] in terms for their potential use in a diverse range of applications. The breakdown of hemicellulose and cyclodehydration of common hexoses leads to 5-hydroxymethyl furfural (HMF)[219], which serves as a platform chemical for the production of the fuel alternatives 2,5-dimethylfuran, 2,5-dihydroxymethyl furan (DHMF), 2,5-furan dicarboxylic acid (terephthalic acid

replacement molecule in PET polymers)[192,220,221] and γ-valerolactone[185] (food additive), among others.[184,222,223] It is of high importance to develop chemical tools that allow chemists to perform transformations on these biomass-derived starting materials to obtain value-added next-generation chemicals[224]. On this note, the synthesis of aryl substituted furans remains an important transformation due the ubiquitous presence of this moiety in a variety of compound classes including natural products[225], pharmaceutical active components[76], polymer synthesis[226], among others.

Several reports have described the synthesis of 2,5-diaryl furans **30**. The employment of coinage metals such as Cu, Ag and Au towards the synthesis of substituted furans has been reported with reactions including cyclization of alkynes with tethered nucleophiles[227], cycloaddition reactions[228], radical cyclization of haloalkenes or haloalkynes[229], among others[230], as well as the use of Rh[231] and Pd-mediated cross-couplings[85].

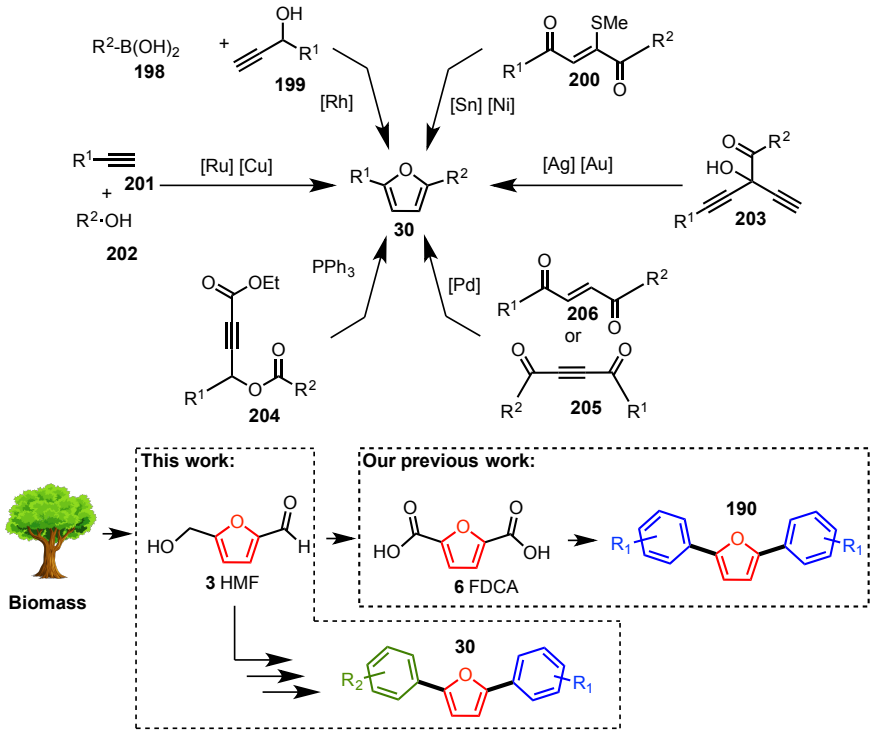

Figure 48. Reported synthetic strategies for the synthesis of 2,5-non symmetric diaryl furans and the proposed present work.

These methodologies, although helpful, require the synthesis of complex non-commercial starting materials, which results in a non-modular approach that could limit their utility.

In our approach, we intend to circumvent longstanding stepwise transformation of non-aromatic precursors with an expedient decarboxylative arylation strategy for the selective cross-coupling of biomass-derived furans with aryl halides. Previously, we reported the employment of a double decarboxylative cross-coupling reaction on biomass-derived 2,5-furandicarboxylic acid for the synthesis of symmetric 2,5-diaryl furans with good to excellent yields[232]. Herein, we aim to expand the scope of biomass-derived starting material by generating 2,5-diaryl non-symmetric furans from HMF. This route would provide significant additional value by not only allowing for differentiation between the 2- and 5- positions of the furan, but also utilizing a biomass-derived starting material (HMF) that is one-step upstream in the biomass processing cycle relative to the previously employed FDCA.

3.2.3. Results and Discussion

The proposed synthetic approach comprises a first oxidation of the aldehyde moiety of HMF to obtain HMFA (**4**, Z=H). There have been several strategies reported for this transformation, mainly using transition metals supported on heterogeneous media for catalysis. Our group previously reported the utilization of a solvent-free mechanochemical disproportionation of HMF into DHMF and HMFA in quantitative yields[233], and we employed this method to obtain the substrate for the first cross-coupling reactions (Table 1). Previous reports had demonstrated that the presence of free alcohols and phenols in the electrophilic coupling partner is detrimental for the decarboxylative cross-coupling arylation[232], but in this case, employment of HMFA in the cross-coupling step includes the presence of a free hydroxymethyl group in the nucleophilic cross-coupling partner, which we hypothesized would help in the stabilization of the intermediates **210**.

Table 13. Optimization of the first cross-coupling.

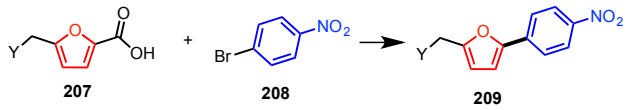

Entry	Y	Pd Source (5 mol%)	Ligand (10 mol%)	Yield (%)
1	TBDMSO	$Pd(OAc)_2$	none	0
2	TBDMSO	$Pd(OAc)_2$	P(*t*-Bu)$_3$	23
3	TBDMSO	$PdCl_2$	P(*t*-Bu)$_3$	28
4	HO	$PdCl_2$	P(*t*-Bu)$_3$	54
5	HO	Pd[P(*t*-Bu$_3$)]$_2$	None	61
6	HO	$Pd(dba)_2$	P(*t*-Bu)$_3$	51
7	HO	$Pd(dba)_2$	PCy_3	44
8	HO	$Pd(acac)_2$	P(*t*-Bu)$_3$	67
9	HO	$Pd(acac)_2$	MePhos	85
10	HO	$Pd(acac)_2$	JohnPhos	93
11	MeO	$Pd(acac)_2$	JohnPhos	72
12	TBDMSO	$Pd(acac)_2$	JohnPhos	53

General conditions: Furan substrate 0.4 mmol, *p*-bromo nitrobenzene 0.2 mmol, Cs_2CO_3 (1.5 equiv.), *n*-Bu_4NCl (30 mol%) DMF [0.1 M], 170 °C μw, 8 min, 900 rpm.

To test this hypothesis, we prepared the silyl ether protected HMFA and tested the reaction with the reported common conditions for decarboxylative cross-coupling. In the absence of a sterically hindered phosphine as ligand (entry 1) the reaction did not yield the desired product, but when P(*t*-Bu)$_2$ was added to the reaction, the desired product was obtained in a 23% yield (entry 2). Switching the Pd source to $PdCl_2$ gave similar results (entry 3). Employing the unprotected alcohol (HMFA) in the cross-coupling, resulted in higher yields (entries 4-7), which supported our hypothesis. Finally, employing a combination of $Pd(acac)_2$ and Buchwald-type ligands[146] yielded the desired product in higher yields. The optimized conditions (entry 10) were finally evaluated with the two other derivatives (entries 11 and 12) to confirm that indeed the presence of bulky groups in the methyl alcohol oxygen would not favour the distal weak stabilization effect. Additionally, the optimized conditions were employed in the coupling of 2-furoic acid, giving a 61% of yield, which supports the positive effect of having the hydroxymethyl handle present in the carboxylic acid coupling partner (Figure 49).

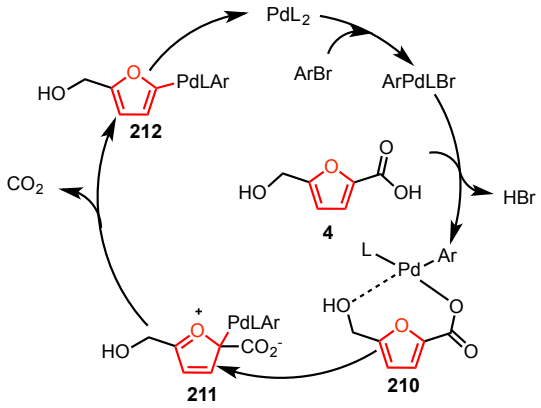

Figure 49. Proposed catalytic cycle for the Pd-mediated cross-coupling of HMFA **4** and aryl bromides.

Single experiments suggest that the presence of the free hydroxyl group on the HMFA **4** is responsible for the improved yields. Weak interactions with palladium in catalysis have been reported by the Yu[234,235] group, based on the findings of Boele[236] and Dick[128] .

Table 14. Additional experiments to evaluate the effects of the presence of the hydroxymethyl handle of HMFA.

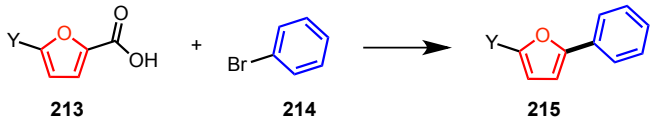

213 214 215

Entry	Y	Yield (%)[a]
1	CH_2OH (213a)	84
2	CH_2OCH_3 (213b)	66
3	H (213c)	55
4	$CH_2Si(t\text{-}Bu)(CH_3)_2$ (213d)	45
5	CH_2OH (213a) H (213c)	73 (1.5:1; 215a:215c)
6	CH_2OH (213a) CH_2OCH_3 (213b) $CH_2Si(t\text{-}Bu)(CH_3)_2$ (213d)	81 (1.7:1.3:1; 215a:215b:215d)

Conditions: Furan substrate 0.4 mmol (each), *p*-bromo benzotrifluoride 0.4 mmol, Cs_2CO_3 (1.5 equiv.), *n*-Bu_4NCl (30 mol%), $Pd(acac)_2$ 5 mol%, JohnPhos 10 mol%, DMF [0.1 M], 170 °C μw, 8 min, 900 rpm. [a]Analysis done by ^{1}HNMR, using 1,3,5-trimethoxybenzene as internal standard.

This hypothesis was further supported (Table 14) in the competition experiments; the product obtained for the cross-coupling with HMFA **213a** was always the most abundant in the

crude mixture analyzed by ^{1}H-NMR. Ongoing studies are focusing on examining the possible interactions of this hydroxyl handle with the palladium complexes involved in the reaction, but a clear trend was observed when comparing the possible weak coordination affinities of all the derivatives evaluated.

Oxidation of the alcohol to the carboxylic acid still remains a challenging reaction since the use of harsh oxidative conditions could lead to a low functional group tolerance or overoxidation of the substrate into undesired by-products (Table 15. Oxidation of the methyl alcohol moiety.). Employing a catalytic TEMPO-NaOCl system with $NaClO_2$ was first evaluated (entries 1 and 2), but the product obtained was a low yield of the corresponding aldehyde for the *p*-OCH_3 substrate[237] We hypothesized that the electron-rich nature of this model substrate may be problematic, so we prepared a second model substrate with an electron-deficient substituent (*p*-CF_3), that improved the yield towards the aldehyde (**217**), but only a small quantity of the desired carboxylic acid (**218**) was obtained (entry 2). Oxidative conditions that involve acidic media were non-compatible with the hydroxymethyl furan derivatives as they induce the formation of a non-desired side-products (entry 3). Interestingly, when metal catalysis with peroxide was employed as oxidant[238], it promoted the formation of a mixture between the desired product and the aldehyde derivative (entries 4 and 5).

Table 15. Oxidation of the methyl alcohol moiety.

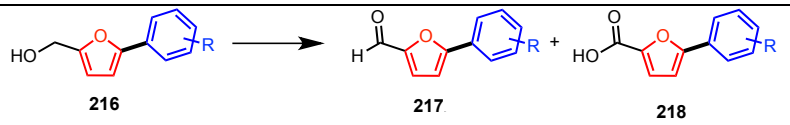

Entry	R	Conditions [a]	%217	%218
1	*p*-OCH_3	$NaClO_2$, $NaOCl_{cat}$, $TEMPO_{cat}$	20	0
2	*p*-CF_3	$NaClO_2$, $NaOCl_{cat}$, $TEMPO_{cat}$	48	<5
3	*p*-CF_3	Jones Reagent	0	0
4	*p*-CF_3	$BiCl_{3cat}$, *t*-BuOOH	<5	68
5	*p*-OCH_3	$BiCl_{3cat}$, *t*-BuOOH	45	19
6	*p*-OCH_3	SiO_2:$KMnO_4$ [b]	0	0
7	*p*-CF_3	$CuBr_{2cat}$, *t*-BuOOH	68	0
8	*p*-OCH_3	$CuBr_{2cat}$, *t*-BuOOH	43	0
9	*p*-CF_3	$Fe(NO_3)_3 9H_2O_{cat}$, $TEMPO_{cat}$, O_2	>98	0
10	*p*-OCH_3	$Fe(NO_3)_3$ $9H_2O_{cat}$, $TEMPO_{cat}$, O_2	90	0
11	*p*-CF_3	$[Cu(CH_3CN)_4]PF_{6cat}$, DBED, O_2	>99	0
12	*p*-OCH_3	$[Cu(CH_3CN)_4]PF_{6cat}$, DBED, O_2	94	0
13	*p*-CF_3	1.$[Cu(CH_3CN)_4]PF_{6cat}$, DBED, O_2 2.$NaClO_2$, Sulphamic Acid	0	95

[a]Full description of the reaction conditions can be found in experimental section. [b]60 % of *p*-methoxybenzoic acid was recovered.

Replacement of the $BiCl_3$ with $CuBr_2$ led to the selective formation of the aldehyde in moderate yields[239]. Harsher oxidation conditions ($KMnO_4$ adsorbed on Silica[240]) cleaved the furan moiety to produce the corresponding benzoic acid (entry 6). The use of TEMPO/O_2 with $Fe(NO_3)_3$ gave excellent yields of the aldehyde derivative[241]. Given the high cost of TEMPO, we envisioned that this step would be non-optimal, particularly for industrial applications.[242] For this matter, we subsequently employed a biomimetic copper system[243], in which the reaction is performed at room temperature under an O_2 atmosphere, obtaining high yields of the corresponding aldehydes in much shorter reaction times. We subsequently employed a two-step oxidation with the conditions reported in entries 11 and 12, including an adapted Pinnick oxidation[244,245] to obtain the carboxylic acids **218**.

With the carboxylic acids prepared, we submitted the furoic acids to a second decarboxylative cross-coupling based on the conditions optimized for the first reaction and with a wide scope of coupling partners (Table 16).

Table 16. Scope of the second decarboxylative cross-coupling reaction.

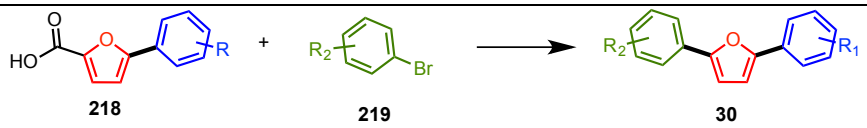

Entry		Product	Yield (%)
1	**30a**	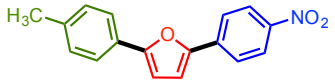	77
2	**30b**	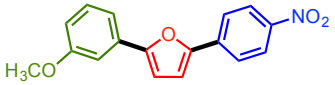	72
3	**30c**	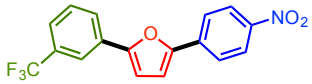	91
4	**30d**	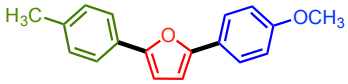	69
5	**30e**	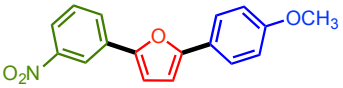	76
6	**30f**	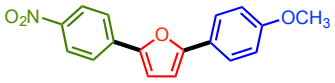	82
7	**30g**	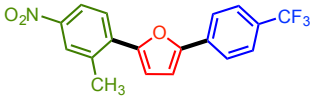	83
8	**30h**	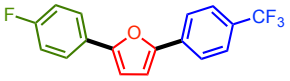	69
9	**30i**	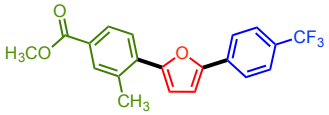	64
10	**30j**	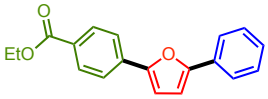	74
11	**30k**	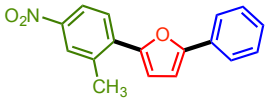	83
12	**30l**	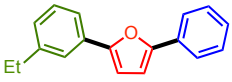	87

General conditions: Furan carboxylic acid (1.5 equiv.), Aryl bromide 1 mmol, $Pd(acac)_2$ (5 mol%), JohnPhos (10 mol%) Cs_2CO_3 (1.5 equiv.), n-Bu_4NCl (30 mol%) DMF [0.1 M], 170 °C μw, 8 min, 900 rpm.

A broad range of aryl coupling partners was evaluated with different 5-aryl-2-furoic acids with good yields in most cases. When performing the reaction with electron deficient carboxylic acids (entries 1-3, 7-9) a trend was observed that correlate the yield outcome with the electronic properties of the aryl bromide, giving higher yields for those aryl bromides with electron withdrawing substituents, possibly due to the more facile oxidative addition of the Pd^0 into the C_{sp2}-Br bond[181,246]. In general, for electron rich carboxylic acids, the yields obtained for the second cross-coupling were moderate in all cases, possibly due to the higher energetic barrier to overcome the decarboxylation step. Overall, a wide cope of reagents was prepared that tolerated a range of functionalities, including substrates bearing ortho functional groups (entries 7, 9 and 11).

3.2.4. Formal synthesis of Dantrolene®

Dantrolene is a hydantoin derivative furan that acts as a postsynaptic muscle relaxant and is the chief drug in the prevention and treatment of malignant hyperthemia.[76,247] The reported patented synthesis[248,249], involves the preparation of a diazonium salt followed by a Cu-catalyzed Meerwein arylation, and an iminium formation with 2-aminohydantoin to form the target drug. Despite this synthetic approach involving only three steps, it represents a challenge in the efficiency of the arylation, because the yield obtained is very low (<20%), and also, requires the preparation of the potentially dangerous diazonium salt. Other methodologies have been reported, that explore the C-H arylation of furan with solid supported catalysis (TiO_2)[250] and Pd-mediated C-H arylations[251]. In our system, we proposed employing a biomass-derived starting material (HMF) for the synthesis of this drug molecule based on the currently reported method. HMFA (**4**) was obtained from HMF (**3**) through a solvent-free mechanochemical base-promoted disproportionation and used as the starting material for the decarboxylative cross-coupling with *p*-bromo nitrobenzene to obtain **220**. This step is critical since it circumvents the two main problems of the patented route, the low yield for the coupling and the commercial availability of the starting materials. This compound was subjected to a biomimetic Cu-catalyzed aerobic oxidation to obtain the corresponding aldehyde **221** in quantitative yield. The overall yield for this three-step process of the key aldehyde intermediate **221** of 93% starting from biomass-derived HMF is the most efficient synthesis reported for Dantrolene®.

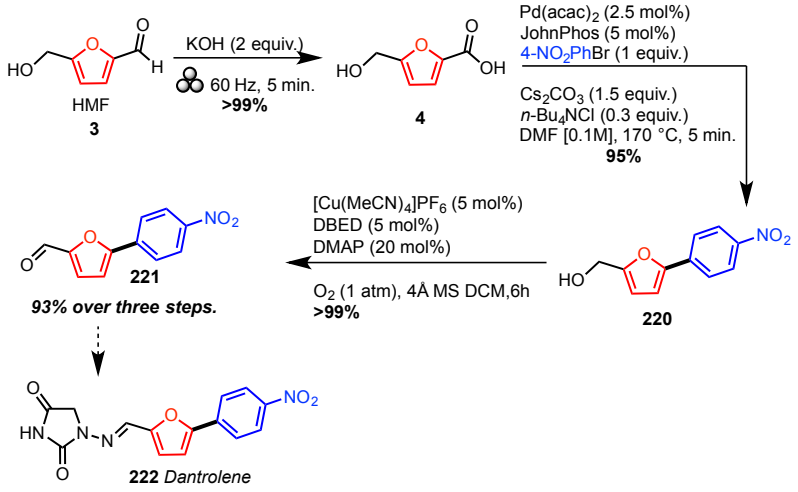

Figure 50. Proposed synthetic route for the formal synthesis of Dantrolene® from biomass-derived HMF.

3.2.5. Conclusions

Biomass-derived HMF was used as a platform chemical starting material for the synthesis of non-symmetric 2,5-diaryl furans with good to excellent yields. Single experiments and competition reactions support the idea of a stabilizing distal coordination of the hydroxyl handle that results in improved yields. Oxidation methodologies were explored for the oxidation of 5-hydroxymethyl-2-aryl furans, and a two-step oxidation was selected to obtain the corresponding carboxylic acids. With this key intermediate, a new formal synthetic pathway for the commercially available muscle relaxant Dantrolene® was achieved, with excellent yields and higher efficiency than reported routes. This work highlights the importance of the employment of renewable resources as starting materials for more complex targets, as a way to contribute in the development of environmentally friendly approaches in the synthesis of high-value target molecules.

3.2.6. Experimental Section

General procedure for the decarboxylative cross-coupling of HMFA and Aryl Bromides: To an oven-dried microwave vial (2-5 mL), with a stir bar, was added 114 mg of HMFA (0.8 mmol, 2 equiv.), 6.1 mg of $Pd(acac)_2$ (0.02 mmol, 5 mol%), 11.9 mg of JohnPhos (0.08 mmol, 10 mol%), 195 mg of Cs_2CO_3 (0.6 mmol, 1.5 equiv.), 0.4 mmol of the corresponding Aryl Bromide, 33 mg of n-Bu_4NCl (0.12 mmol, 30 mol%) and 4 mL of anhydrous DMF. The reaction is pre-stirred for 30 seconds and then submitting to microwave irradiation to achieve 170 °C for 8 min at 900 rpm. The reaction crude is transferred to a 125 mL separatory funnel and diluted with 30 mL

of EtOAc, washed with brine (2x20 mL), $NaHCO_{3(sat)}$ (1x20 mL). The combined aqueous phases are re-extracted with EtOAc (1x15 mL), and the combined organics are dried over Na_2SO_4. The solvent is removed under vaccuo and the crude is purified by Silica Gel chromatography to obtain the pure desired product.

Cu-catalyzed Oxidation of the primary alcohol to the aldehyde: In a nitrogen glovebox, a Schlenk tube equipped with a stir bar was charged with alcohol (0.5 mmol), $[Cu(CH_3CN)_4]PF_6$ (0.025 mmol), ligand (0.025 mmol), additive (0.1 mmol), 4Å molecular sieves (100 mg), CH_2Cl_2 (4 mL), The tube was sealed, brought out of the glovebox, the nitrogen headspace was evacuated, and then replaced with a constant pressure of 1 atm O2. The resulting mixture was stirred at room temperature for 6 h. After this time 10% wt. $NaHSO_4$ (15 mL) was added to quench the reaction. The product was extracted with additional CH_2Cl_2 (3X10 mL) and the combined organic layers were dried with Na_2SO_4, filtered and concentrated to afford the product. Purification was done (when needed) with Silica gel Combiflash using Hexanes:EtOAc (10:0 to 8:2) as eluent. This reaction was scaled up according to the corresponding yield of the first cross-coupling.

Adapted Pinnick Oxidation of the aldehyde to the Carboxylic Acid: The corresponding aldehyde (limiting reagent, 1 equiv.) was added in a 10 mL round bottom flask and equipped with a stir bar. To this flask was added MeCN:H_2O (3:1, 0.65M to the corresponding alcohol), NaH_2PO_4 (0.26 equiv.), $NaClO_2$ (1.39 equiv.) and H_2O_2 30% (1 equiv.). The flask was covered with aluminum foil to avoid photoinduced decomposition and stirred at room temperature for 18 hr. In those cases where the reaction was not completed in 18 hr (electron-rich substrates), the reaction vessel was opened and $NaClO_2$ (1.05 equiv.) and H_2O_2 30% (1 equiv.) was added, and stirred for another 18 hr. When the reaction was completed, the stir bar was removed and the MeCN was removed under vaccuo. The aqueous remaining solution was checked for high acidity (pH 2, adjusted with 2M HCl when necessary), and extracted with EtOAc (3x10 mL). The combined organics were dried with Na_2SO_4, and the solvent was removed under vaccuo to obtain the product, usually a solid. When needed, purification of the product can be done with acid-base extraction, or silica-gel chromatography with DCM:MeOH (10:0 to 8:2, and trace amount of AcOH).

General procedure for the decarboxylative cross-coupling of 5-aryl-2-furoic acids and Aryl Bromides: To an oven-dried microwave vial (0.5-2 mL), with a stir bar, was added 0.2 mmol

of the 5-aryl-2-furoic acid (1 equiv.), 3.1 mg of $Pd(acac)_2$ (0.01 mmol, 5 mol%), 6.0 mg of JohnPhos (0.02 mmol, 10 mol%), 98 mg of Cs_2CO_3 (0.3 mmol, 1.5 equiv.), 0.4 mmol of the corresponding Aryl Bromide, 16 mg of n-Bu_4NCl (0.06 mmol, 30 mol%) and 2 mL of anhydrous DMF. The reaction is pre-stirred for 30 seconds and then submitting to microwave irradiation to achieve 170 °C for 8 min at 900 rpm. The reaction crude is transferred to a 125 mL separatory funnel and diluted with 30 mL of EtOAc, washed with brine (2x20 mL), $NaHCO_{3(sat)}$ (1x20 mL). The combined aqueous phases are re-extracted with EtOAc (1x15 mL), and the combined organics are dried over Na_2SO_4. The solvent is removed under vaccuo and the crude is purified by Silica Gel chromatography to obtain the pure desired product.

3.2.7. Characterization Data

Compound **216a** - (5-(4-nitrophenyl)furan-2-yl)methanol

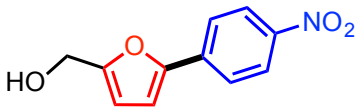

Compound **216a** was prepared following the general procedure for decarboxylative cross-coupling of HMFA and Aryl Bromides on a 0.4 mmol scale. The compound was isolated with column chromatography (R_f = 0.42) Hexanes:DCM:EtOAC (4:4:2) as a yellow solid. **^{1}H NMR** (500 MHz, $CDCl_3$) δ ppm 8.23 (d, *J* = 9.0 Hz, 2H), 7.78 (d, *J* = 9.0 Hz, 2H), 6.83 (d, *J* = 3.4 Hz, 1H), 6.46 (d, *J* = 3.4 Hz, 1H), 4.71 (s, 2H), 1.86 (bs, 1H). **^{13}C NMR** (125 MHz, $CDCl_3$) δ ppm 155.8 (1C), 151.6 (1C), 146.4 (1C), 136.2 (1C), 124.3 (2C), 123.9 (2C), 110.5 (1C), 109.7 (1C), 57.6 (1C). **HRMS (EI):** Exact mass calculated for $C_{11}H_8NO_4^-$ $[M-1]^{-\cdot}$ 218.0459, found 218.0455 (-1.8 ppm)

Compound **216b** – (5-(4-methoxyphenyl)furan-2-yl)methanol

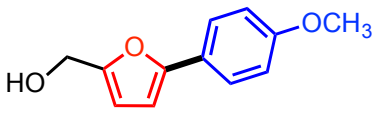

Compound **216b** was prepared following the general procedure for decarboxylative cross-coupling of HMFA and Aryl Bromides on a 0.4 mmol scale. The compound was isolated with column chromatography (R_f = 0.53) Hexanes:DCM:EtOAC (4:4:2) as a pale yellow solid. **^{1}H NMR** (500 MHz, $CDCl_3$) δ ppm 7.60 (d, *J* = 8.9 Hz, 2H), 6.92 (d, *J* = 8.9 Hz, 2H), 6.46 (d, *J* = 3.2 Hz, 1H),

6.34 (d, J = 3.2 Hz, 1H), 4.64 (s, 2H), 3.83 (s, 3H), 2.19 (bs, 1H). **^{13}C NMR** (125 MHz, $CDCl_3$) δ ppm 159.1 (1C), 154.2 (1C), 152.9 (1C), 125.3 (2C), 123.8 (1C), 114.1 (2C), 109.9 (1C), 104.1 (1C), 57.6 (1C), 55.3 (1C). **HRMS (EI):** Exact mass calculated for $C_{12}H_{11}O_3^-$ $[M-1]^{-\cdot}$ 203.0708, found 203.0705 (-1.3 ppm)

Compound **216c** - (5-(4-(trifluoromethyl)phenyl)furan-2-yl)methanol

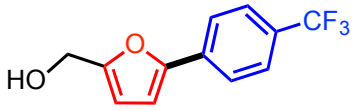

Compound **216c** was prepared following the general procedure for decarboxylative cross-coupling of HMFA and Aryl Bromides on a 0.4 mmol scale. The compound was isolated with column chromatography (R_f = 0.30) Hexanes:DCM:EtOAC (4:4:2) as a white solid. **^{1}H NMR** (500 MHz, $CDCl_3$) δ ppm 7.74 (d, J = 8.0 Hz, 2H), 7.61 (d, J = 8.0 Hz, 2H), 6.70 (d, J = 3.3 Hz, 1H), 6.40 (d, J = 3.3 Hz, 1H), 4.68 (s, 2H), 2.34 (bs, 1H). **^{13}C NMR** (125 MHz, $CDCl_3$) δ ppm 154.7 (1C), 152.4 (1C), 133.7 (1C), 129.0 (q, J = 32.5 Hz, 1C), 125.7 (q, J = 3.9 Hz, 2C), 124.1 (q, J = 271.2 Hz, 1C), 123.7 (2C), 110.1 (1C), 107.7 (1C), 57.5 (1C). **HRMS (EI):** Exact mass calculated for $C_{12}H_8F_3O_2^-$ $[M-1]^{-\cdot}$ 241.0477, found 241.0472 (-1.9 ppm)

Compound **216d** – (5-phenylfuran-2-yl)methanol

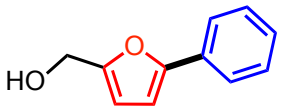

Compound **216d** was prepared following the general procedure for decarboxylative cross-coupling of HMFA and Aryl Bromides on a 0.4 mmol scale. The compound was isolated with column chromatography (R_f = 0.34) Hexanes:DCM:EtOAC (4:4:2) as a white solid. **^{1}H NMR** (500 MHz, $CDCl_3$) δ ppm 7.69 (m, 2H), 7.39 (m, 2H), 7.28 (m, 1H), 6.61 (d, J = 3.3 Hz, 1H), 6.39 (d, J = 3.3 Hz, 1H), 4.68 (s, 2H), 1.98 (bs, 1H). **^{13}C NMR** (125 MHz, $CDCl_3$) δ ppm 154.0 (1C), 153.6 (1C), 130.7 (1C), 128.7 (2C), 127.5 (1C), 123.8 (2C), 110.0 (1C), 105.7 (1C), 57.7 (1C). **HRMS (EI):** Exact mass calculated for $C_{11}H_9O_2^-$ $[M-1]^{-\cdot}$ 173.0603, found 173.0599 (-2.1 ppm)

Compound **30a** - 2-(4-nitrophenyl)-5-(p-tolyl)furan

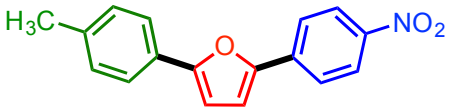

Compound **30a** was prepared following the general procedure for decarboxylative cross-coupling of 5-aryl-2-furoic acids and Aryl Bromides on a 0.2 mmol scale. The compound was isolated with column chromatography (R_f = 0.43) Hexanes:DCM (1:1) as a yellow solid. **^{1}H NMR** (500 MHz, $CDCl_3$) δ ppm 8.25 (d, *J* = 9.0 Hz, 2H), 7.82 (d, *J* = 9.0 Hz, 2H), 7.66 (d, *J* = 8.2 Hz, 2H), 7.24(d, *J* = 8.2 Hz, 2H) 6.95 (d, *J* = 3.6 Hz, 1H), 6.74 (d, *J* = 3.6 Hz, 1H), 2.40 (s, 3H) **^{13}C NMR** (125 MHz, $CDCl_3$) δ ppm 155.9(1C), 150.6(1C), 146.1(1C), 138.3(1C), 136.4(1C), 129.5(2C), 127.3(1C), 124.4(2C), 124.1(2C), 123.6(2C), 111.4(1C), 107.2(1C), 21.4(1C). **HRMS (EI):** Exact mass calculated for $C_{17}H_{13}NO_3$ [$M^{+\cdot}$]: 279.0895, found 279.0898 (1.1 ppm)

Compound **30b** – 2-(3-methoxyphenyl)-5-(4-nitrophenyl)furan

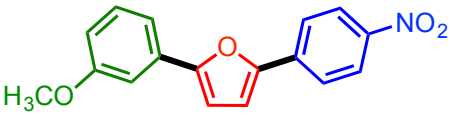

Compound **30b** was prepared following the general procedure for decarboxylative cross-coupling of 5-aryl-2-furoic acids and Aryl Bromides on a 0.2 mmol scale. The compound was isolated with column chromatography (R_f = 0.36) Hexanes:DCM (1:1) as a yellow solid. **^{1}H NMR** (500 MHz, $CDCl_3$) δ ppm 8.25 (d, *J* = 9.0 Hz, 2H), 7.83 (d, *J* = 9.0 Hz, 2H), 7.36 (d, *J* = 5.1 Hz, 2H), 7.30 (dt, *J* = 2.4, 0.9 Hz, 1H), 6.96 (d, *J* = 3.6 Hz, 1H), 6.91 – 6.87 (m, 1H), 6.80 (d, *J* = 3.6 Hz, 1H), 3.90 (s, 2H). **^{13}C NMR** (125 MHz, $CDCl_3$) δ ppm 160(1C), 155.4(1C), 150.9(1C), 146.2(1C), 136.2(1C), 131.2(1C), 124.37(2C), 123.7(2C), 116.74(1C), 113.6(1C), 111.3(1C), 109.8(1C), 108.1(1C), 55.37(1C). **HRMS (EI):** Exact mass calculated for $C_{17}H_{13}NO_4$ [$M^{+\cdot}$]: 295.0845, found 295.0851 (2.0 ppm)

Compound **30c** - 2-(4-nitrophenyl)-5-(3-(trifluoromethyl)phenyl)furan

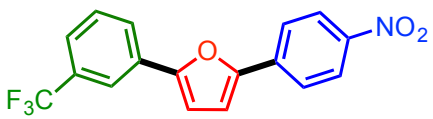

Compound **30c** was prepared following the general procedure for decarboxylative cross-coupling of 5-aryl-2-furoic acids and Aryl Bromides on a 0.2 mmol scale. The compound was isolated with column chromatography (R_f = 0.38) Hexanes:DCM (1:1) as an orange/yellow solid. **^{1}H NMR** (500 MHz, $CDCl_3$) δ ppm 8.29 (d, *J* = 9.0 HZ, 2H), 7.99 (m, 1H), 7.93 (m, 1H), 7.87 (d, *J* = 9.0 Hz, 2H), 7.57 (m, 2H), 7.00 (d, *J* = 3.6 Hz, 1H), 6.91 (d, *J* = 3.6 Hz, 1H). **^{13}C NMR** (125 MHz, $CDCl_3$) δ ppm 153.8(1C), 151.7(1C), 146.5(1C), 135.8(1C), 131.4 (q, *J* = 32.5, 1C), 130.7(1C), 129.4(1C), 127.1(q, *J* = 1.4 Hz, 1C), 124.6(q, J = 3.8 Hz, 1C), 124.4 (2C), 124.0 (q, *J* = 272.0 Hz, 1C), 123.9(2C), 120.7(q, *J* = 3.9 Hz, 1C), 111.2(1C), 109.1(1C). **HRMS (EI):** Exact mass calculated for $C_{17}H_{10}F_3NO_3$ [$M^{+\cdot}$]: 333.0613, found 333.0618 (1.5 ppm)

Compound **30d**- 2-(4-methoxyphenyl)-5-(p-tolyl)furan

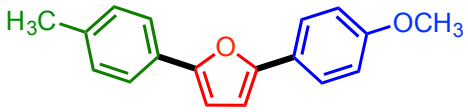

Compound **30d** was prepared following the general procedure for decarboxylative cross-coupling of 5-aryl-2-furoic acids and Aryl Bromides on a 0.2 mmol scale. The compound was isolated with column chromatography (R_f = 0.43) Hexanes:DCM (1:1) as a pale yellow solid. **^{1}H NMR** (500 MHz, $CDCl_3$) δ ppm 7.70 – 7.65 (m, 2H), 7.65 – 7.60 (m, 2H), 7.23 – 7.18 (m, 2H), 6.98 – 6.91 (m, 2H), 6.66 (d, *J* = 3.4 Hz, 1H), 6.59 (d, *J* = 3.4 Hz, 1H). **^{13}C NMR** (125 MHz, $CDCl_3$) δ ppm 158.9(1C), 153(1C), 152.9(1C), 136.9(1C), 129.3(2C), 128.2(1C), 125.1(2C), 124(1C), 123.5(2C), 114.1(2C), 106.4(1C), 105.5(1C), 55.3(1C), 21.2(1C). **HRMS (EI):** Exact mass calculated for $C_{18}H_{16}O_2$ [$M^{+\cdot}$]: 264.1150, found 264.1152 (0.8 ppm)

Compound **30e** – 2-(4-methoxyphenyl)-5-(3-nitrophenyl)furan

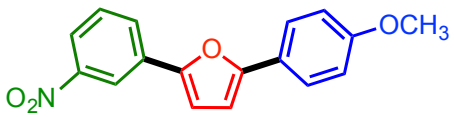

Compound **30e** was prepared following the general procedure for decarboxylative cross-coupling of 5-aryl-2-furoic acids and Aryl Bromides on a 0.2 mmol scale. The compound was isolated with column chromatography (R_f = 0.31) Hexanes:DCM (7:3) as a yellow solid. **^{1}H NMR** (500 MHz, $CDCl_3$) δ ppm 8.51 (ddd, *J* = 2.2, 1.6, 0.4 Hz, 1H), 8.06 (ddd, *J* = 8.0, 2.2, 1.0 Hz, 1H), 7.98 (ddd,

J = 8.0, 1.6, 1.0 Hz, 1H), 7.69 (d, J = 8.9 Hz, 2H), 7.55 (dd, J = 8.0, 0.4 Hz, 1H), 6.97 (d, J = 8.9 Hz, 2H), 6.86 (d, J = 3.5 Hz, 1H), 6.64 (d, J = 3.5 Hz, 1H), 3.86 (s, 3H). **^{13}C NMR** (125 MHz, $CDCl_3$) δ ppm 159.5(1C), 154.8(1C), 150(1C), 148.7(1C), 132.4(1C), 129.6(1C), 128.8(2C), 125.5(1C), 123.1(1C), 121.2(1C), 118,08(1C), 114.2(2C), 109.5(1C), 105.8(1C), 55.36(1C). **HRMS (EI):** Exact mass calculated for $C_{17}H_{13}NO_4$ [$M^{+\cdot}$]: 295.0845, found 295.0852 (2.4 ppm)

Compound **30f**– 2-(4-methoxyphenyl)-5-(4-nitrophenyl)furan

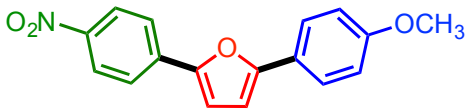

Compound **30f** was prepared following the general procedure for decarboxylative cross-coupling of 5-aryl-2-furoic acids and Aryl Bromides on a 0.2 mmol scale. The compound was isolated with column chromatography (R_f = 0.38) Hexanes:DCM (7:3) as a yellow solid. **^{1}H NMR** (500 MHz, $CDCl_3$) δ ppm 8.24 (d, J = 9.0 Hz, 2H), 7.81 (d, J = 9.0 Hz, 2H), 7.70 (d, J = 8.8 Hz, 2H), 6.97 (d, J = 8.8 Hz, 2H), 6.94 (d, J = 3.6 Hz, 1H), 6.67 (d, J = 3.56Hz, 1H), 3.86 (s, 3H). **^{13}C NMR** (125 MHz, $CDCl_3$) δ ppm 159.8 (1C), 155.8 (1C), 150.3 (1C), 146.0 (1C), 136.4 (1C), 125.6 (2C), 124.4 (2C), 123.4 (2C), 122.9 (2C), 114.3 (1C), 111.5 (1C), 106.4 (1C), 55.4 (1C). **HRMS (EI):** Exact mass calculated for $C_{17}H_{13}NO_4$ [$M^{+\cdot}$]: 295.0845, found 295.0851 (2.0 ppm)

Compound **30g** - 2-(2-methyl-4-nitrophenyl)-5-(4-(trifluoromethyl)phenyl)furan

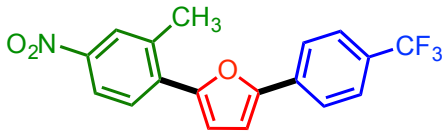

Compound **30g** was prepared following the general procedure for decarboxylative cross-coupling of 5-aryl-2-furoic acids and Aryl Bromides on a 0.2 mmol scale. The compound was isolated with column chromatography (R_f = 0.58) Hexanes:DCM (7:3) as a yellow solid. **^{1}H NMR** (500 MHz, $CDCl_3$) δ ppm 8.63 (d, J = 2.5 Hz, 1H), 8.05 (dd, J = 8.4, 2.5 Hz, 1H), 7.85 (d, J = 8.1 Hz, 2H), 7.68 (d, J = 8.1 Hz, 2H), 7.42(d, J = 8.4 Hz, 1H), 6.92 (d, J = 3.6 Hz, 1H), 6.82 (d, J = 3.6 Hz, 1H), 2.67 (s, 3H). **^{13}C NMR** (125 MHz, $CDCl_3$) δ ppm 152.6 (1C), 151.6 (1C), 146.6 (1C), 141.6 (1C), 133.2 (q, J = 1.4 Hz, 1C), 132.3 (1C), 130.8 (1C), 129.5 (q, J = 32.6 Hz, 1C), 125.9 (q, J =

3.8 Hz, 2C), 124.0 (q, J = 271.7 Hz, 1C), 124.0 (2C), 121.9 (1C), 121.7 (1C), 112.7 (1C), 109.1 (1C), 22.3 (1C). **HRMS (EI):** Exact mass calculated for $C_{18}H_{12}F_3NO_3$ [$M^{+\cdot}$]: 347.0769, found 347.0774 (1.4 ppm)

Compound **30h** – 2-(4-fluorophenyl)-5-(4-(trifluoromethyl)phenyl)furan

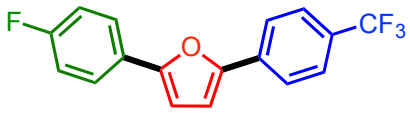

Compound **30h** was prepared following the general procedure for decarboxylative cross-coupling of 5-aryl-2-furoic acids and Aryl Bromides on a 0.2 mmol scale. The compound was isolated with column chromatography (R_f = 0.39) Hexanes:DCM (7:3) as a yellow solid. **^{1}H NMR** (500 MHz, $CDCl_3$) δ ppm 7.81 (d, J = 7.4 Hz, 2H), 7.72 (m, 2H), 7.65 (d, J = 7.4, 2H), 7.12 (m, 2H), 6.84 (d, J = 3.5 Hz, 1H), 6.70 (d, J = 3.5 Hz, 1H). **^{13}C NMR** (125 MHz, $CDCl_3$) δ ppm 162.4 (d, J = 248.3 Hz, 1C), 153.6 (1C), 151.8 (1C), 133.7 (q, J = 1.23 Hz, 2C), 128.9 (q, J = 32.8 Hz, 1C), 126.7 (d, J = 3.3 Hz, 1C), 125.7 (q, J = 3.8 Hz, 2C), 125.7 (d, J = 8.0 Hz, 2C), 124.2 (q, J = 271.4 Hz, 1C), 123.6 (1C), 115.8 (d, J = 22.0 Hz, 2C) , 109.2 (1C), 107.1 (d, J = 1.4 Hz, 1C). **HRMS (EI):** Exact mass calculated for $C_{17}H_{10}F_4O$ [$M^{+\cdot}$]: 306.0668, found 306.0669 (0.3 ppm)

Compound **30i** – methyl 3-methyl-4-(5-(4-(trifluoromethyl)phenyl)furan-2-yl)benzoate

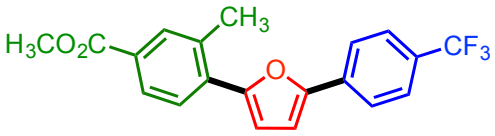

Compound **30i** was prepared following the general procedure for decarboxylative cross-coupling of 5-aryl-2-furoic acids and Aryl Bromides on a 0.2 mmol scale. The compound was isolated with column chromatography (R_f = 0.38) Hexanes:DCM (7:3) as a pale yellow solid. **^{1}H NMR** (500 MHz, $CDCl_3$) δ ppm 7.90 (m, 2H), 7.87 (d, J = 8.1 Hz, 1H), 7.83 (d, J = 8.1 Hz, 2H), 7.66 (d, J = 8.1 Hz, 2H), 6.90 (d, J = 3.5 Hz, 1H), 6.80 (d, J = 3.5 Hz, 1H), 3.94 (s, 3H), 2.62 (s, 3H). **^{13}C NMR** (125 MHz, $CDCl_3$) δ ppm 166.8 (1C), 153.1 (1C), 152.3 (1C), 134.3 (1C), 133.5 (2C), 132.6 (1C), 129.3 (q, J = 32.3 Hz, 1C), 128.8 (1C), 127.3 (1C), 126.5 (1C), 125.8 (q, J = 3.8 Hz, 2C),

124.1 (q, J = 272.0 Hz, 1C), 123.8 (2C), 112.6 (1C), 109.1 (1C), 52.1 (1C), 22.2 (1C). **HRMS (EI):** Exact mass calculated for $C_{20}H_{15}F_3O_3$ [$M^{+\cdot}$]: 360.0973, found 360.0979 (1.7 ppm)

Compound **30j** – ethyl 4-(5-phenylfuran-2-yl)benzoate

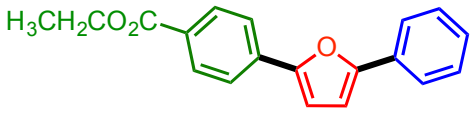

Compound **30j** was prepared following the general procedure for decarboxylative cross-coupling of 5-aryl-2-furoic acids and Aryl Bromides on a 0.2 mmol scale. The compound was isolated with column chromatography (R_f = 0.41) Hexanes:DCM (7:3) as a white solid. **^{1}H NMR** (500 MHz, $CDCl_3$) δ ppm 8.08 (d, J = 8.7 Hz, 2H), 8.08 (d, J = 8.7 Hz, 2H), 7.76 (m, 2H), 7.42 (m, 2H), 7.30 (m, 1H), 6.87 (d, J = 3.5 Hz, 1H), 6.77 (d, J = 3.5 Hz, 1H), 4.40 (q, J = 7.1 Hz, 2H), 1.42 (t, J = 7.2 Hz, 3H). **^{13}C NMR** (125 MHz, $CDCl_3$) δ ppm 166.3 (1C), 154.4 (1C), 152.3 (1C), 134.5 (1C), 130.4 (2C), 130.1 (1C), 128.8 (1C), 128.7 (2C), 127.8 (1C), 123.9 (2C), 123.2 (2C), 109.5 (1C), 107.5 (1C), 61.0 (1C), 14.4 (1C). **HRMS (EI):** Exact mass calculated for $C_{19}H_{16}O_3$ [$M^{+\cdot}$]: 292.1099, found 292.1105 (2.1 ppm)

Compound **30k** – 2-(2-methyl-4-nitrophenyl)-5-phenylfuran

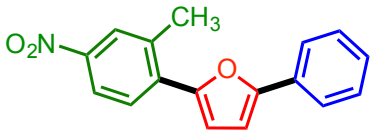

Compound **30k** was prepared following the general procedure for decarboxylative cross-coupling of 5-aryl-2-furoic acids and Aryl Bromides on a 0.2 mmol scale. The compound was isolated with column chromatography (R_f = 0.40) Hexanes:DCM (7:3) as a yellow solid. **^{1}H NMR** (500 MHz, $CDCl_3$) δ ppm 8.63 (d, J = 2.5 Hz, 1H), 8.01 (dd, J = 8.3, 2.5 Hz, 1H), 7.75 (m, 2H), 7.44 (dd, J = 8.4, 7.2 Hz, 2H), 7.39 (dd, J = 8.4, 0.8 Hz, 1H), 7.32 (m, 1H), 6.80 (d, J = 3.5 Hz, 1H), 6.78 (d, J = 3.5 Hz, 1H), 2.65 (s, 3H). **^{13}C NMR** (125 MHz, $CDCl_3$) δ ppm 154.2 (1C), 150.5 (1C), 146.6 (1C), 141.3 (1C), 132.2 (1C), 131.1 (1C), 130.1 (1C), 128.8 (2C), 128.0 (1C), 124.0 (2C), 121.4 (1C), 121.4 (1C), 112.6 (1C), 107.1 (1C), 22.4 (1C). **HRMS (EI):** Exact mass calculated for $C_{17}H_{13}NO_3$ [$M^{+\cdot}$]: 279.0895, found 279.0893 (-0.7 ppm)

Compound **30l** – 2-(3-ethylphenyl)-5-phenylfuran

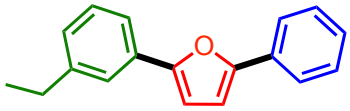

Compound **30l** was prepared following the general procedure for decarboxylative cross-coupling of 5-aryl-2-furoic acids and Aryl Bromides on a 0.2 mmol scale. The compound was isolated with column chromatography (R_f = 0.52) Hexanes:DCM (7:3) as a white solid. **^{1}H NMR** (500 MHz, $CDCl_3$) δ ppm 7.76 (m, 2H), 7.72 (m, 1H), 7.43 (m, 2H), 7.31 (m, 2H), 6.79 (d, *J* = 3.4 Hz, 1H), 6.64 (d, *J* = 3.4 Hz, 1H), 2.97 (q, *J* = 7.5 Hz, 2H), 1.35 (t, *J* = 7.5 Hz, 3H). **^{13}C NMR** (125 MHz, $CDCl_3$) δ ppm 153.4 9 (1C), 153.2 (1C), 141.2 (1C), 130.9 (1C), 129.7 (1C), 129.5 (1C), 128.7 (2C), 128.0 (1C), 127.9 (1C), 127.3 (1C), 125.9 (1C), 123.7 (2C), 110.3 (1C), 106.8 (1C), 27.4 (1C), 15.4 (1C). **HRMS (EI):** Exact mass calculated for $C_{18}H_{16}O$ [$M^{+\cdot}$]: 248.1201, found 248.1203 (0.8 ppm).

Chapter 4. Efficient synthesis of Bis(5-arylfuran-2-yl)methane scaffolds utilizing biomass-derived staring materials.

4.1. Introduction

The increasing demand for materials and energy has boosted the research in the development of renewable chemicals for a sustainable economy. In this regard, biomass has been the main target as the resource where many chemicals could be obtained with potential uses either for novel applications or even direct replacements of common petroleum-derived starting materials. Defunctionalization of carbohydrates has been in particular de most attractive target for the variety of products that can be acquired. The US Department of Energy identified the top 12 compounds obtained from carbohydrates defunctionalization with the potential of becoming industrially important in large scales as renewable starting materials. Within these chemicals, 5-hydroxymethyl furfural was highlighted as a *"sleeping giant"* because of its versatility and ease to obtain. This report discusses the employment of this biomass-derived starting materials for the efficient synthesis of bis(5-arylfuran-2-yl)methane scaffolds, an attractive class of compounds that is present in licorice flavors, coffee volatiles and have been used as conveniently as precursors in the synthesis or various condensed heterocyclic systems and as monomers and cross-linking reagents in polymer manufacturing.

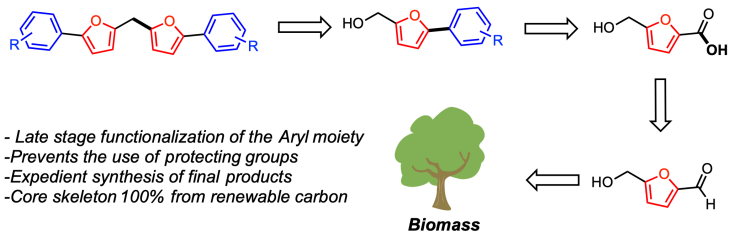

Figure 51. Retrosynthetic analysis for the synthesis of bis(5-arylfuran-2-yl)methane scaffolds from HMF.

Several reports have discussed the synthesis of these important compounds. In general, the synthetic strategies could be classified into two big classes. The first one includes those reaction where the furan ring is reacted with another furan ring bearing the bridge carbon, like the reports by Gillman and Wright that utilized organometallic reagents (mercury, lithium and copper) as nucleophiles to react with furfural derivatives, that after reduction gave satisfactorily the methane

scaffold. Another important class is the utilization of electrophilic compounds to bridge the carbon to assemble both furan rings, like the approach presented Denisov *et al.*, in which they used furylalkynylcarbinol derivatives and studied their reaction utilizing pre-complexation of the triple bond with cobalt complexes. Even though several strategies have been reported, we decided to pursue a different route for the synthesis of these scaffolds with a biomass conversion approach that utilizes 5-hydroxymethyl furfural as starting material, and also, the route herein presented, tries to overcome limitation of existing routes regarding the late stage functionalization of the aryl moiety, and the availability of the starting materials.

4.2. Results and Discussion

A defunctionalization of biomass was reported by Tiwaru et al., for the synthesis of these scaffolds comencing with Tartaric acid (or erithrol). In their report, a synthetic pathway of 9 steps with overall yields ranging from 20 to 25% was reported. Inspired by this green approach, we decided to start our synthesis utilizing our previously reported conditions for the solvent-free disproportionation of HMF to obtain the HMFA necessary for cross coupling. HMFA was cross-coupled with several aryl bromides, under the conditions optimized for this type of cross-coupling on chapter 3. The bigger scope of coupling partners used allowed for a detailed analysis of the influence of the electronic and steric situation of the electrophilic coupling partner in this reaction (Table 17).

Table 17. Scope of the decarboxylative cross-coupling of HMFA and aryl bromides.

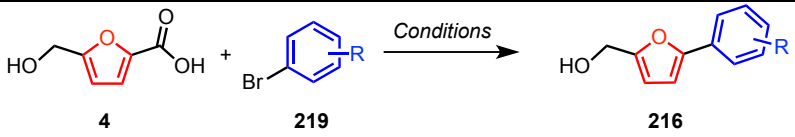

4 219 216

Entry	R	Product	Yield (%)
1	4-NO_2	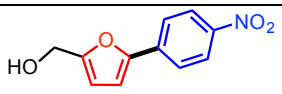	93
2	4-OCH_3	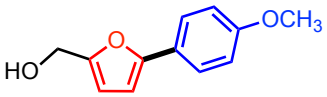	89
3	4-CF_3		87
4	H	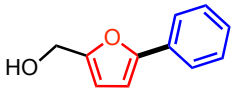	88

5	3-CF_3	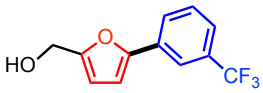	82
6	4-CH_3	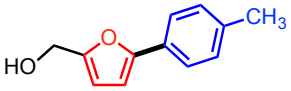	76
7	2-CH_3	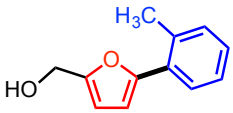	68
8	4-F	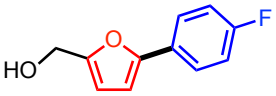	84
9	4-CO_2CH_3-2-CH_3	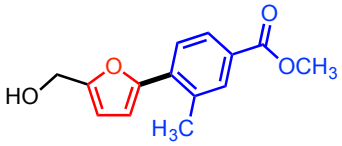	74
10	2-CH_3-5-NO_2	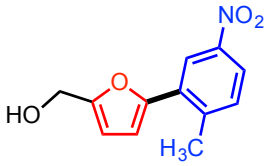	91
11	4-CN	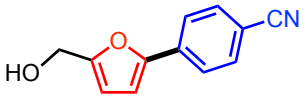	90
12	4-Ph	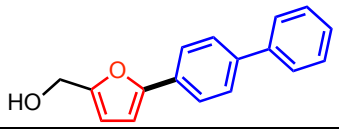	78

Conditions: Aryl bromide (1 equiv.), HMFA (2 equiv.), $Pd(acac)_2$ (5 mol%), JohnPhos (10 mol%), Cs_2CO_3 (1.5 equiv.), *n*-Bu_4NCl (0.3 equiv.), anhydrous DMF [0.1M], 170 °C, 8 min.

The decarboxylative cross-coupling reaction between HMFA and aryl bromides is robust and gives the corresponding products in good to excellent yields. Certain differences in the efficiency of the cross-coupling were observed due to the electronic effects of the cross-coupling partners. In general, higher yields were obtained for those coupling partners bearing functionalities that are electron withdrawing (nitro-, nitrile-, and CF_3-). Electron donating groups had a slightly lower yields (-OCH_3 and toluene derivatives). A small steric influence was observed with aryl halides bearing functionalities *ortho* to the bromide (entries 4 and 8), with a small decrease in yield. Overall, the results obtained proved to be positive to continue with the synthetic route, and different reaction conditions were tested for the synthesis of the bis(5-arylfuryl-2-yl)methane scaffolds (Figure 52 ,Table 18).

Table 18. Optimization of the reaction conditions for the acid-catalyzed pseudo-dimerization of 2-aryl-5-hydroxymethyl furans.

216 223

Entry	Solvent [0.2 M]	Acid (equiv.)	*n*-Bu$_4$NCl (1 equiv.)	Conditions	Yield (%)[a]
1	H_2O:DMA (1:1)	HCl (10)	No	30 min, 120 °C, μw	76
2	H_2O:DMA (1:1)	HCl (10)	Yes	30 min, 120 °C, μw	55
3	H_2O:DMA (1:1)	HCl (10)	No	18 h, 120 °C, Δ	50
4	H_2O	HCl (10)	No	30 min, 120 °C, μw	43
5	H_2O	HCl (10)	No	60 min, 120 °C, μw	73
6	H_2O	HCl (10)	Yes	30 min, 120 °C, μw	67
7	H_2O	HCl (10)	Yes	18 h, 120 °C, Δ	96
8	H_2O	HCl (10)	Yes	60 min, 120 °C, μw	81
9	H_2O:THF (1:3)	HCl (10)	Yes	18 h, 100 °C, Δ	85
10	H_2O:THF (1:3)	HCl (10)	Yes	30 min, 100 °C, μw	62
11	H_2O:THF (1:3)	TFA (10)	Yes	18 h, 40 °C, Δ	87
12	H_2O:THF (1:3)	TFA (10)	Yes	8 h, 40 °C, Δ	85
13	H_2O:THF (1:3)	TFA (10)	No	8 h, 40 °C, Δ	89
14	H_2O:THF (1:3)	TFA (15)	No	8 h, 40 °C, Δ	>99
15	H_2O:THF (1:3)	TFA (15)	No	4 h, 40 °C, Δ	>99

[a] HNMR using TMB as an internal standard

Initially, an organic co-solvent (DMA) was employed to fully dissolve 5-aryl-2-hydroxymethyl, and then mixed with HCl (entry 1) and heated in the microwave for 30 min. To

our surprise, these initial conditions gave a satisfactory 76% yield of the desired product, and equally as important, the 24% yield remaining was observed as unreacted starting material. This result suggested that optimization of the rection conditions could potentially result in even better yields. For this, we decided to add an alkyl ammonium salt, to facilitate the mixing of all the components of the reaction, but it resulted in an overall decrease in yield (entry 2), and some side-products were observed (alkylation of the hydroxy group on the starting material by the alkyl ammonium ion). Thermal heating conditions were tested (entry 3) but no improvement in yield was observed. The mixed solvent was replaced solely for water, and several heating modes were tested (entries 4 to 8), obtaining excellent results for termal reactions with the use of an additive (entry 7). The biggest concern at this point was the long reaction time and the use of relatively high temperatures, even when excellent yields were obtained for the *p*-benzotrifluoro derivative, it was known from parallel experiments, that those substrates bearing electron donating functionanilities had a low stability towards light and elevated temperature when exposed for prolonged time. The addition of a co-solvent with a lower boiling point (THF) allowed for lower reaction temperatures (entries 9 and 10), and the employment of trifluoroacetic acid (TFA) allowed for even lower reaction temperatures and shorter reaction times overall. The optimized conditions (entry 15) revealed a quantitative yield for the model reaction with a short reaction time and low temperature.

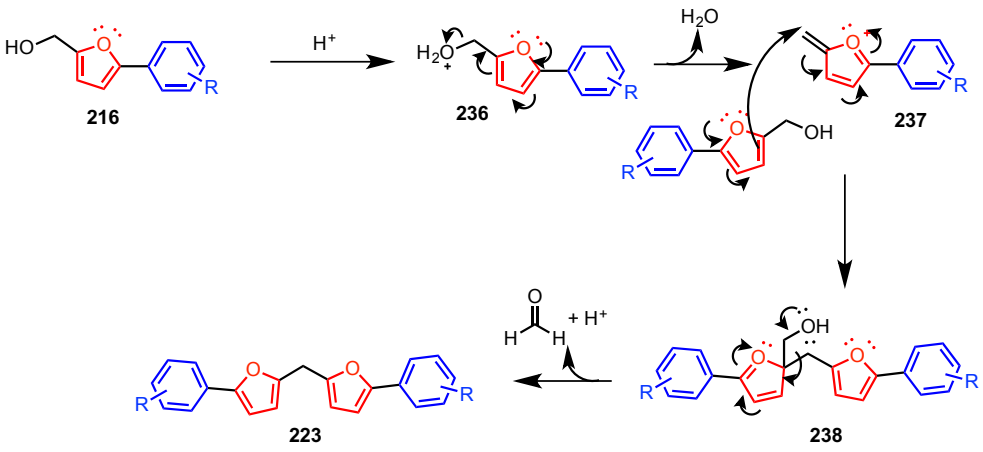

Figure 52. Mechanism for the acid-catalyzed formation of bis(5-arylfuran-2-yl)methane scaffolds.

Eventhough these conditions gave an excellent yield for the model reaction, when tested for the scope, the reaction times and temperature can vary (reactions monitored by TLC) according to the electronic nature of the aryl substituent. In table 19, time and temperature conditions are reported (additional to the 4 hours at 40 °C) if the reaction was not completed during that time.

Table 19. Scope of the pseudo-dimerization of 5-aryl-2-hydroxymethyl furan scaffolds.

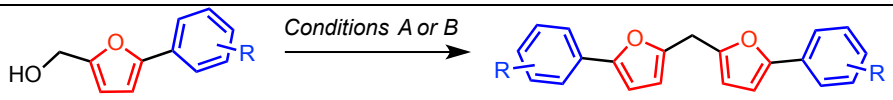

216 **223**

Entry	R	Product	Conditions[a]	Yield (%)[b]
1	4-NO_2	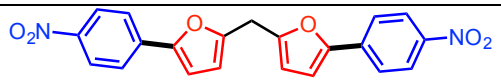	A	93
2	4-OCH_3	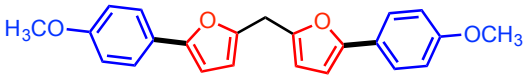	B	73
3	4-CF_3	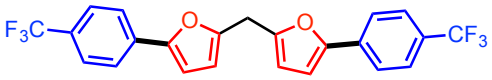	A	97
4	H	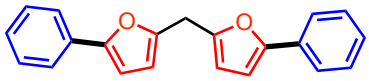	A	83
5	3-CF_3	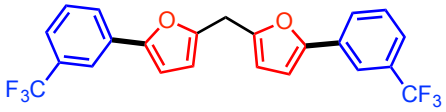	A	95
6	4-CH_3	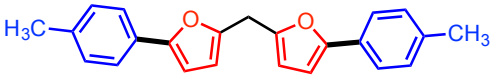	B	84
7	2-CH_3	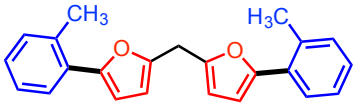	B	78
8	4-F	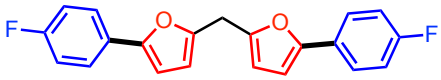	B	83
9	4-CO_2CH_3-2-CH_3	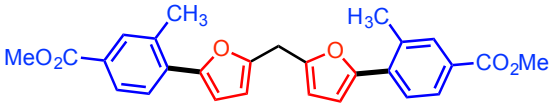	B	79
10	2-CH_3-5-NO_2	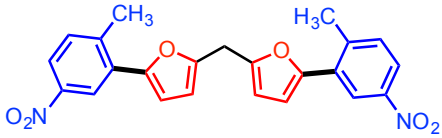	A	82
11	4-CN	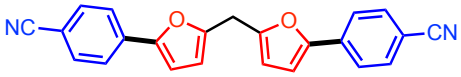	A	85
12	4-Ph	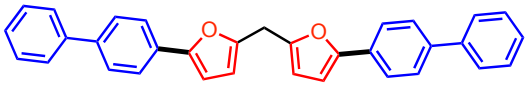	B	89

[a]Conditions: H_2O:THF (1:3), TFA (15 equiv.): (A) 40 °C for 4 h; (B) 40 °C for 4h and then increase to 60 °C for an additional 12 h. [b] Isolated yields using combiflash chromatography with silica gel and DCM:Hexanes (0:10 to 3:7).

When testing the scope of the reaction, some compound gave unsatisfactory yields (below 60 %) with the optimized conditions (Table 19, entry 15), specifically those bearing electron rich aryl groups. For this set of experiments, we decided to increase the temperature of the reaction to 60 °C after the 4 h at 40 °C, for an additional 12 h of heating. This behaviour suggest that even though the electron richness of substrates like the 4-OCH_3 derivative (entry 6) makes the furan ring a better nucleophile, it is the formation of the carbocation intermediate X the rate-limiting step of the overall reaction. Also, the products of these electron rich substrates tend to decompose faster when exposed to light (as seen by HNMR). Other substrates bearing electron neutral or electron defficient functionalities gave satisfactory yields when only heated for 4 h. In most cases, the reaction behave so neatly that no further purification after work-up was needed.

4.3. Conclusions

In conclusion, the influence of the steric and electronic nature of different aryl bromides in the efficiency of the decarboxylative cross-coupling with HMFA was studied, determining that electron defficient coupling partners favoured the reaction when compared to those electron defficient substrates. The optimization of the acid-mediated pseudo-dimerization of 5-aryl-2-hydroxymethyl furan scaffolds was achieved utilizing trifluoroacetic acid and a mixed solvent (THF:H_2O). The optimized conditions were adapted to those electron rich subtrates to obtain higher yields in the dimerization. In general, a new approach for the synthesis of bis(5-arylfuran-2-yl)methane scaffolds was developed utlizing biomass-derived resources as the starting point and environmentally friendly reaction conditions.

4.4. Experimental Section

Synthesis of 5-aryl-2-hydroxymethyl furans: To an oven-dried microwave vial (2-5 mL), with a stir bar, was added 114 mg of HMFA (0.8 mmol, 2 equiv.), 6.1 mg of $Pd(acac)_2$ (0.02 mmol, 5 mol%), 11.9 mg of JohnPhos (0.08 mmol, 10 mol%), 195 mg of Cs_2CO_3 (0.6 mmol, 1.5 equiv.), 0.4 mmol of the corresponding Aryl Bromide, 33 mg of *n*-Bu_4NCl (0.12 mmol, 30 mol%) and 4 mL of anhydrous DMF. The reaction is pre-stirred for 30 seconds and then submitting to

microwave irradiation to achieve 170 °C for 8 min at 900 rpm. The reaction crude is transferred to a 125 mL separatory funnel and diluted with 30 mL of EtOAc, washed with brine (2x20 mL), $NaHCO_{3(sat)}$ (1x20 mL). The combined aqueous phases are re-extracted with EtOAc (1x15 mL), and the combined organics are dried over Na_2SO_4. The solvent is removed under vaccuo and the crude is purified by Silica Gel chromatography to obtain the pure desired product.

Synthesis of bis(5-arylfuran-2-yl)methane scaffolds: To an oven-dried 5 mL amber vial, with a stir bar, was added 0.5 mmol of the corresponding 5-aryl-2hydroxymethyl furan (1 equiv.), 2.5 mL of THF:H_2O (3:1) and 575 µL of TFA (7.5 mmol, 15 equiv.). The vial is sealed and heated to 40 °C for 4 h. For those substrates with electron rich nature, and additional heating for 12 h at 60 °C was allowed. After the reaction is done, the crude is transferred to a diluted with EtOAc (20 mL), washed with $NaHCO_{3(sat)}$ (2x20 mL) and $NaCl_{(sat)}$ (1x20mL). The combined organics were dried over Na2SO4. The solvent is removed under vaccuo and the crude is purified by silica Gel Chromatography (when needed) utilizing DCM:Hex as eluent (0:10 to 3:7).

4.5. Characterization Data

Compound **216a** - (5-(4-nitrophenyl)furan-2-yl)methanol

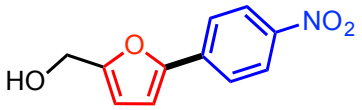

Compound **216a** was prepared following the general procedure for decarboxylative cross-coupling of HMFA and Aryl Bromides on a 0.4 mmol scale. The compound was isolated with column chromatography (R_f = 0.42) Hexanes:DCM:EtOAc (4:4:2) as a yellow solid. **^{1}H NMR** (500 MHz, $CDCl_3$) δ ppm 8.23 (d, *J* = 9.0 Hz, 2H), 7.78 (d, *J* = 9.0 Hz, 2H), 6.83 (d, *J* = 3.4 Hz, 1H), 6.46 (d, *J* = 3.4 Hz, 1H), 4.71 (s, 2H), 1.86 (bs, 1H). **^{13}C NMR** (125 MHz, $CDCl_3$) δ ppm 155.8 (1C), 151.6 (1C), 146.4 (1C), 136.2 (1C), 124.3 (2C), 123.9 (2C), 110.5 (1C), 109.7 (1C), 57.6 (1C). **HRMS (EI):** Exact mass calculated for $C_{11}H_8NO_4^-$ $[M-1]^{-\cdot}$ 218.0459, found 218.0455 (-1.8 ppm).

Compound **216b** – (5-(4-methoxyphenyl)furan-2-yl)methanol

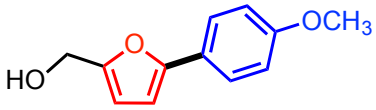

Compound **216b** was prepared following the general procedure for decarboxylative cross-coupling of HMFA and Aryl Bromides on a 0.4 mmol scale. The compound was isolated with column chromatography (R_f = 0.53) Hexanes:DCM:EtOAc (4:4:2) as a pale yellow solid. **^{1}H NMR** (500 MHz, $CDCl_3$) δ ppm 7.60 (d, *J* = 8.9 Hz, 2H), 6.92 (d, *J* = 8.9 Hz, 2H), 6.46 (d, *J* = 3.2 Hz, 1H), 6.34 (d, *J* = 3.2 Hz, 1H), 4.64 (s, 2H), 3.83 (s, 3H), 2.19 (bs, 1H). **^{13}C NMR** (125 MHz, $CDCl_3$) δ ppm 159.1 (1C), 154.2 (1C), 152.9 (1C), 125.3 (2C), 123.8 (1C), 114.1 (2C), 109.9 (1C), 104.1 (1C), 57.6 (1C), 55.3 (1C). **HRMS (EI):** Exact mass calculated for $C_{12}H_{11}O_3^-$ $[M-1]^{-\cdot}$ 203.0708, found 203.0705 (-1.3 ppm)

Compound **216c** - (5-(4-(trifluoromethyl)phenyl)furan-2-yl)methanol

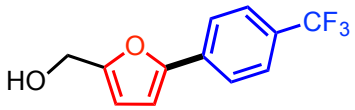

Compound **216c** was prepared following the general procedure for decarboxylative cross-coupling of HMFA and Aryl Bromides on a 0.4 mmol scale. The compound was isolated with column chromatography (R_f = 0.30) Hexanes:DCM:EtOAc (4:4:2) as a white solid. **^{1}H NMR** (500 MHz, $CDCl_3$) δ ppm 7.74 (d, *J* = 8.0 Hz, 2H), 7.61 (d, *J* = 8.0 Hz, 2H), 6.70 (d, *J* = 3.3 Hz, 1H), 6.40 (d, *J* = 3.3 Hz, 1H), 4.68 (s, 2H), 2.34 (bs, 1H). **^{13}C NMR** (125 MHz, $CDCl_3$) δ ppm 154.7 (1C), 152.4 (1C), 133.7 (1C), 129.0 (q, *J* = 32.5 Hz, 1C), 125.7 (q, *J* = 3.9 Hz, 2C), 124.1 (q, *J* = 271.2 Hz, 1C), 123.7 (2C), 110.1 (1C), 107.7 (1C), 57.5 (1C). **HRMS (EI):** Exact mass calculated for $C_{12}H_8F_3O_2^-$ $[M-1]^{-\cdot}$ 241.0477, found 241.0472 (-1.9 ppm)

Compound **216d** – (5-phenylfuran-2-yl)methanol

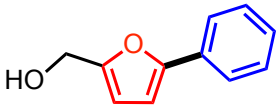

Compound **216d** was prepared following the general procedure for decarboxylative cross-coupling of HMFA and Aryl Bromides on a 0.4 mmol scale. The compound was isolated with column chromatography (R_f = 0.34) Hexanes:DCM:EtOAc (4:4:2) as a white solid. **^{1}H NMR** (500 MHz, $CDCl_3$) δ ppm 7.69 (m, 2H), 7.39 (m, 2H), 7.28 (m, 1H), 6.61 (d, *J* = 3.3 Hz, 1H), 6.39 (d, *J* = 3.3 Hz, 1H), 4.68 (s, 2H), 1.98 (bs, 1H). **^{13}C NMR** (125 MHz, $CDCl_3$) δ ppm 154.0 (1C), 153.6 (1C), 130.7 (1C), 128.7 (2C), 127.5 (1C), 123.8 (2C), 110.0 (1C), 105.7 (1C), 57.7 (1C). **HRMS (EI):** Exact mass calculated for $C_{11}H_9O_2^-$ $[M-1]^{-\cdot}$ 173.0603, found 173.0599 (-2.1 ppm)

Compound **216e** – (5-(3-(trifluoromethyl)phenyl)furan-2-yl)methanol

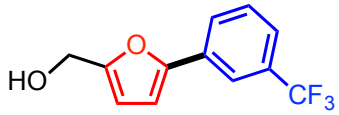

Compound **216e** was prepared following the general procedure for decarboxylative cross-coupling of HMFA and Aryl Bromides on a 0.4 mmol scale. The compound was isolated with column chromatography (R_f = 0.39) Hexanes:DCM:EtOAc (4:4:2) as a white solid. **^{1}H NMR** (500 MHz, $CDCl_3$) δ ppm 7.89 (s, 1H), 7.79 (s, 1H), 7.50 (m, 2H), 6.40 (d, *J* = 2.5 Hz, 1H), 6.25 (d, *J* = 2.5 Hz, 2H), 4.56 (s, 2H).**^{13}C NMR** (125 MHz, $CDCl_3$) δ ppm 154.5 (1C), 152.6 (1C), 131.5 (1C), 131.4 (q, *J* = 32.6 Hz, 1C), 129.3 (1C), 126.9 (q, *J* = 1.0 Hz, 1C), 124.2 (q, J = 272.6 Hz, 1C), 124.0 (q, J = 3.8 Hz, 1C), 120.7 (q, *J* = 4.0 Hz, 1C), 110.3 (1C), 107.2 (1C), 57.8 (1C). **HRMS (EI):** Exact mass calculated for $C_{12}H_8F_3O_2$ $[M-1]^{-\cdot}$ 241.0477, found 241.0472 (-1.9 ppm).

Compound **216f** – (5-(*p*-tolyl)furan-2-yl)methanol

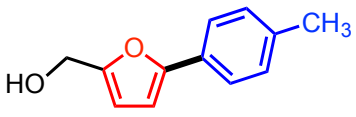

Compound 216f was prepared following the general procedure for decarboxylative cross-coupling of HMFA and Aryl Bromides on a 0.4 mmol scale. The compound was isolated with column chromatography (Rf = 0.44) Hexanes:DCM:EtOAc (4:4:2) as a light-yellow oil. **^{1}H NMR** (500

MHz, CDCl3) δ ppm 7.55 (d, *J* = 8.0 Hz, 2H), 7.17 (d, *J* = 8.0 Hz, 2H), 6.51 (d, *J* = 3.2 Hz, 1H), 6.34 (d, *J* = 3.2 Hz, 1H), 4.63 (s, 2H), 2.34 (s, 3H). **^{13}C NMR** (125 MHz, CDCl3) δ ppm 154.2 9 (1C), 153.2 (1C), 137.3 (1C), 129.3 (2C), 128.0 (1C), 123.75 (2C), 109.9 (1C), 104.9 (1C), 57.6 (1C), 21.3 (1C). HRMS (EI): Exact mass calculated for $C_{12}H_{11}O_2$ $[M-1]^{\cdot-}$ 187.0759, found 187.0753 (-3.0 ppm).

Compound **216g** – (5-(*o*-tolyl)furan-2-yl)methanol

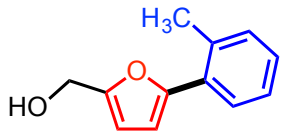

Compound 216g was prepared follow ing the general procedure for decarboxylative cross-coupling of HMFA and Aryl Bromides on a 0.4 mmol scale. The compound was isolated with column chromatography (Rf = 0.45) Hexanes:DCM:EtOAc (4:4:2) as a light-yellow oil. **^{1}H NMR** (500 MHz, CDCl3) δ ppm 7.69 (d, *J* = 7.7 Hz, 1H), 7.24 (m, 3H), 6.48 (d, *J* = 3.2 Hz, 1H), 6.40 (d, *J* = 3.2 Hz, 1H), 4.67 (s, 2H), 2.49 (s, 3H). **^{13}C NMR** (125 MHz, CDCl3) δ ppm 153.5 (1C), 153.1 (1C), 134.6 (1C), 131.1 (1C), 130.0 (1C), 127.6 (1C), 127.0 (1C), 126.0 (1C), 109.6 (1C), 109.3 (1C), 57.7 (1C), 21.8 (1C). HRMS (EI): Exact mass calculated for $C_{12}H_{11}O_2$ $[M-1]^{\cdot-}$ 187.0759, found 187.0754 (-2.5 ppm).

Compound **216h** – (5-(4-fluorophenyl)furan-2-yl)methanol

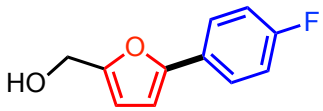

Compound 216h was prepared following the general procedure for decarboxylative cross-coupling of HMFA and Aryl Bromides on a 0.4 mmol scale. The compound was isolated with column chromatography (Rf = 0.39) Hexanes:DCM:EtOAc (4:4:2) as a white solid. **^{1}H NMR** (500 MHz, CDCl3) δ ppm 7.67 – 7.61 (m, 2H), 7.07 (t, *J* = 8.7 Hz, 2H), 6.53 (d, *J* = 3.3 Hz, 1H), 6.37 (d, *J* =

3.2 Hz, 1H), 4.66 (s, 2H).**^{13}C NMR** (125 MHz, CDCl3) δ ppm 163.2 (1C), 161.2 (1C), 153.4(d, *J* = 40.0 Hz, 1C), 153.22, 127.0 (d, *J* = 3.2 Hz, 1C), 125.6 (d, *J* = 8.1 Hz, 2C), 115.7 (d, *J* = 22.0 Hz, 2C), 110.0 (1C), 105.3 (1C), 57.6 (1C). HRMS (EI): Exact mass calculated for $C_{11}H_8FO_2$ $[M-1]^{\cdot}$ 191.0509, found 191.0507 (-0.8 ppm).

Compound **216i** – methyl 4-(5-(hydroxymethyl)furan-2-yl)-3-methylbenzoate

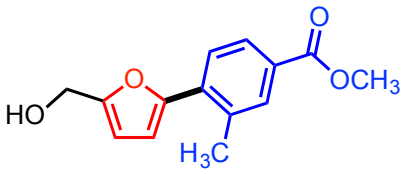

Compound 216i was prepared following the general procedure for decarboxylative cross-coupling of HMFA and Aryl Bromides on a 0.4 mmol scale. The compound was isolated with column chromatography (Rf = 0.34) Hexanes:DCM:EtOAc (4:4:2) as a white solid. **^{1}H NMR** (500 MHz, CDCl3) δ ppm 7.89 (m, 2H), 7.79 (d, *J* = 8.2 Hz, 1H), 6.62 (d, *J* = 3.4 Hz, 1H), 6.44 (d, *J* = 3.4 Hz, 1H), 4.70 (s, 2H), 3.92 (s, 3H), 2.54 (s, 3H). **^{13}C NMR** (125 MHz, CDCl3) δ ppm 167.0 (1C), 154.1 (1C), 152.4 (1C), 134.2 (1C), 132.4 (1C), 128.4 (1C), 127.2 (1C), 126.5 (1C), 111.3 (1C), 109.9 (1C), 57.6 (1C), 52.1 (1C), 22.1 (1C). HRMS (EI): Exact mass calculated for $C_{14}H_{13}O_4$ $[M-1]^{\cdot}$ 245.0814, found 245.0809 (-1.9 ppm).

Compound **216j** – (5-(2-methyl-5-nitrophenyl)furan-2-yl)methanol

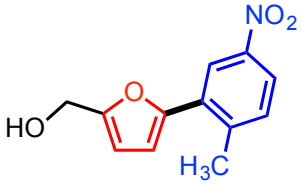

Compound 216j was prepared following the general procedure for decarboxylative cross-coupling of HMFA and Aryl Bromides on a 0.4 mmol scale. The compound was isolated with column chromatography (Rf = 0.45) Hexanes:DCM:EtOAc (4:4:2) as a golden yellow solid. **^{1}H NMR**

(500 MHz, CDCl3) δ ppm 8.57 (d, *J* = 2.4 Hz, 1H), 8.01 (dd, *J* = 8.4, 2.4 Hz, 1H), 7.38 (d, *J* = 8.4 Hz, 1H), 6.63 (d, *J* = 3.4 Hz, 1H), 6.46 (d, *J* = 3.4 Hz, 1H), 4.72 (s, 2H), 2.59 (s, 3H).**^{13}C NMR** (125 MHz, CDCl3) δ ppm 154.4 (1C), 150.9 (1C), 146.6 (1C), 141.6 (1C), 132.1 (1C), 131.1 (1C), 121.7 (1C), 121.7 (1C), 111.3 (1C), 109.9 (1C), 57.6 (1C), 22.2(1C). HRMS (EI): Exact mass calculated for $C_{12}H_{10}NO_4$ $[M-1]^{-\cdot}$ 232.0610, found 232.0606 (-1.6 ppm).

Compound **216k** – 4-(5-(hydroxymethyl)furan-2-yl)benzonitrile

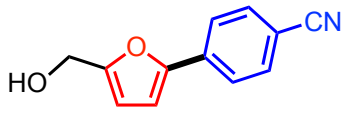

Compound 216k was prepared following the general procedure for decarboxylative cross-coupling of HMFA and Aryl Bromides on a 0.4 mmol scale. The compound was isolated with column chromatography (Rf = 0.34) Hexanes:DCM:EtOAc (4:4:2) as a white solid. **^{1}H NMR** (500 MHz, CDCl3) δ ppm 7.73 (d, *J* = 8.5 Hz, 2H), 7.64 (d, *J* = 8.5 Hz, 2H), 6.76 (d, *J* = 3.4 Hz, 1H), 6.43 (d, *J* = 3.4 Hz, 1H), 4.69 (d, *J* = 4.6 Hz, 2H). **^{13}C NMR** (125 MHz, CDCl3) δ 155.34, 151.9 (1C), 134.4 (1C), 132.6 (2C), 123.9 (2C), 118.9 (1C), 110.4 (1C), 110.0 (1C), 108.9 (1C), 77.3 (1C), 77.2 (1C), 77.0 (1C), 76.8 (1C), 57.6 (1C). HRMS (EI): Exact mass calculated for $C_{12}H_8NO_2$ $[M-1]^{-\cdot}$ 198.0555, found 198.0551 (-1.8 ppm).

Compound **216l** – (5-([1,1'-biphenyl]-4-yl)furan-2-yl)methanol

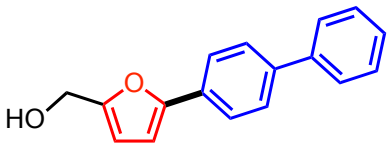

Compound 216l was prepared following the general procedure for decarboxylative cross-coupling of HMFA and Aryl Bromides on a 0.4 mmol scale. The compound was isolated with column chromatography (Rf = 0.40) Hexanes:DCM:EtOAc (4:4:2) as a white solid. **^{1}H NMR** (500 MHz, CDCl3) δ ppm 7.73 (m, 2H), 7.62 (m, 4H), 7.45 (m, 3H), 7.35 (m, 1H), 6.64 (d, *J* = 3.3 Hz, 1H),

6.40 (d, *J* = 3.3 Hz, 1H), 4.69 (s, 2H). **^{13}C NMR** (125 MHz, CDCl3) δ 15.8 (1C), 153.7 (1C), 140.5 (1C), 140.1 (1C), 129.6 (2C), 128.8 (1C), 127.4 (1C), 127.3 (2C), 126.9 (2C), 124.2 (2C), 110.1 (1C), 105.8 (1C), 57.7 (1C). HRMS (EI): Exact mass calculated for , $C_{17}H_{13}O_2$ $[M-1]^{-\cdot}$ 249.0916, found 249.0915 (-0.2 ppm).

Compound **223a** – bis(5-(4-nitrophenyl)furan-2-yl)methane

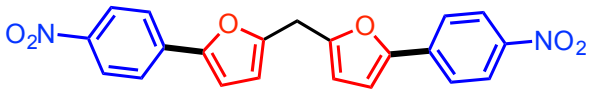

Compound 223a was prepared following the general procedure. The compound was isolated with column chromatography (Rf = 0.78) Hexanes:DCM (7:3) as a yellow solid. **^{1}H NMR** (500 MHz, CDCl3) δ ppm 8.24 (d, *J* = 9.0 Hz, 4H), 7.76 (d, *J* = 9.0 Hz, 4H), 6.84 (d, *J* = 3.4 Hz, 2H), 6.33 (d, *J* = 3.4 Hz, 2H), 4.21 (s, 2H). **^{13}C NMR** (125 MHz, CDCl3) δ 152.8 (2C), 151.1 (2C), 146.3 (2C), 136.3 (2C), 124.3 (4C), 123.6 (4C), 110.0 (2C), 109.9 (2C), 27.9 (1C). HRMS (EI): Exact mass calculated for $C_{21}H_{14}N_2O_6$ $M^{+\cdot}$ 390.0852, found 390.0855 (0.8 ppm).

Compound **223b** – bis(5-(4-methoxyphenyl)furan-2-yl)methane

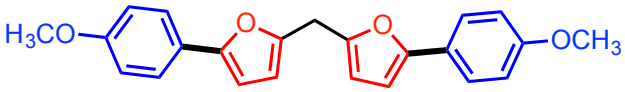

Compound 223b was prepared following the general procedure. The compound was isolated with column chromatography (Rf = 0.80) Hexanes:DCM (7:3) as a white solid. **^{1}H NMR** (500 MHz, CDCl3) δ ppm 7.58 (d, *J* = 8.4 Hz, 4H), 6.90 (d, *J* = 8.4 Hz, 4H), 6.44 (d, *J* = 3.0 Hz, 2H), 6.17 (d, *J* = 3.0 Hz, 2H), 4.11 (s, 2H), 3.82 (s, 6H). **^{13}C NMR** (125 MHz, CDCl3) δ 158.8 (2C), 153.0 (2C), 150.5 (2C), 124.9 (4C), 124.1 (2C), 114.0 (4C), 108.5 (2C), 104.2 (2C), 55.3 (2C), 27.8 (1C). HRMS (EI): Exact mass calculated for $C_{23}H_{20}O_4$ $M^{+\cdot}$ 360.1362, found 360.1367 (1.4 ppm).

Compound **223c** – bis(5-(4-(trifluoromethyl)phenyl)furan-2-yl)methane

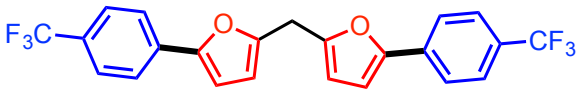

Compound 223c was prepared following the general procedure. The compound was isolated with column chromatography (Rf = 0.67) Hexanes:DCM (7:3) as a white solid. **^{1}H NMR** (500 MHz, CDCl3) δ ppm 7.73 (d, *J* = 8.2 Hz, 4H), 7.61 (d, *J* = 8.2 Hz, 4H), 6.71 (d, *J* = 3.3 Hz, 2H), 6.27 (d, *J* = 3.3 Hz, 2H), 4.17 (s, 2H). **^{13}C NMR** (125 MHz, CDCl3) δ 151.9 (2C), 121.7 (2C), 133.9 (q, *J* = 1.4 Hz, 4C), 128.7 (q, *J* = 32.2 Hz, 2C), 125.6 (q, *J* = 4.0 Hz, 4C), 124.1 (q, *J* = 271.7 Hz, 2C), 123.4 (2C), 109.3 (2C), 107.9 (2C), 27.8 (1C). HRMS (EI): Exact mass calculated for $C_{23}H_{14}F_6O_2$ $M^{+\cdot}$ 436.0898, found 436.0901 (0.7 ppm).

Compound **223d** – bis(5-phenylfuran-2-yl)methane

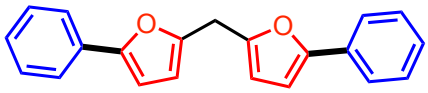

Compound 223d was prepared following the general procedure. The compound was isolated with column chromatography (Rf = 0.70) Hexanes:DCM (7:3) as a white solid (low melting point). **^{1}H NMR** (500 MHz, CDCl3) δ ppm 7.65 (d, *J* = 8.2 Hz, 4H), 7.36 (t, *J* = 8.0 Hz, 4H), 7.23 (m, 2H), 6.59 (d, *J* = 3.3 Hz, 2H), 6.21 (d, *J* = 3.3 Hz, 2H), 4.14 (s, 2H). **^{13}C NMR** (125 MHz, CDCl3) δ 153.0 (2C), 151.1 (2C), 130.9 (2C), 128.6 (4C), 127.0 (2C), 123.5 (4C), 108.7 (2C), 105.8 (2C), 27.8 (1C). HRMS (EI): Exact mass calculated for $C_{21}H_{16}O_2$ $M^{+\cdot}$ 300.1150, found 330.1153 (1.0 ppm).

Compound **223e** – bis(5-(3-(trifluoromethyl)phenyl)furan-2-yl)methane

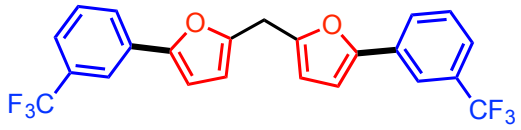

Compound 223e was prepared following the general procedure. The compound was isolated with column chromatography (Rf = 0.87) Hexanes:DCM (7:3) as a white solid. **^{1}H NMR** (500 MHz, CDCl3) δ ppm 7.88 (s, 2H), 7.80 (s, 2H), 7.48 (m, 4H), 6.68 (d, *J* = 2.5 Hz, 2H), 6.26 (d, *J* = 2.5 Hz, 2H), 4.16 (s, 2H).**^{13}C NMR** (125 MHz, CDCl3) δ 151.7 (2C), 151.6 (2C), 131.5 (2C), 131.1(q, *J* = 32.3 Hz, 2C), 129.1 (2C), 126.5 (2C), 123.0 (q, *J* = 272.4 Hz, 2C), 123.5 (q, *J* = 3.8 Hz, 2C), 120.2 (q, J = 3.9 Hz, 2C), 109.1 (2C), 107.2 (2C), 27.8 (1C). HRMS (EI): Exact mass calculated for , $C_{23}H_{14}F_6O_2$ $M^{+\cdot}$ 436.0898, found 436.0902 (0.9 ppm).

Compound **223g** – bis(5-(*o*-tolyl)furan-2-yl)methane

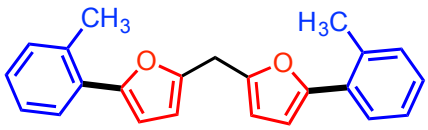

Compound 223g was prepared following the general procedure. The compound was isolated with column chromatography (Rf = 0.80) Hexanes:DCM (7:3) as a light-yellow liquid. **^{1}H NMR** (500 MHz, CDCl3) δ ppm 7.69 (d, *J* = 7.9 Hz, 2H), 7.20 (m, 6H), 6.47 (d, *J* = 3.3 Hz, 2H), 6.24 (d, *J* = 3.3 Hz, 2H), 4.15 (s, 2H), 2.48 (s, 6H). **^{13}C NMR** (125 MHz, CDCl3) δ ppm 152.6 (2C), 150.7 (2C), 134.3 (2C), 131.1 (2C), 130.2 (2C), 127.1 (2C), 126.7 (2C), 125.9 (2C), 109.4 (2C), 108.4 (2C), 27.8 (2C), 21.9 (1C). HRMS (EI): Exact mass calculated for $C_{23}H_{20}O_2$ $M^{+\cdot}$ 328.1463, found 328.1472 (2.7 ppm).

Compound **223i** – dimethyl 4,4'-(methylenebis(furan-5,2-diyl))bis(3-methylbenzoate)

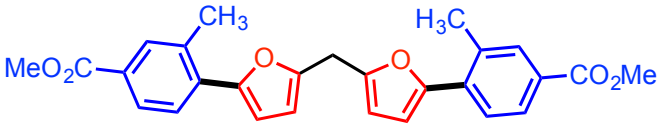

Compound 223i was prepared following the general procedure. The compound was isolated with column chromatography (Rf = 0.65) Hexanes:DCM (7:3) as a pale yellow solid. **^{1}H NMR** (500 MHz, CDCl3) δ ppm ^{1}H NMR (500 MHz, Chloroform-*d*) δ 7.89 (m, 4H), 7.78 (d, *J* = 8.1 Hz, 2H),

6.63 (d, *J* = 3.3 Hz, 2H), 6.30 (d, *J* = 3.3 Hz, 2H), 4.18 (s, 2H), 3.92 (s, 6H), 2.53 (s, 6H). **^{13}C NMR** (125 MHz, CDCl3) δ ppm ^{13}C NMR (126 MHz, cdcl$_3$) δ 166.9 (2C), 151.7 (2C), 151.4 (2C), 134.0 (2C), 133.9 (2C), 132.5 (2C), 128.1 (2C), 127.2 (2C), 126.1 (2C), 111.5 (2C), 109.0 (2C), 27.8 (1C), 22.1 (2C). HRMS (EI): Exact mass calculated for $C_{27}H_{24}O_6$ $M^{+\cdot}$ 444.1573, found 444.1579 (1.4 ppm).

Compound **223j** – bis(5-(2-methyl-5-nitrophenyl)furan-2-yl)methane

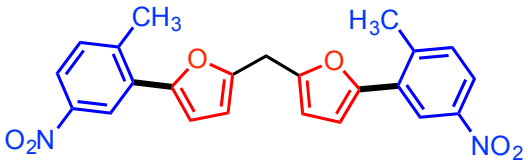

Compound 223j was prepared following the general procedure. The compound was isolated with column chromatography (Rf = 0.63) Hexanes:DCM (7:3) as a yellow gold solid. **^{1}H NMR** (500 MHz, CDCl3) δ ppm ^{1}H NMR (500 MHz, Chloroform-*d*) δ 8.56 (d, *J* = 2.3 Hz, 2H), 8.00 (dd, *J* = 8.5, 2.3 Hz, 2H), 7.37 (d, *J* = 8.4 Hz, 2H), 6.65 (d, *J* = 3.3 Hz, 2H), 6.33 (d, *J* = 3.3 Hz, 2H), 4.22 (s, 2H), 2.59 (s, 6H). **^{13}C NMR** (125 MHz, CDCl3) δ ppm 151.6 (2C), 150.3 (2C), 146.6 (2C), 141.3 (2C), 132.1 (2C), 131.2 (2C), 121.4 (2C), 121.4 (2C), 111.5 (2C), 109.1 (2C), 27.3 (1C), 22.3 (2C). HRMS (EI): Exact mass calculated for $C_{23}H_{18}N_2O_6$ $M^{+\cdot}$ 418.1165, found 418.1171 (1.4 ppm).

Compound **223k** – 4,4'-(methylenebis(furan-5,2-diyl))dibenzonitrile

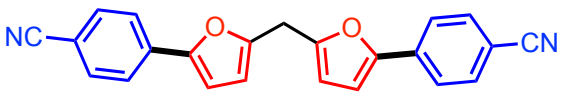

Compound 223k was prepared following the general procedure. The compound was isolated with column chromatography (Rf = 0.78) Hexanes:DCM (7:3) as a pale yellow solid. **^{1}H NMR** (500 MHz, CDCl3) δ ppm 7.70 (d, *J* = 8.6 Hz, 4H), 7.63 (d, *J* = 8.6 Hz, 4H), 6.76 (d, *J* = 3.4 Hz, 2H), 6.28 (d, *J* = 3.3 Hz, 2H), 4.16 (s, 2H). **^{13}C NMR** (125 MHz, CDCl3) δ ppm 152.3 (2C), 151.2 (2C), 134.5 (2C), 132.6 (4C), 123.6 (4C), 118.9 (2C), 110.1 (2C), 109.6 (2C), 109.2 (2C), 27.8

(1C). HRMS (EI): Exact mass calculated for $C_{23}H_{14}N_2O_2$ $M^{+\cdot}$ 350.1055, found 350.1057 (0.6 ppm).

Compound **223l** – bis(5-([1,1'-biphenyl]-4-yl)furan-2-yl)methane

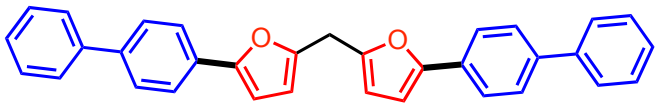

Compound 223l was prepared following the general procedure. The compound was isolated with column chromatography (Rf = 0.79) Hexanes:DCM (7:3) as a white solid. **^{1}H NMR** (500 MHz, CDCl3) δ ppm 7.72 (d, J = 7.5 Hz, 4H), 7.61 (m, 8H), 7.44 (m, 4H), 7.34 (m, 2H), 6.64 (s, 2H), 6.25 (s, 2H), 4.18 (s, 2H). **^{13}C NMR** (125 MHz, CDCl3) δ ppm 152.8 (2C), 151.2 (2C), 140.7 (2C), 139.7 (2C), 129.9 (2C), 128.8 (4C), 127.3 (4C), 127.2 (2C), 126.9 (4C), 123.9 (4C), 108.9 (2C), 106.1 (2C), 27.9 (1C). HRMS (EI): Exact mass calculated for $C_{33}H_{24}O_2$ $M^{+\cdot}$ 452.1776, found 452.1785 (2.0 ppm).

Chapter 5. General Conclusions and Future Directions

5.1. General Conclusions

The general objective of the research described in this thesis was to develop new chemical tools to achieve the transformation of biomass-derived furans into value-added commodity chemicals useful in many areas. Initially, the decarboxylative cross-coupling of 2,5-furandicarboxylic acid represented a challenge in both substrate and the transformation. A detailed optimization of reaction parameters overcame the limitations of the previously reported methods for the decarboxylative cross-coupling reactions on five-membered heteroaromatic rings. Good to excellent yields were obtained for a variety of aryl bromide and iodides, from which it was found that the iodine analogs reacted more efficiently to overall higher yields. The limitations for the scope of this project were tested, and it was concluded that employing aryl tosylates and/or free phenol groups in the aryl halide partner, was detrimental for the reaction and no product was isolated. Keeping in mind the importance on creating the green reaction condition, we decided to study the possibility of recycling the stoichiometric amount of Ag_2CO_3 used in the reaction, with recovery percentages that ranged between 79-84%.

After a successful synthesis of 2,5-diaryl symmetric furans, we decided to analyze the possibility of coming up with a non-symmetric route that could lead to two different aryl groups on either side of the furan. 5-hydroxymethyl furfural became the clear starting point for this route. Initially, some experimentation regarding the protection of the alcohol moiety and posterior oxidation were done, where it was found that conventional oxidation methods for the formyl group were not successful. After many attempts to oxidize this aldehyde, we explored the Cannizzaro disproportionation reaction, as a way to obtain simultaneously two important building blocks, HMFA and DHMF. For this purpose, a solvent-free methodology was developed where HMF was converted quantitatively to HMFA (acid or salt) and DHMF utilizing a planetary ball milling. This reaction is done in 5 minutes with an E_{factor} of 0.5 (which is 7 times smaller than the previous reports). We decided to test the scope of this reaction with a range of aromatic aldehydes. All examples gave excellent yields, and even a scale up (up to 12.8 g) of HMF was reacted successfully. With this HMFA in hand, the cross-coupling with Aryl bromides was tested, and to our surprise, the presence of the free alcohol on the HMFA favoured the yield of the reaction. To

inspect this behaviour deeply, we prepared some other modified HMFA derivatives, and the decarboxylative cross-coupling experiments followed a trend. The bulkier the group on the alcohol moiety, the lower the yield obtained for the decarboxylative cross-coupling reaction. Based on these findings we proposed a stabilizing interaction of the hydroxymethyl handle that could stabilize the Pd-complex and favour the C2 Palladation step. The carboxylic acid was obtained with a two-step oxidation. First a Cu-catalyzed biomimetic oxidation was done under aerobic conditions, and then an adapted Pinnick protocol was performed to oxidize the aldehyde to the carboxylic acids. These 5-aryl-2-furoic acids were submitted to a second decarboxylative cross-coupling reaction to obtain a large range of 2,5-diaryl non-symmetric furans with good to excellent overall yields. This synthetic route was used to achieve the formal synthesis of Dantrolene®, the chief drug in the treatment and prevention of malignant hyperthermia. The synthesis of the intermediate towards Dantrolene® was achieved with a high efficiency and circumventing the problems of the patented synthesis.

Finally, we decided to design a new approach for the synthesis of bis(5-arylfuran-2-yl)methane scaffolds. These synthetic targets have been reported to be important components of licorice, and used empirically as an ointment for the treatment of eczema. Synthetically, these scaffolds have been used in the synthesis of various condensed heterocyclic systems and as monomers and cross-linking reagents in polymer manufacturing. We envisioned that the 5-aryl-2-hydroxymethyl furan intermediates synthesized in the previous project, could be also utilized for the pseudo-dimerization into the desired new targets. First, we tested the scope of the decarboxylative cross-coupling of HMFA and a variety of aryl bromides, ranging in both electronic ad steric situations. Those electrophilic coupling partners bearing electron withdrawing groups had higher efficiencies in the cross-coupling than those with electron donating groups, but overall, we obtained good to excellent yields for all the coupling aryl bromides tested. We then optimized the acid-catalyzed pseudo-dimerization of these intermediates. We began to explore aqueous solutions and the influence of adding *n*-Bu_4NCl to help in the mixing of the reagents. We also explored the possibility of utilizing two different heating modes, microwave and conventional heating. The optimized conditions for the dimerization gave quantitative yields of the desired product with the model reaction [5-(4-benzotrifluoro)2-hydroxymethyl furan], and these conditions were later tested for a large scope. The intermediates that have electronic rich situations

needed to be heated for longer times in order to have good yields of the dimerization, and these reactions were ran in amber vials wrapped with aluminum foil, to prevent the degradation of the synthesized products.

In general, we developed three synthetic approaches for the synthesis of different derivatives 2- and or 5-arylated furans, which are motifs ubiquitously present in natural products, bioactive compounds of the pharmaceutical industry and modern materials for engineering applications.

References

(1) Stocker, T. *Climate Change Lecture Series*. 2014, pp 1–9.

(2) Graham, S. John Tyndall (1820-1893) https://earthobservatory.nasa.gov/features/Tyndall (accessed Aug 28, 2019).

(3) Callendar, G. S. *Q. J. R. Meteorol. Soc.* **1938**, *64* (275), 223–240.

(4) US Department of Commerce, N. O. and A. A. Mauna Loa Carbon Dioxide Record https://celebrating200years.noaa.gov/datasets/mauna/welcome.html#ded (accessed Aug 28, 2019).

(5) Revelle, R. R.; Shapero, D. C. *Environ. Conserv.* **1978**, *5* (2), 81–91.

(6) National Aeronautics and Space Administration. Global Climate Change: Vital Signs of the Planet https://climate.nasa.gov/effects/ (accessed Aug 28, 2019).

(7) United Nations. Vienna Convention for the Protection of the Ozone Layer https://treaties.un.org/pages/ViewDetails.aspx?src=TREATY&mtdsg_no=XXVII-2&chapter=27&clang=_en (accessed Aug 28, 2019).

(8) United Nations. (1988). The 1987 Montreal Protocol on Substances that Deplete the Ozone Layer. Montreal: United Nations Treaty Collection

(9) United Nations. Kyoto Protocol to the United Nations Framework Convention on Climate Change https://treaties.un.org/pages/ViewDetails.aspx?src=TREATY&mtdsg_no=XXVII-7-a&chapter=27&lang=en (accessed Aug 28, 2019).

(10) United Nations. The Paris Agreement | UNFCCC https://unfccc.int/process-and-meetings/the-paris-agreement/the-paris-agreement (accessed Aug 28, 2019).

(11) United States Environmental Protection Agency. Green Chemistry https://www.epa.gov/greenchemistry (accessed Aug 28, 2019).

(12) Anastas , P . T ., Warner, J. C. (1988), *Green Chemistry: Theory and Practice.* Oxford, England: Oxford University Press., 135.

(13) Kristin Seyboth; Sverrisson, F.; Appavou, F.; Brown, A.; Epp, B.; Leidreiter, A.; Lins, C.; Musolino, E.; Murdock, H. E.; Petrichenko, K.; Farrell, T. C.; Krader, T. T.; Tsakiris, A.; Sawin, J. L.; Skeen, J.; Sovacool, B. *Renewables 2016 Global Status Report*; Paris, France, 2016.

(14) Office of Energy Efficiency and Renewable Energy. Biomass Feedstocks https://www.energy.gov/eere/bioenergy/biomass-feedstocks (accessed Aug 28, 2019).

(15) Wynne, K. *Newsweek*. New York September 12, 2018.

(16) Dodds, D. R.; Gross, R. A. *Science*. 2007, pp 1250–1251.

(17) McNaught, A. D.; Wilkinson, A. *IUPAC. Compendium of Chemical Terminology*, 2nd ed.; Chalk, S., Ed.; IUPAC: Research Triagle Park, NC, 2019.

(18) Ur-Rehman, S.; Mushtaq, Z.; Zahoor, T.; Jamil, A.; Murtaza, M. A. *Crit. Rev. Food Sci. Nutr.* **2015**, *55* (11), 1514–1528.

(19) Tuck, C. O.; Perez, E.; Horvath, I.; Sheldon, R.; Poliakoff, M. *Science.* **2012**, *337* (6095), 695–699.

(20) Ballesteros, M.; Manzanares, P. In *The Role of Bioenergy in the Bioeconomy*; Academic Press, 2019; pp 113–144.

(21) Rubin, E. M. *Nature*. **2008**, *454* (7206), 841–845.

(22) Zhang, Y. H. P.; Lynd, L. R. *Proc. Natl. Acad. Sci. U. S. A.* **2005**, *102* (20), 7321–7325.

(23) Scheller, H. V.; Ulvskov, P. *Annu. Rev. Plant Biol.* **2010**, *61* (1), 263–289.

(24) Cherubini, F. *Energy Convers. Manag.* **2010**, *51*, 1412–1421.

(25) Kucherov, F. A.; Romashov, L. V; Galkin, K. I.; Ananikov, V. P. *ACS Sustain. Chem. Eng.* **2018**, *6* (7), 8064–8092.

(26) Dapsens, P. Y.; Mondelli, C.; Pérez-Ramírez, J. *ACS Catal.* **2012**, *2* (7), 1487–1499.

(27) Clark, J. H.; Luque, R.; Matharu, A. S. *Annu. Rev. Chem. Biomol. Eng.* **2012**, *3*, 183–207.

(28) Kang, E. S.; Hong, Y. W.; Chae, D. W.; Kim, B.; Kim, B.; Kim, Y. J.; Cho, J. K.; Kim, Y. G. *ChemSusChem* **2015**, *8* (7), 1179–1188.

(29) Kuster, B. F. M. *Starch - Stärke.* **1990**, *42* (8), 314–321.

(30) Agirrezabal-Telleria, I.; Gandarias, I.; Arias, P. L. *Catal. Today* **2014**, *234*, 42–58.

(31) van Dam, H. E.; Kieboom, A. P. G.; van Bekkum, H. *Starch - Stärke* **1986**, *38* (3), 95–101.

(32) Ståhlberg, T.; Fu, W.; Woodley, J. M.; Riisager, A. *ChemSusChem*. **2011**, *4*, 451–458.

(33) Chheda, J. N.; Huber, G. W.; Dumesic, J. A. *Angew. Chemie Int. Ed.* **2007**, *46* (38), 7164–7183.

(34) Dumesic, J.; Motagamwala, A. H. Method to produce furandicarboxylic acid (FDCA) from 5-hydroxymethylfurfural (HMF). US9617234B1, 2017.

(35) McKenna, S. M.; Leimkühler, S.; Herter, S.; Turner, N. J.; Carnell, A. J. *Green Chem.* **2015**, *17* (6), 3271–3275.

(36) Lolli, A.; Albonetti, S.; Utili, L.; Amadori, R.; Ospitali, F.; Lucarelli, C.; Cavani, F. *Appl. Catal. A Gen.* **2015**, *504*, 408–419.

(37) Sahu, R.; Dhepe, P. L. *React. Kinet. Mech. Catal.* **2014**, *112* (1), 173–187.

(38) Rathod, P. V; Jadhav, V. H. *ACS Sustain. Chem. Eng.* **2018**, *6* (5), 5766–5771.

(39) Ait Rass, H.; Essayem, N.; Besson, M. *Green Chem.* **2013**, *15* (8), 2240–2251.

(40) Siyo, B.; Schneider, M.; Pohl, M. M.; Langer, P.; Steinfelt, N. *Catal. Letters* **2014**, *144* (3), 498–506.

(41) Kumar Gupta, N.; Nishimura, S.; Takagaki, A.; Ebitani, K. *Green Chem.* **2011**, *13*, 824–

827.

(42) Yi, G.; Teong, S. P.; Zhang, Y. *Green Chem.* **2016**, *18* (4), 979–983.

(43) Grabowski, G.; Lewkowski, J.; Skowroński, R. *Electrochim. Acta* **1991**, *36* (13), 1995.

(44) Krystof, M.; Perez-Sanchez, M.; De Maria, P. D. *ChemSusChem* **2013**, *6* (5), 826–830.

(45) Qin, Y.-Z.; Li, Y.-M.; Zong, M.-H.; Wu, H.; Li, N. *Green Chem.* **2015**, *17* (7), 3718–3722.

(46) Thiyagarajan, S.; Pukin, A.; Van Haveren, J.; Lutz, M.; Van Es, D. S. *RSC Adv.* **2013**, *3* (36), 15678–15686.

(47) Bozell, J. J.; Petersen, G. R. *Green Chem.* **2010**, *12* (4), 539–554.

(48) Rieser, K.-P. (BASF); de Vries, A. (Avantium). *BASF and Avantium intend to establish joint venture*; 2016.

(49) Rosen, W.; Anderson, J. *DuPont Industrial Biosciences and ADM Announce Breakthrough Platform Technology for Long Sought-After Molecule Opens Up Vast Landscape of Bio-based Materials Offerings*; 2016.

(50) MetGen. METGEN INVENTS NOVELCHEMO-ENZYMATICROUTE TO FDCA - MetGen http://www.metgen.com/metgen-invents-new-technology-renewable-chemicals/ (accessed May 24, 2017).

(51) Corma Canos, A.; Iborra, S.; Velty, A. *Chem. Rev.* **2007**, *107* (6), 2411–2502.

(52) Villard, R.; Robert, F.; Blank, I.; Bernardinelli, G.; Soldo, T.; Hofmann, T. *J. Agric. Food Chem.* **2003**, *51* (14), 4040–4045.

(53) Katsuhisa Kojiri, Hisao Kondo, Hiroharu Arakawa, Mitsuru Ohkubo, H. S. Indolopyrrolocarbazole derivatives and antitumor agents. US6703373 B1, 2004.

(54) Fumagalli, T.; Sello, G.; Orsini, F. *Synth. Commun.* **2009**, *39* (12), 2178–2195.

(55) Goodman, S. N.; Jacobsen, E. N. *Adv. Synth. Catal.* **2002**, *344* (9), 953–956.

(56) Yu, C.; Liu, B.; Hu, L. *J. Org. Chem.* **2001**, *66* (16), 5413–5418.

(57) Chengzhi, Y.; Hu, L. *J. Org. Chem.* **2002**, *67* (1), 219–223.

(58) Cottier, L.; Descotes, G.; Soro, Y. *J. Carbohydr. Chem.* **2005**, *24* (1), 55–71.

(59) Lichtenthaler, F.; Willgraben, A. 5-(alpha-D-Glucopyranosyloxymethyl)-furan-2-carboxaldehyd und dessen Derivate und Folgerprodukte sowie Verfahren zur Herstellung der Verbindungen und deren Verwendung. 0426176A2, 1990.

(60) Williams, C. L.; Chang, C.-C.; Do, P.; Nikbin, N.; Caratzoulas, S.; Vlachos, D. G.; Lobo, R. F.; Fan, W.; Dauenhauer, P. J. *ACS Catal.* **2012**, *2* (6), 935–939.

(61) Mahmoud, E.; Yu, J.; Gorte, R. J.; Lobo, R. F. *ACS Catal.* **2015**, *5* (11), 6946–6955.

(62) Settle, A. E.; Berstis, L.; Rorrer, N. A.; Roman-Leshkóv, Y.; Beckham, G. T.; Richards, R. M.; Vardon, D. R. *Green Chem.* **2017**, *19* (15), 3468–3492.

(63) Sutton, A. D.; Waldie, F. D.; Wu, R.; Schlaf, M.; 'Pete'Silks, L. A.; Gordon, J. C. *Nat. Chem.* **2013**, *5* (5), 428–432.

(64) van Berkel, J. G. Process for enhancing the molecular weight of a polyester by solid state polimerization, WO2017043974A1. WO 2017/043974, 2017.

(65) Dai, Z. H.; Yang, Z. W.; Chen, Z. W.; Zhao, Z. X.; Lou, Y. J.; Zhang, Y. Y.; Liu, T. X.; Fu, F. Y.; Fu, Y. Q.; Liu, X. D. *ACS Sustain. Chem. Eng.* **2018**, *6* (11), 15056–15063.

(66) Kucherov, F. A.; Gordeev, E. G.; Kashin, A. S.; Ananikov, V. P. *Angew. Chemie - Int. Ed.* **2017**, *56* (50), 15931–15935.

(67) Elliot, B. A.; Liao, K.-H.; Shiftlett, M. B. Gas Separation Membrane using Furan-based Polymers. WO 2017/019435, 2017.

(68) De Jong, E.; Dam, M. A.; Sipos, L.; Gruter, G.-J. J. M. In *ACS Symposium Series*; 2012; Vol. 1105, pp 1–13.

(69) Miao, J. T.; Yuan, L.; Guan, Q.; Liang, G.; Gu, A. *ACS Sustain. Chem. Eng.* **2017**, *5* (8),

7003–7011.

(70) Li, H.; Liu, X.; Yang, T.; Zhao, W.; Saravanamurugan, S.; Yang, S. *ChemSusChem* **2017**, *10* (8), 1761–1770.

(71) Chang, F.; Hsu, W.-H.; Mascal, M. *Sustain. Chem. Pharm.* **2015**, *1*, 14–18.

(72) Ilkei, V.; Faragó, K.; Sánta, Z.; Dékány, M.; Hazai, L.; Szántay Jr., C.; Szántay, C.; Kalaus, G. *Int. J. Org. Chem.* **2014**, *04* (05), 309–313.

(73) Rajeena Ch, A.; Nayak, S. P.; Kamat, V.; Revanasiddappa, B. C.; Kumar, H. *J. Chem. Pharm. Res.* **2018**, *10* (6), 184–189.

(74) Haddach, M.; Michaux, J.; Schwaebe, M. K.; Pierre, F.; O'Brien, S. E.; Borsan, C.; Tran, J.; Raffaele, N.; Ravula, S.; Drygin, D.; Siddiqui-Jain, A.; Darjania, L.; Stansfield, R.; Proffitt, C.; MacAlino, D.; Streiner, N.; Bliesath, J.; Omori, M.; Whitten, J. P.; Anderes, K.; Rice, W. G.; Ryckman, D. M. *ACS Med. Chem. Lett.* **2012**, *3* (2), 135–139.

(75) Jiang, S.; Tala, S. R.; Lu, H.; Zou, P.; Avan, I.; Ibrahim, T. S.; Abo-Dya, N. E.; Abdelmajeid, A.; Debnath, A. K.; Katritzky, A. R. *Bioorganic Med. Chem. Lett.* **2011**, *21* (22), 6895–6898.

(76) Krause, T.; Gerbershagen, M. U.; Fiege, M.; Weißhorn, R.; Wappler, F. *Anaesthesia* **2004**, *59* (4), 364–373.

(77) Migulin, V. A.; Lvov, A. G.; Krayushkin, M. M. *Tetrahedron* **2017**, *73* (30), 4439–4449.

(78) Kim, J. T.; Kel'In, A. V.; Gevorgyan, V. *Angew. Chemie - Int. Ed.* **2003**, *42* (1), 98–101.

(79) Sromek, A. W.; Rubina, M.; Gevorgyan, V. *J. Am. Chem. Soc.* **2005**, *127* (30), 10500–10501.

(80) Jung, C. K.; Wang, J. C.; Krische, M. J. *J. Am. Chem. Soc.* **2004**, *126* (13), 4118–4119.

(81) Sromek, A. W.; Kel'in, A. V.; Gevorgyan, V. *Angew. Chemie - Int. Ed.* **2004**, *43* (17), 2280–2282.

(82) Dheur, J.; Sauthier, M.; Castanet, Y.; Mortreuxa, A. *Adv. Synth. Catal.* **2010**, *352* (2–3), 557–561.

(83) Zhang, M.; Jiang, H.-F.; Neumann, H.; Beller, M.; Dixneuf, P. H. *Angew. Chemie Int. Ed.* **2009**, *48* (9), 1681–1684.

(84) Yin, G.; Wang, Z.; Chen, A.; Gao, M.; Wu, A.; Pan, Y. *J. Org. Chem.* **2008**, *73* (9), 3377–3383.

(85) Rao, H. S. P.; Jothilingam, S. *J. Org. Chem.* **2003**, *68* (13), 5392–5394.

(86) Ackermann, L. *Modern arylation methods*; Weinheim: Wiley-VCH, 2009.

(87) Negishi, E.; de Meijere, A. *Handbook of Organopalladium Chemistry for Organic Synthesis*; 2002; Vol. 2.

(88) Ahlquist, M. S. G.; Norrby, P. O. *Angew. Chemie - Int. Ed.* **2011**, *50* (49), 11794–11797.

(89) Johansson Seechurn, C. C. C.; Kitching, M. O.; Colacot, T. J.; Snieckus, V. *Angew. Chemie Int. Ed.* **2012**, *51* (21), 5062–5085.

(90) Nicolaou, K. C.; Bulger, P. G.; Sarlah, D. *Angew. Chemie - Int. Ed.* **2005**, *44* (29), 4442–4489.

(91) Heck, R. F. *J. Am. Chem. Soc.* **1968**, *90* (20), 5518–5526.

(92) Fitton, P.; Johnson, M. P.; McKeon, J. E. *Chem. Commun.* **1968**, No. 1, 6–7.

(93) Mizoroki, T.; Mori, K.; Ozaki, A. *Bull. Chem. Soc. Jpn.* **1971**, *44* (2), 581–581.

(94) Heck, K. F.; Nolley, J. P. *J. Org. Chem.* **1972**, *37* (14), 2320–2322.

(95) Beletskaya, I. P.; Cheprakov, A. V. *Chem. Rev.* **2000**, *100* (8), 3009–3066.

(96) Wu, X. F.; Neumann, H.; Beller, M. *Angew. Chemie - Int. Ed.* **2010**, *49* (31), 5284–5288.

(97) Tamao, K.; Sumitani, K.; Kumada, M. *J. Am. Chem. Soc*. **1972**, *94* (12), 4374–4376.

(98) Corriu, R. J. P.; Masse, J. P. *Chem. Commun.* **1972**, *3*, 144.

(99) Job, A.; Reich, R. *C. R. Hebd. Seances Acad. Sci.* **1924**, *179*, 330–332.

(100) Kharasch, M. S.; Tawney, P. O. *J. Am. Chem. Soc.* **1941**, *63* (9), 2308–2316.

(101) Knappke, C. E. I.; Jacobi Von Wangelin, A. *Chem. Rev*. 2011, pp 4948–4962.

(102) Furstner, A. *Angew. Chem. - Int. Ed*. **2009**, *48* (8), 1364–1367.

(103) Hassan, J.; Sévignon, M.; Gozzi, C.; Schulz, E.; Lemaire, M. *Chem. Rev.* **2002**, *102* (5), 1359–1469.

(104) Ullmann, F.; Bielecki, J. *Berichte der Dtsch. Chem. Gesellschaft.* **1901**, *34* (2), 2174–2185.

(105) Glaser, C. *Berichte der Dtsch. Chem. Gesellschaft.* **1869**, *2* (1), 422–424.

(106) Li, J. J. *Name reactions : a collection of detailed reaction mechanisms*, Fourth Edition; Springer: London, 2009.

(107) Stephens, R. D.; Castro, C. E. *J. Org. Chem.* **1963**, *28* (12), 3313–3315.

(108) Sonogashira, K.; Tohda, Y.; Hagihara, N. *Tetrahedron Lett.* **1975**, *16* (50), 4467–4470.

(109) Liang, B.; Dai, M.; Chen, J.; Yang, Z. *J. Org. Chem.* **2005**, *70* (1), 391–393.

(110) Negishi, E.; King, A. O.; Okukado, N. *J. Org. Chem.* **1977**, *42* (10), 1821–1823.

(111) Fauvarque, J. F.; Jutand, A. *J. Organomet. Chem.* **1977**, *132* (2), C17–C19.

(112) Jin, L.; Lei, A. *Org. Biomol. Chem.* **2012**, *10* (34), 6817–6825.

(113) Milstein, D.; Stille, J. K. *J. Am. Chem. Soc.* **1978**, *100* (11), 3636–3638.

(114) Nagasawa, T.; Kuwahara, S. *Org. Lett.* **2013**, *15* (12), 3002–3005.

(115) Masse, C. E.; Yang, M.; Solomon, J.; Panek, J. S. *J. Am. Chem. Soc.* **1998**, *120* (17), 4123–4134.

(116) Miyaura, N.; Yamada, K.; Suzuki, A. *Tetrahedron Lett.* **1979**, *20* (36), 3437–3440.

(117) Roughley, S. D.; Jordan, A. M. *J. Med. Chem*. **2011**, *54* (1), 3451–3479.

(118) Alberico, D.; Scott, M. E.; Lautens, M. *Chem. Rev.* **2007**, *107* (1), 174–238.

(119) Chen, X.; Engle, K. M.; Wang, D. H.; Jin-Quan, Y. *Angew. Chem. - Int. Ed*. **2009**, *48* (28), 5094–5115.

(120) Seregin, I. V; Gevorgyan, V. *Chem. Soc. Rev.* **2007**, *36* (7), 1173–1193.

(121) Cho, S. H.; Kim, J. Y.; Kwak, J.; Chang, S. *Chem. Rev*. **2011**, *40* (10), 5068–5083.

(122) Wendlandt, A. E.; Suess, A. M.; Stahl, S. S. *Angew. Chem. - Int. Ed.* **2011**, *50* (47), 11062–11087.

(123) Kleiman, J. P.; Dubeck, M. *J. Am. Chem. Soc.* **1963**, *85* (10), 1544–1545.

(124) Chatt, J.; Davidson, J. M. *J. Am. Chem. Soc.* **1965**, *111*, 843–855.

(125) van Helden, R.; Verberg, G. *Recl. des Trav. Chim. des Pays-Bas* **1965**, *84* (10), 1263–1273.

(126) Fujiwara, Y.; Moritani, I.; Danno, S.; Asano, R.; Teranishi, S. *J. Am. Chem. Soc.* **1969**, *91* (25), 7166–7169.

(127) Kalyani, D.; Deprez, N. R.; Desai, L. V.; Sanford, M. S. *J. Am. Chem. Soc.* **2005**, *127* (20), 7330–7331.

(128) Dick, A. R.; Hull, K. L.; Sanford, M. S. *J. Am. Chem. Soc.* **2004**, *126* (8), 2300–2301.

(129) Daugulis, O.; Zaitsev, V. G. *Angew. Chemie - Int. Ed.* **2005**, *44* (26), 4046–4048.

(130) Dong, J. J.; Roy, D.; Roy, R. J.; Ionita, M.; Doucet, H. *Synthesis (Stuttg).* **2011**, *21*, 3530–3546.

(131) Holton, R. A.; Natalie, K. J. *Tetrahedron Lett.* **1981**, *22* (4), 267–270.

(132) Horino, H.; Inoue, N. *J. Org. Chem.* **1981**, *46* (22), 4416–4422.

(133) Canty, A. J.; van Koten, G. *Acc. Chem. Res.* **1995**, *28* (10), 406–413.

(134) Murai, S.; Kakiuchi, F.; Sekine, S.; Tanaka, Y.; Kamatani, A.; Sonoda, M.; Chatani, N. *Nature* **1993**, *366* (6455), 529–531.

(135) Chen, H.; Schlecht, S.; Semple, T. C.; Hartwig, J. F. *Science.* **2000**, *287* (5460), 1995–1997.

(136) Glover, B.; Harvey, K. A.; Liu, B.; Sharp, M. J.; Tymoschenko, M. F. *Org. Lett.* **2003**, *5* (3), 301–304.

(137) Krapcho, A. P.; Weimaster, J. F.; Eldridge, J. M.; Jahngen, E. G. E.; Lovey, A. J.; Stephens, W. P. *J. Org. Chem.* **1978**, *43* (1), 138–147.

(138) Krapcho, A. P. *ARKIVOC* **2007**, *2007* (ii), 1–53.

(139) Gong, Y.; Lin, L.; Shi, J.; Liu, S. *Molecules* **2010**, *15* (11), 7946–7960.

(140) Nilsson, M. *Acta Chem. Scand.* **1966**, *20*, 423–426.

(141) Heim, A.; Terpin, A.; Steglich, W. *Angew. Chem. Int. Ed.* **1997**, *36* (1), 155–156.

(142) Peschko, C.; Winklhofer, C.; Steglich, W. *Chem. - A Eur. J.* **2000**, *6* (7), 1147–1152.

(143) Myers, A. G.; Tanaka, D.; Mannion, M. R. *J. Am. Chem. Soc.* **2002**, *124* (38), 11250–11251.

(144) Tanaka, D.; Myers, A. G. *Org. Lett.* **2004**, *6* (3), 433–436.

(145) Goossen, L. J.; Guojun, D.; Levy, L. *Science* **2006**, *313* (5787), 662–664.

(146) Surry, D. S.; Buchwald, S. L. *Chem. Sci.* **2011**, *2* (1), 27–50.

(147) Goossen, L. J.; Zimmermann, B.; Knauber, T. *Angew. Chem. - Int. Ed.* **2008**, *47* (37), 7103–7106.

(148) Goossen, L. J.; Rodríguez, N.; Lange, P. P.; Linder, C. *Angew. Chemie - Int. Ed.* **2010**, *49* (6), 1111–1114.

(149) Goossen, L. J.; Rodríguez, N.; Linder, C. *J. Am. Chem. Soc.* **2008**, *130* (46), 15248–15249.

(150) Becht, J. M.; Catala, C.; Le Drian, C.; Wagner, A. *Org. Lett.* **2007**, *9* (9), 1781–1783.

(151) Becht, J.-M.; Le Drian, C. *Org. Lett.* **2008**, *10* (14), 3161–3164.

(152) Wang, Z.; Ding, Q.; He, X.; Wu, J. *Tetrahedron* **2009**, *65* (24), 4635–4638.

(153) Forgione, P.; Brochu, M.-C.; St-Onge, M.; Thesen, K. H.; Bailey, M. D.; Bilodeau, F. *J. Am. Chem. Soc.* **2006**, *128* (35), 11350–11351.

(154) Bilodeau, F.; Brochu, M. C.; Guimond, N.; Thesen, K. H.; Forgione, P. *J. Org. Chem.* **2010**, *75* (5), 1550–1560.

(155) Hassanpour, A.; De Carufel, C. A. nne; Bourgault, S.; Forgione, P. *Chemistry* **2014**, *20* (9), 2522–2528.

(156) Chen, F.; Wong, N. W. Y.; Forgione, P. *Adv. Synth. Catal.* **2014**, *356* (8), 1725–1730.

(157) Corma Canos, A.; Iborra, S.; Velty, A. *Chem. Rev*. **2007**, *107* (6), 2411–2502.

(158) Zhang, Z.; Deng, K. *ACS Catal.* **2015**, *5*, 6529–6544.

(159) Kroger, M.; Prueße, U.; Vorlop, K.-D. *Top. Catal.* **2000**, *13*, 237–242.

(160) De Jong, E.; Dam, M. A.; Sipos, L.; Gruter, G. J. M. In *ACS Symposium Series*; American Chemical Society: Washington, DC., 2012; Vol. 1105, pp 1–13.

(161) Myers, A. G.; Tanaka, D.; Mannion, M. R. *J. Am. Chem. Soc.* **2002**, *124*, 11250–11251.

(162) Tanaka, D.; Romeril, S. P.; Myers, A. G. *J. Am. Chem. Soc.* **2005**, *127* (29), 10323–10333.

(163) Goossen, L. J.; Rodríguez, N.; Melzer, B.; Linder, C.; Deng, G.; Levy, L. M. *J. Am. Chem. Soc.* **2007**, *129*, 4824–4833.

(164) Gooßen, L. J.; Zimmermann, B.; Knauber, T. *Angew. Chemie - Int. Ed.* **2008**, *47* (37), 7103–7106.

(165) Goossen, L. J.; Linder, C.; Rodríguez, N.; Lange, P. P. *Chem. - A Eur. J.* **2009**, *15* (37),

9336–9349.

(166) Goossen, L. J.; Lange, P. P.; Rodriguez, N.; Linder, C. *Chem. - A Eur. J.* **2010**, *16* (13), 3906–3909.

(167) Lange, P. P.; Goossen, L. J.; Podmore, P.; Underwood, T.; Sciammetta, N. *Chem. Commun.* **2011**, *47* (12), 3628.

(168) Bhadra, S.; Dzik, W. I.; Goossen, L. J. *J. Am. Chem. Soc.* **2012**, *134*, 9938–9941.

(169) Nandi, D.; Jhou, Y. M.; Lee, J. Y.; Kuo, B. C.; Liu, C. Y.; Huang, P. W.; Lee, H. M. *J. Org. Chem.* **2012**, *77* (20), 9384–9390.

(170) Jafarpour, F.; Zarei, S.; Olia, M. B. A.; Jalalimanesh, N.; Rahiminejadan, S. *J. Org. Chem.* **2013**, *78* (7), 2957–2964.

(171) Song, B.; Knauber, T.; Gooßen, L. J. *Angew. Chem. - Int. Ed.* **2013**, *52* (10), 2954–2958.

(172) Lovett, G. H.; Sparling, B. A. *Org. Lett.* **2016**, *18* (14), 3494–3497.

(173) Noble, A.; McCarver, S. J.; Macmillan, D. W. C. *J. Am. Chem. Soc.* **2015**, *137* (2), 624–627.

(174) Jin, Y.; Fu, H. *Asian J. Org. Chem.* **2017**, *6* (4), 368–385.

(175) Mangel, D.; Buonomano, C.; Sévigny, S.; Di Censo, G.; Thevendran, G.; Forgione, P. *Heterocycles* **2015**, *90* (2), 1228–1239.

(176) Goossen, L. J.; Rodríguez, N.; Melzer, B.; Linder, C.; Deng, G.; Levy, L. M. *J. Am. Chem. Soc.* **2007**, *129* (15), 4824–4833.

(177) Goossen, L. J.; Rodríguez, N.; Linder, C.; Lange, P. P.; Fromm, A. *ChemCatChem* **2010**, *2* (4), 430–442.

(178) Becht, J.-M.; Catala, C.; Le Drian, C.; Wagner, A. *Org. Lett.* **2007**, *9* (9), 1781–1783.

(179) Martin, R.; Buchwald, S. L. *Acc. Chem. Res.* **2008**, *41* (11), 1461–1473.

(180) Barrios-Landeros, F.; Carrow, B. *J. Am. Chem. Soc.* **2009**, *131*, 8141–8154.

(181) McMullin, C. L.; Jover, J.; Harvey, J. N.; Fey, N. *Dalt. Trans.* **2010**, *39*, 10833–10836.

(182) Tan, G.; He, S.; Huang, X.; Liao, X.; Cheng, Y.; You, J. *Angew. Chem. Int. Ed.* **2016**, *55* (35), 10414–10418.

(183) Gallezot, P. *Chem. Soc. Rev.* **2011**, *41* (41), 1538–1558.

(184) Werpy, T.; Petersen, G. *Top Value Added Chemicals from Biomass Volume I — Results of Screening for Potential Candidates from Sugars and Synthesis Gas Top Value Added Chemicals From Biomass Volume I : Results of Screening for Potential Candidates*; Springfield, VA., 2004; Vol. 1.

(185) Deng, L.; Li, J.; Lai, D. M.; Fu, Y.; Guo, Q. X. *Angew. Chemie - Int. Ed.* **2009**, *48* (35), 6529–6532.

(186) Li, C.; Xu, G.; Liu, X.; Zhang, Y.; Fu, Y. *Ind. Eng. Chem. Res.* **2017**, *56* (31), 8843–8849.

(187) Röper, H. *Starch/Staerke*. **2002**, *54* (3-4), 89.

(188) Van Putten, R.-J.; Van Der Waal, J. C.; De Jong, E.; Rasrendra, C. B.; Heeres, H. J.; De Vries, J. G. *Chem. Rev.* **2013**, *113*, 1499–1597.

(189) Mika, L. T.; Cséfalvay, E.; Németh, Á. *Chem. Rev*. **2018**, *118* (2), 505–613.

(190) Rosatella, A. A.; Simeonov, S. P.; Frade, R. F. M.; Afonso, C. A. M. *Green Chem.* **2011**, *13*, 754–793.

(191) Gupta, N. K.; Nishimura, S.; Takagaki, A.; Ebitani, K.; Jitsukawa, K.; Kaneda, K. *Green Chem.* **2011**, *13* (4), 824.

(192) Fang, R.; Luque, R.; Li, Y. *Green Chem.* **2016**, *18* (10), 3152–3157.

(193) Fang, R.; Luque, R.; Li, Y. *Green Chem.* **2017**, *19* (3), 647–655.

(194) Tan, P.; Li, G.; Fang, R.; Chen, L.; Luque, R.; Li, Y. *ACS Catal.* **2017**, *7* (4), 2948–2955.

(195) Fang, R.; Tian, P.; Yang, X.; Luque, R.; Li, Y. *Chem. Sci.* **2018**, *9* (7), 1854–1859.

(196) Xu, S.; Zhou, P.; Zhang, Z.; Yang, C.; Zhang, B.; Deng, K.; Bottle, S.; Zhu, H. *J. Am. Chem. Soc.* **2017**, *139* (41), 14775–14782.

(197) Gandini, A.; Belgacem, M. *Prog. Polym. Sci.* **1997**, *22*, 1203–1379.

(198) Boufi, S.; Gandini, A.; Belgacem, M. N. *Polymer (Guildf).* **1995**, *36* (8), 1689–1696.

(199) Subbiah, S.; Simenon, S.; Esperanca, J.; Rebelo, L. P.; Afonso, C. *Green Chem.* **2013**, *15*, 2849–2853.

(200) Cannizzaro, S. *Ann. der Chemie und Pharm.* **1853**, *88* (1), 129–130.

(201) Geissman, T. A. In *Organic Reactions*; John Wiley & Sons, Inc.: Hoboken, NJ, USA, 2011; pp 94–113.

(202) Kang, E. S.; Chae, D. W.; Kim, B.; Kim, Y. G. *J. Ind. Eng. Chem.* **2012**, *18* (1), 174–177.

(203) Ohyama, J.; Esaki, A.; Yamamoto, Y.; Arai, S.; Satsuma, A. *RSC Adv.* **2013**, *3*, 1033–1036.

(204) Constable, D. J. C.; Jimenez-Gonzalez, C.; Henderson, R. K. *Org. Process Res. Dev.* **2007**, *11* (1), 133–137.

(205) Nasir Baig, R. B.; Varma, R. S. *Chem. Soc. Rev* **2012**, *41* (41), 1559–1584.

(206) Varma, R. S. *ACS Sustain. Chem. Eng.* **2016**, *4* (11), 5866–5878.

(207) Margetić, D.; Štrukil, V. (2016). In *Mechanochemical Organic Synthesis: Chapter 1 - Practical Considerations in Mechanochemical Organic Synthesis*; Elsevier, pp 1–54.

(208) Fang, Y.; Salamé, N.; Woo, S.; Bohle, D. S.; Friščić, T.; Cuccia, L. A. *CrystEngComm* **2014**, *16* (31), 7180–7185.

(209) Stolle, A.; Ondruschka, B.; Krebs, A.; Bolm, C. In *Innovative Catalysis in Organic Synthesis*; Wiley-VCH Verlag GmbH & Co. KGaA: Weinheim, Germany, 2012; pp 327–349.

(210) Stolle, A.; Szuppa, T.; Leonhardt, S. E. S.; Ondruschka, B. *Chem. Soc. Rev*. 2011, pp 2317–2329.

(211) Sheldon, R. A. *Green Chem.* **2007**, *9* (12), 1273.

(212) Hazlet, S. E.; Stauffer, D. A. *J. Org. Chem.* **1962**, *27* (6), 2021–2024.

(213) Tiwari, R. D.; Srivastava, N. P. *Recl. des Trav. Chim. des Pays-Bas* **2010**, *75* (3), 254–256.

(214) Cheng, J. P.; Handoo, K. L.; Xue, J.; Parker, V. D. *J. Org. Chem.* **1993**, *58* (19), 5050–5054.

(215) Clark, J. H.; Luque, R.; Matharu, A. S. *Annu. Rev. Chem. Biomol. Eng.* **2012**, *3* (3), 183–207.

(216) Doods, D.; Gross, R. *Science* **2007**, *318* (5854), 1250–1251.

(217) Vennestrøm, P. N. R.; Osmundsen, C. M.; Christensen, C. H.; Taarning, E. *Angew. Chem. Int. Ed.* **2011**, *50* (45), 10502–10509.

(218) Bicker, M.; Kaiser, D.; Ott, L.; Vogel, H. *J. Supercrit. Fluids* **2005**, *36*, 118–126.

(219) Fan, W.; Verrier, C.; Queneau, Y.; Popowycz, F. *Curr. Org. Synth.* **2019**, *16* (4), 583–614.

(220) Vijjamarri, S.; Streed, S.; Serum, E. M.; Sibi, M. P.; Du, G. *ACS Sustain. Chem. Eng.* **2018**, *6* (2), 2491–2497.

(221) Rao, K. T. V.; Rogers, J. L.; Souzanchi, S.; Dessbesell, L.; Ray, M. B.; Xu, C. (Charles). *ChemSusChem* **2018**, *11* (18), 3323–3334.

(222) Kobayashi, H.; Fukuoka, A. *Green Chem.* **2013**, *15* (7), 1740.

(223) Dapsens, P. Y.; Mondelli, C.; Perez-Ramirez, J. *ACS Catal.* **2012**, *2* (7), 1487–1499.

(224) Serum, E. M.; Selvakumar, S.; Zimmermann, N.; Sibi, M. P. *Green Chem.* **2018**, *20* (7), 1448–1454.

(225) Lin, Y. L.; Tsai, Y. L.; Kuo, Y. H.; Liu, Y. H.; Shiao, M. S. *J. Nat. Prod.* **1999**, *62* (11),

1500–1503.

(226) Woo, C. H.; Beaujuge, P. M.; Holcombe, T. W.; Lee, O. P.; Fréchet, J. M. J. *J. Am. Chem. Soc.* **2010**, *132* (44), 15547–15549.

(227) Kel'in, A. V.; Gevorgyan, V. *J. Org. Chem.* **2002**, *67* (1), 95–98.

(228) Kamijo, S.; Kanazawa, C.; Yamamoto, Y. *J. Am. Chem. Soc.* **2005**, *127* (25), 9260–9266.

(229) Iqbal, J.; Bhatia, B.; Nayyar, N. K. *Chem. Rev.* **1994**, *94* (2), 519–564.

(230) Patil, N. T.; Yamamoto, Y. *Chem. Rev.* **2008**, *108*, 3395–3442.

(231) Dheur, J.; Sauthier, M.; Castanet, Y.; Mortreuxa, A. *Adv. Synth. Catal.* **2010**, *352* (2–3), 557–561.

(232) Chacón-Huete, F.; Mangel, D.; Ali, M.; Sudano, A.; Forgione, P. *ACS Sustain. Chem. Eng.* **2017**, *5* (8), 7071–7076.

(233) Chacón-Huete, F.; Messina, C.; Chen, F.; Cuccia, L.; Ottenwaelder, X.; Forgione, P. *Green Chem.* **2018**, *20* (23), 5261–5265.

(234) Li, G.; Wan, L.; Zhang, G.; Leow, D.; Spangler, J.; Yu, J. Q. *J. Am. Chem. Soc.* **2015**, *137* (13), 4391–4397.

(235) Ma, S.; Villa, G.; Thuy-Boun, P. S.; Homs, A.; Yu, J. Q. *Angew. Chem. - Int. Ed.* **2014**, *53* (3), 734–737.

(236) Boele, M. D. K.; Van Strijdonck, G. P. F.; De Vries, A. H. M.; Kamer, P. C. J.; De Vries, J. G.; Van Leeuwen, P. W. N. M. *J. Am. Chem. Soc.* **2002**, *124* (8), 1586–1587.

(237) Zhao, M.; Li, J.; Mano, E.; Song, Z.; Tschaen, D. M.; Grabowski, E. J. J.; Reider, P. J. *J. Org. Chem.* **1999**, *64* (7), 2564–2566.

(238) Malik, P.; Chakraborty, D. *Synthesis* **2010**, *21*, 3736–3740.

(239) Das, R.; Chakraborty, D. *Appl. Organomet. Chem.* **2011**, *25* (6), 437–442.

(240) Takemoto, T.; Yasuda, K.; Ley, S. V. *Synlett* **2001**, No. 10, 1555–1556.

(241) Jiang, X.; Ma, S. *Synth.* **2018**, *50* (8), 1629–1639.

(242) Ciriminna, R.; Pagliaro, M. *Org. Process Res. Dev.* **2010**, *14* (1), 245–251.

(243) Xu, B.; Lumb, J. P.; Arndtsen, B. A. *Angew. Chem. - Int. Ed.* **2015**, *54* (14), 4208–4211.

(244) Lindgren, B. O.; Nilsson, T. *Acta Chem. Scand.* **1973**, *27*, 888–890.

(245) Bal, B. S.; Childers, W. E.; Pinnick, H. W. *Tetrahedron* **1981**, *37* (11), 2091–2096.

(246) Senn, H. M.; Ziegler, T. *Organometallics* **2004**, *23* (12), 2980–2988.

(247) Hosoya, T.; Aoyama, H.; Ikemoto, T.; Kihara, Y.; Hiramatsu, T.; Endo, M.; Suzuki, M. *Bioorganic Med. Chem.* **2003**, *11* (5), 663–673.

(248) Davis, C. S.; Snyder, H. R. 1-(5-SUBSTITUTED)FURFURYLIDENEAMINO HYDANTONS AND MIDAZOLIDINONES. US 3415821, 1968.

(249) Snyder, H. R.; Davis, C. S.; Bickerton, R. K.; Halliday, R. P. *J. Med. Chem.* **1967**, *10* (5), 807–810.

(250) Fabry, D. C.; Ho, Y. A.; Zapf, R.; Tremel, W.; Panthöfer, M.; Rueping, M.; Rehm, T. H. *Green Chem.* **2017**, *19* (8), 1911–1918.

(251) Ahmed, J.; Sau, S. C.; P, S.; Hota, P. K.; Vardhanapu, P. K.; Vijaykumar, G.; Mandal, S. K. *European J. Org. Chem.* **2017**, *2017* (5), 1004–1011.

(252) Durola, F.; Hanss, D.; Roesel, P.; Sauvage, J. P.; Wenger, O. S. *European J. Org. Chem.* **2007**, *1*, 125–135.

Appendices

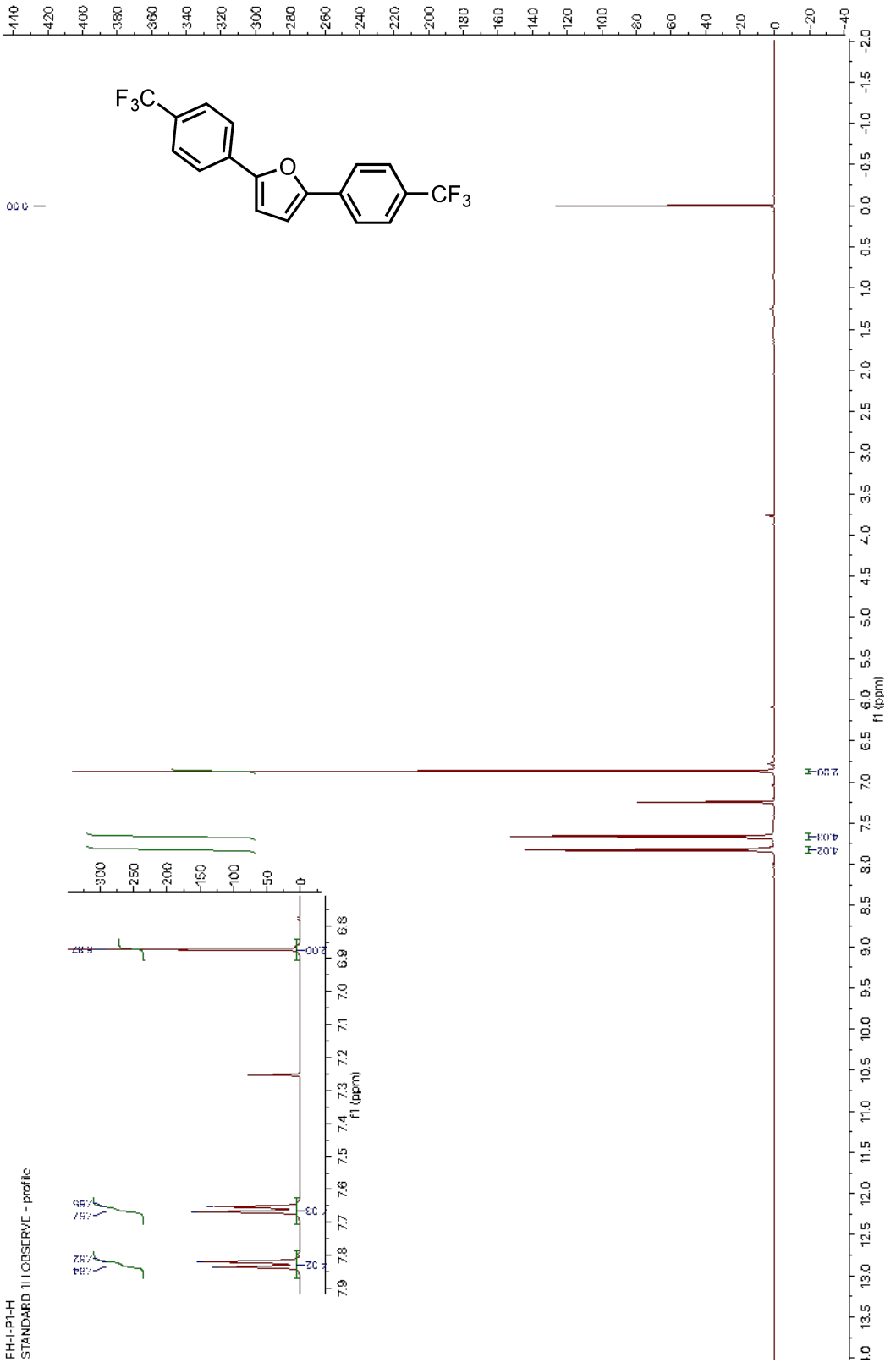

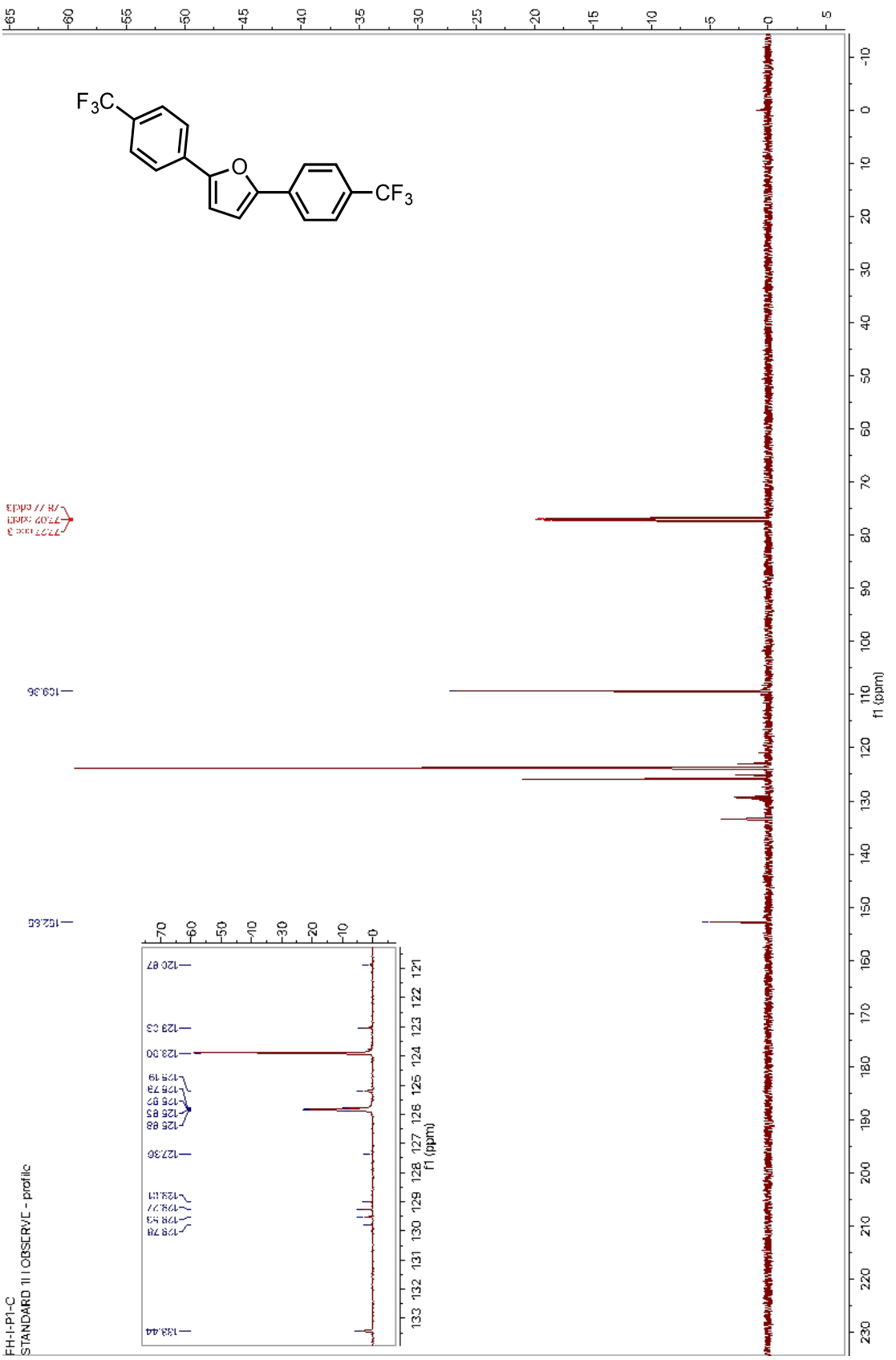
F3C
O
CF3
FH-I-P1-C
STANDARD 1H OBSERVE - profile
f1 (ppm)

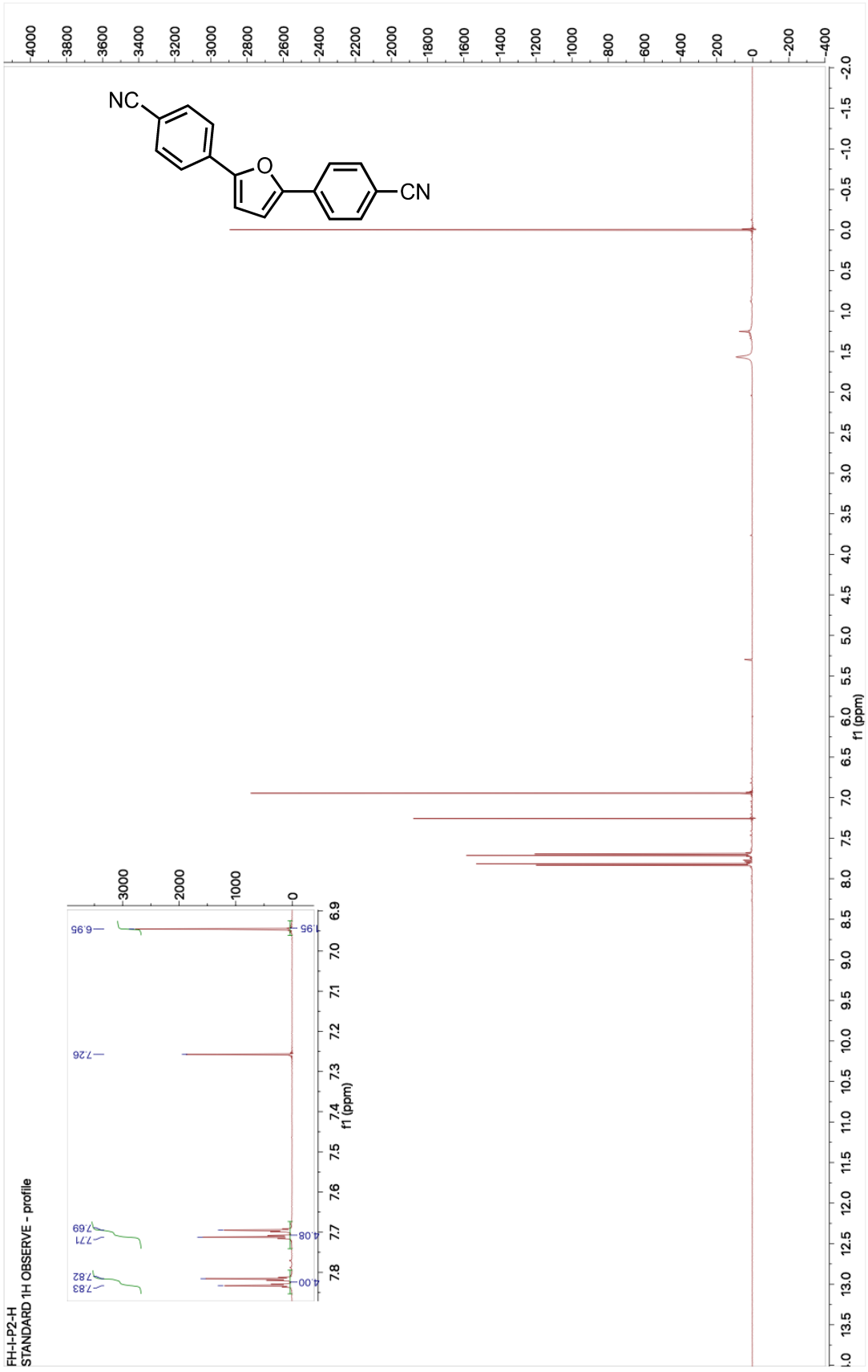
NC
O
CN
FH-I-P2-H
STANDARD 1H OBSERVE - profile
f1 (ppm)
6.95
7.26
7.69
7.71
7.82
7.83
1.95
4.08
4.00

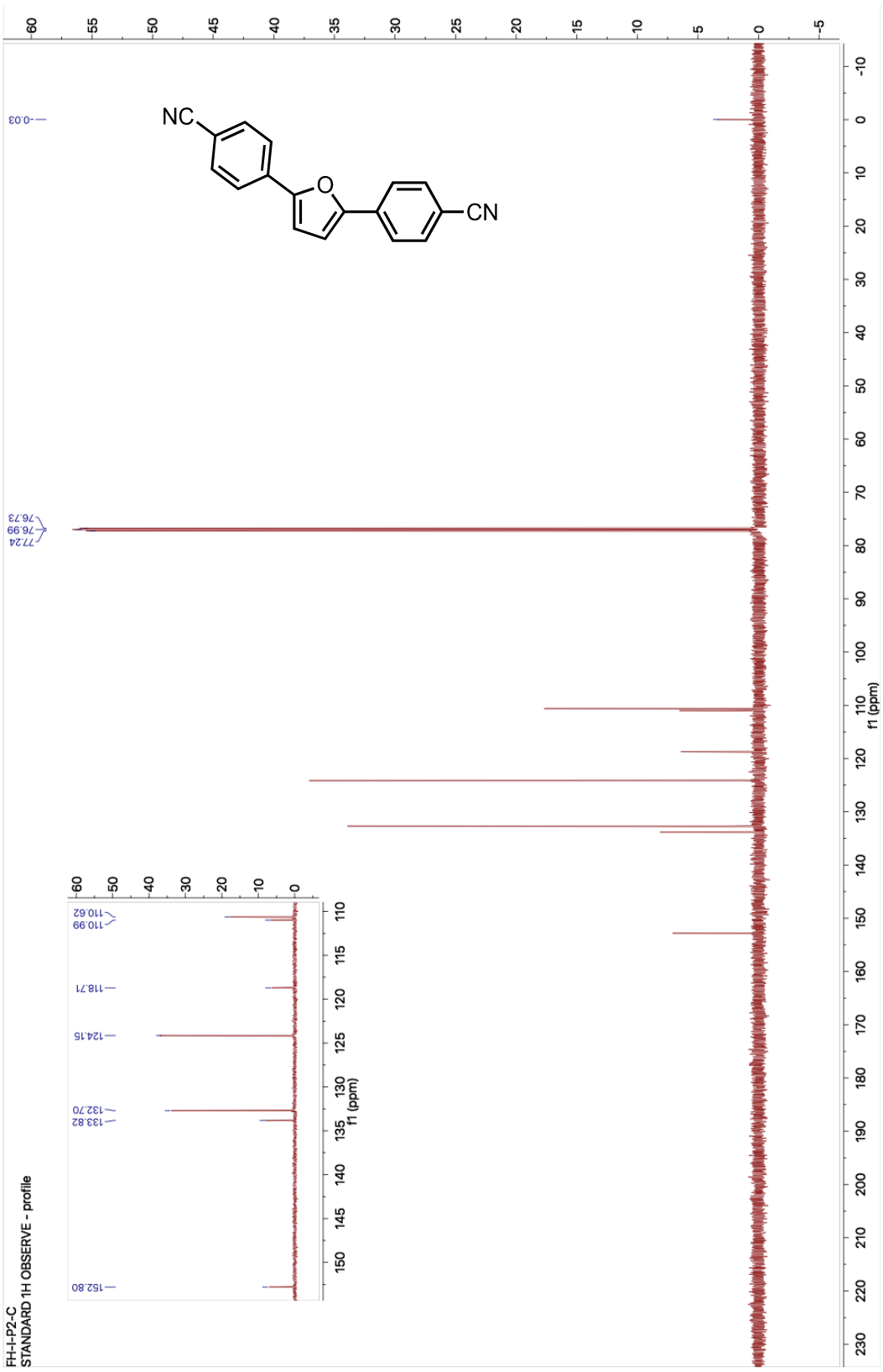
NC
O
CN
-0.03
77.24
76.99
76.73
110.99
110.62
118.71
124.15
133.82
132.70
152.80
f1 (ppm)
FH-I-P2-C
STANDARD 1H OBSERVE - profile

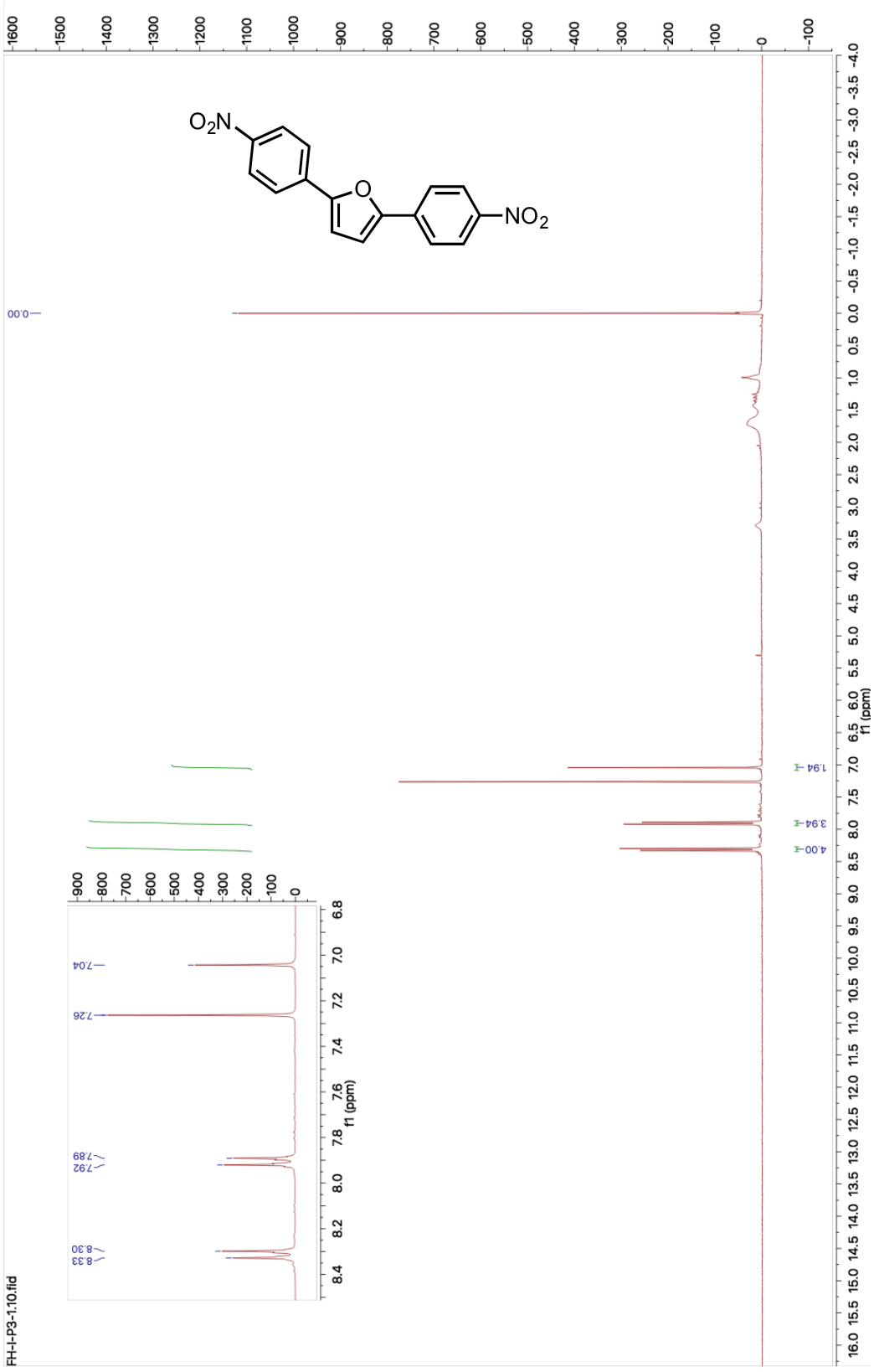
O2N
O
NO2
0.00
1.94
3.94
4.00
7.04
7.26
7.89
7.92
8.30
8.33
f1 (ppm)
FH-I-P3-1.10.fid

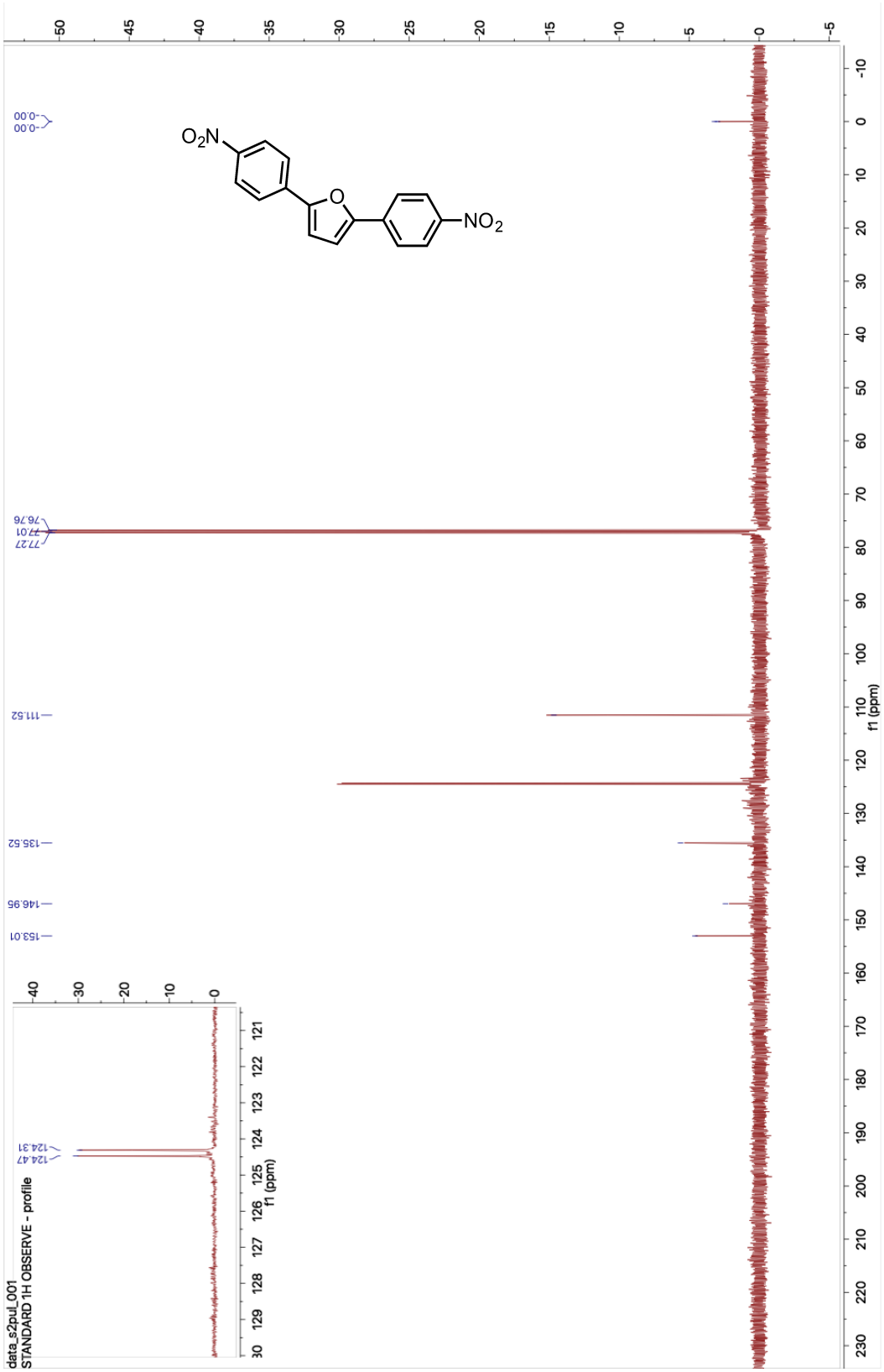
O2N
O
NO2
f1 (ppm)
data_s2pul_001
STANDARD 1H OBSERVE - profile

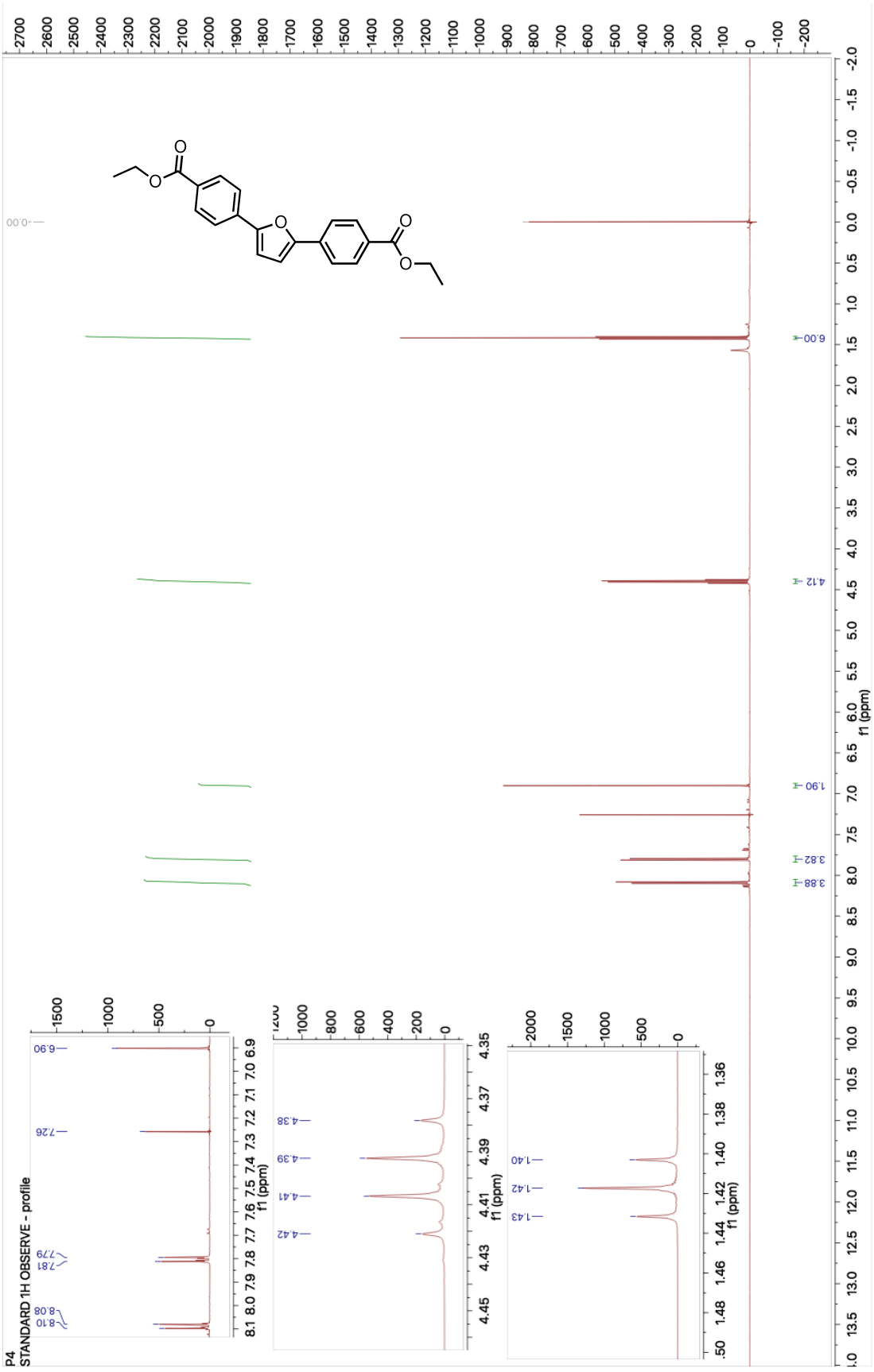
P4
STANDARD 1H OBSERVE - profile
f1 (ppm)
6.00
4.12
1.90
3.82
3.88

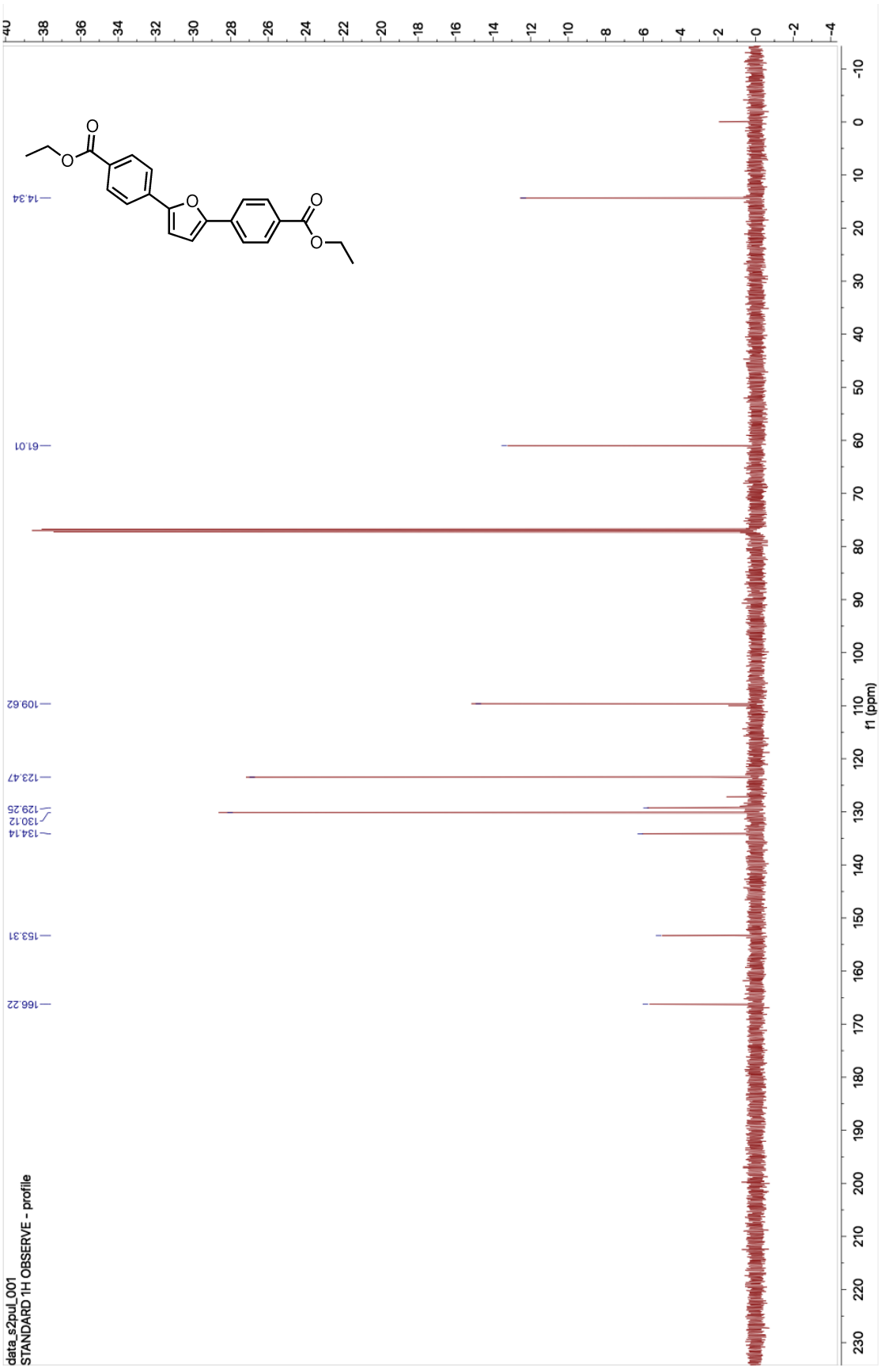
14.34
61.01
109.62
123.47
129.25
130.12
134.14
153.31
166.22
f1 (ppm)
data_s2pul_001
STANDARD 1H OBSERVE - profile

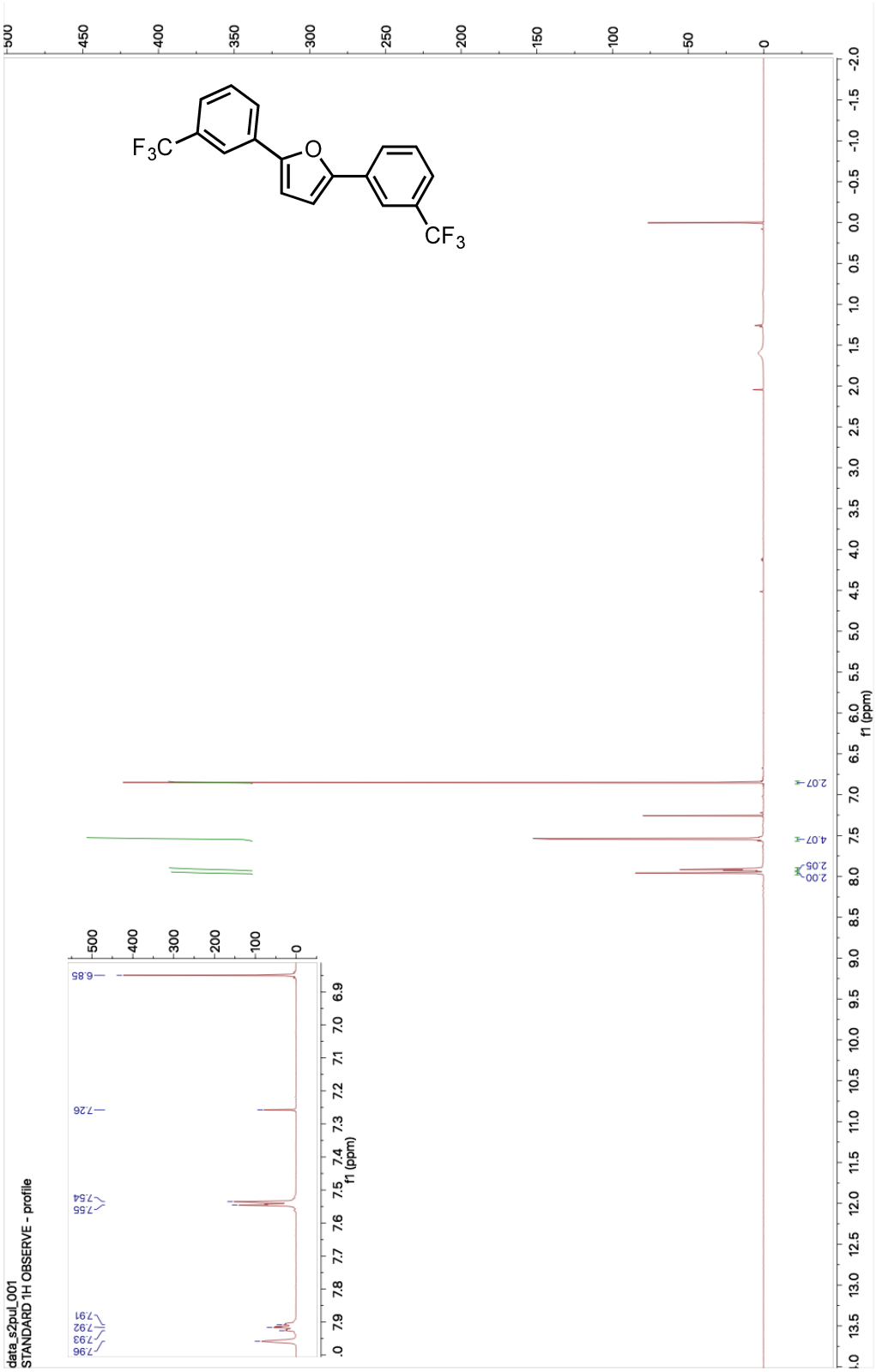
F3C
O
CF3
2.07
4.07
2.05
2.00
f1 (ppm)
data_s2pul_001
STANDARD 1H OBSERVE - profile
6.85
7.26
7.55
7.54
7.93
7.92
7.91
7.96
f1 (ppm)

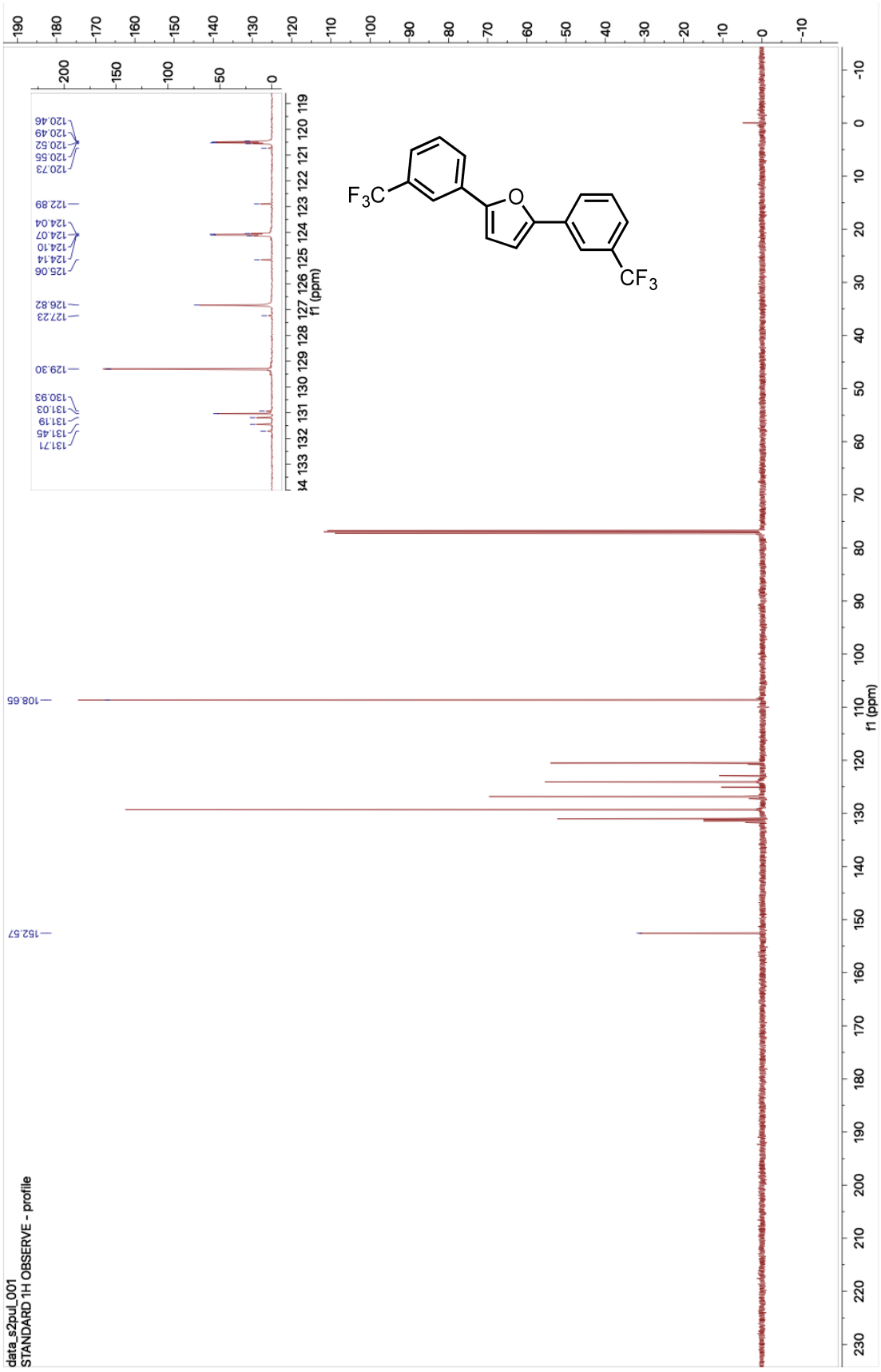
data_s2pul_001
STANDARD 1H OBSERVE - profile
f1 (ppm)
F3C
O
CF3
152.57
108.65
131.71
131.45
131.19
131.03
130.93
129.30
127.23
126.82
125.06
124.14
124.10
124.07
124.04
122.89
120.73
120.55
120.52
120.49
120.46

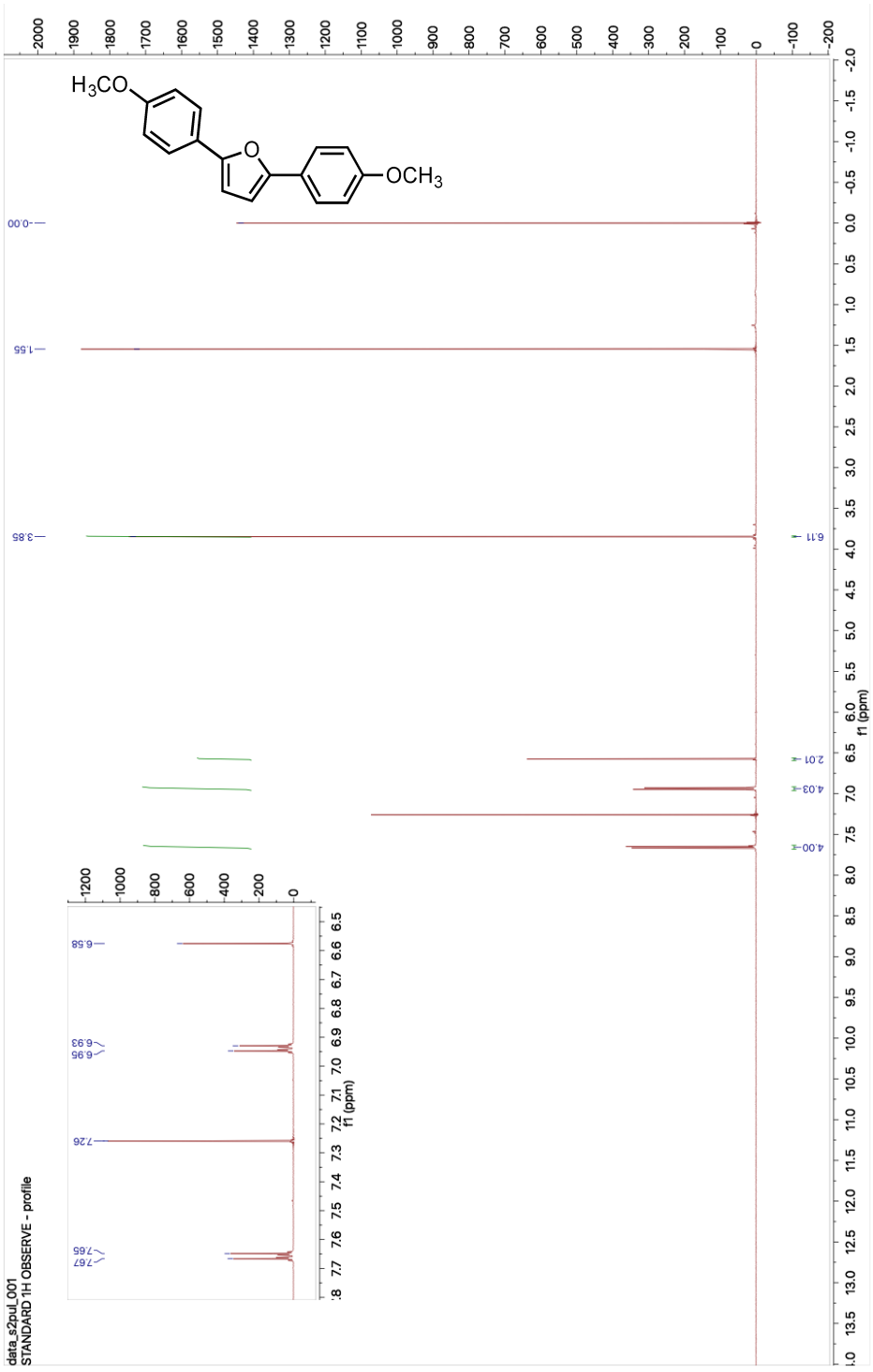
H3CO
O
OCH3
data_s2pul_001
STANDARD 1H OBSERVE - profile
f1 (ppm)
0.00
1.55
3.85
6.11
2.01
4.03
4.00
6.58
6.95
6.93
7.26
7.67
7.65

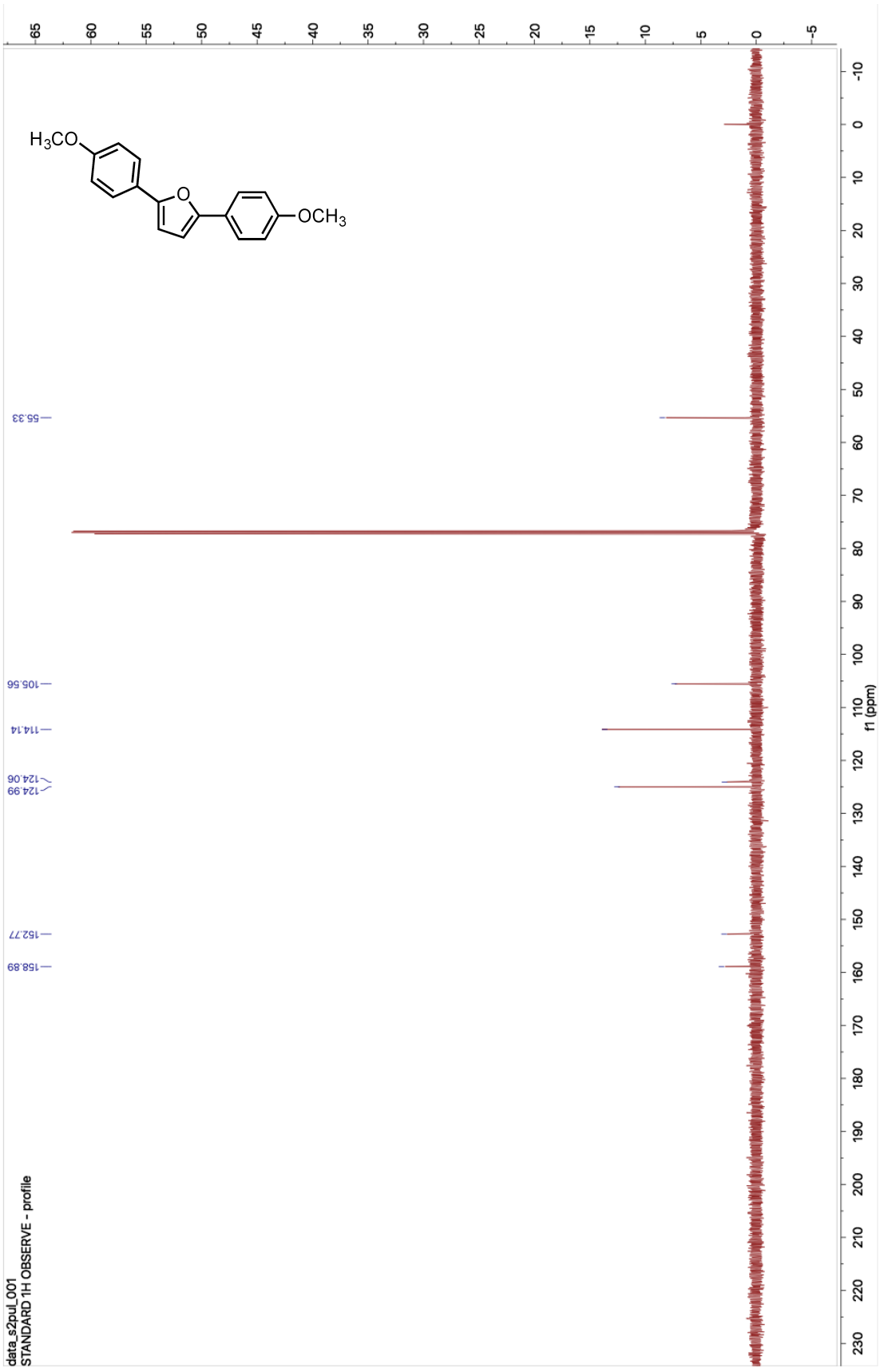
H3CO
O
OCH3
55.33
105.56
114.14
124.06
124.99
152.77
158.89
f1 (ppm)
data_s2pul_001
STANDARD 1H OBSERVE - profile

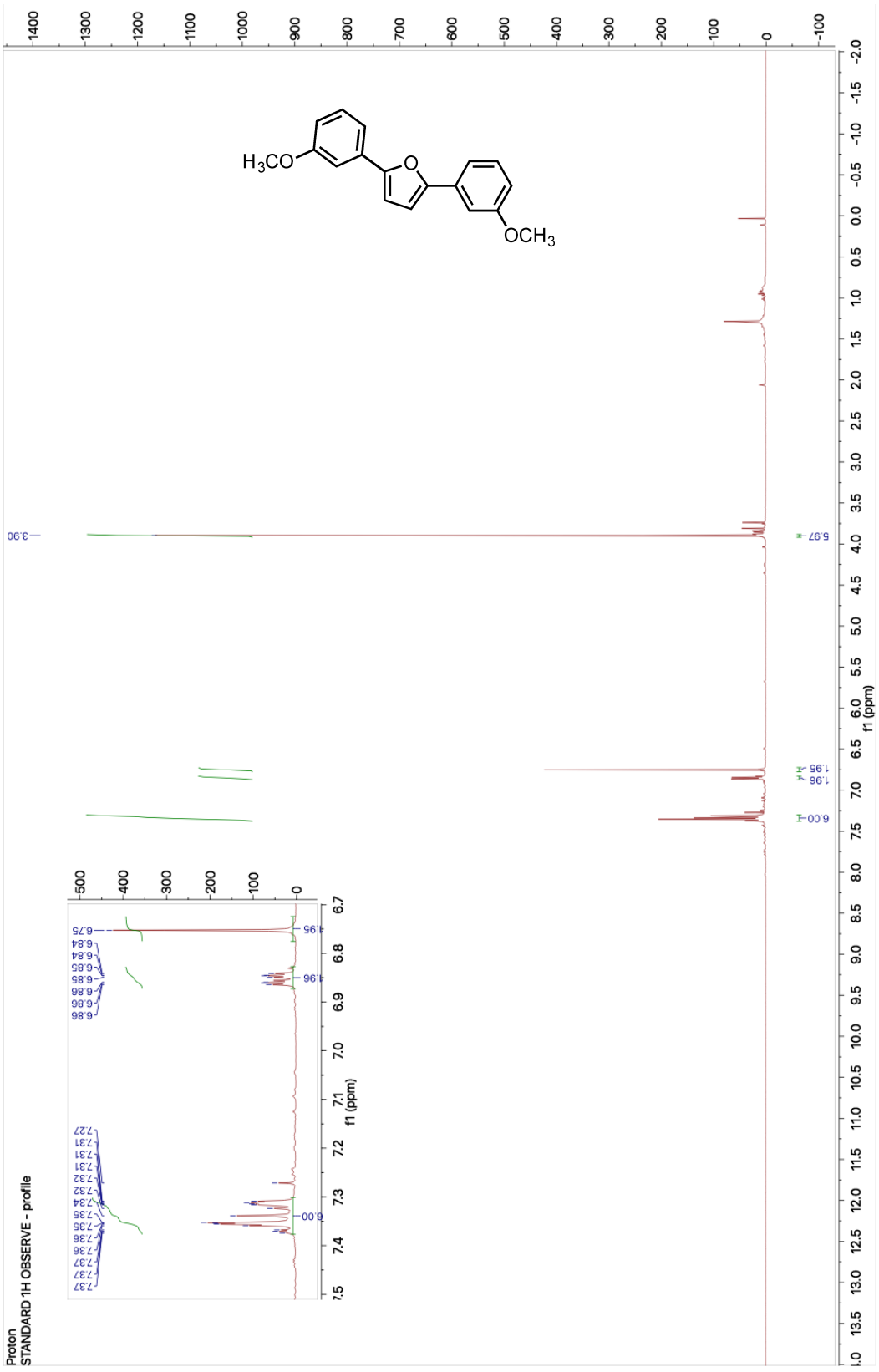
Proton
STANDARD 1H OBSERVE - profile
H3CO
O
OCH3
3.90
5.97
1.96
1.95
6.00
f1 (ppm)

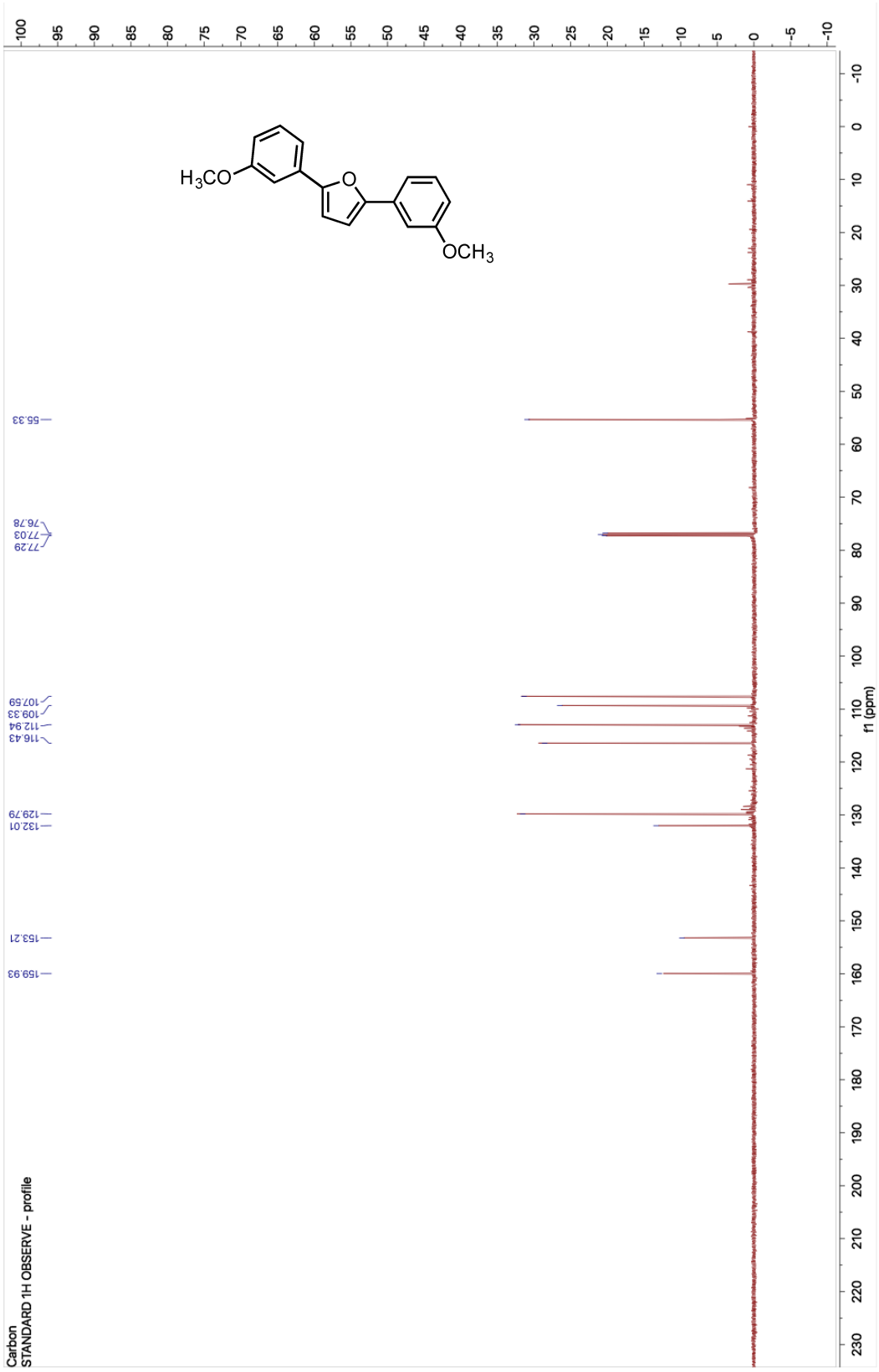
Carbon
STANDARD 1H OBSERVE - profile
H3CO
O
OCH3
55.33
76.78
77.03
77.29
107.59
109.33
112.94
116.43
129.79
132.01
153.21
159.93
f1 (ppm)

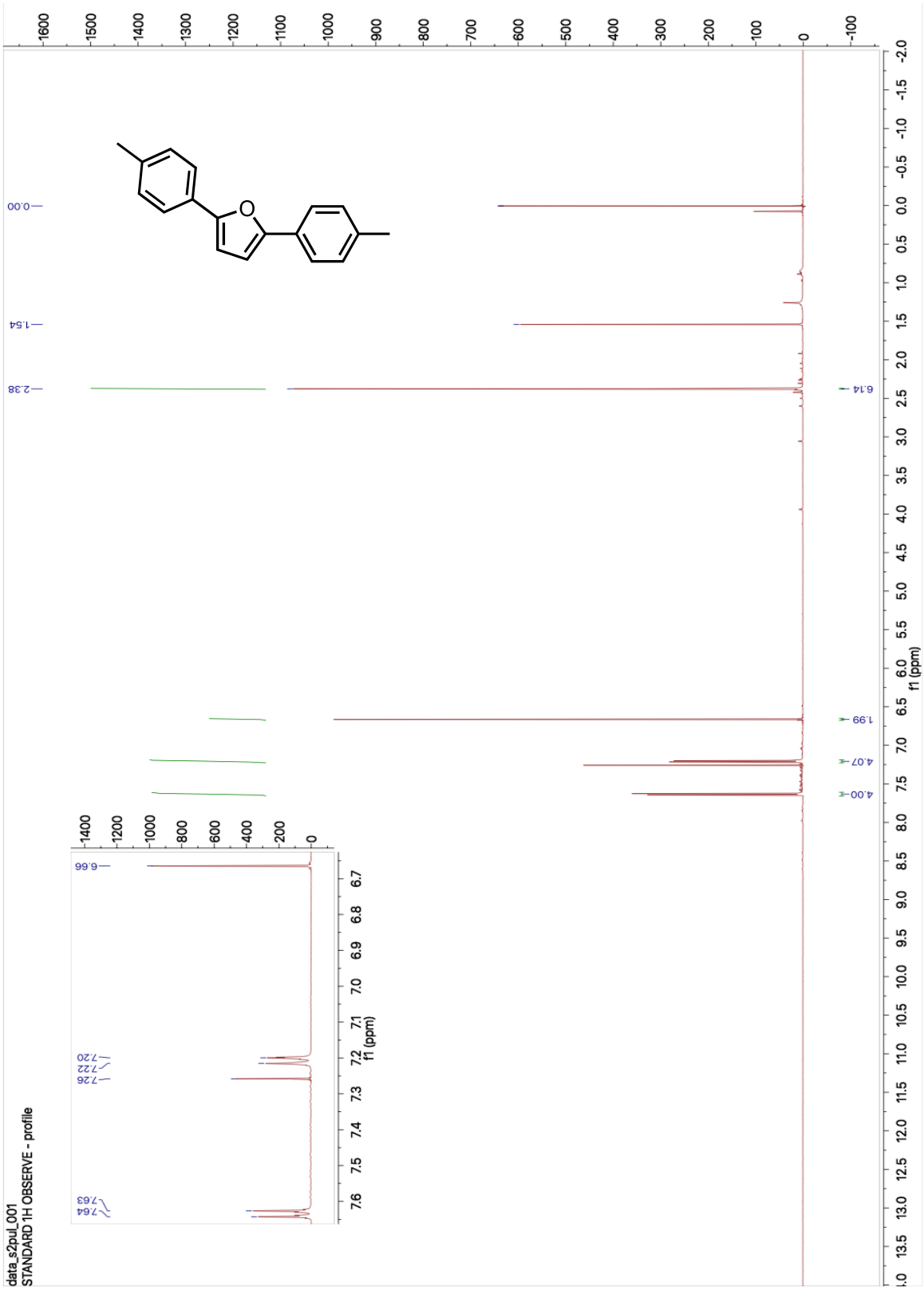
data_s2pul_001
STANDARD 1H OBSERVE - profile
f1 (ppm)
6.14
1.99
4.07
4.00
2.38
1.54
0.00
7.64
7.63
7.26
7.22
7.20
6.66

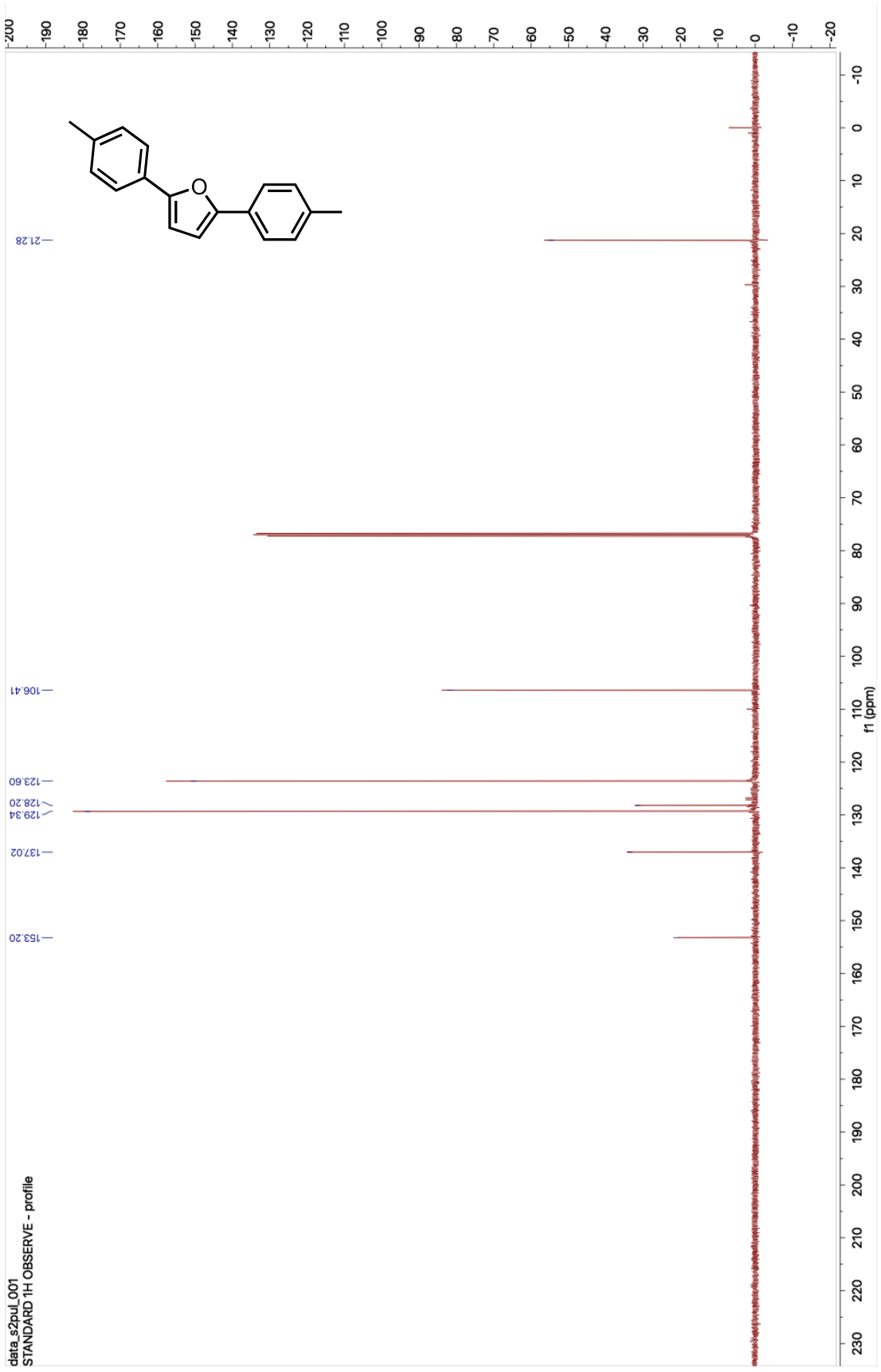
21.28
106.41
123.60
128.20
129.34
137.02
153.20
f1 (ppm)
data_s2pul_001
STANDARD 1H OBSERVE - profile

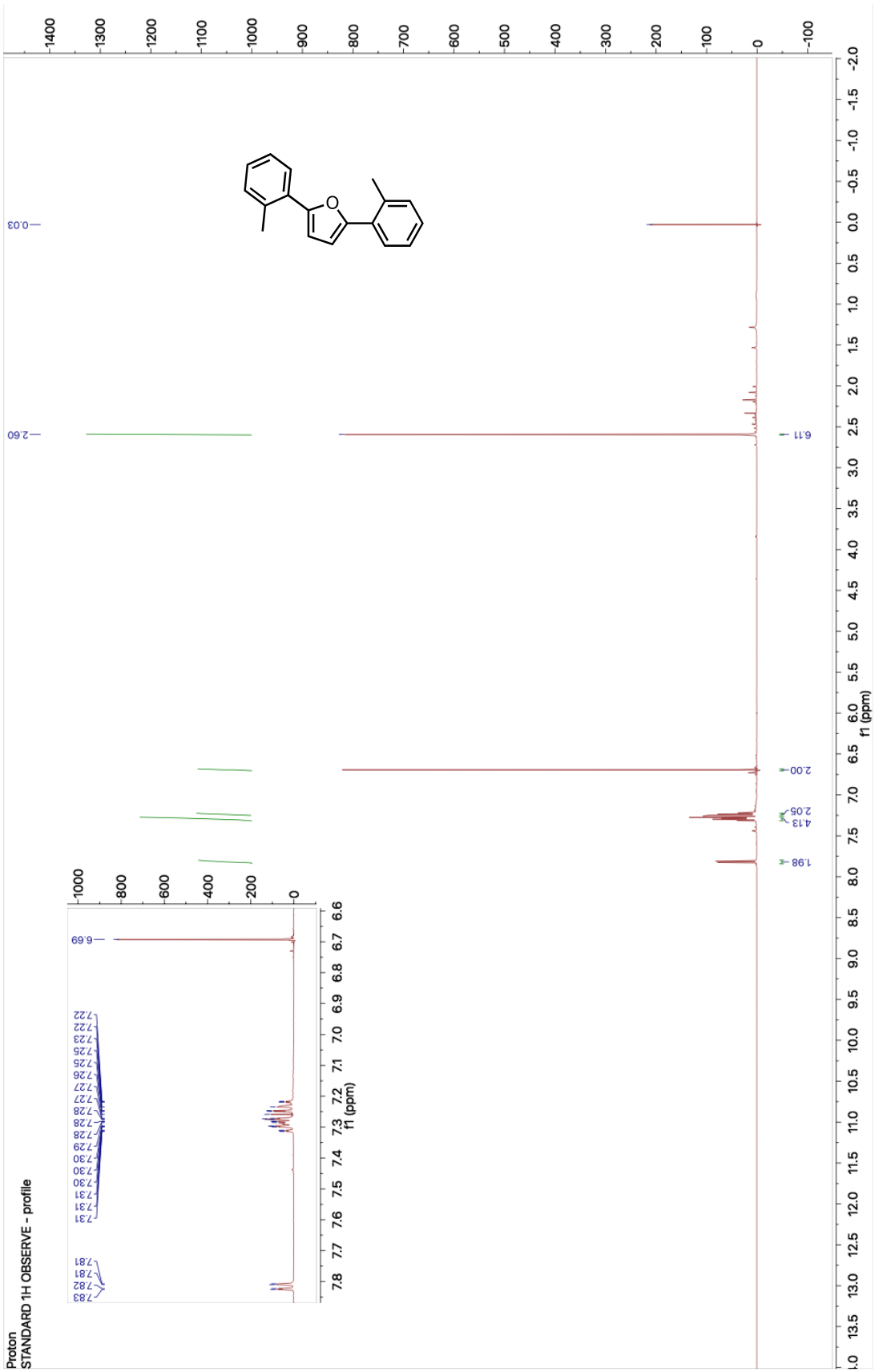
Proton
STANDARD 1H OBSERVE - profile
f1 (ppm)
0.03
2.60
6.11
2.00
4.13
2.05
1.98
6.69

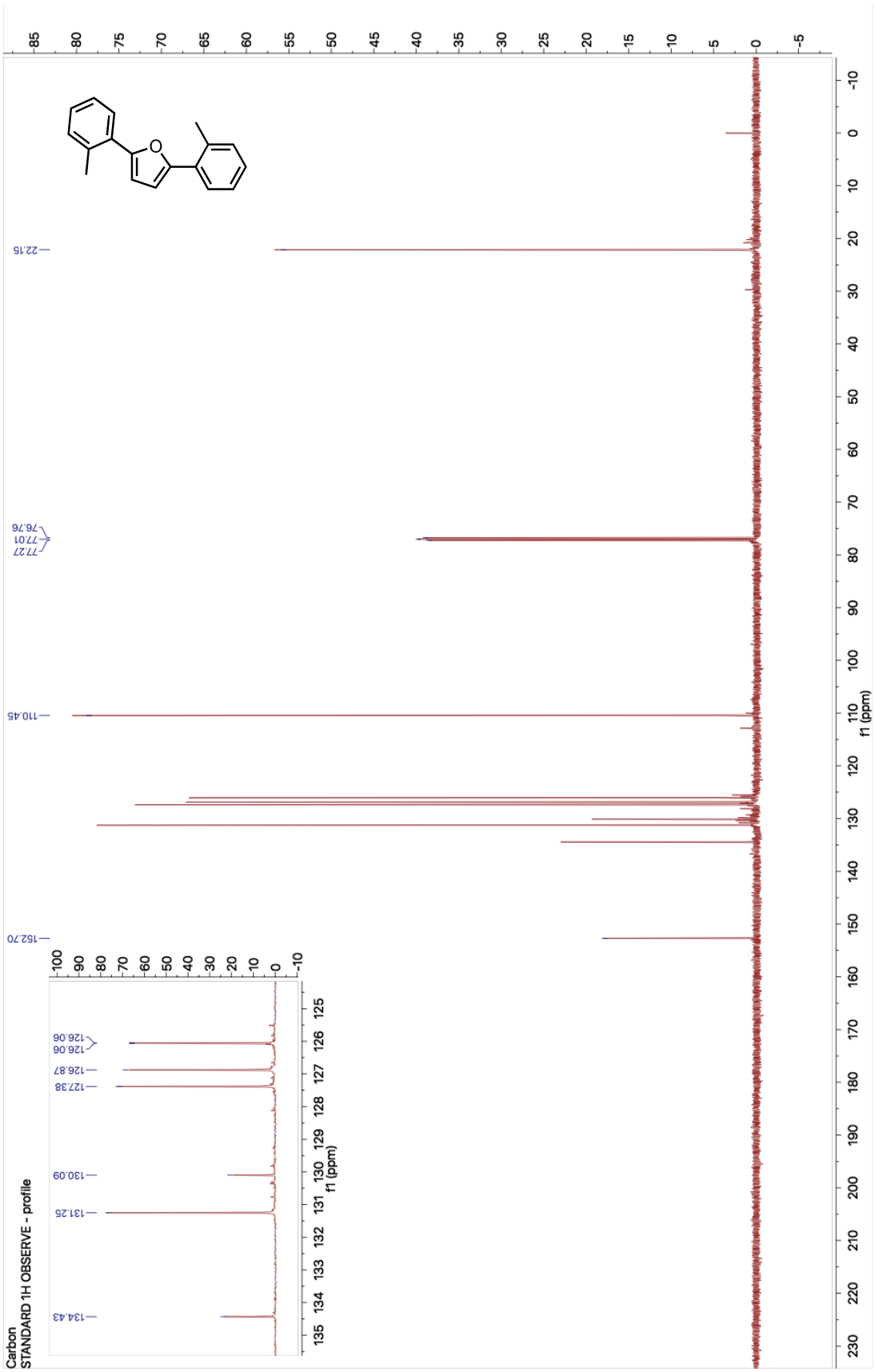
Carbon
STANDARD 1H OBSERVE - profile
f1 (ppm)
22.15
76.76
77.01
77.27
110.45
152.70
126.06
126.87
127.38
130.09
131.25
134.43

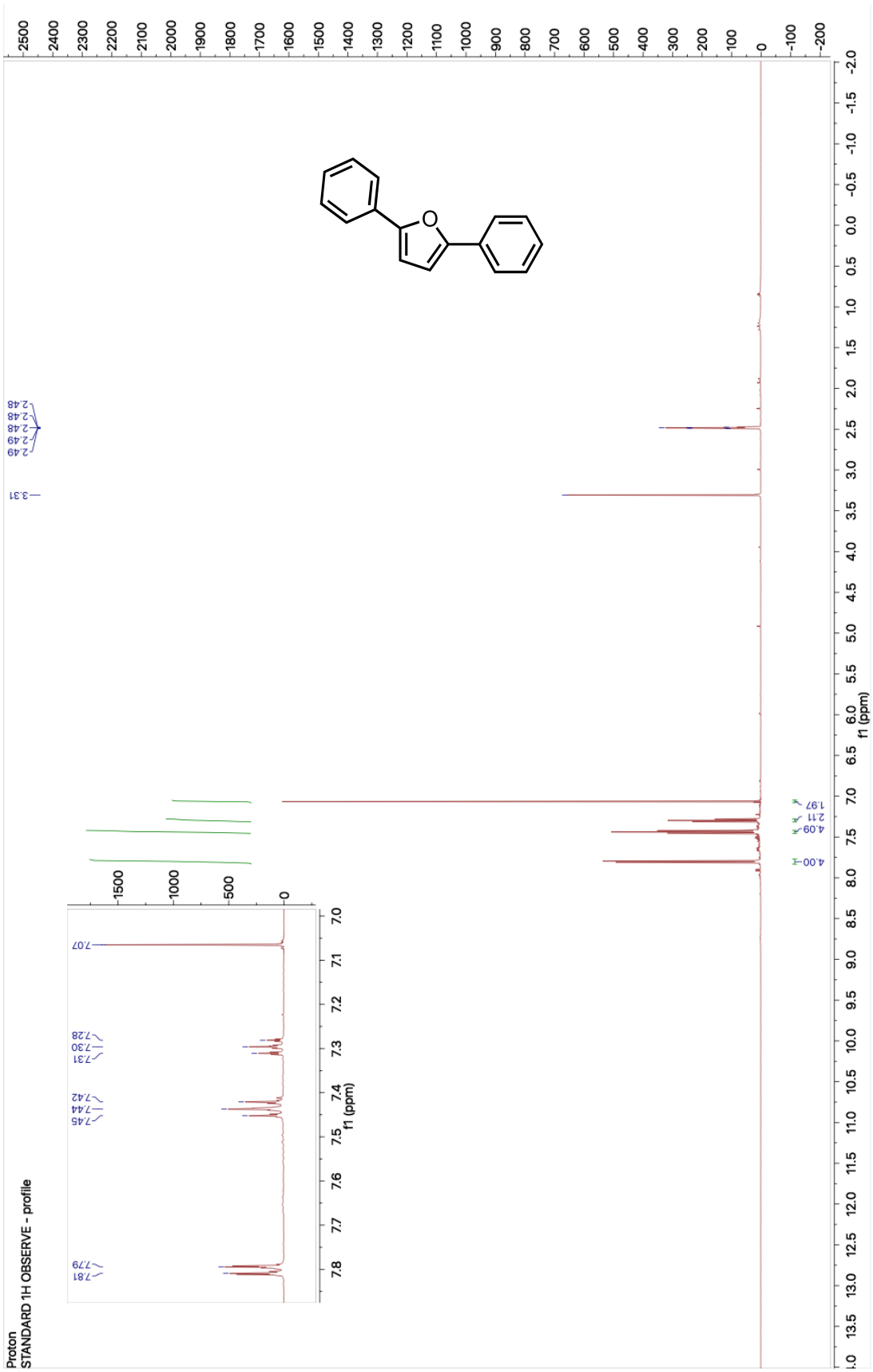
Proton
STANDARD 1H OBSERVE - profile
f1 (ppm)
4.00
4.09
2.11
1.97
3.31
2.48
2.48
2.48
2.49
2.49
7.07
7.28
7.30
7.31
7.42
7.44
7.45
7.79
7.81

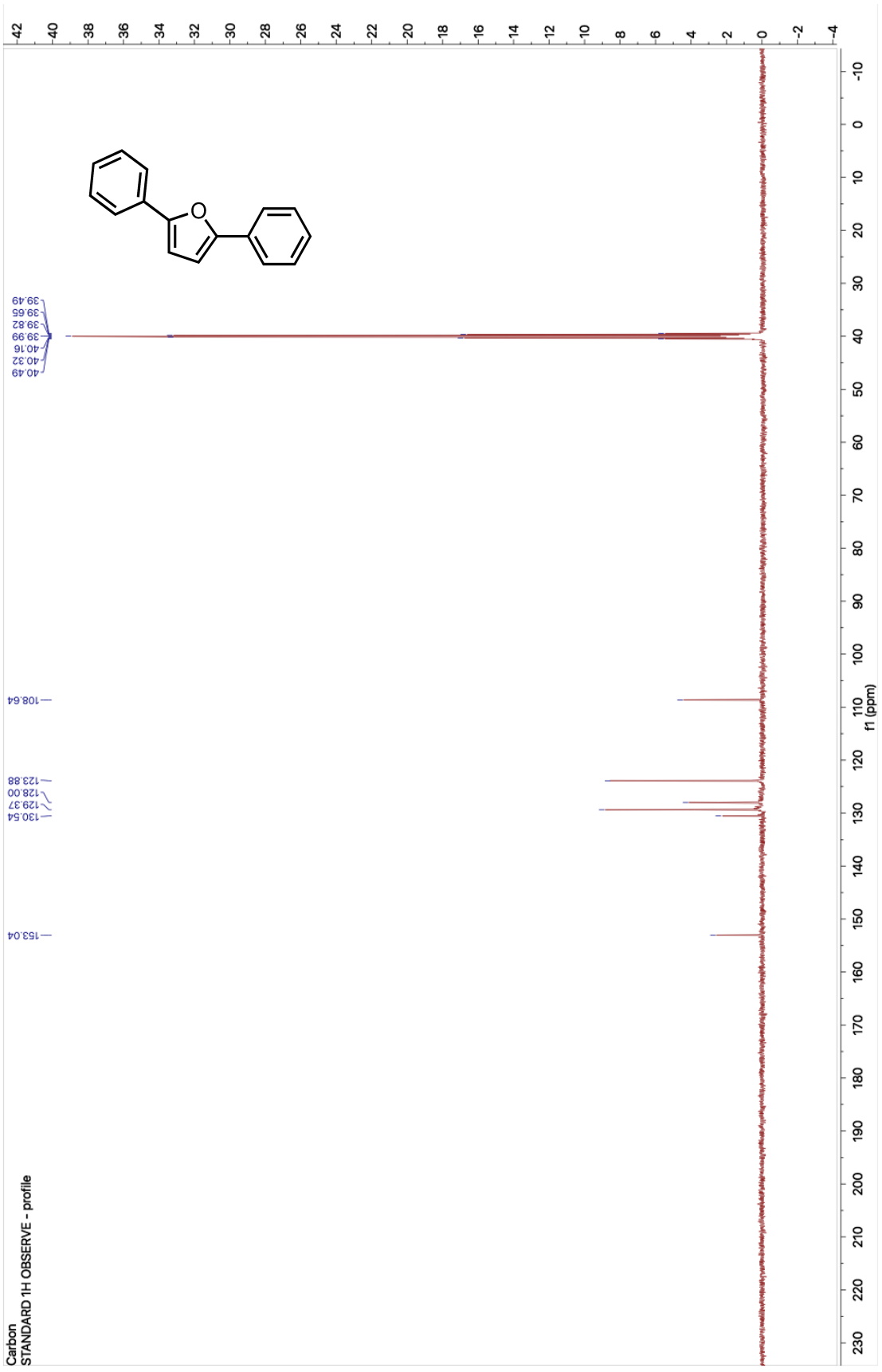
Carbon
STANDARD 1H OBSERVE - profile
153.04
130.54
129.37
128.00
123.88
108.64
40.49
40.32
40.16
39.99
39.82
39.65
39.49
f1 (ppm)

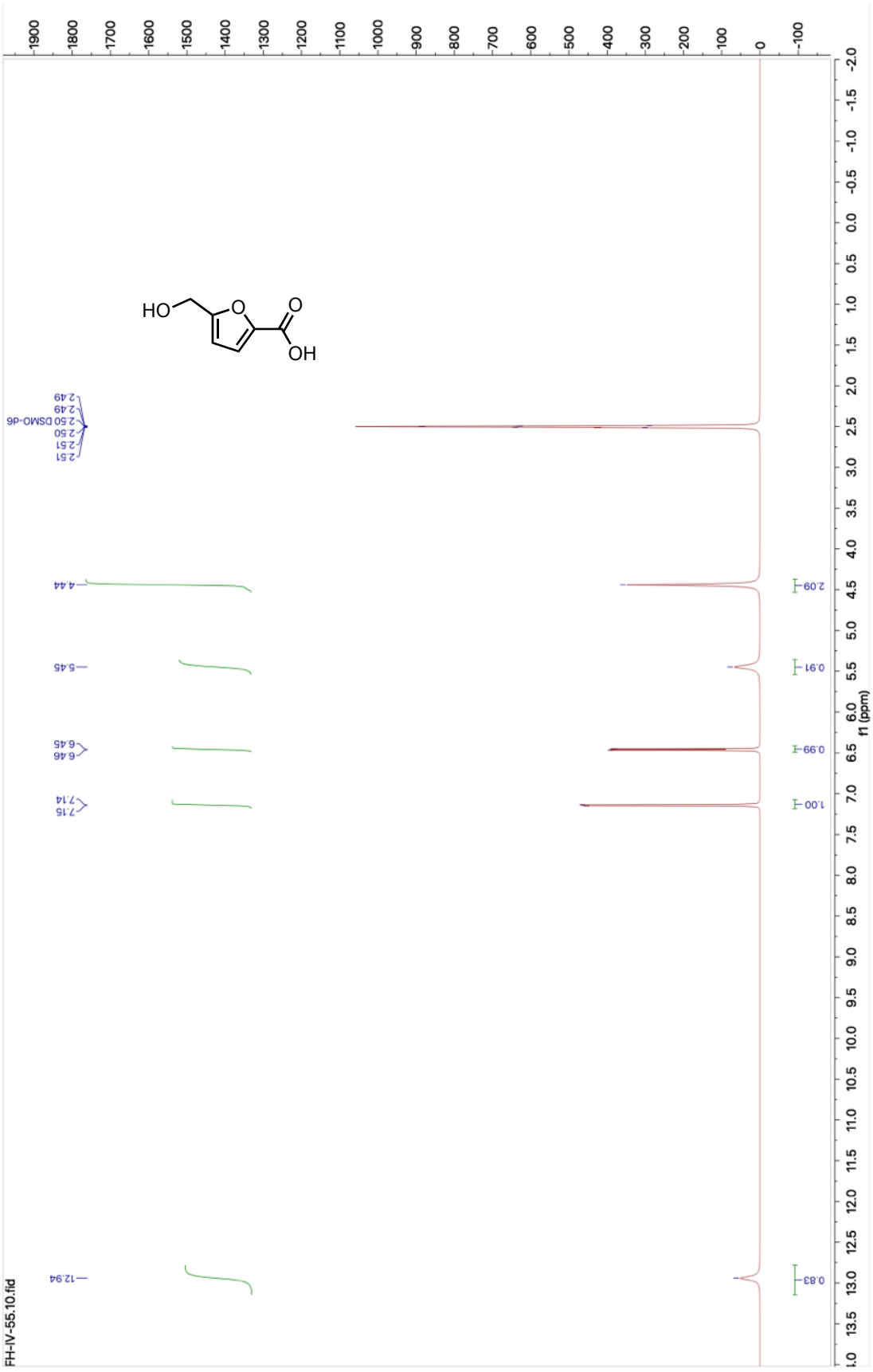
HO
O
O
OH
FH-IV-55.10.fid
f1 (ppm)
DSMO-d6
2.09
0.91
0.99
1.00
0.83

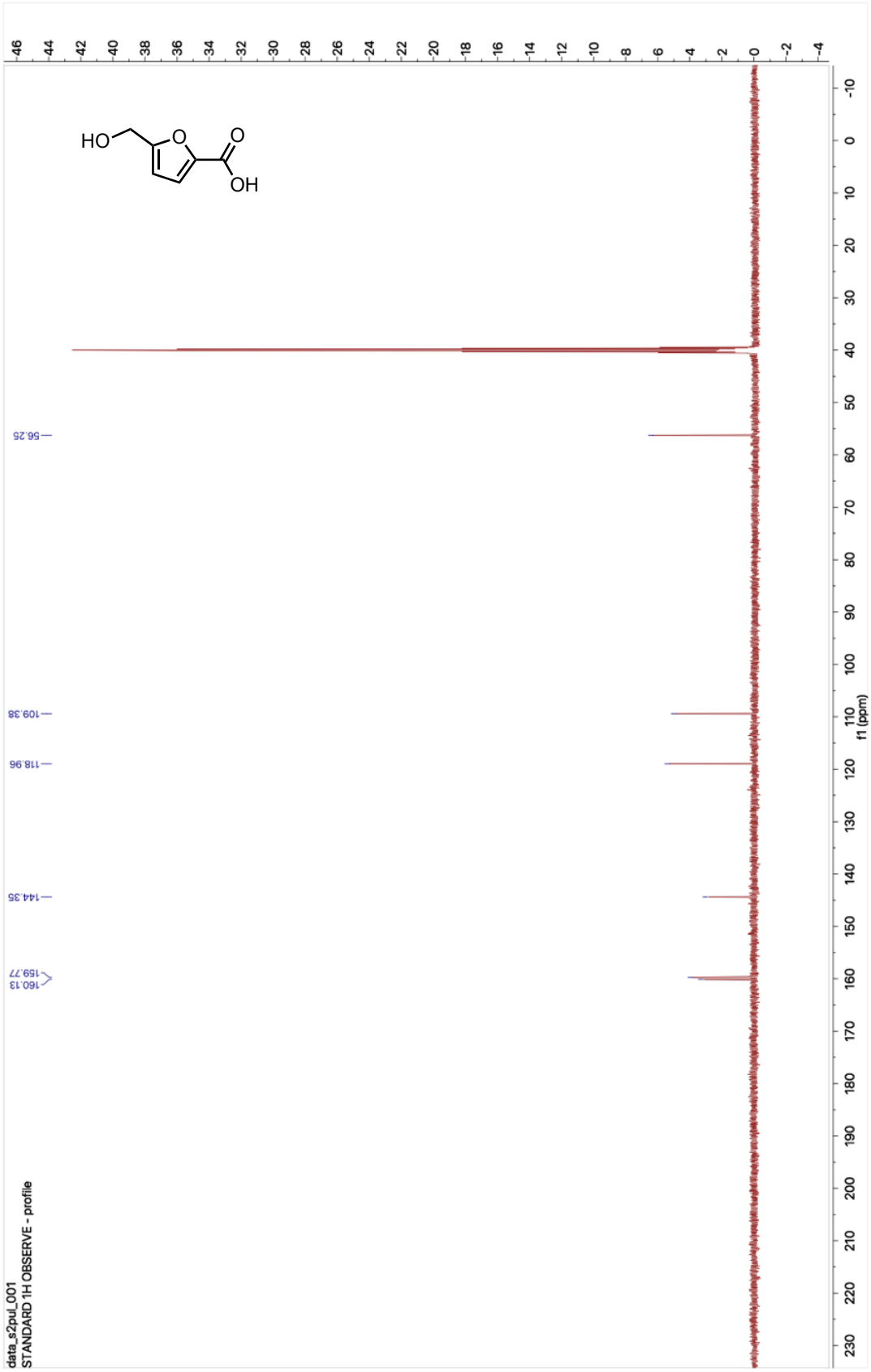
HO
O
O
OH
56.25
109.38
118.96
144.35
160.13
159.77
f1 (ppm)
data_s2pul_001
STANDARD 1H OBSERVE - profile

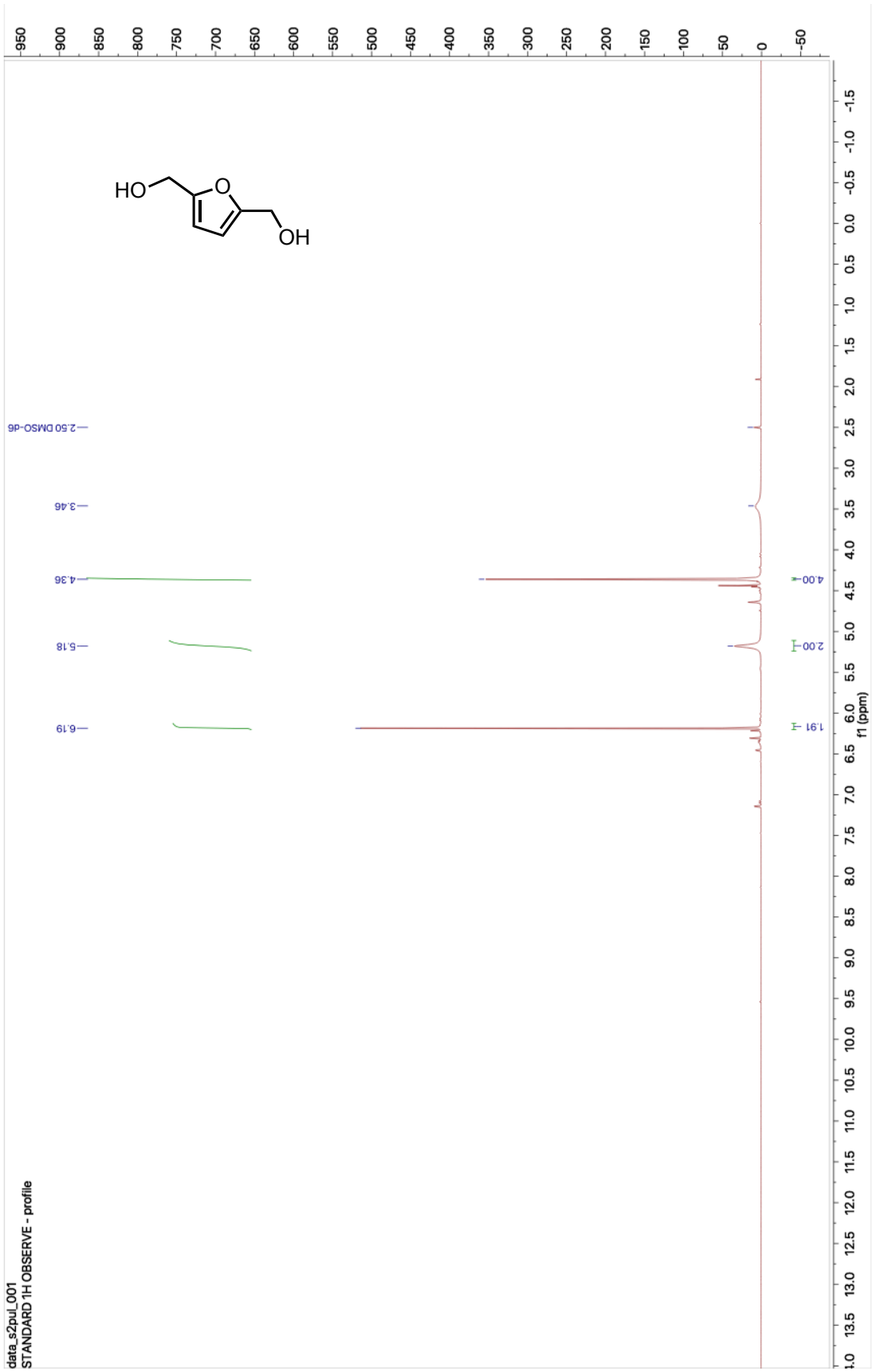
HO
O
OH
2.50 DMSO-d6
3.46
4.36
5.18
6.19
4.00
2.00
1.91
f1 (ppm)
data_s2pul_001
STANDARD 1H OBSERVE - profile

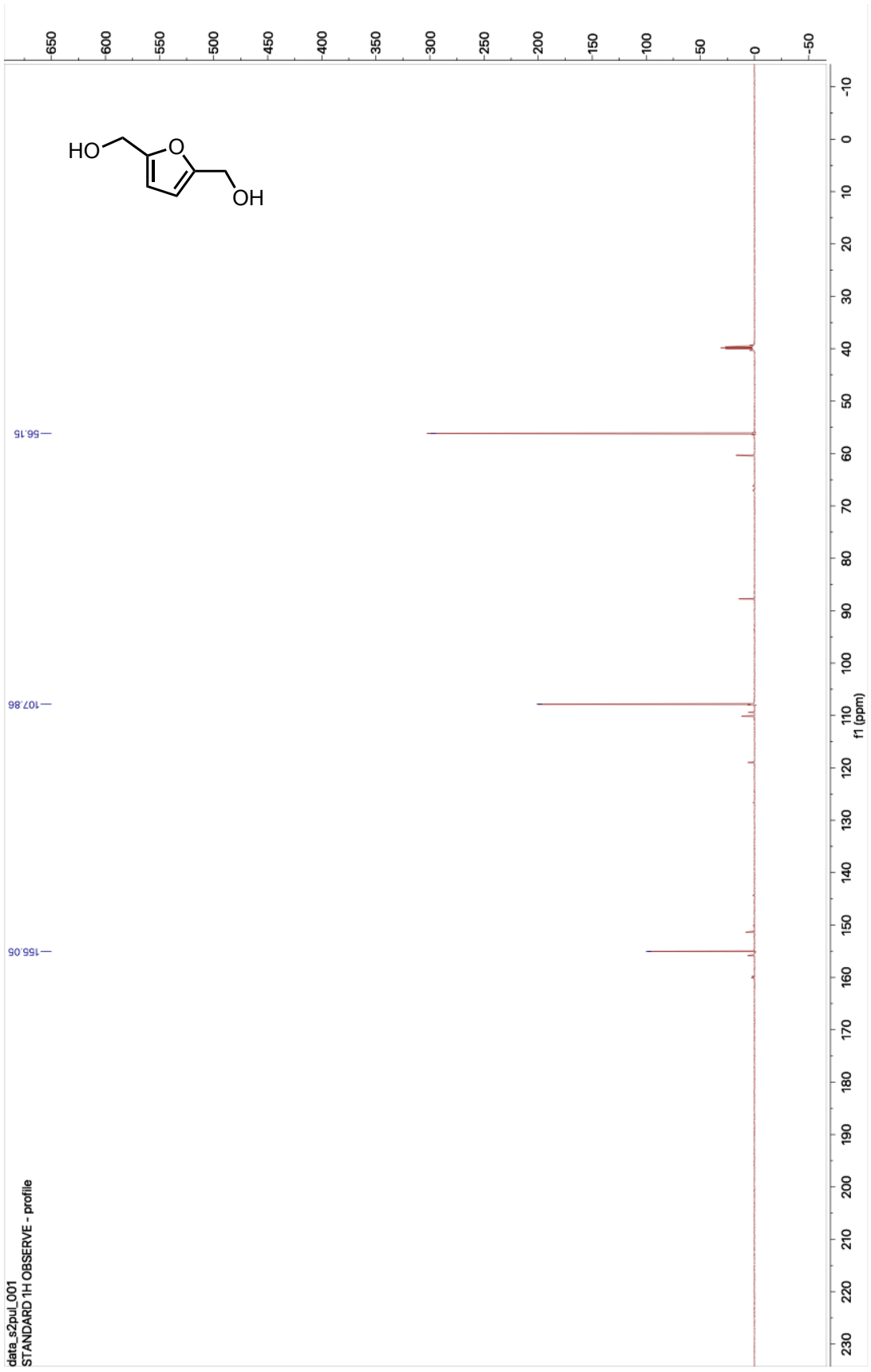
HO
O
OH
56.15
107.86
155.05
f1 (ppm)
data_s2pul_001
STANDARD 1H OBSERVE - profile

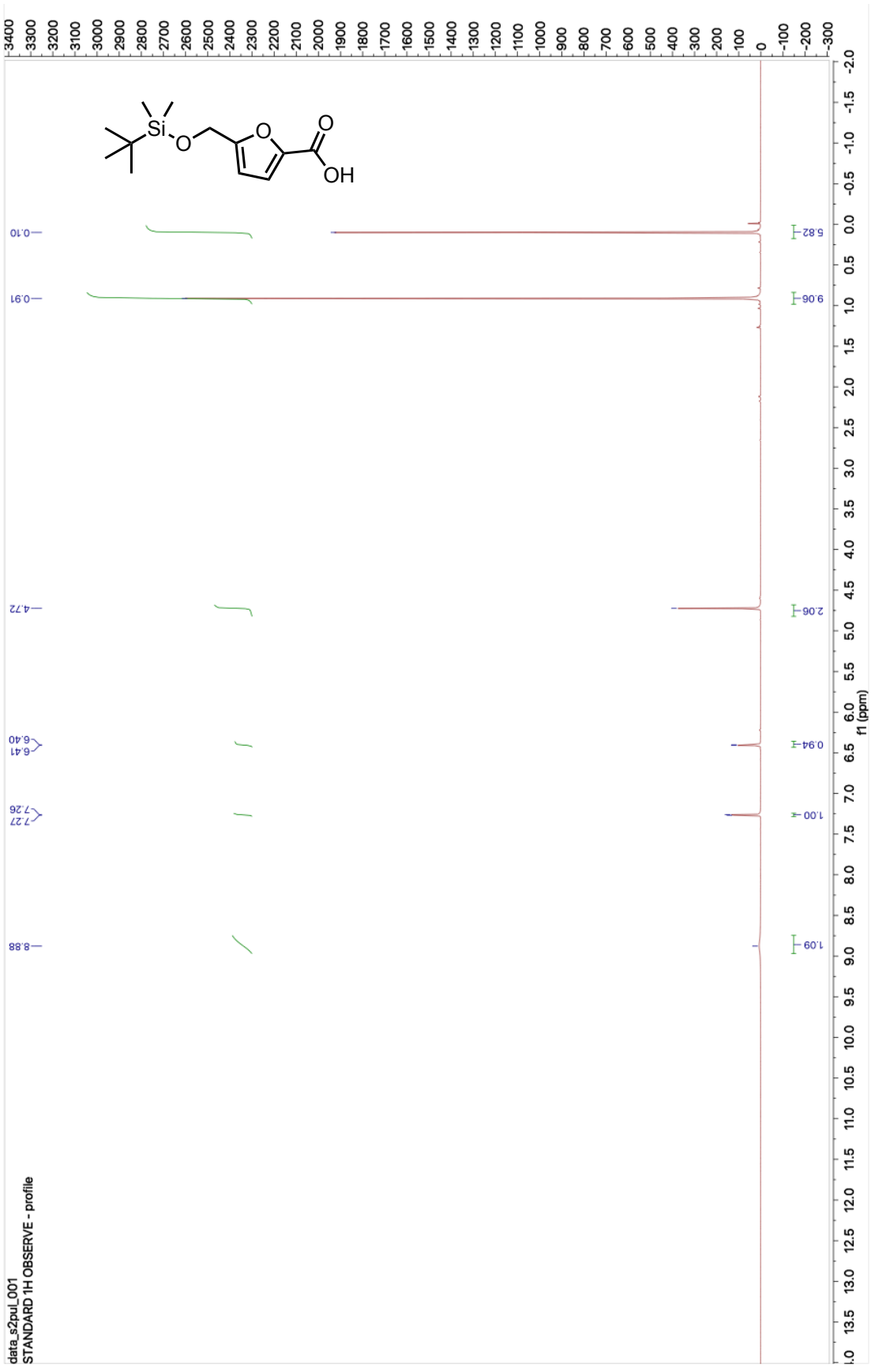
Si
O
O
O
OH
0.10
0.91
4.72
6.41
6.40
7.27
7.26
8.88
5.82
9.06
2.06
0.94
1.00
1.09
f1 (ppm)
data_s2pul_001
STANDARD 1H OBSERVE - profile

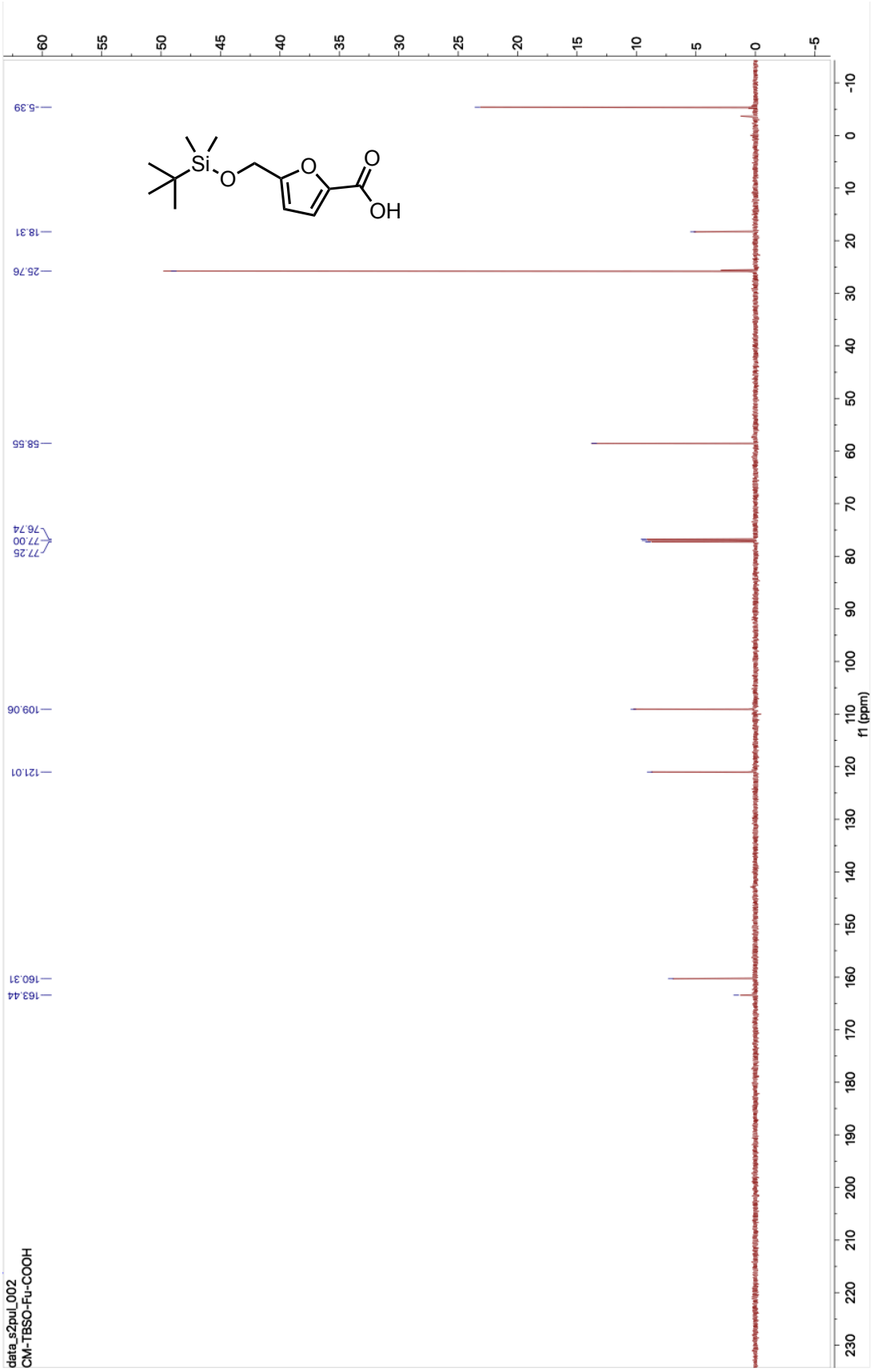
-5.39
18.31
25.76
58.55
76.74
77.00
77.25
109.06
121.01
160.31
163.44
Si
O
O
O
OH
f1 (ppm)
data_s2pul_002
CM-TBSO-Fu-COOH


data_s2pul_001
STANDARD 1H OBSERVE - profile
f1 (ppm)
0.07
0.89
4.60
4.54
6.20
6.19
6.16
6.15
7.26
6.19
9.06
2.14
2.13
1.00
1.03
Si
O
O
OH

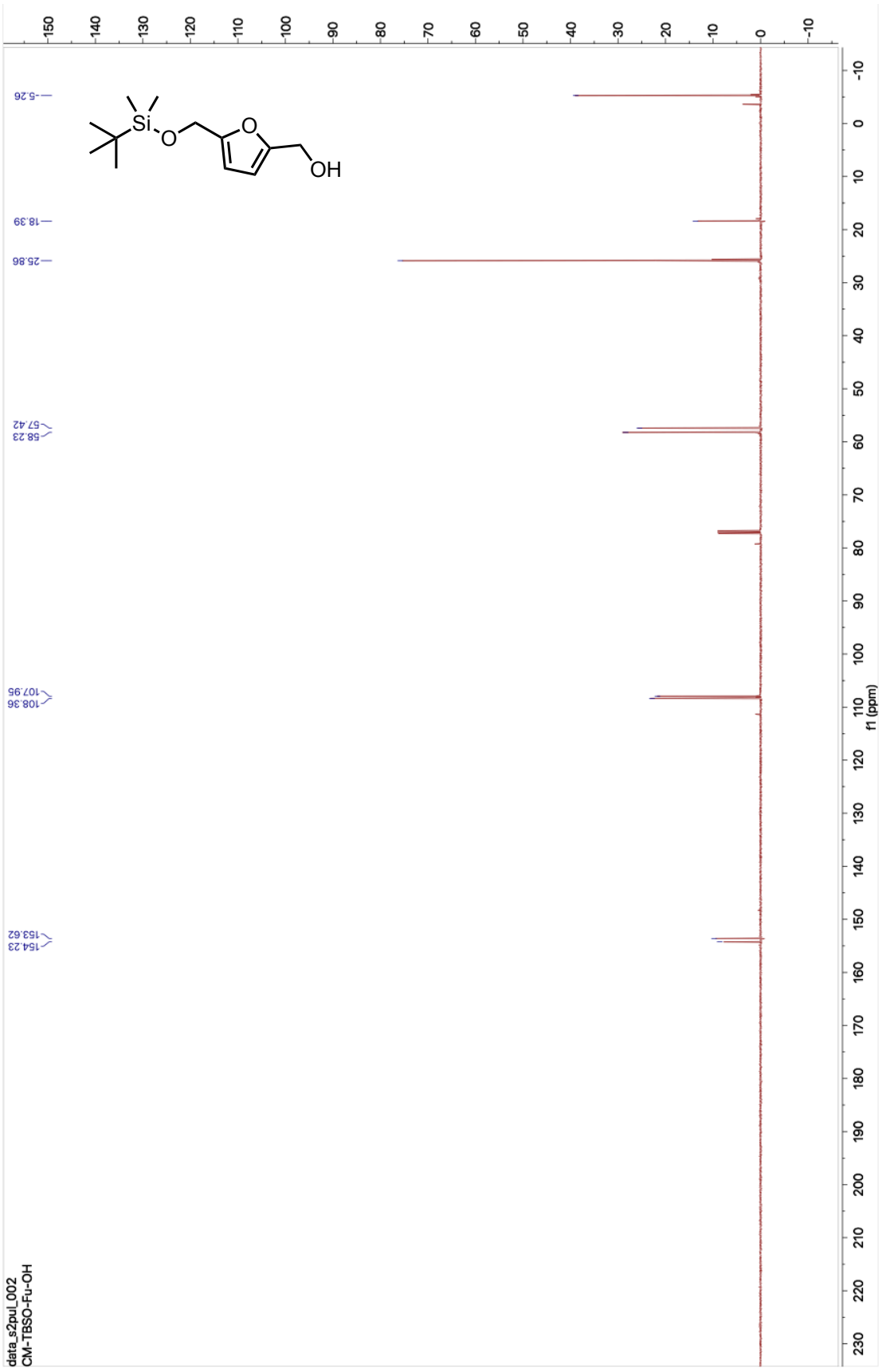
-5.26
18.39
25.86
57.42
58.23
107.95
108.36
153.62
154.23
Si
O
O
OH
f1 (ppm)
data_s2pul_002
CM-TBSO-Fu-OH

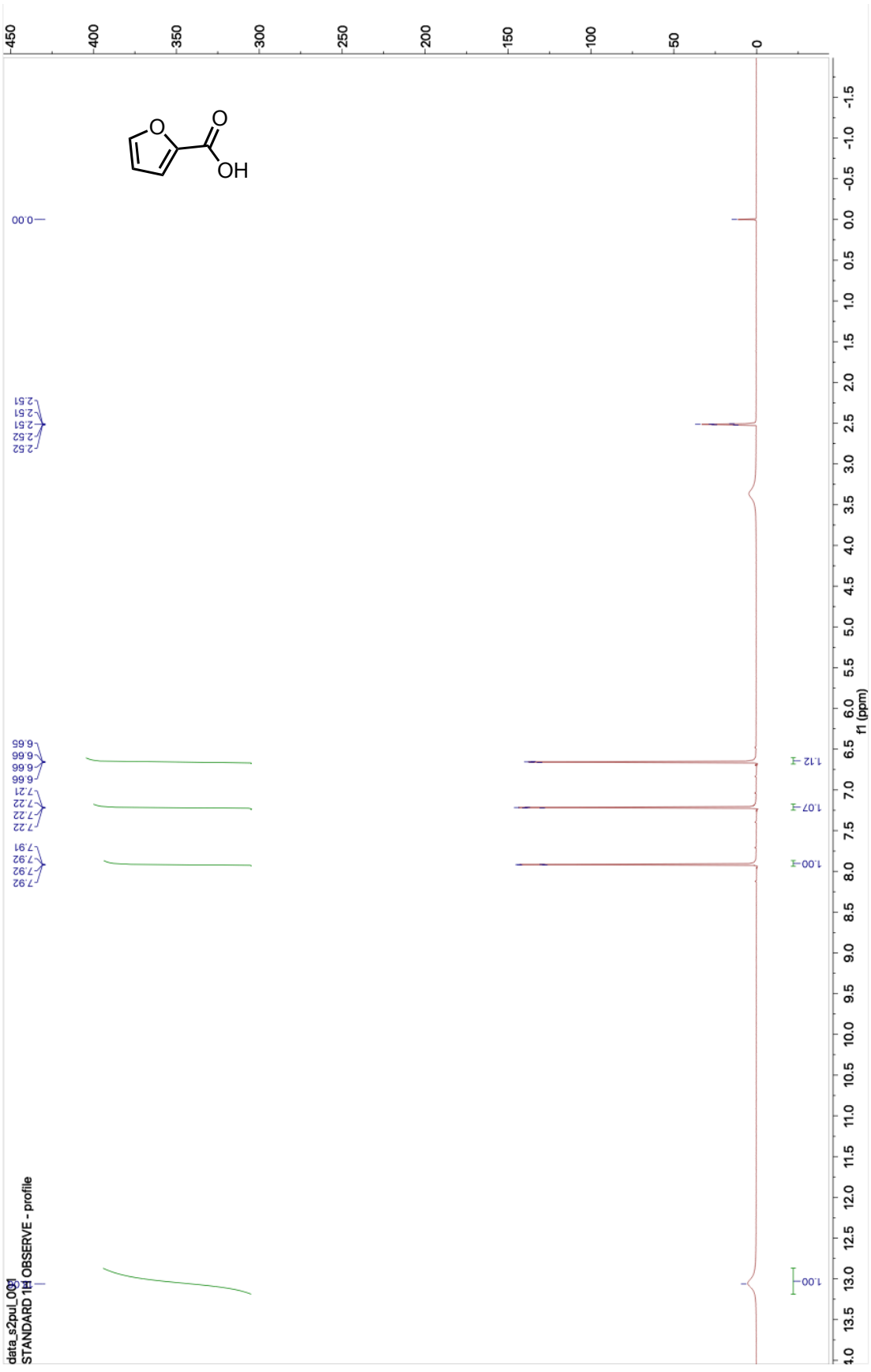
O
OH
data_s2pul_001
STANDARD 1H OBSERVE - profile
f1 (ppm)

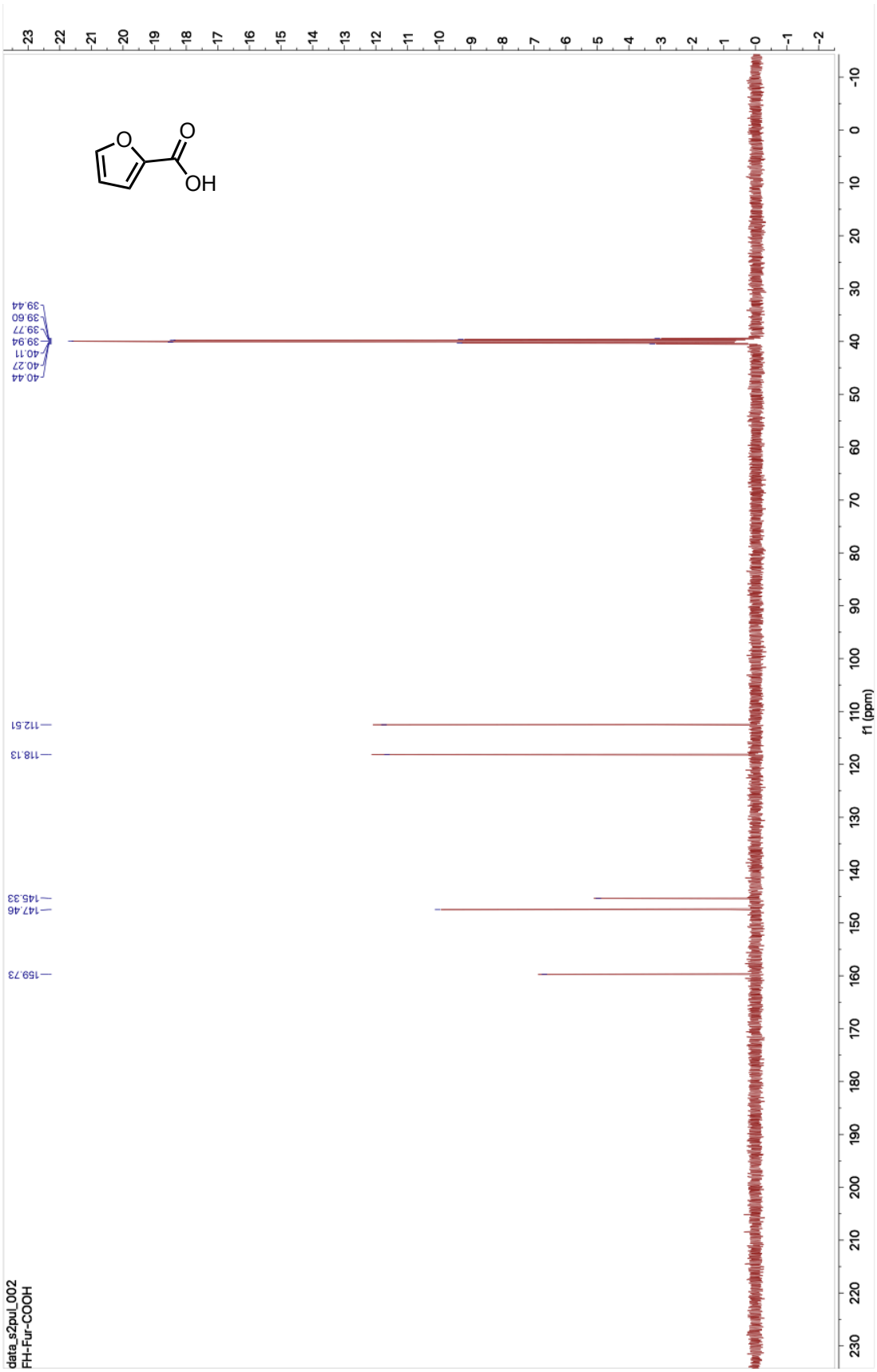
O
O
OH
39.44
39.60
39.77
39.94
40.11
40.27
40.44
112.51
118.13
145.33
147.46
159.73
f1 (ppm)
data_s2pul_002
FH-Fur-COOH

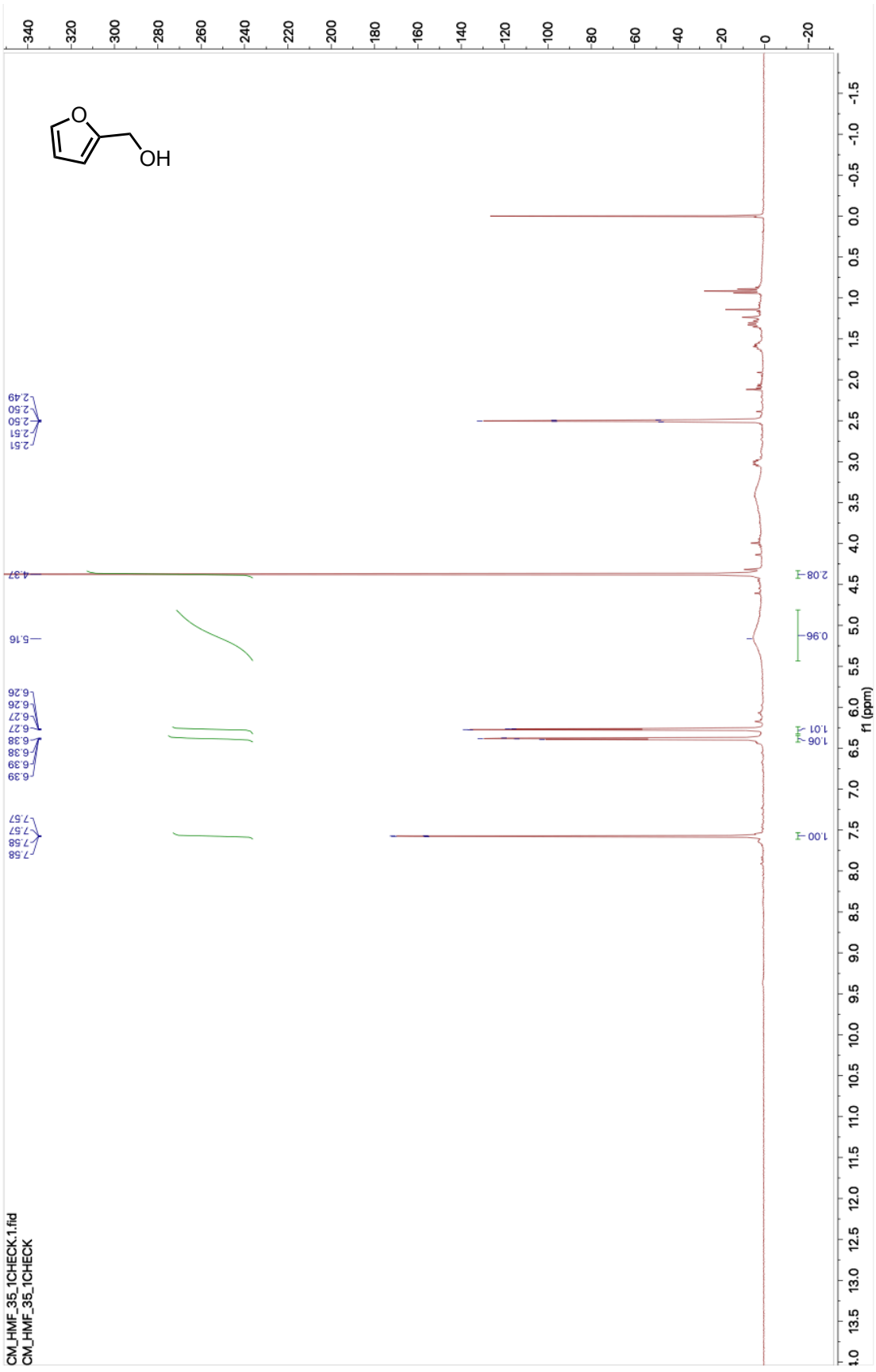
OH
CM_HMF_35_1CHECK.1.fid
CM_HMF_35_1CHECK
f1 (ppm)

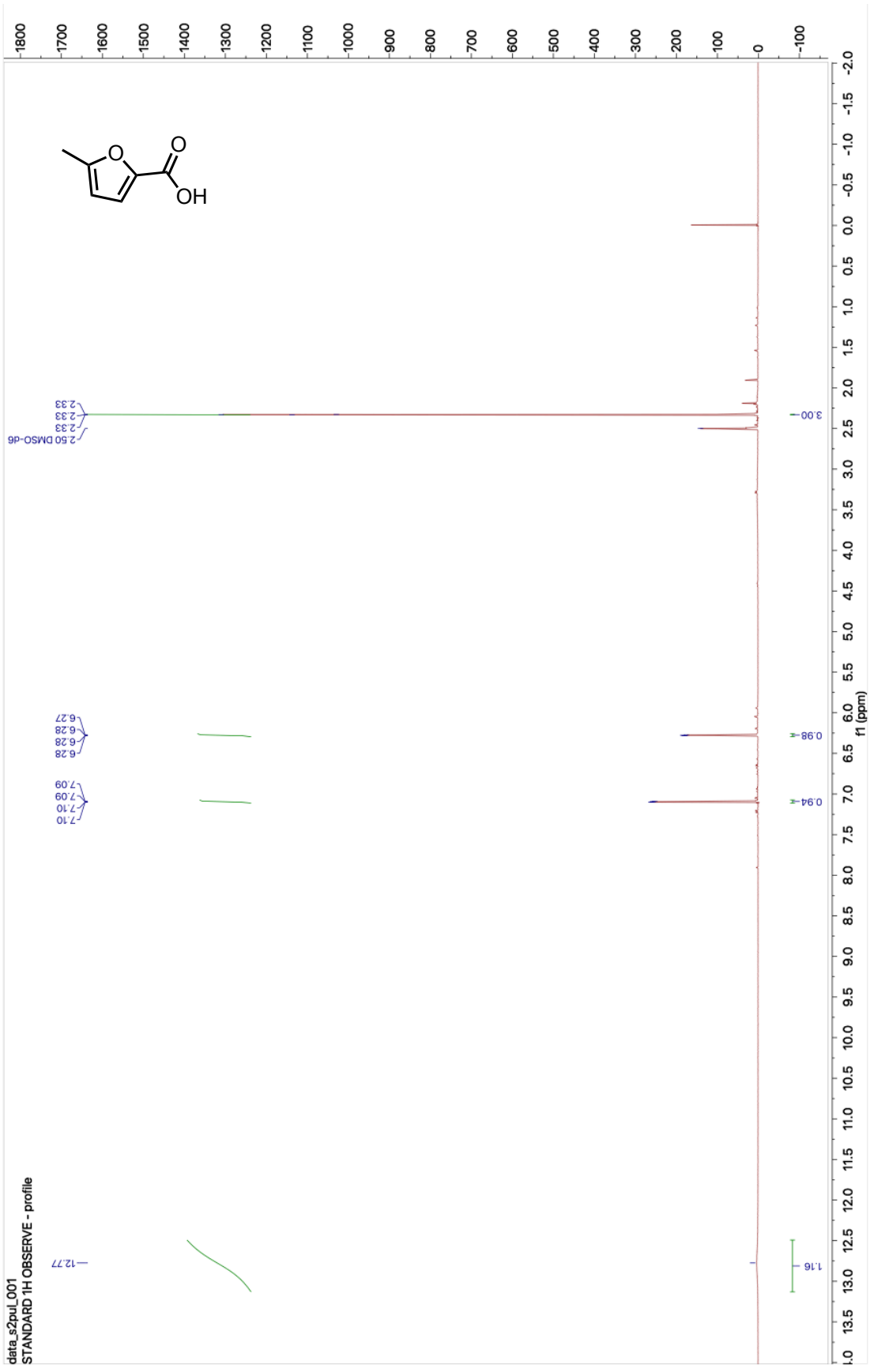
data_s2pul_001
STANDARD 1H OBSERVE - profile
f1 (ppm)
OH
O
O
2.50 DMSO-d6
2.33
2.33
2.33
6.27
6.28
6.28
6.28
7.09
7.09
7.10
7.10
12.77
3.00
0.98
0.94
1.16

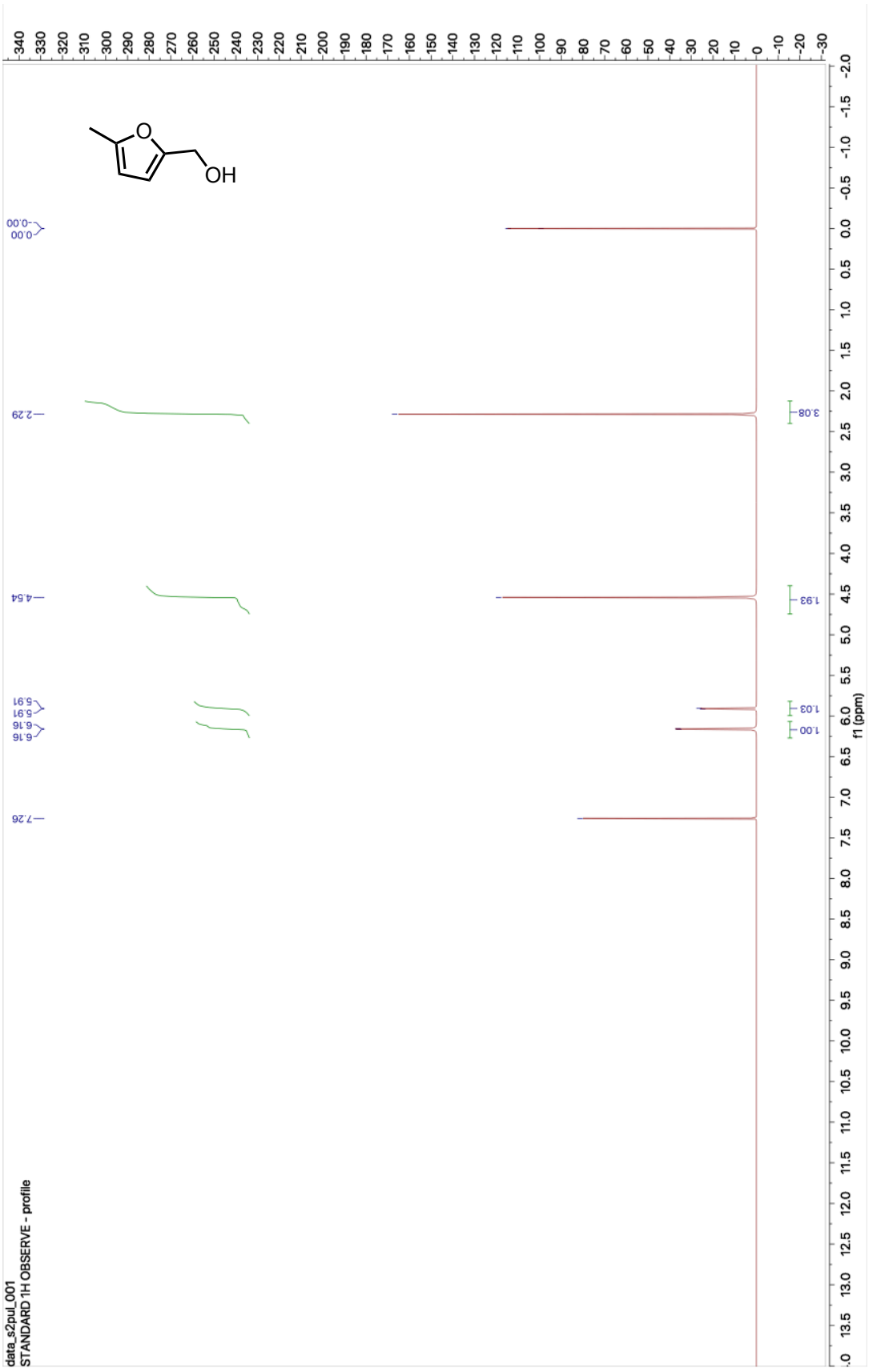
data_s2pul_001
STANDARD 1H OBSERVE - profile
OH
O
0.00
2.29
4.54
5.91
5.91
6.16
6.16
7.26
3.08
1.93
1.03
1.00
f1 (ppm)

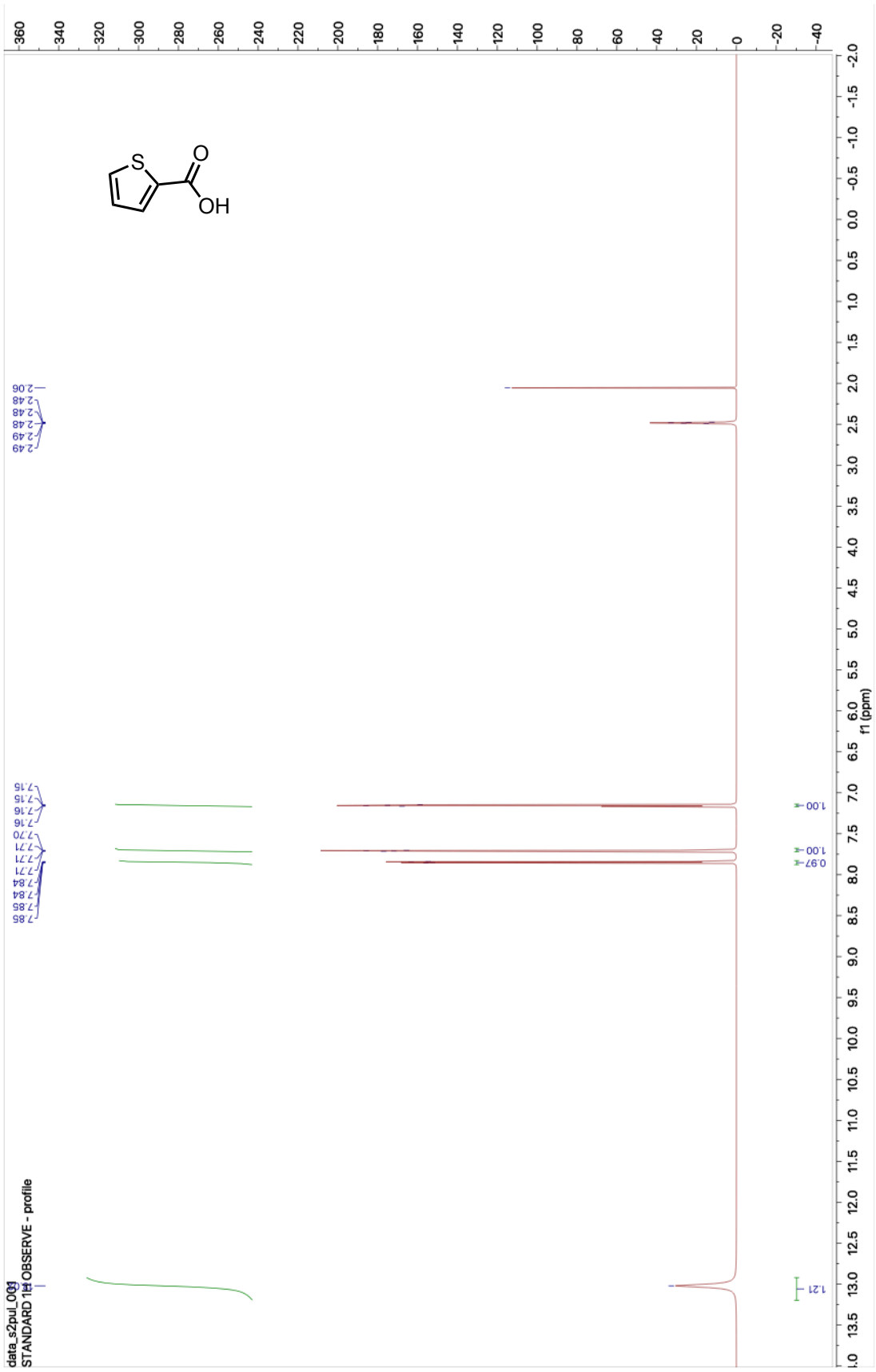
S
O
OH
f1 (ppm)
data_s2pul_001
STANDARD 1H OBSERVE - profile

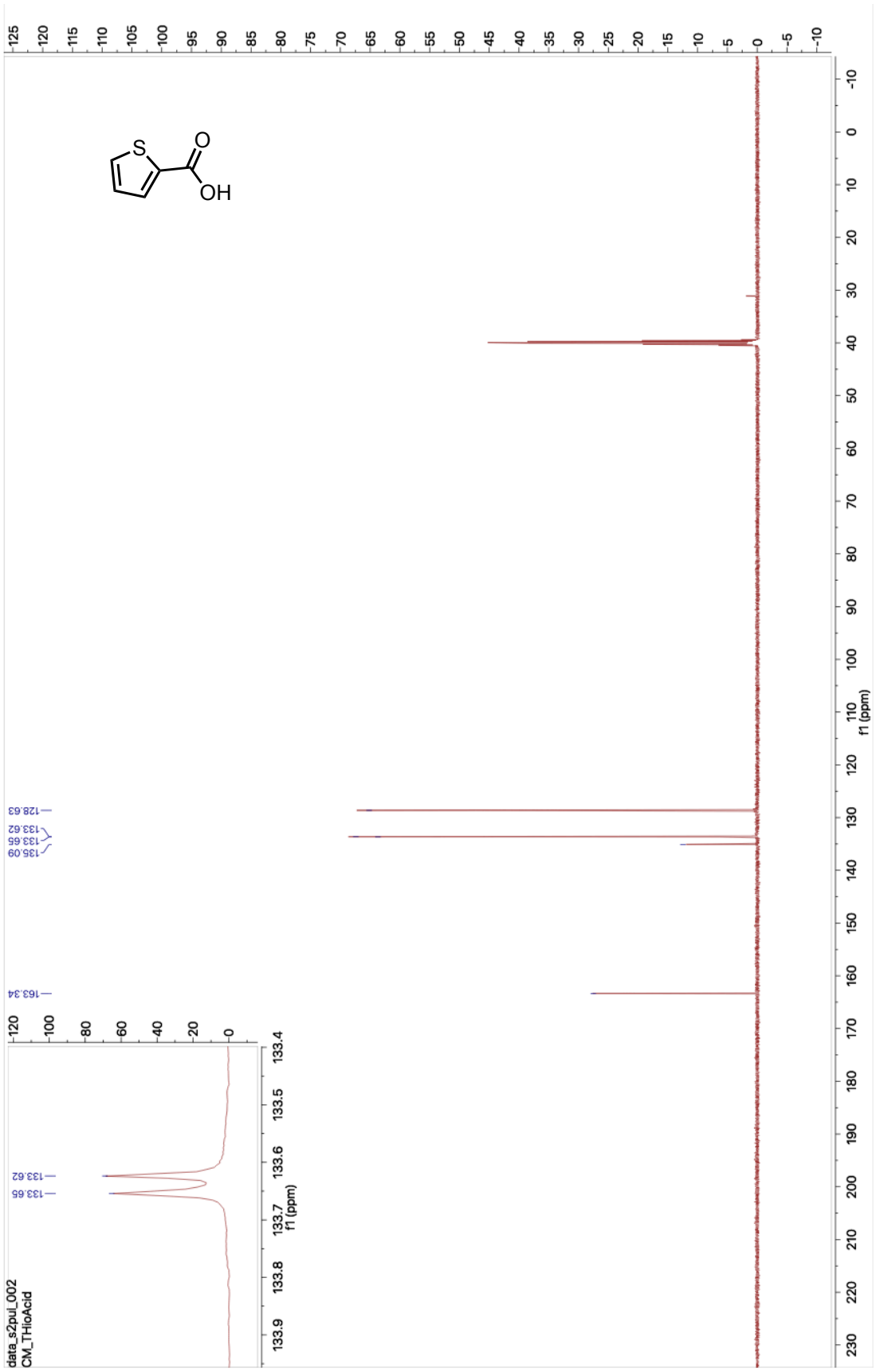
S
O
OH
163.34
136.09
133.65
133.62
128.63
133.62
133.65
data_s2pul_002
CM_ThioAcid
f1 (ppm)

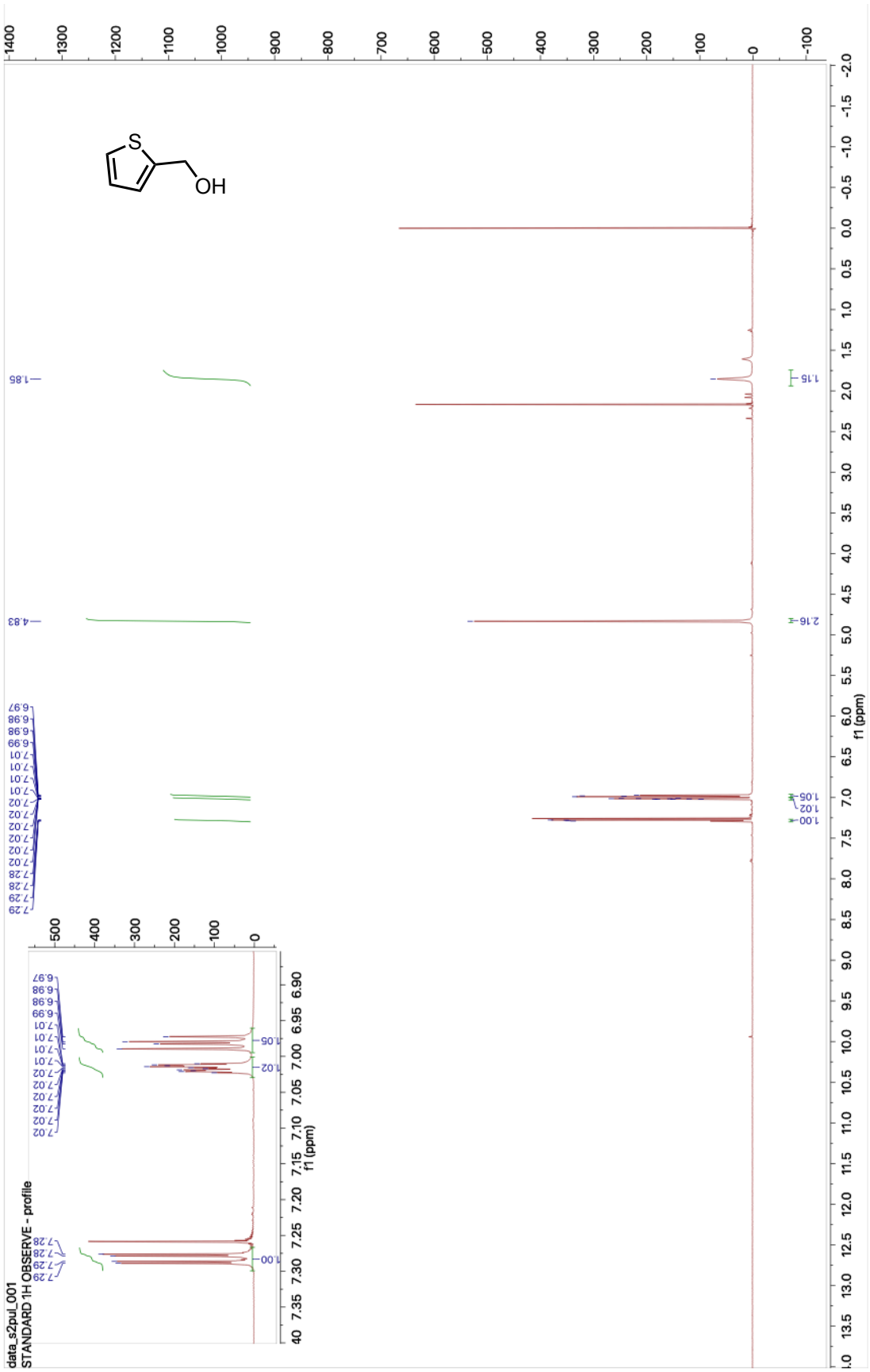
S
OH
data_s2pul_001
STANDARD 1H OBSERVE - profile
f1 (ppm)

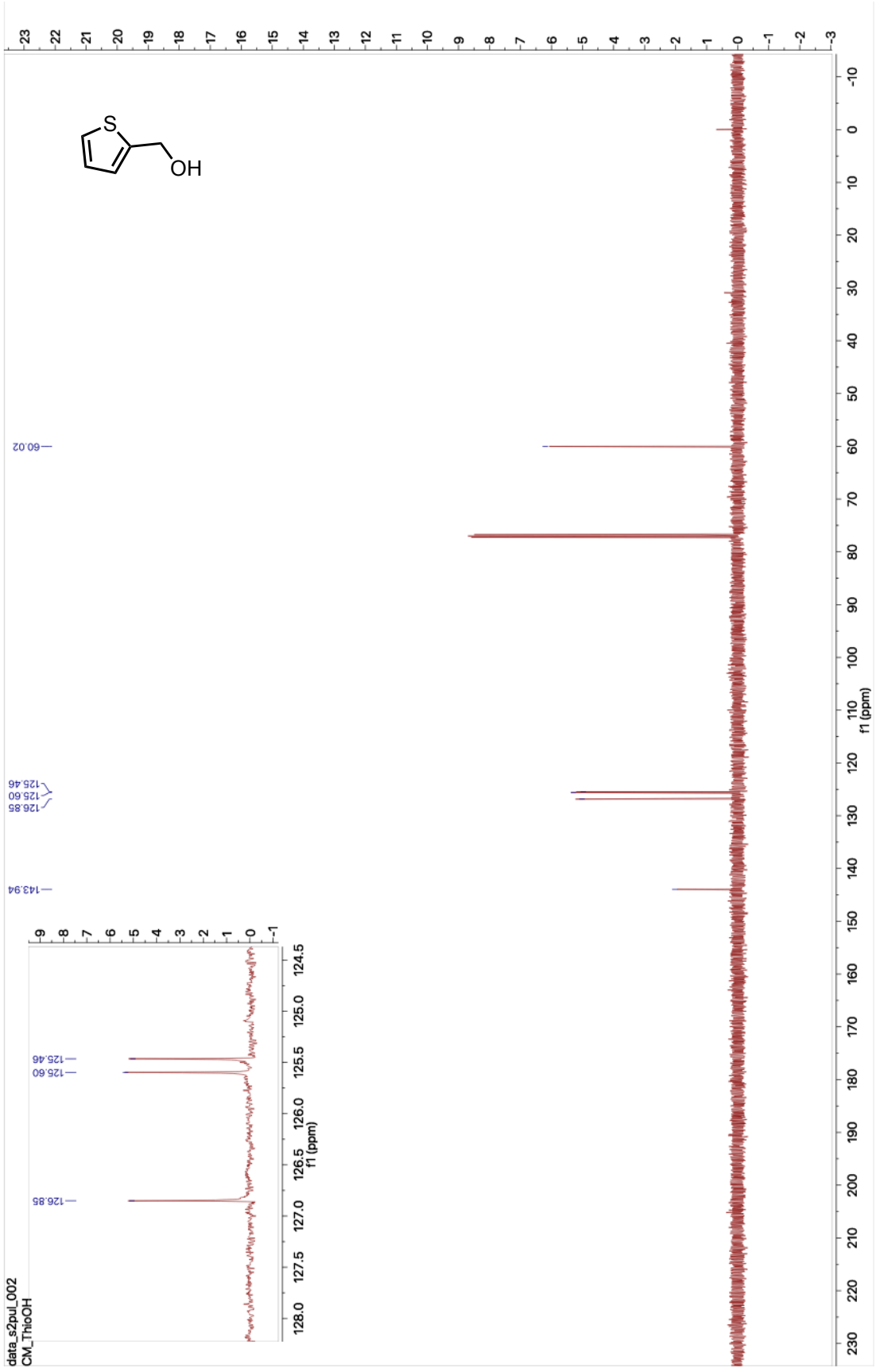
S
OH
60.02
143.94
126.85
125.60
125.46
f1 (ppm)
data_s2pul_002
CM_ThioOH

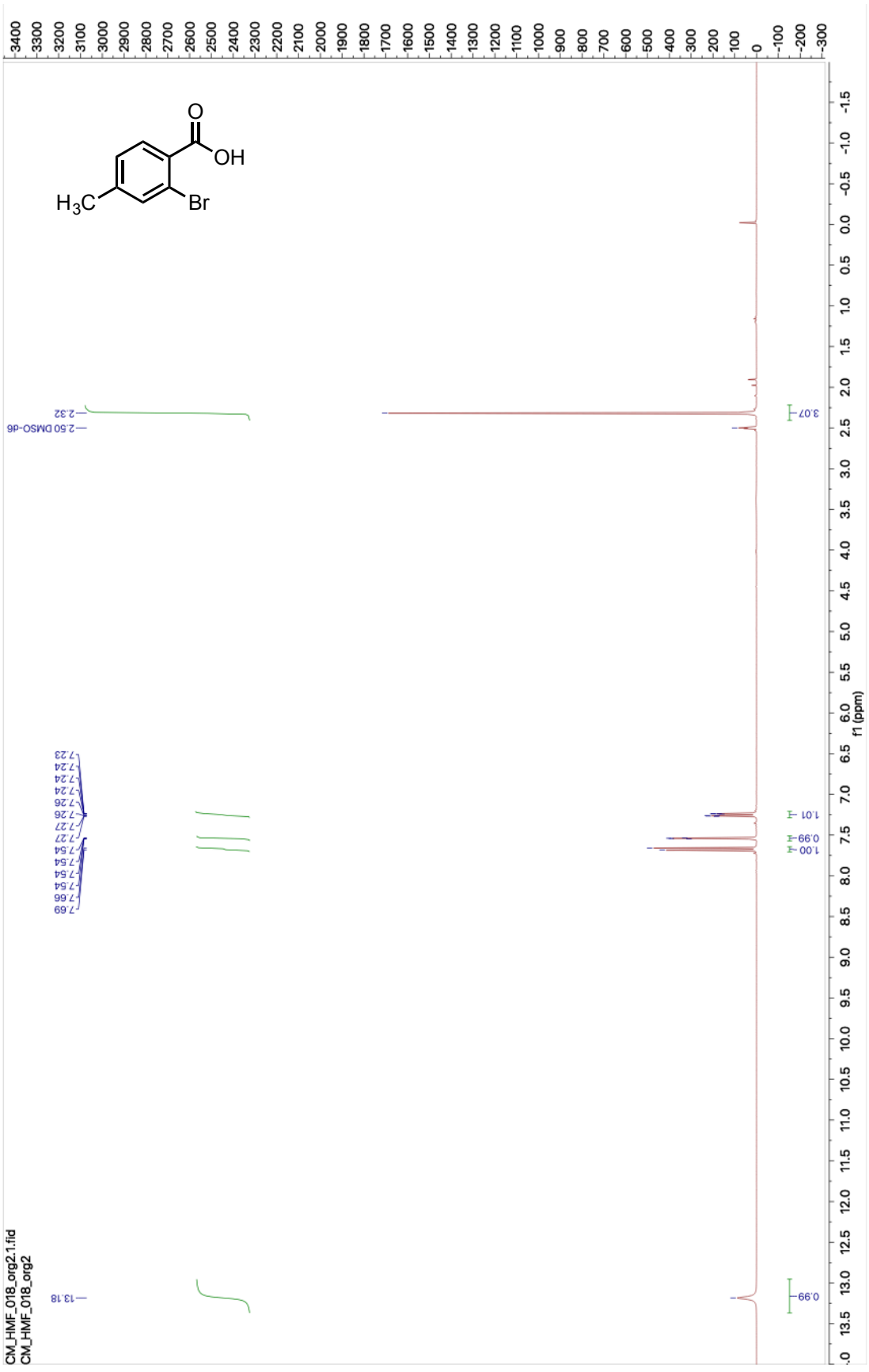
O
OH
H3C
Br
2.32
2.50 DMSO-d6
7.23
7.24
7.24
7.24
7.26
7.26
7.27
7.27
7.54
7.54
7.54
7.54
7.66
7.69
13.18
3.07
1.01
0.99
1.00
0.99
f1 (ppm)
CM_HMF_018_org2.1.fid
CM_HMF_018_org2

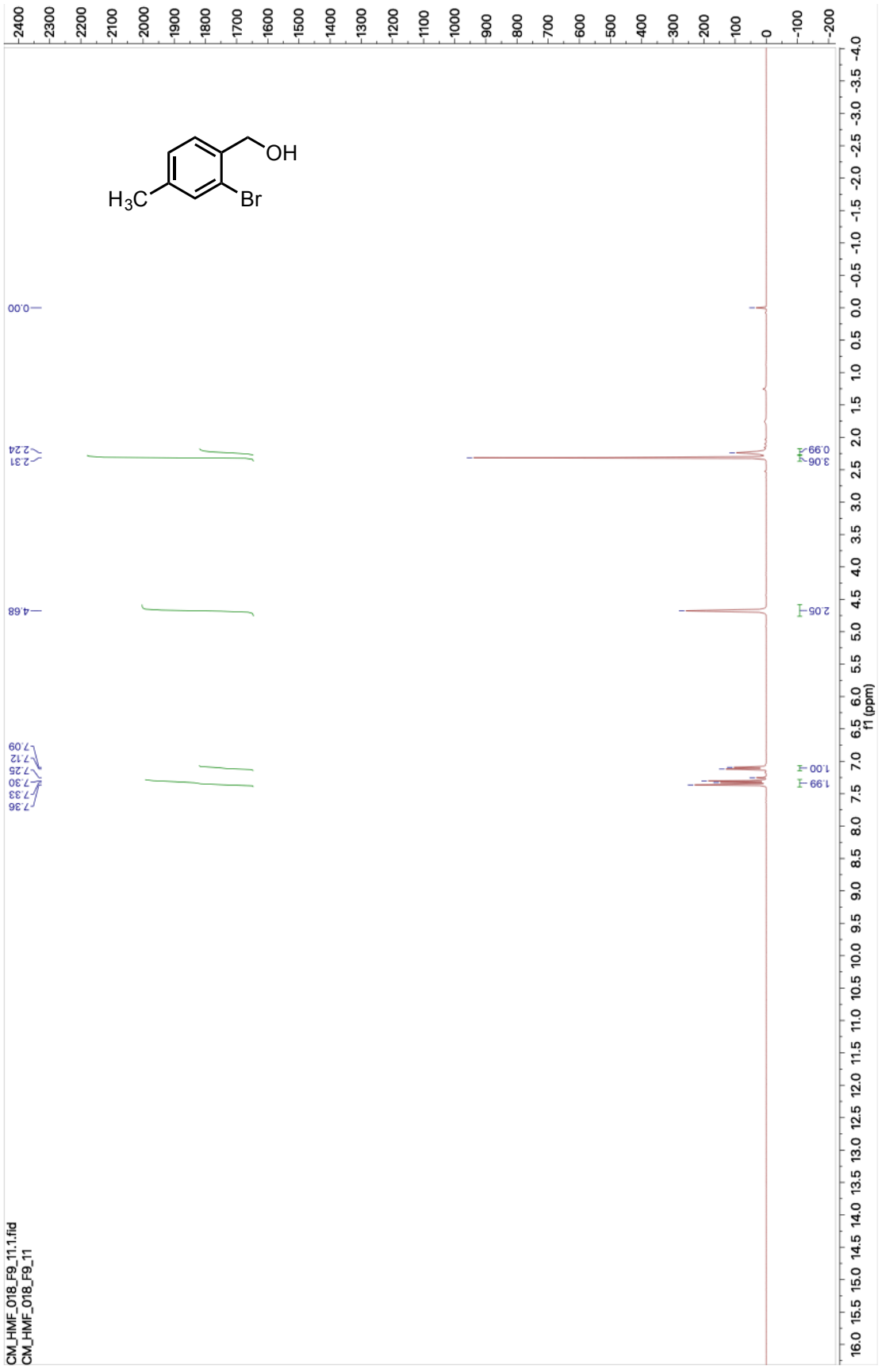
OH
H3C
Br
CM_HMF_018_F9_11.1.fid
CM_HMF_018_F9_11
f1 (ppm)

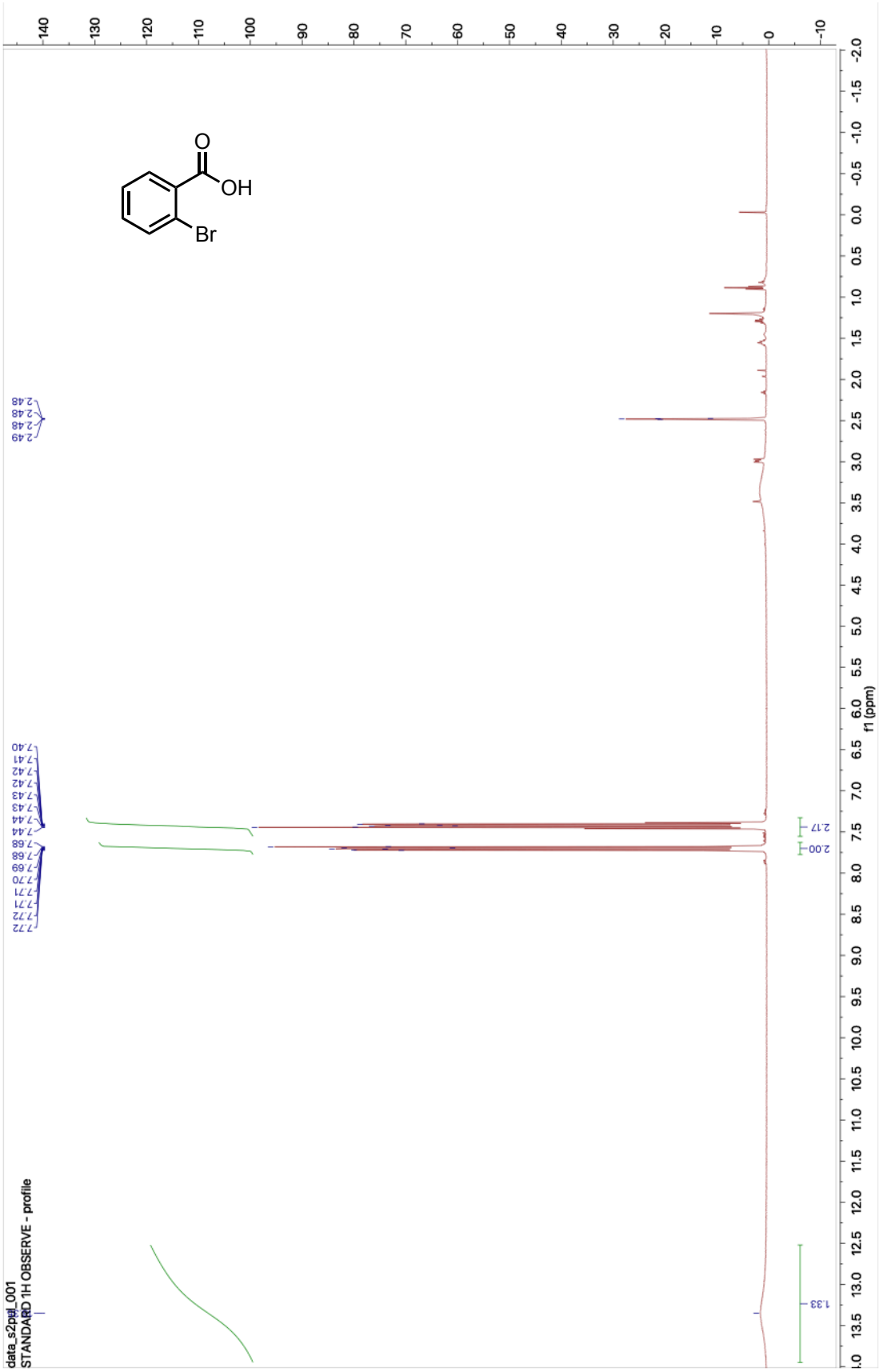
O
OH
Br
data_s2pul_001
STANDARD 1H OBSERVE - profile
f1 (ppm)

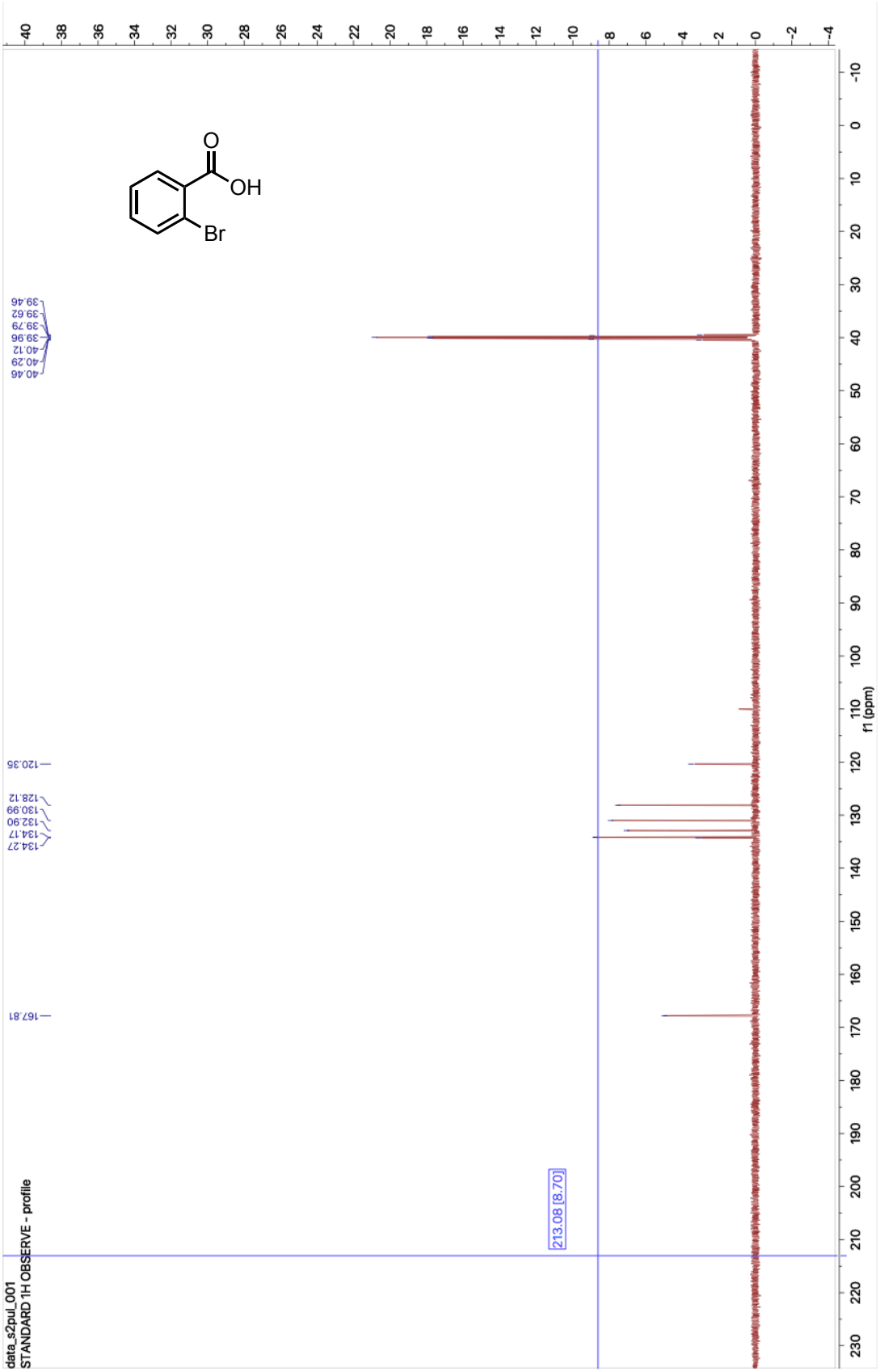
O
OH
Br
39.46
39.62
39.79
39.96
40.12
40.29
40.46
120.35
128.12
130.99
132.90
134.17
134.27
167.81
213.08 [8.70]
f1 (ppm)
data_s2pul_001
STANDARD 1H OBSERVE - profile

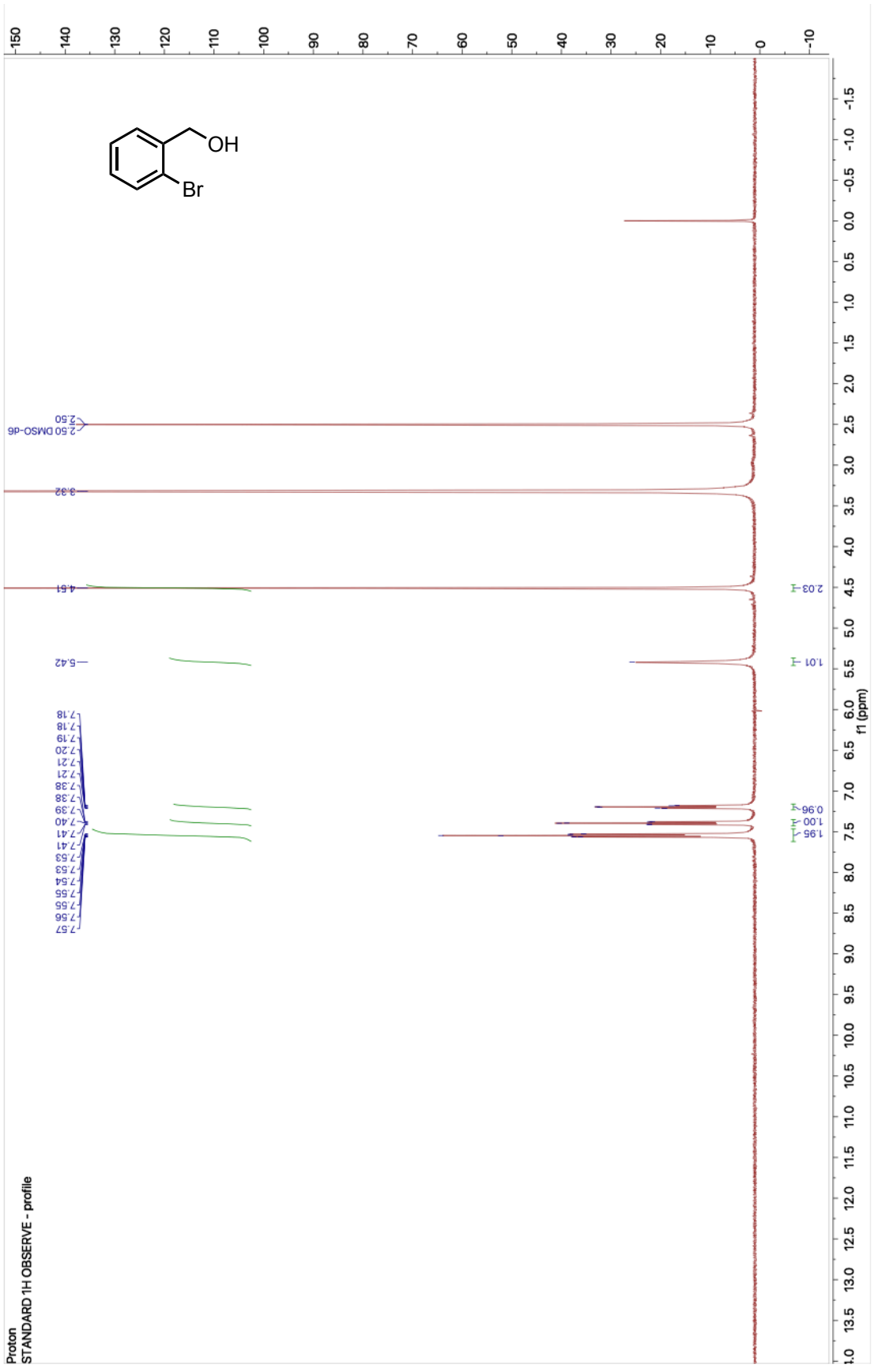
OH
Br
Proton
STANDARD 1H OBSERVE - profile
f1 (ppm)

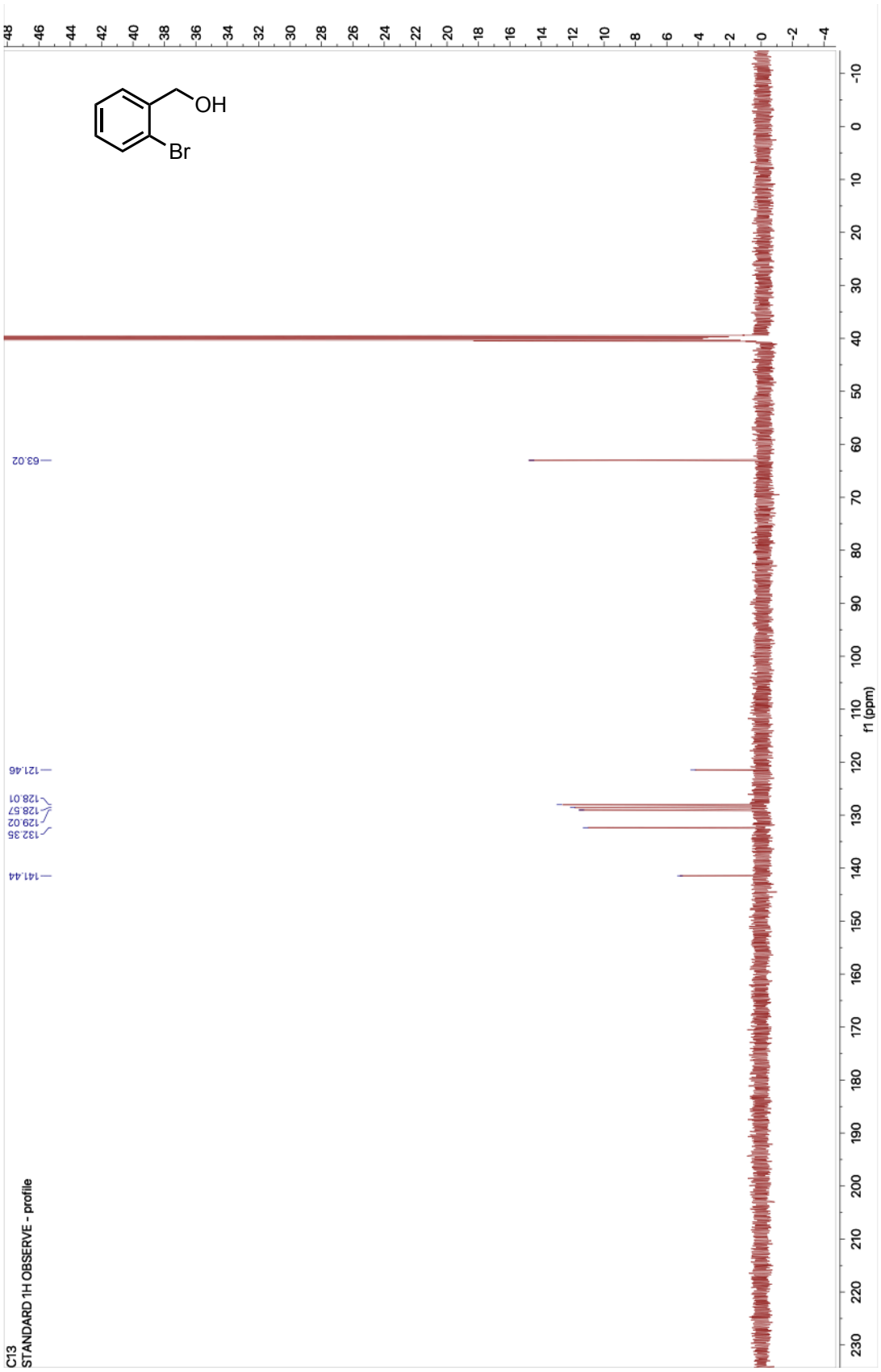
OH
Br
63.02
121.46
128.01
128.57
129.02
132.35
141.44
C13
STANDARD 1H OBSERVE - profile
f1 (ppm)


O
OH
2.48
3.32
7.48
7.60
7.92
2.00
0.96
1.95
1.09
f1 (ppm)
data_s2pul_001
STANDARD 1H OBSERVE - profile

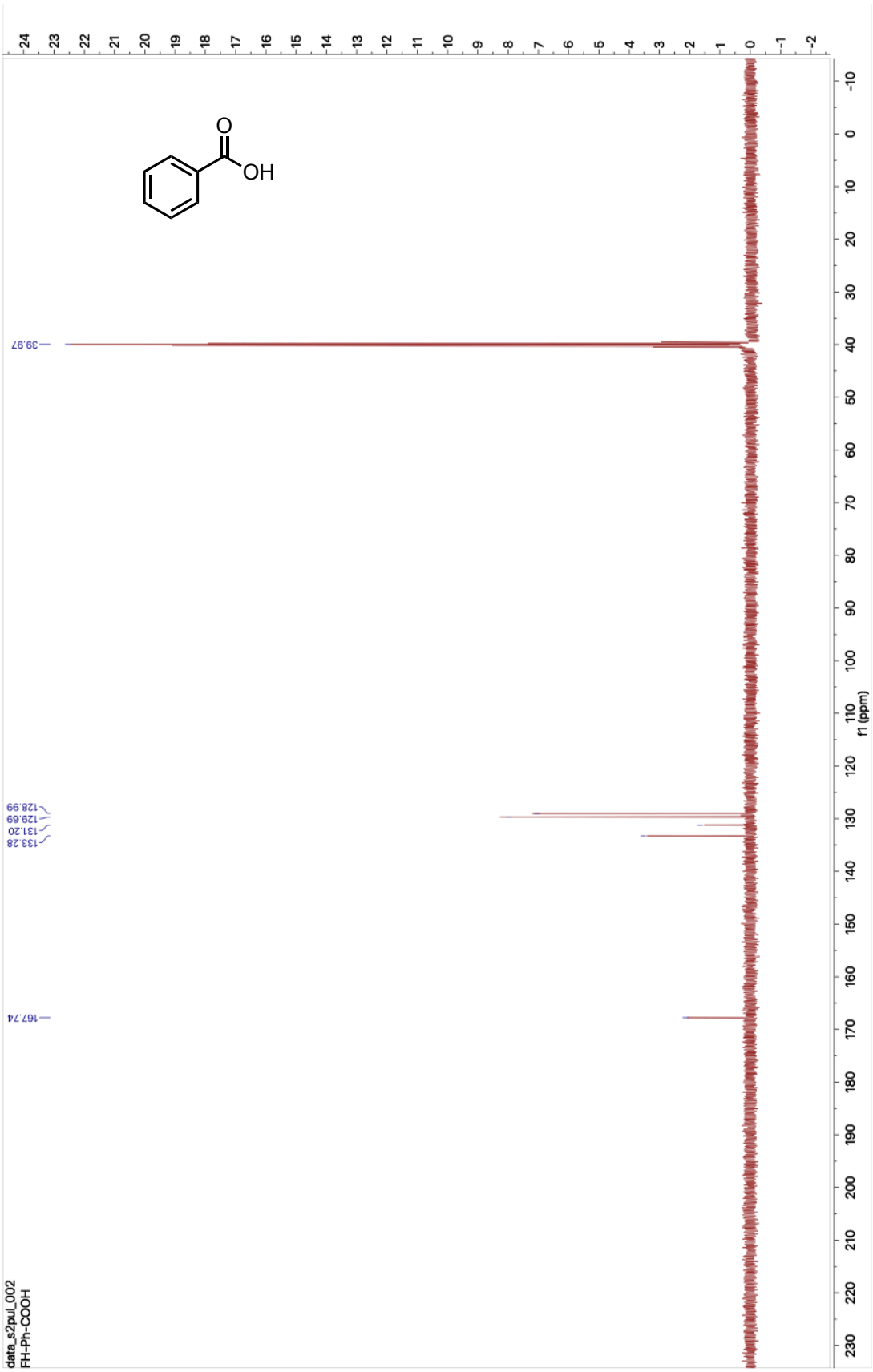
O
OH
39.97
128.99
129.69
131.20
133.28
167.74
f1 (ppm)
data_s2pul_002
FH-Ph-COOH

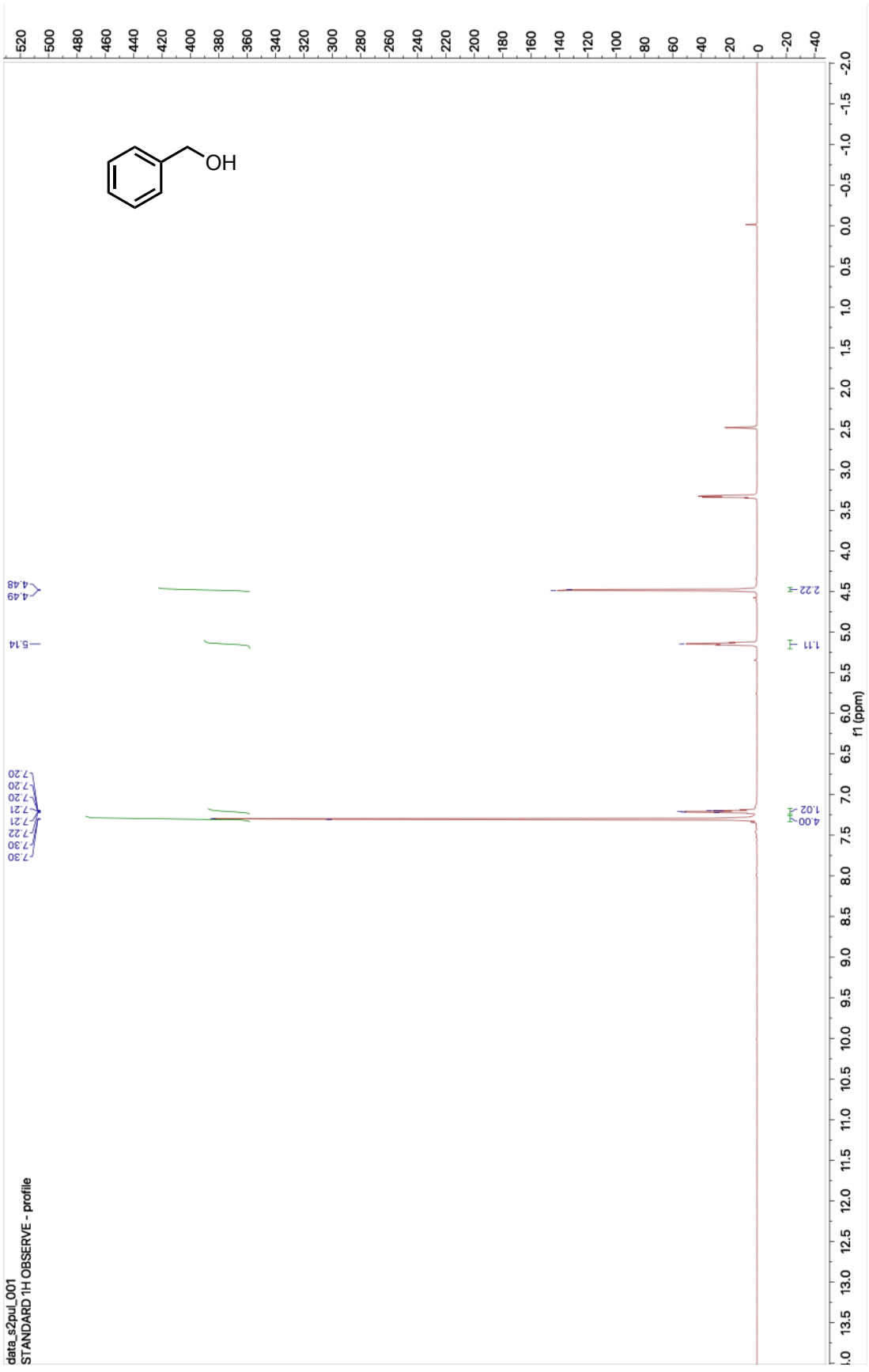
OH
data_s2pul_001
STANDARD 1H OBSERVE - profile
f1 (ppm)

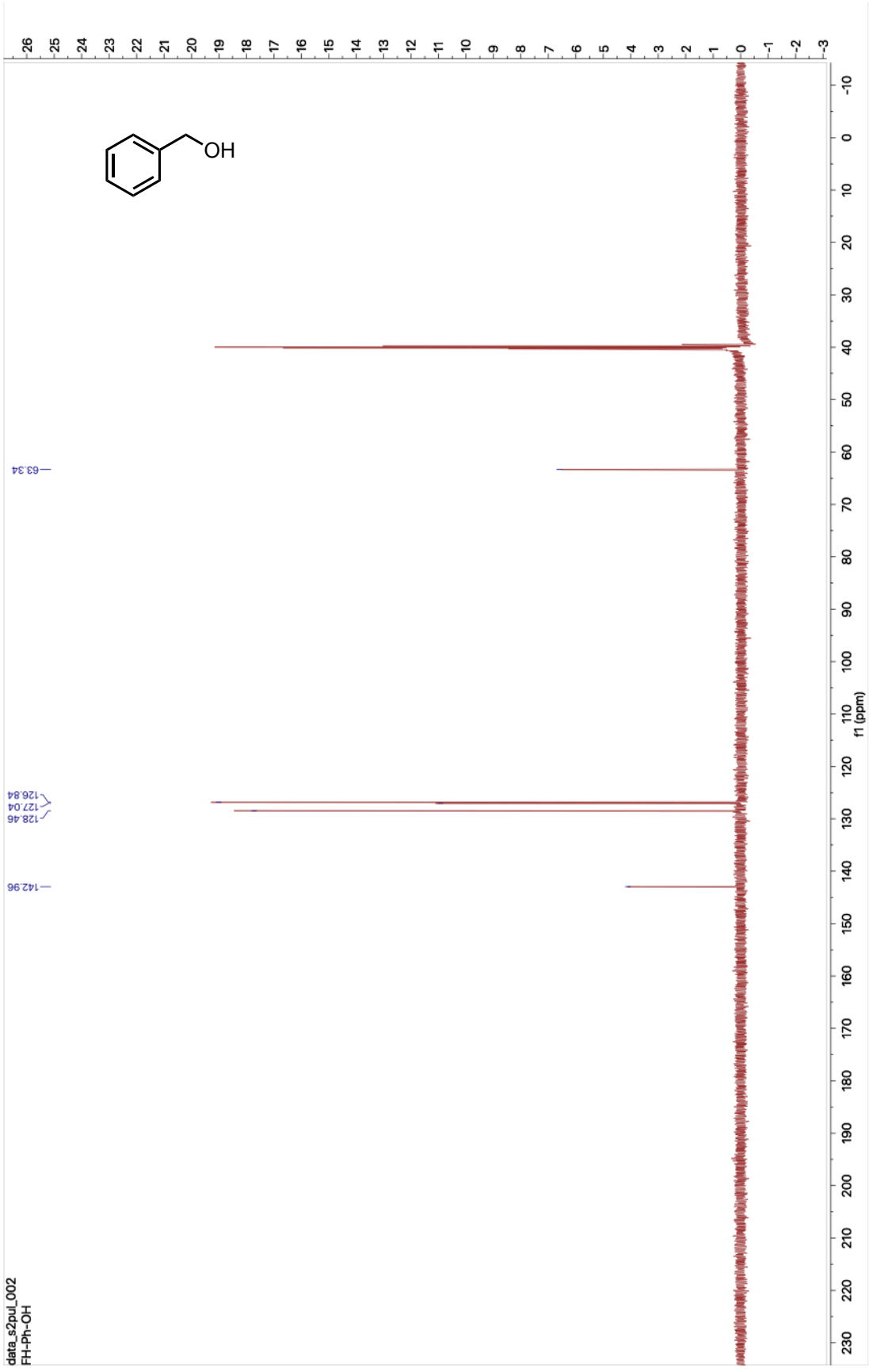
OH
63.34
128.46
127.04
126.84
142.96
f1 (ppm)
data_s2pul_002
FH-Ph-OH

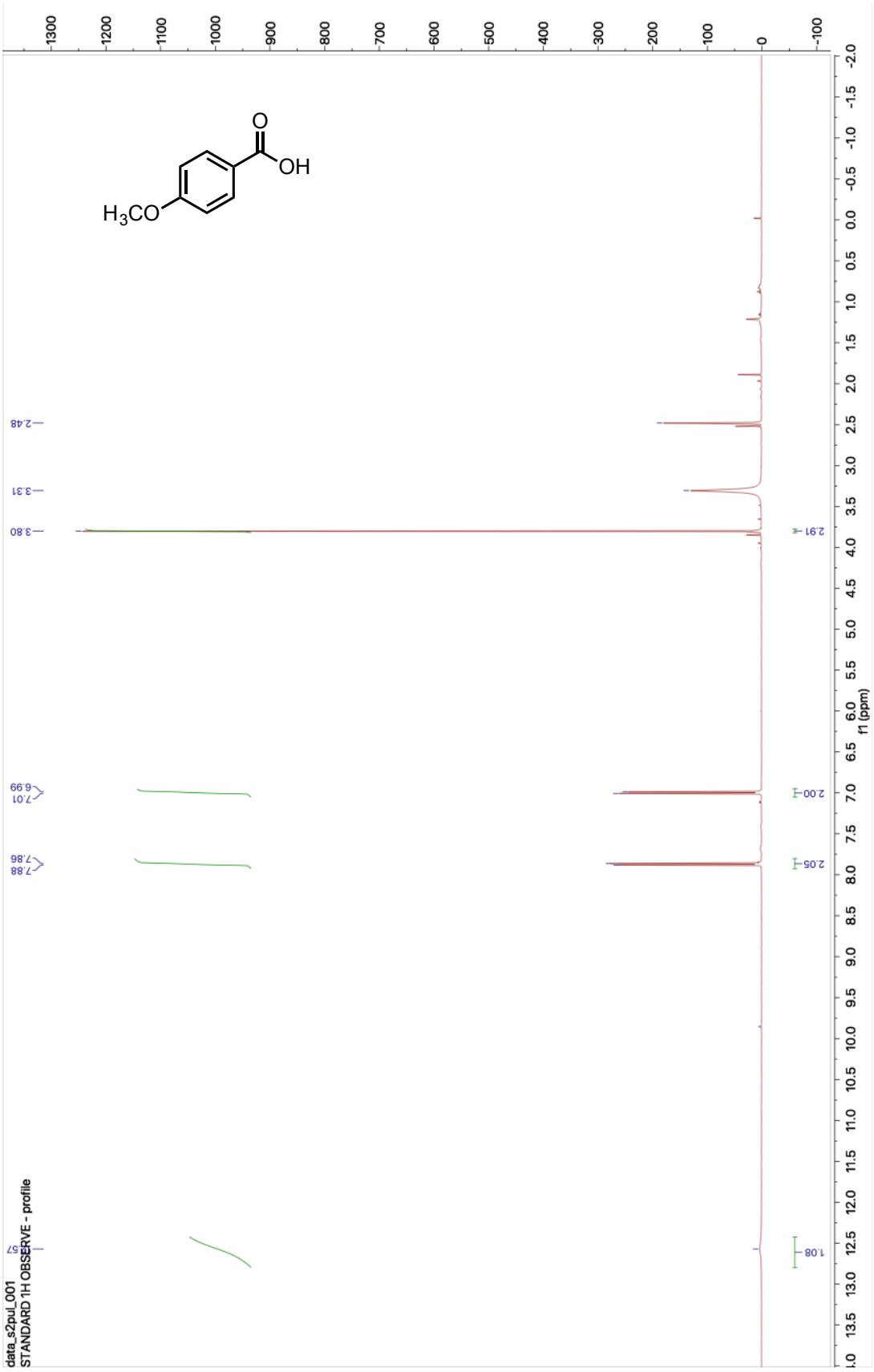
O
OH
H3CO
2.48
3.31
3.80
7.01
6.99
7.88
7.86
2.91
2.00
2.05
1.08
f1 (ppm)
data_s2pul_001
STANDARD 1H OBSERVE - profile

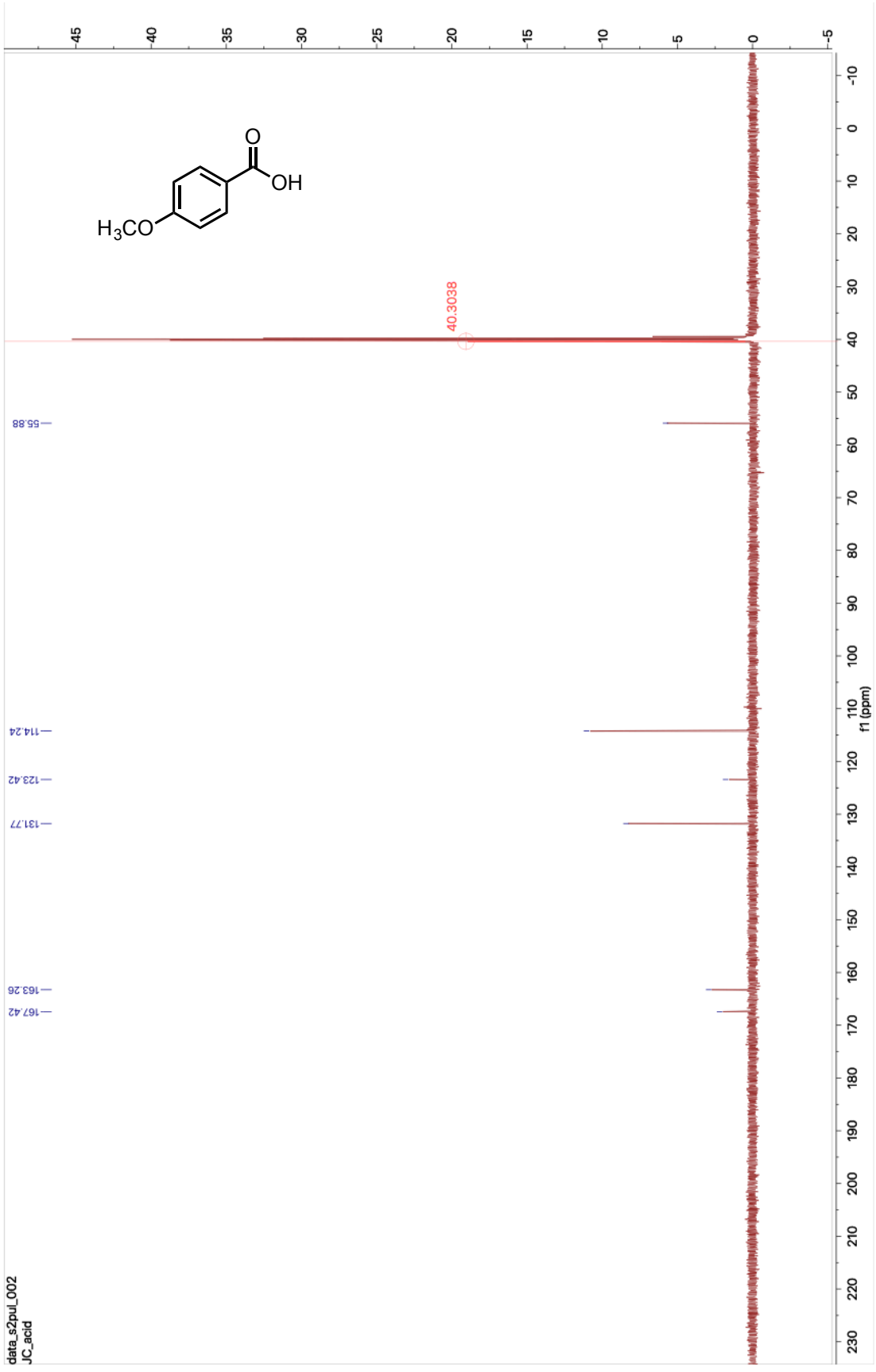
O
OH
H3CO
40.3038
55.88
114.24
123.42
131.77
163.26
167.42
f1 (ppm)
data_s2pul_002
JC_acid

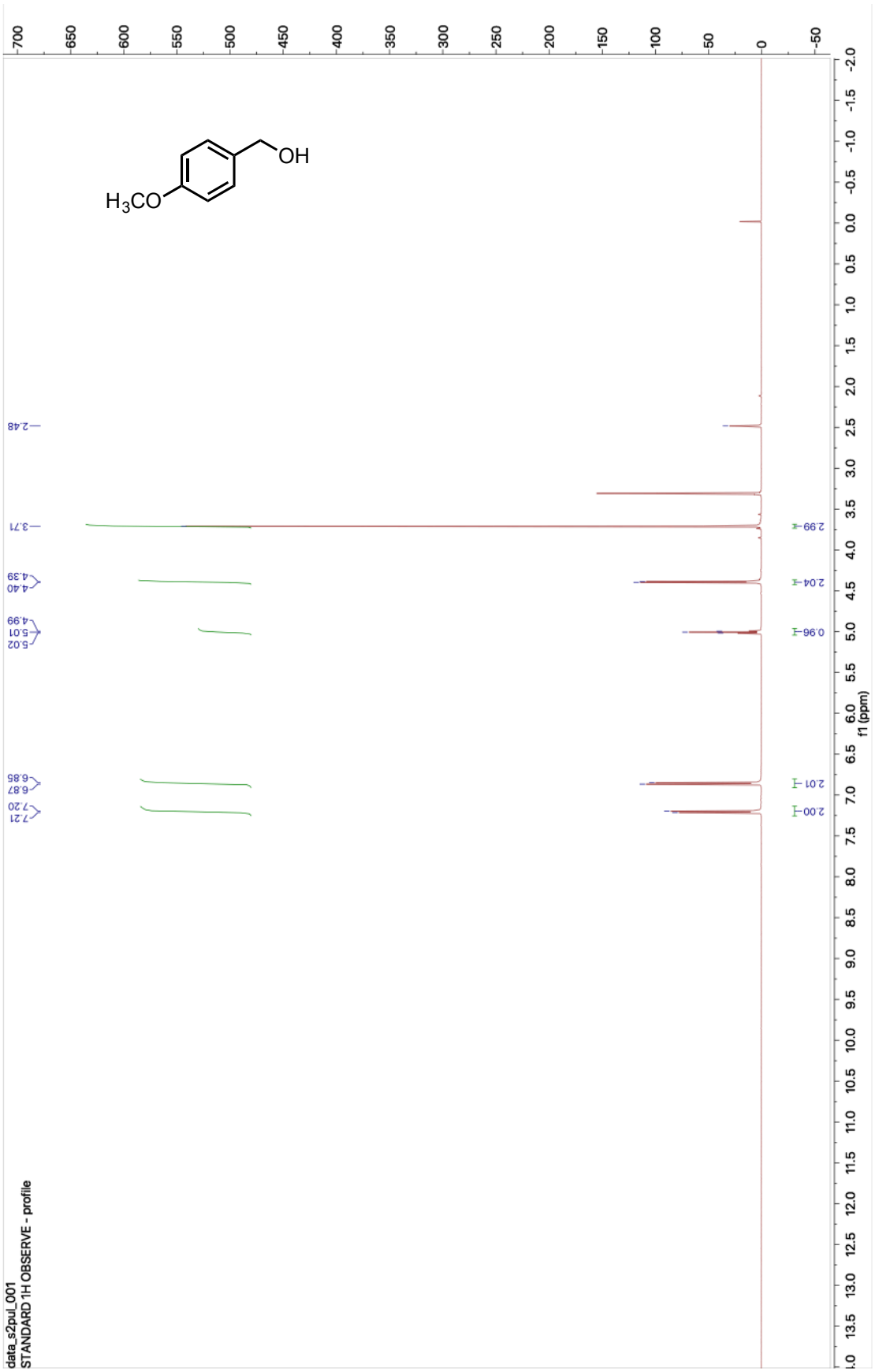
OH
H3CO
data_s2pul_001
STANDARD 1H OBSERVE - profile
f1 (ppm)

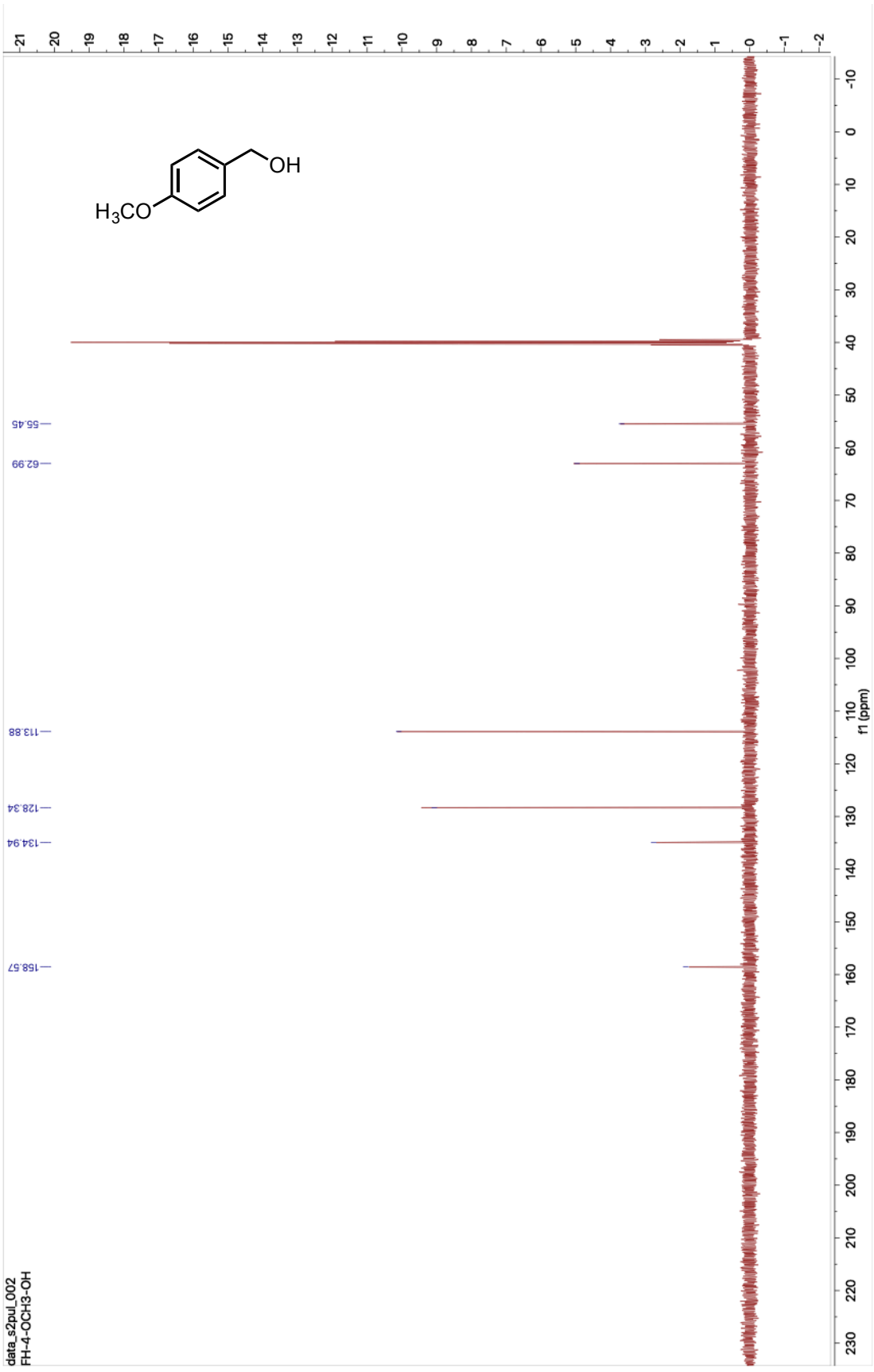
OH
H3CO
55.45
62.99
113.88
128.34
134.94
158.57
f1 (ppm)
data_s2pul_002
FH-4-OCH3-OH

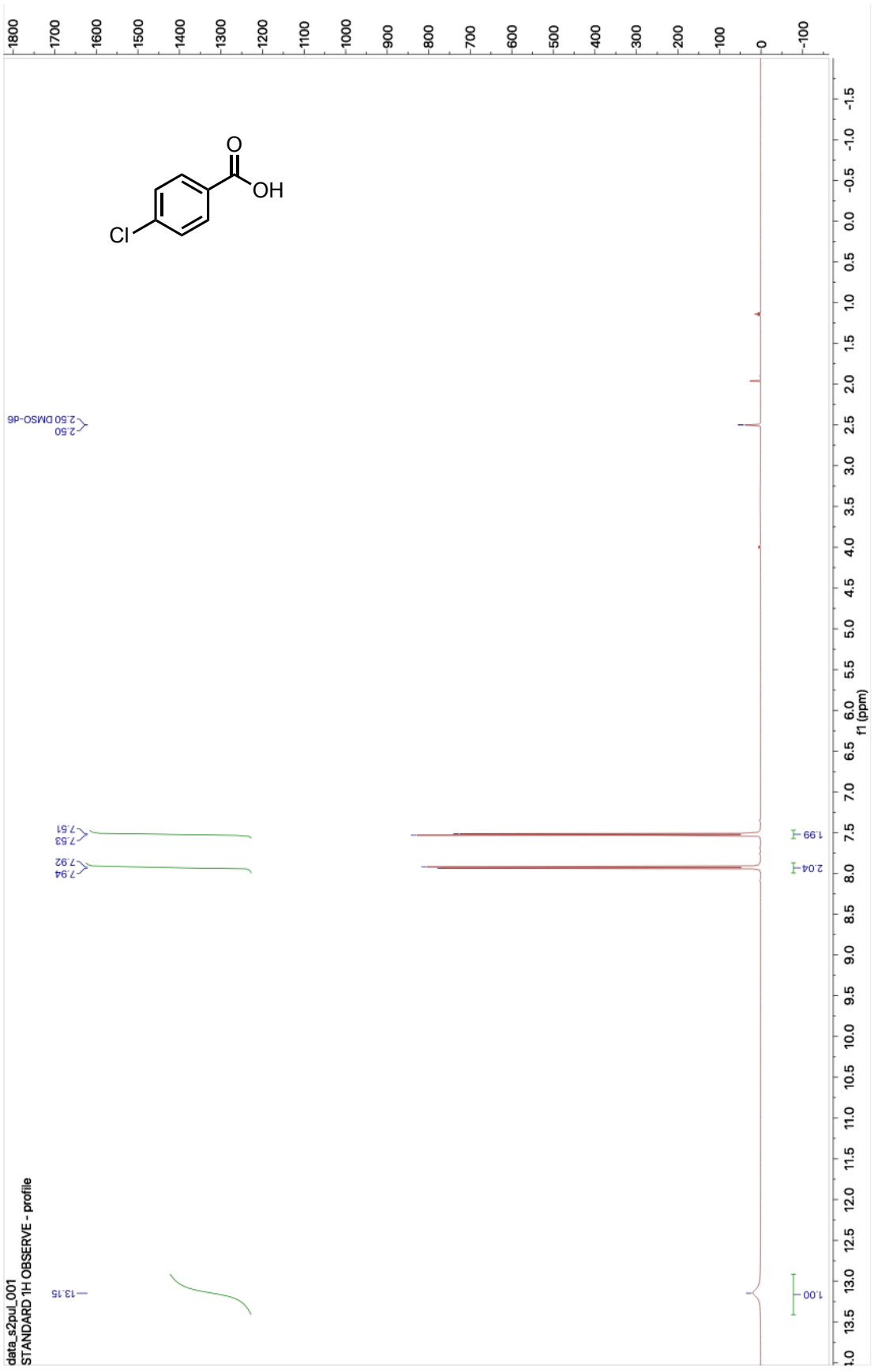
O
OH
Cl
2.50 DMSO-d6
7.51
7.53
7.92
7.94
1.99
2.04
1.00
13.15
f1 (ppm)
data_s2pul_001
STANDARD 1H OBSERVE - profile

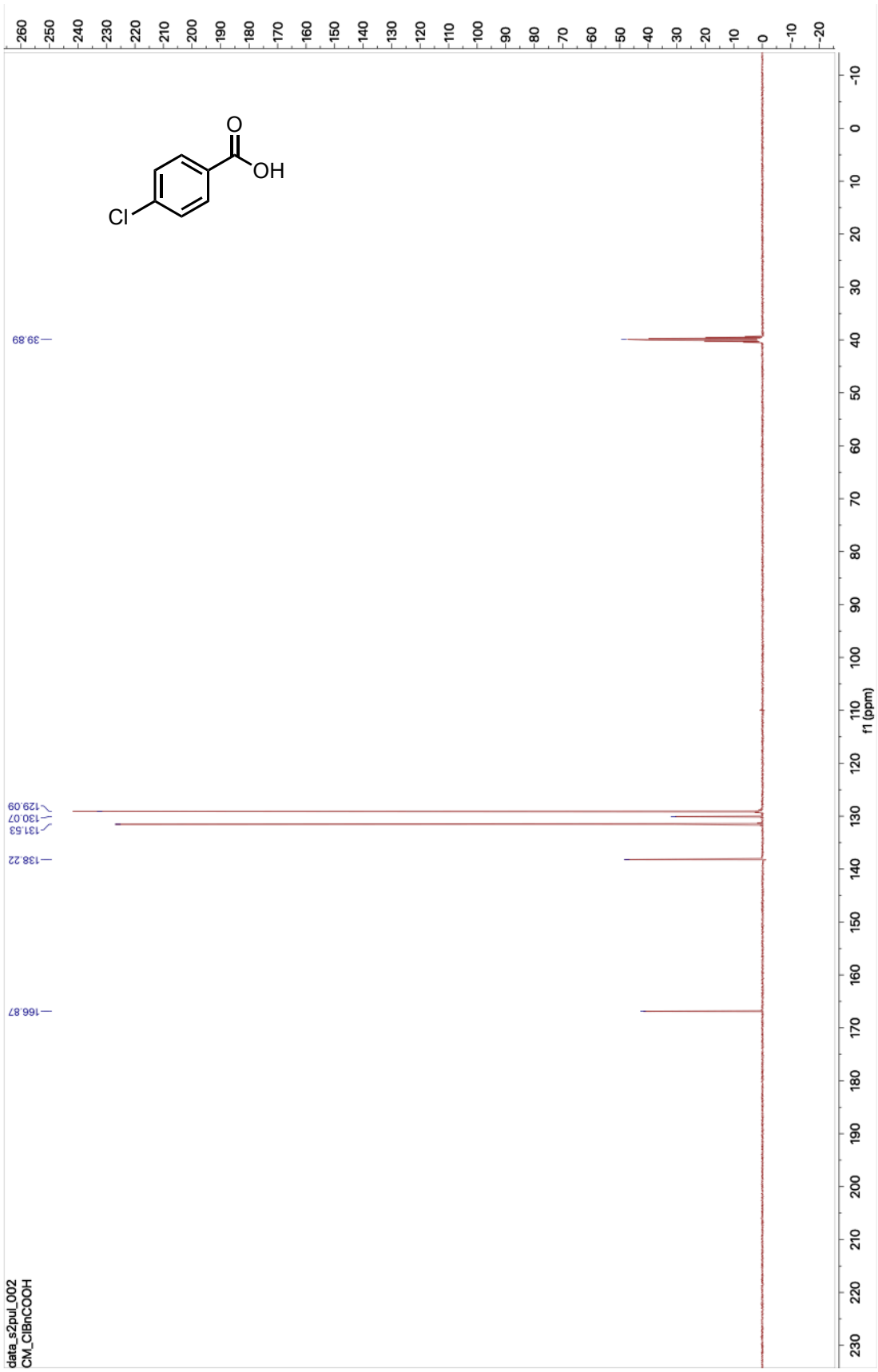
O
OH
Cl
39.89
129.09
130.07
131.53
138.22
166.87
f1 (ppm)
data_s2pul_002
CM_ClBnCOOH

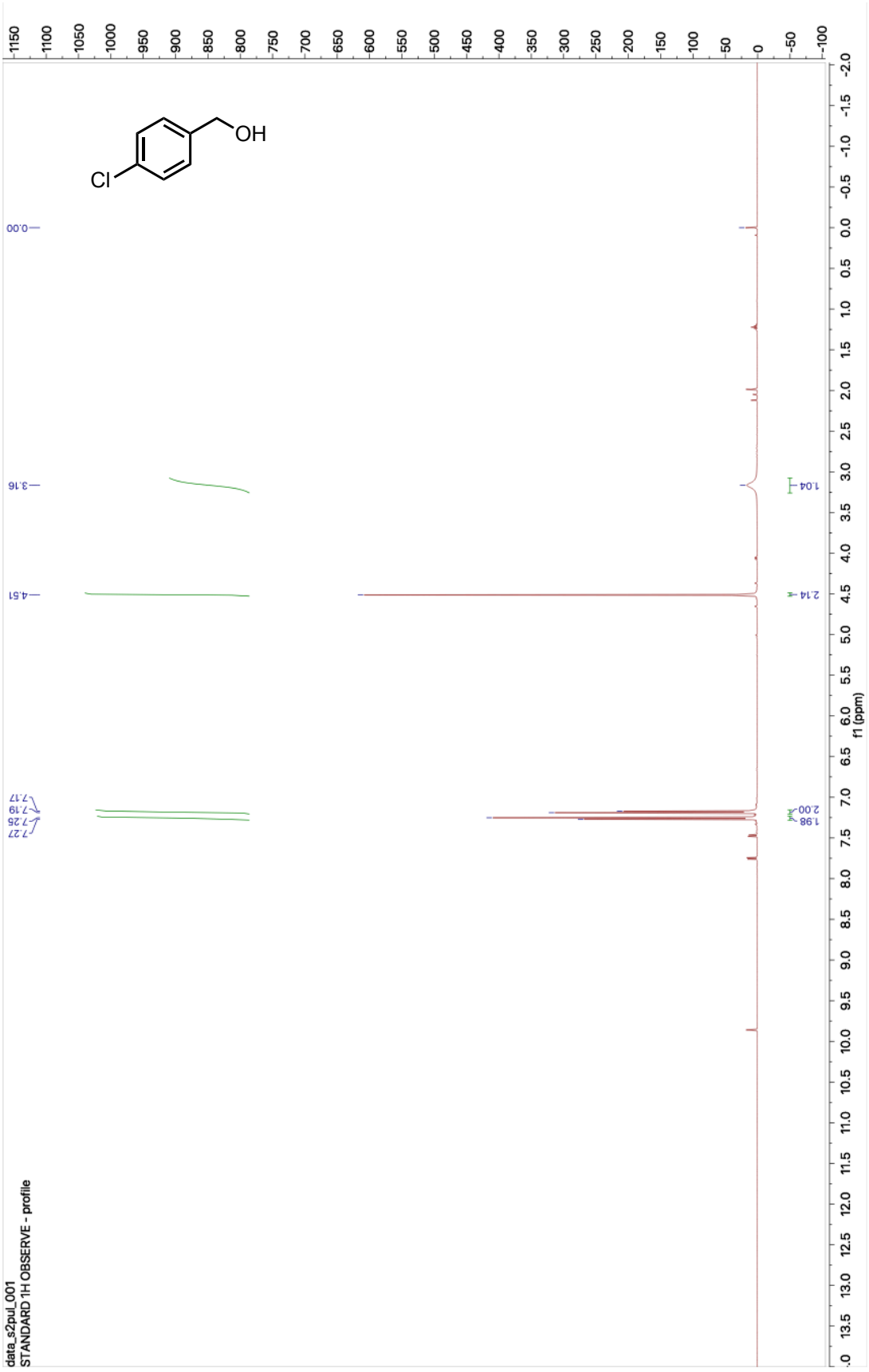
OH
Cl
data_s2pul_001
STANDARD 1H OBSERVE - profile
f1 (ppm)

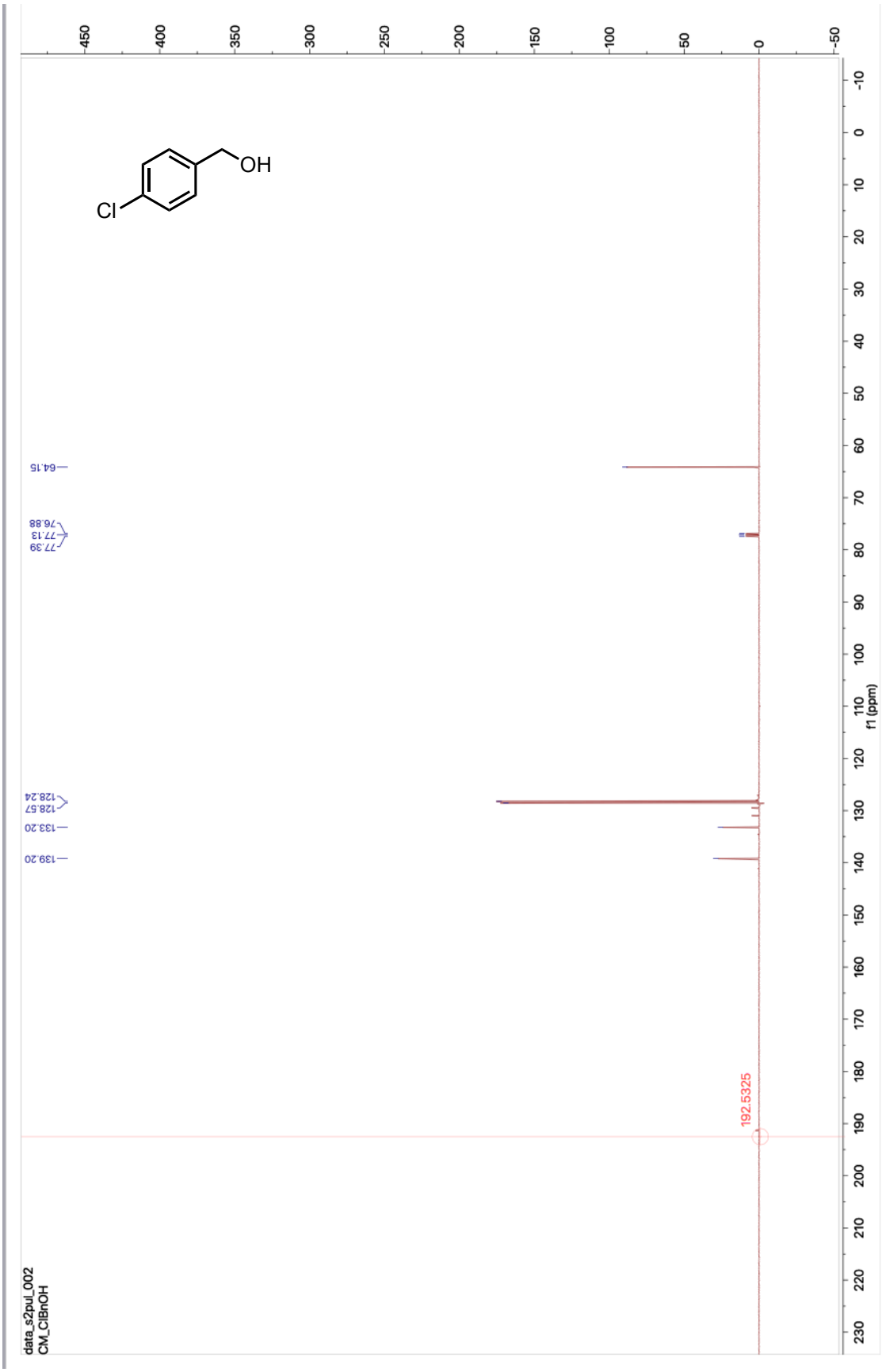
OH
Cl
64.15
76.88
77.13
77.39
128.24
128.57
133.20
139.20
192.5325
f1 (ppm)
data_s2pul_002
CM_ClBnOH

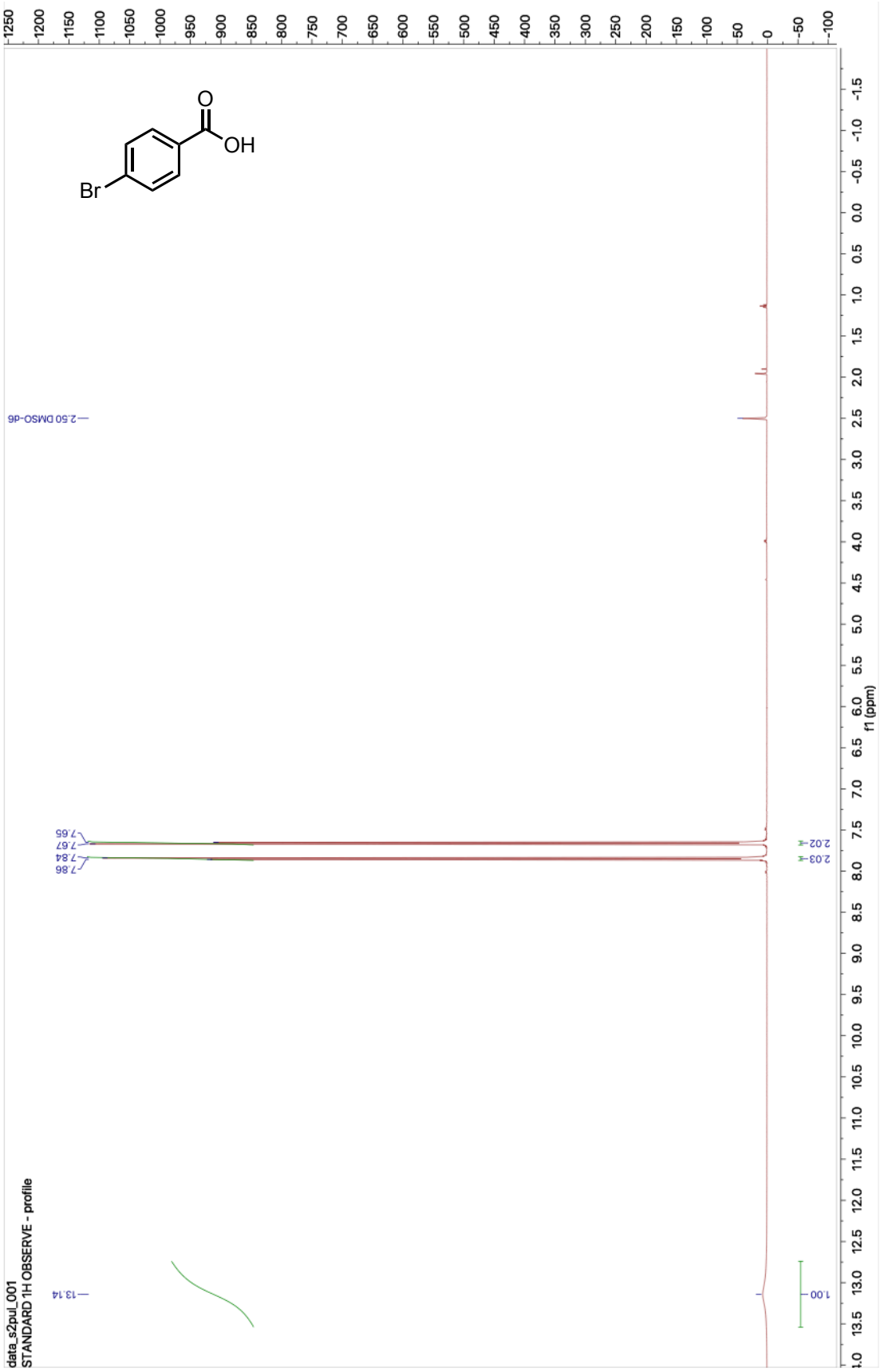
O
OH
Br
2.50 DMSO-d6
7.86
7.84
7.67
7.65
2.03
2.02
1.00
13.14
data_s2pul_001
STANDARD 1H OBSERVE - profile
f1 (ppm)

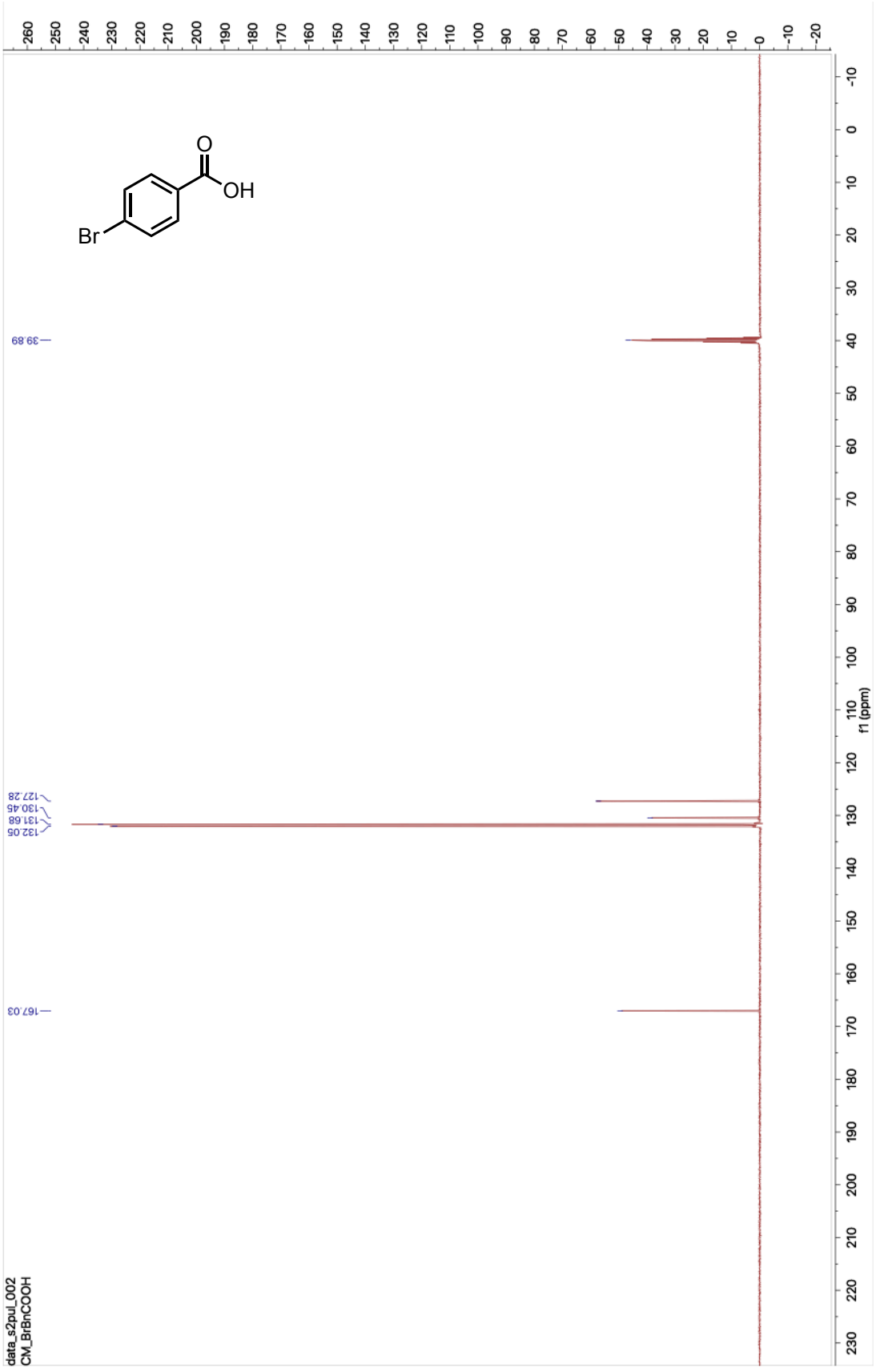
O
OH
Br
39.89
127.28
130.45
131.68
132.05
167.03
f1 (ppm)
data_s2pul_002
CM_BrBnCOOH

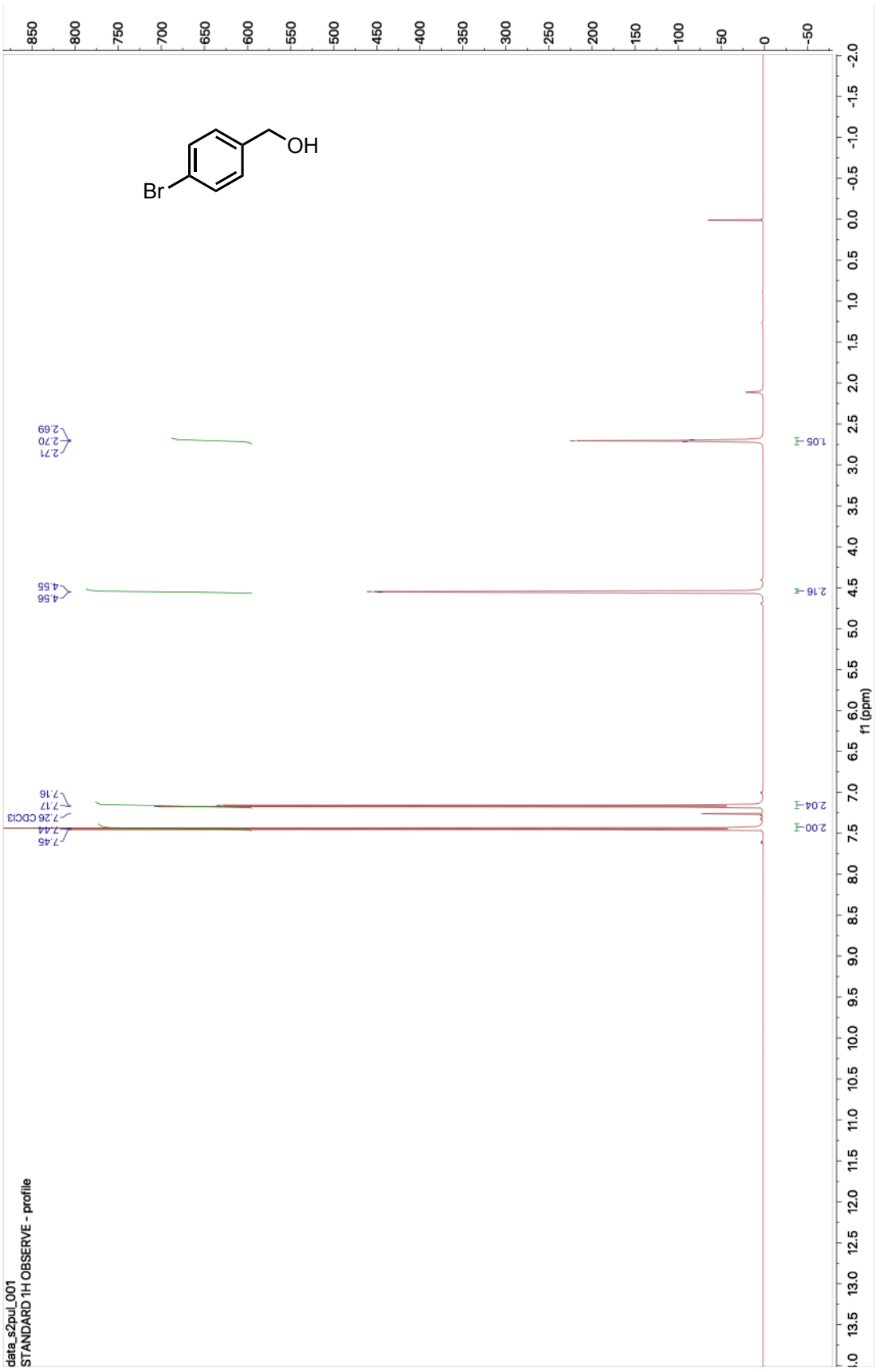
OH
Br
2.69
2.70
2.71
4.55
4.56
7.16
7.17
7.26 CDCl3
7.44
7.45
1.05
2.16
2.04
2.00
f1 (ppm)
data_s2pul_001
STANDARD 1H OBSERVE - profile

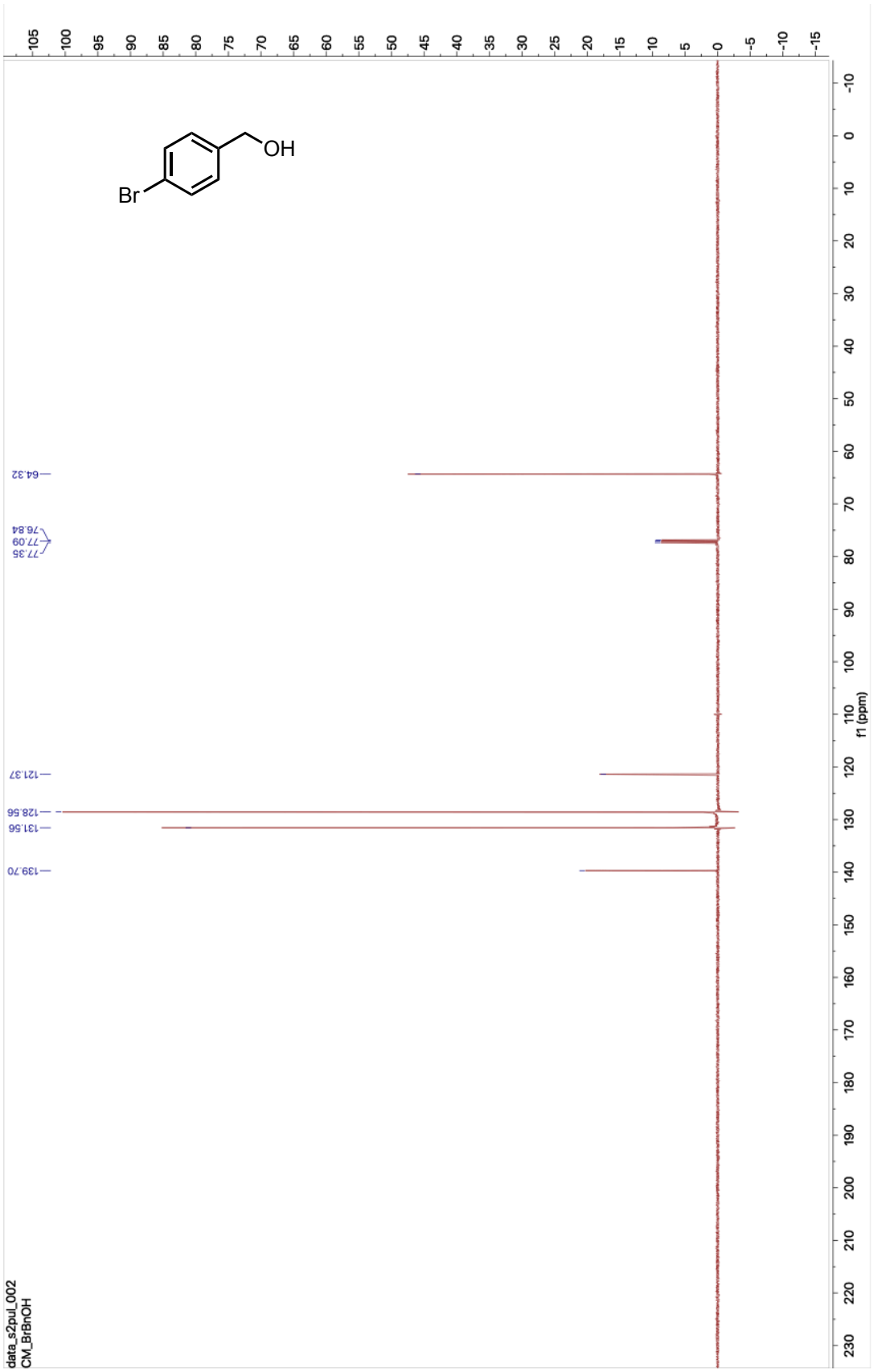
OH
Br
64.32
76.84
77.09
77.35
121.37
128.56
131.56
139.70
f1 (ppm)
data_s2pul_002
CM_BrBnOH

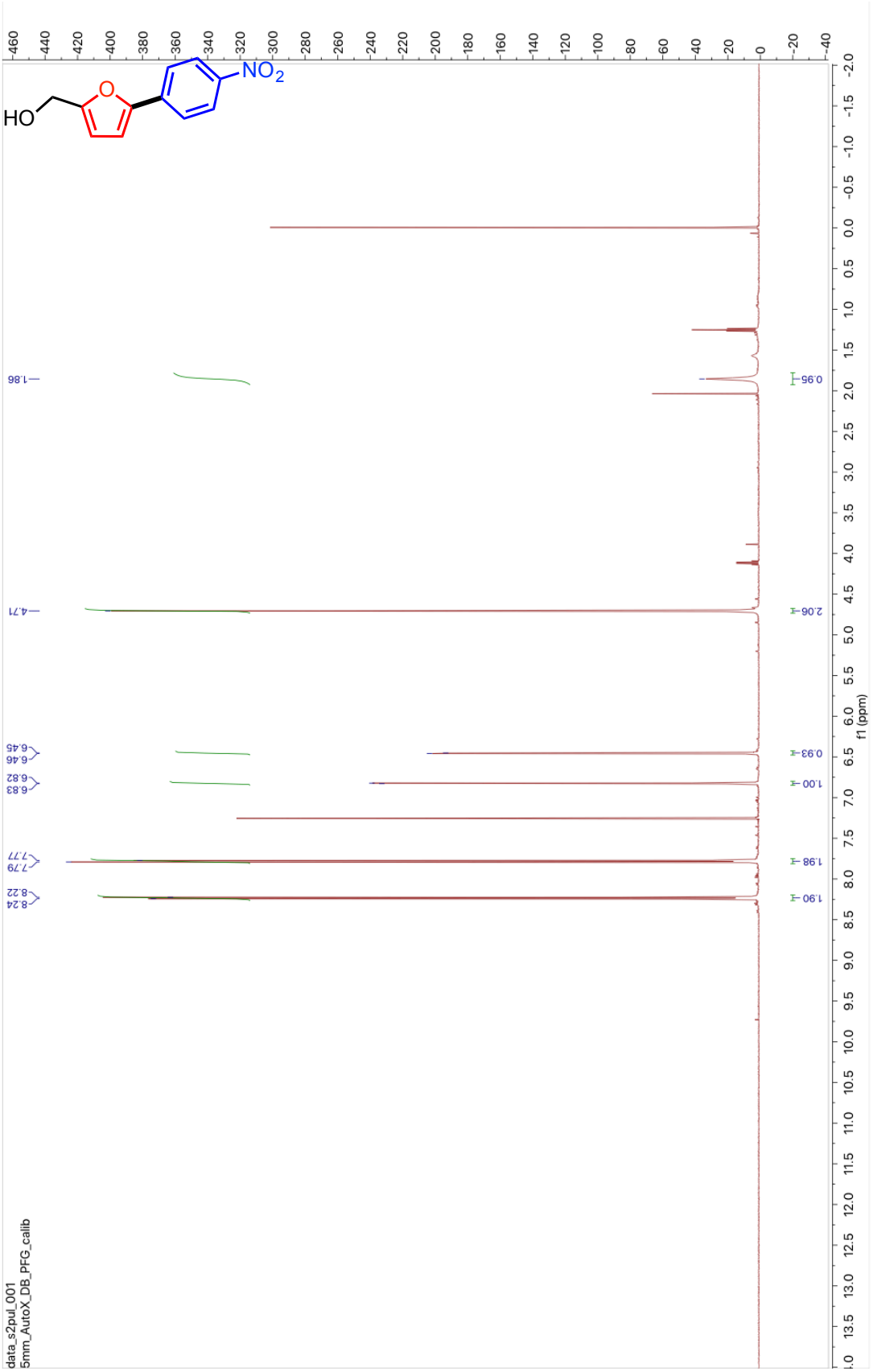
HO
O
NO2
1.86
4.71
6.45
6.46
6.82
6.83
7.77
7.79
8.22
8.24
0.95
2.06
0.93
1.00
1.98
1.90
f1 (ppm)
data_s2pul_001
5mm_AutoX_DB_PFG_calib

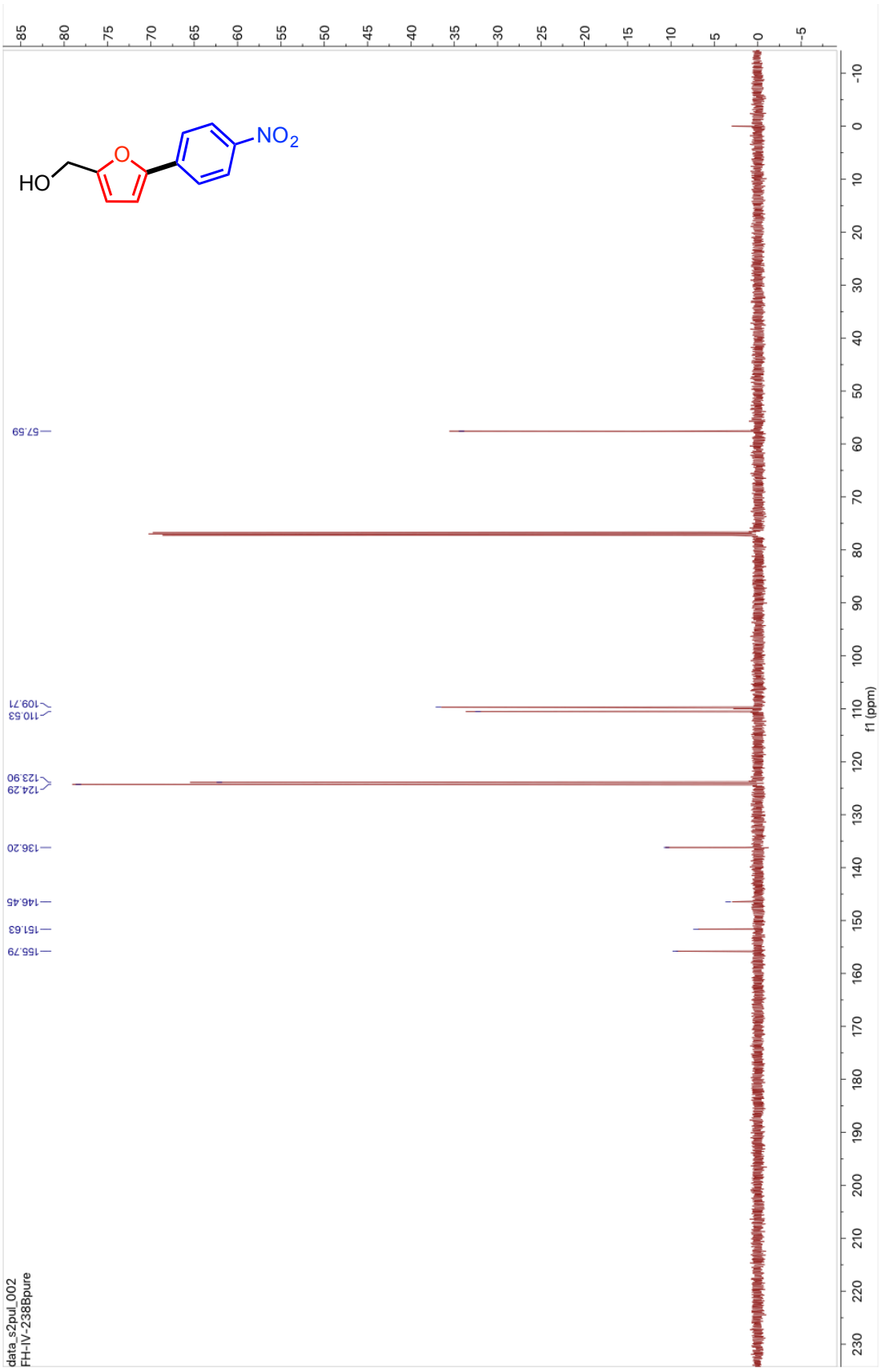
HO
O
NO2
57.59
109.71
110.53
123.90
124.29
136.20
146.45
151.63
155.79
f1 (ppm)
data_s2pul_002
FH-IV-238Bpure

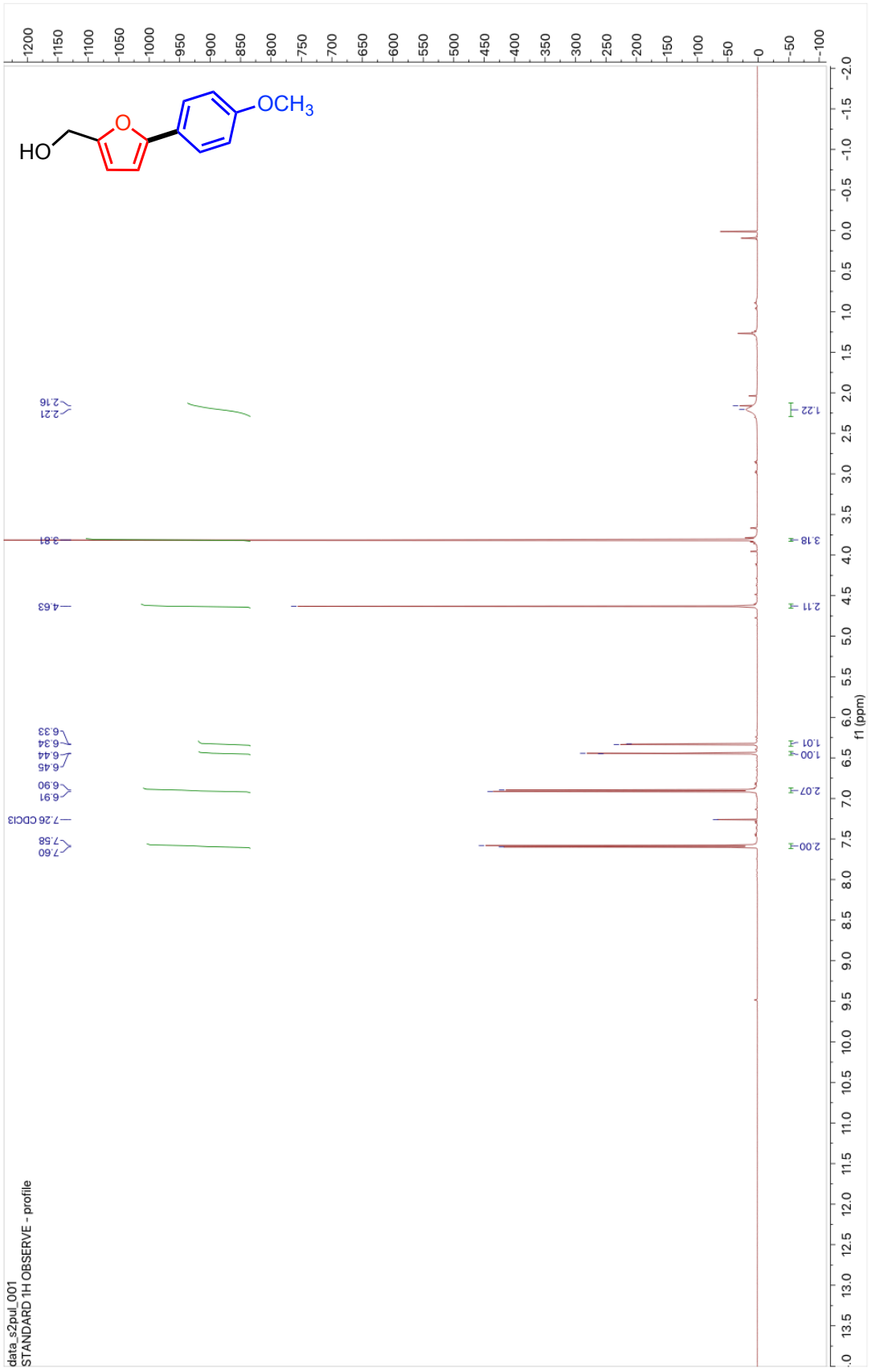
HO
O
OCH3
2.16
2.21
3.81
4.63
6.33
6.34
6.44
6.45
6.90
6.91
7.26 CDCl3
7.58
7.60
1.22
3.18
2.11
1.01
1.00
2.07
2.00
f1 (ppm)
data_s2pul_001
STANDARD 1H OBSERVE - profile

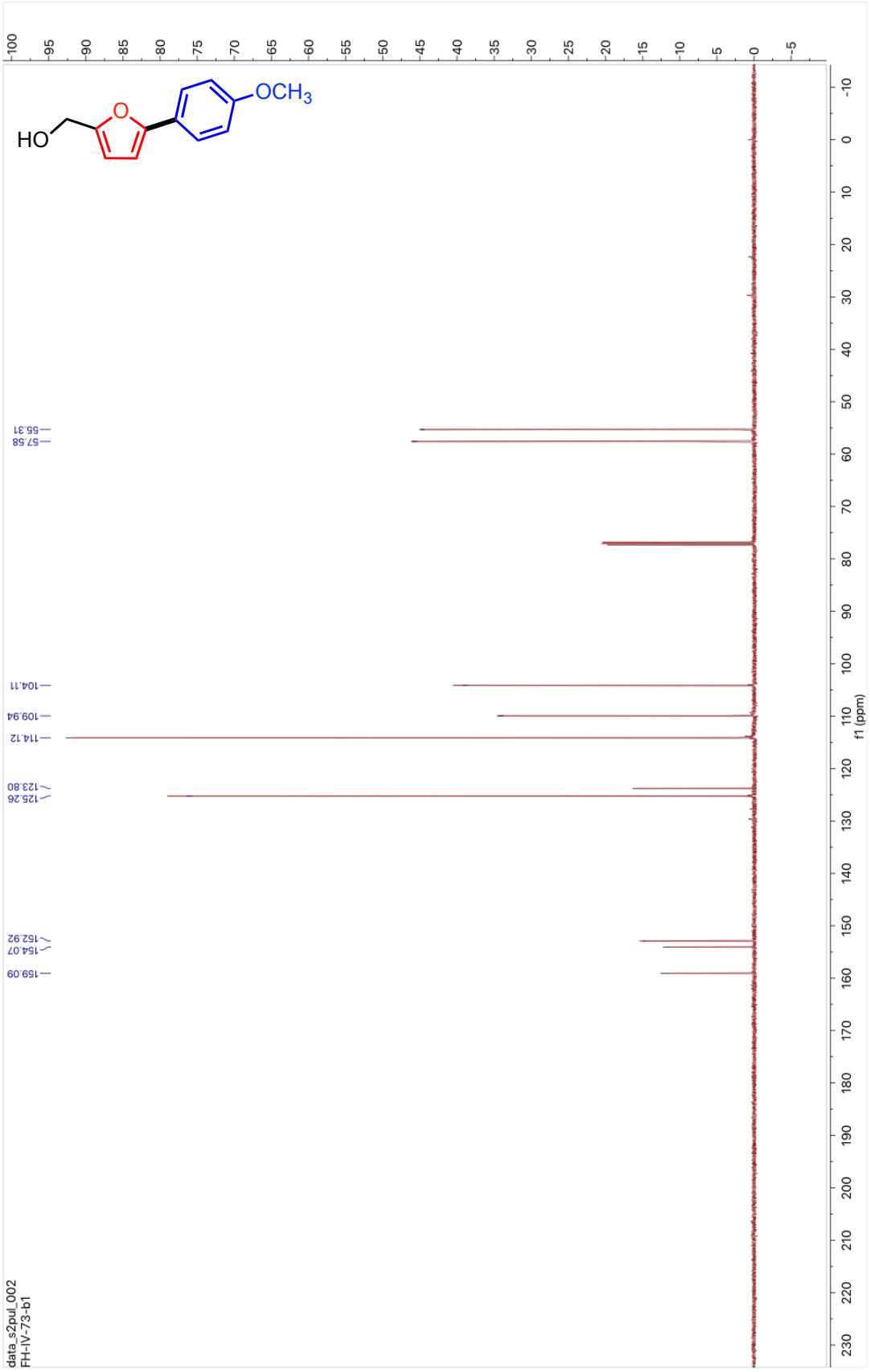
HO
O
OCH3
55.31
57.58
104.11
109.94
114.12
123.80
125.26
152.92
154.07
159.09
f1 (ppm)
data_s2pul_002
FH-IV-73-b1

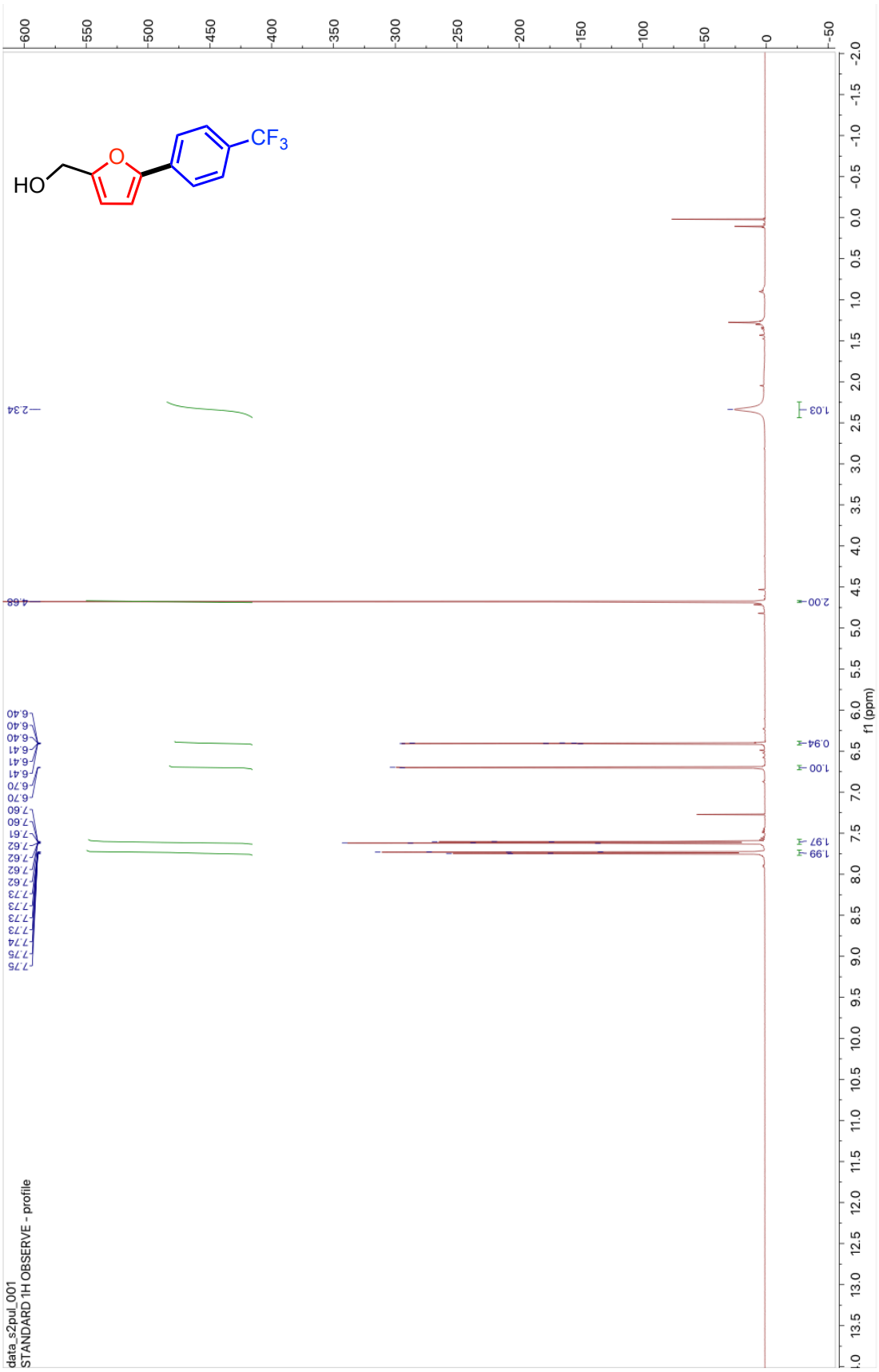
HO
O
CF3
data_s2pul_001
STANDARD 1H OBSERVE - profile
f1 (ppm)

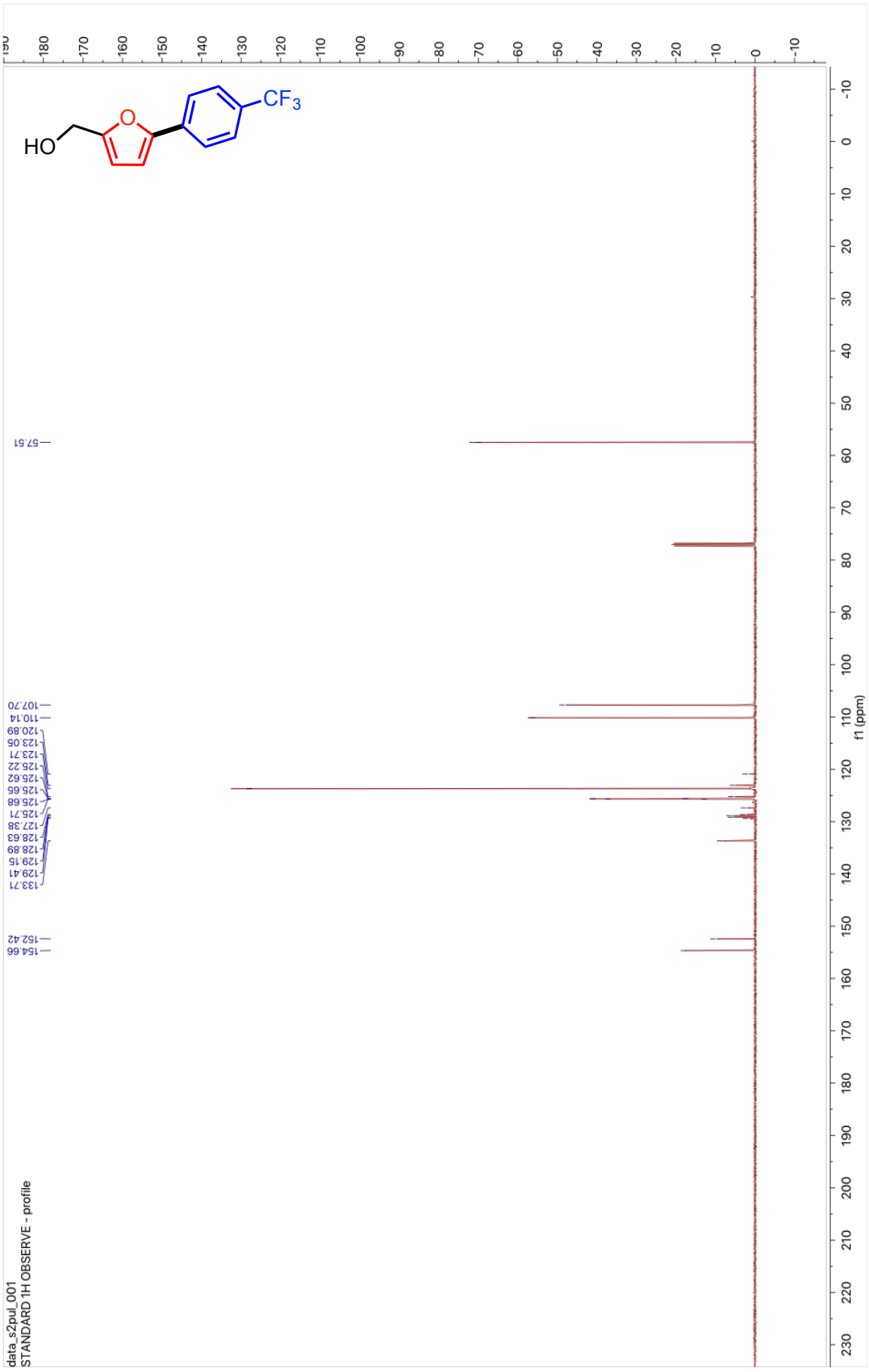
HO
O
CF3
57.51
107.70
110.14
120.89
123.06
123.71
125.22
125.62
125.65
125.68
125.71
127.38
128.63
128.89
129.15
129.41
133.71
152.42
154.66
f1 (ppm)
data_s2pul_001
STANDARD 1H OBSERVE - profile

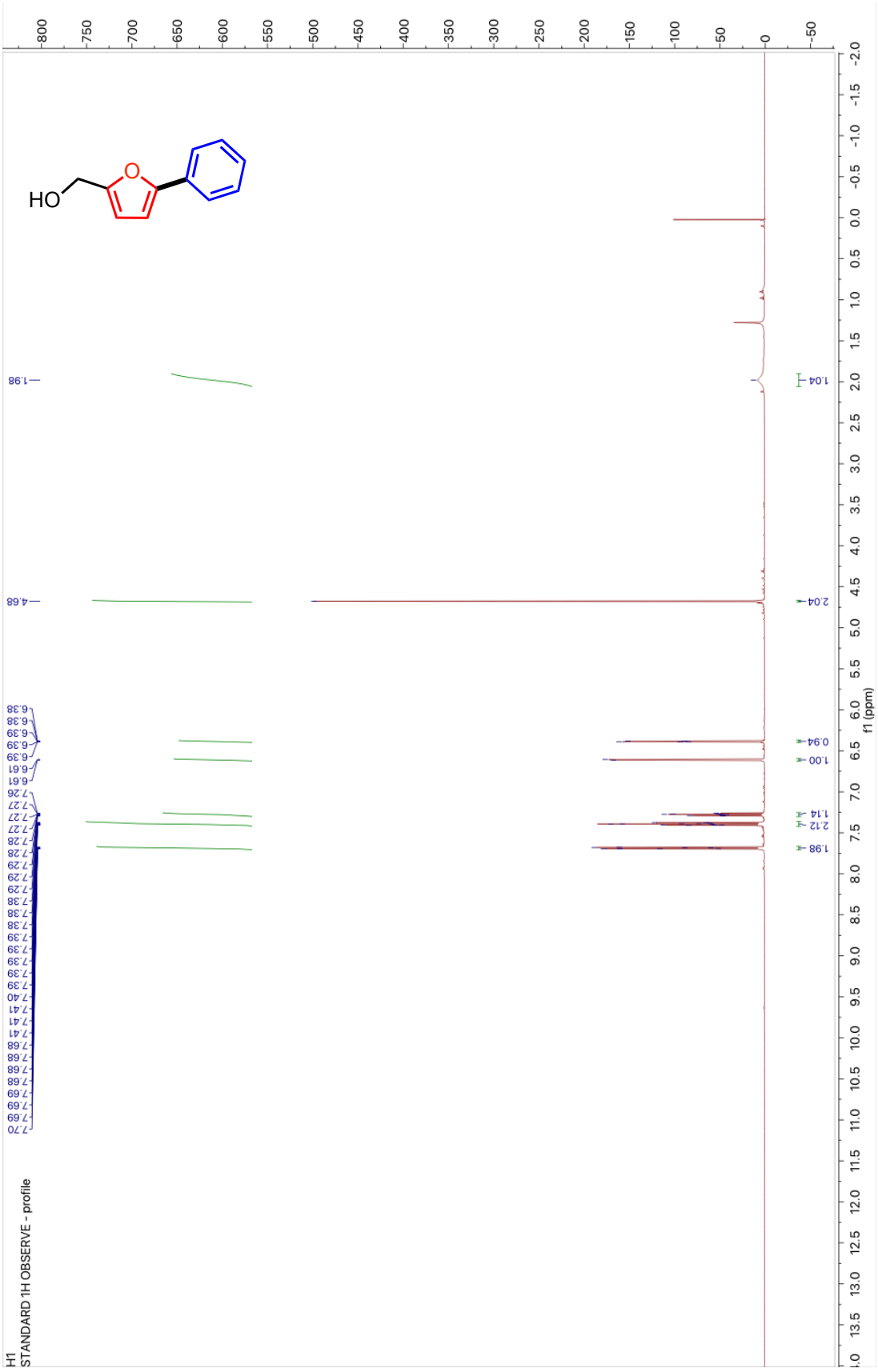
HO
O
H1
STANDARD 1H OBSERVE - profile
f1 (ppm)

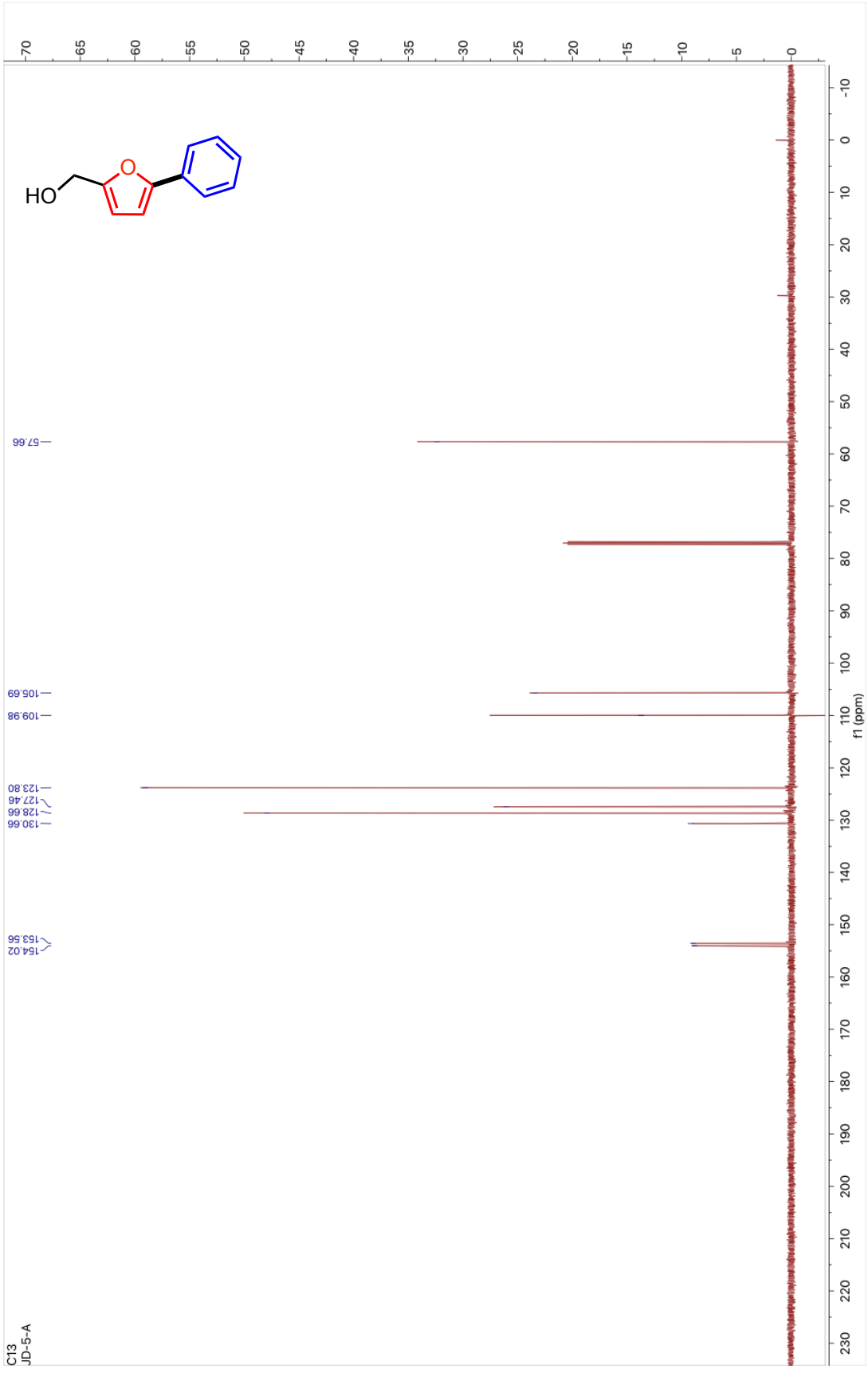
HO
O
57.66
105.69
109.98
123.80
127.46
128.66
130.66
153.56
154.02
C13
JD-5-A
f1 (ppm)

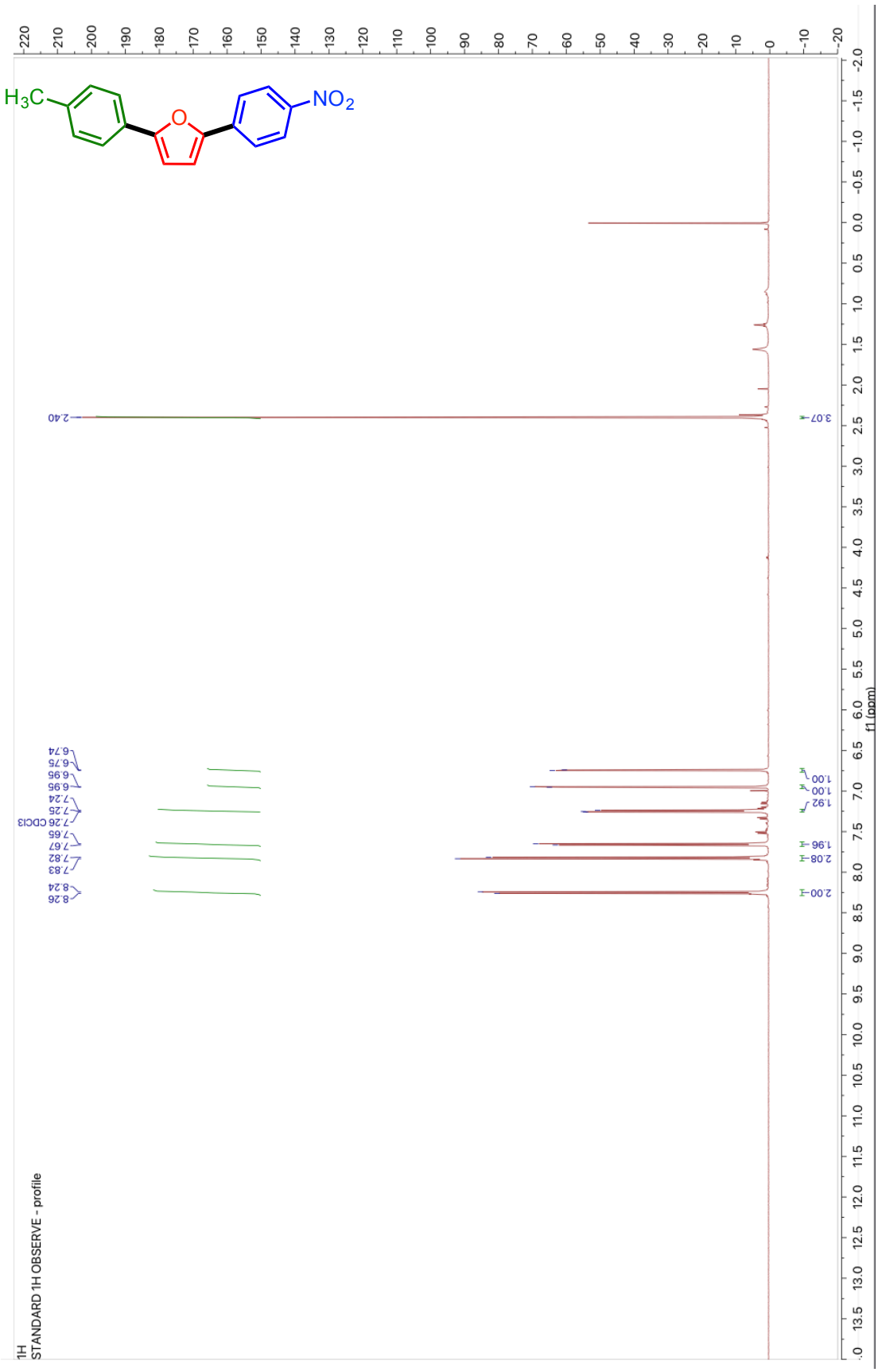
H3C
O
NO2
2.40
3.07
6.74
6.75
6.96
6.96
7.24
7.25
7.26 CDCl3
7.65
7.67
7.82
7.83
8.24
8.26
1.00
1.00
1.92
1.96
2.08
2.00
f1 (ppm)
1H
STANDARD 1H OBSERVE - profile

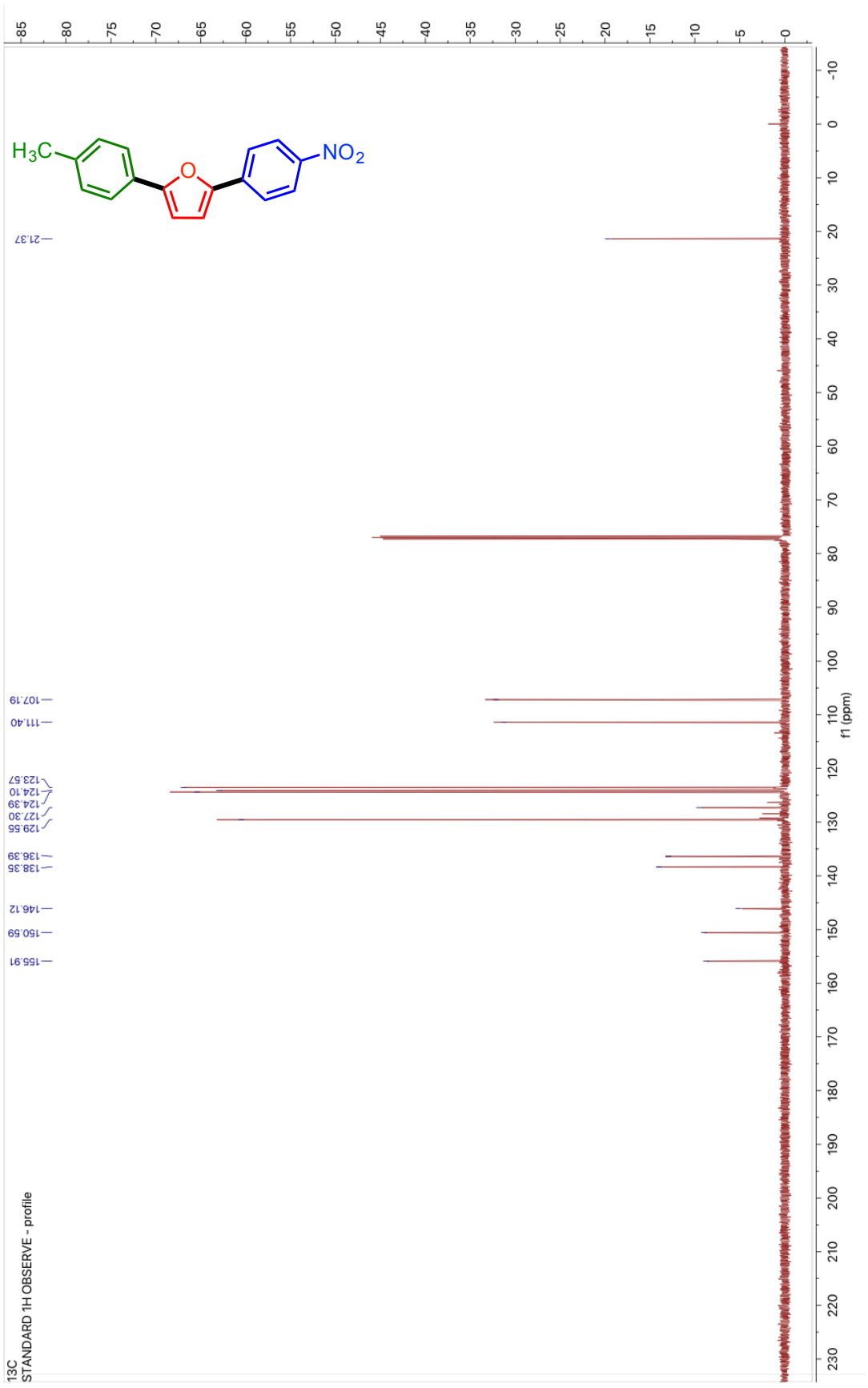
H3C
O
NO2
21.37
107.19
111.40
123.57
124.10
124.39
127.30
129.55
136.39
138.35
146.12
150.59
155.91
13C
STANDARD 1H OBSERVE - profile
f1 (ppm)

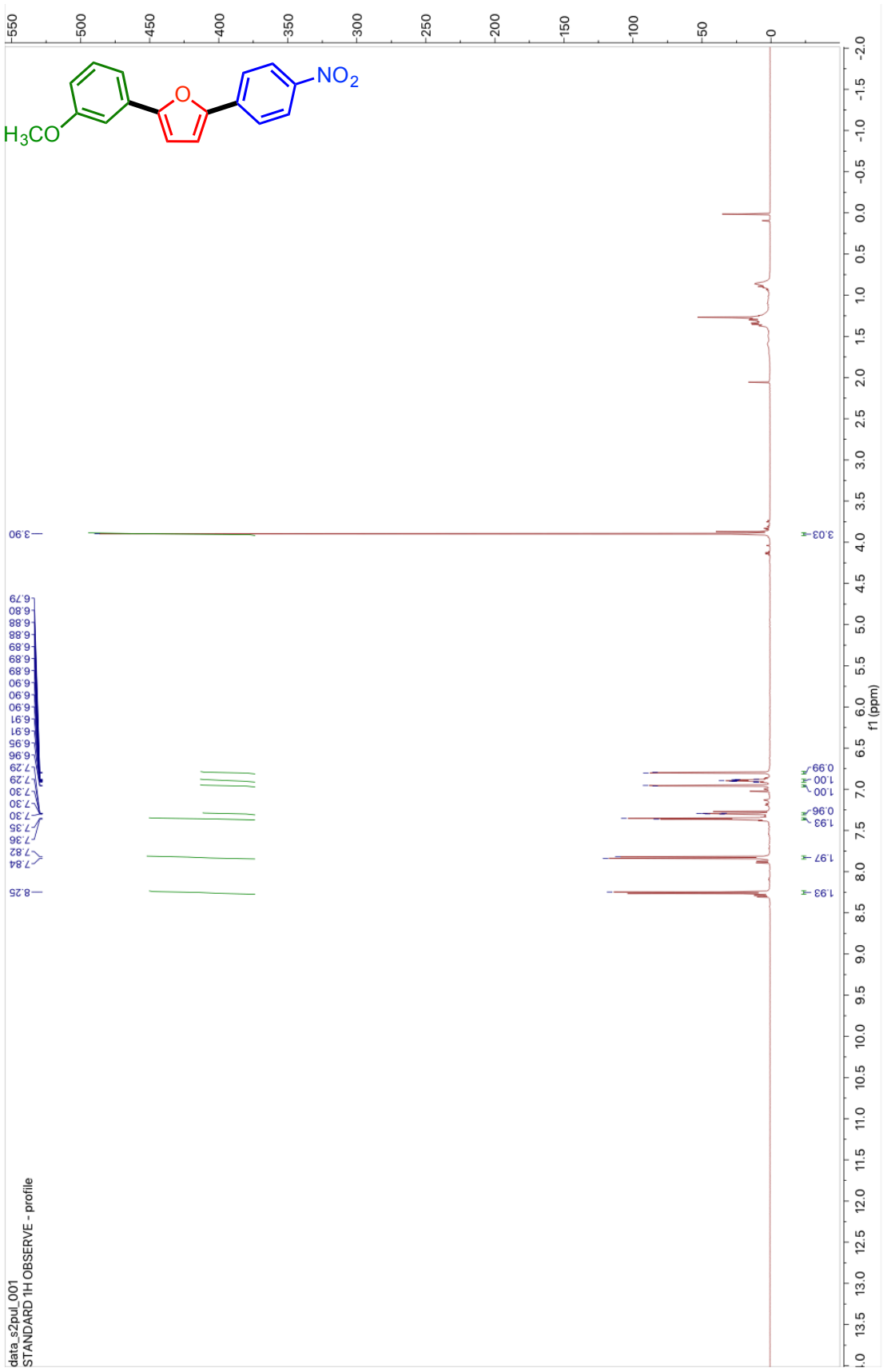
NO2
O
H3CO
f1 (ppm)
data_s2pul_001
STANDARD 1H OBSERVE - profile

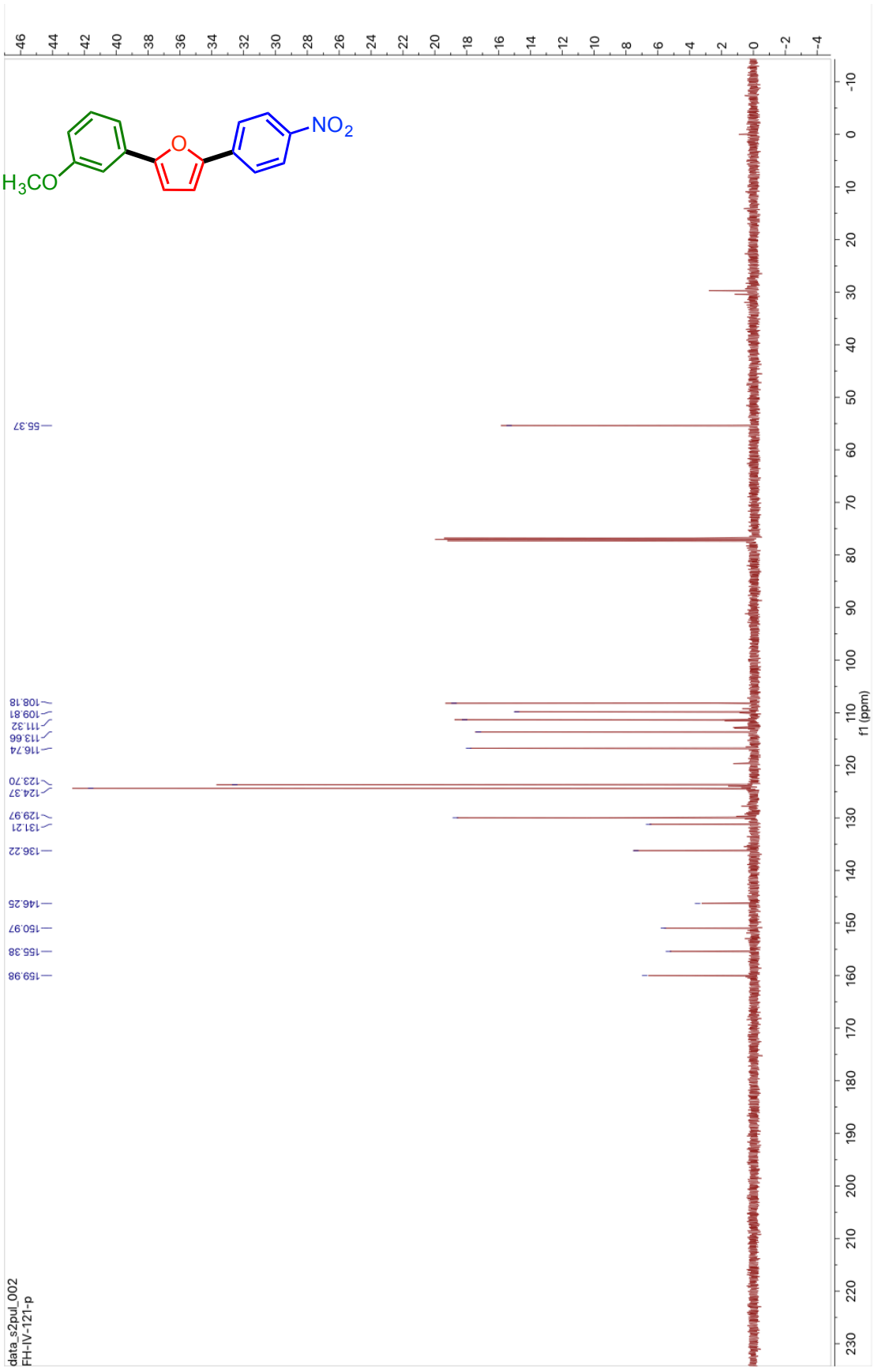
NO2
O
H3CO
55.37
108.18
109.81
111.32
113.66
116.74
123.70
124.37
129.97
131.21
136.22
146.25
150.97
155.38
159.98
f1 (ppm)
data_s2pul_002
FH-IV-121-p

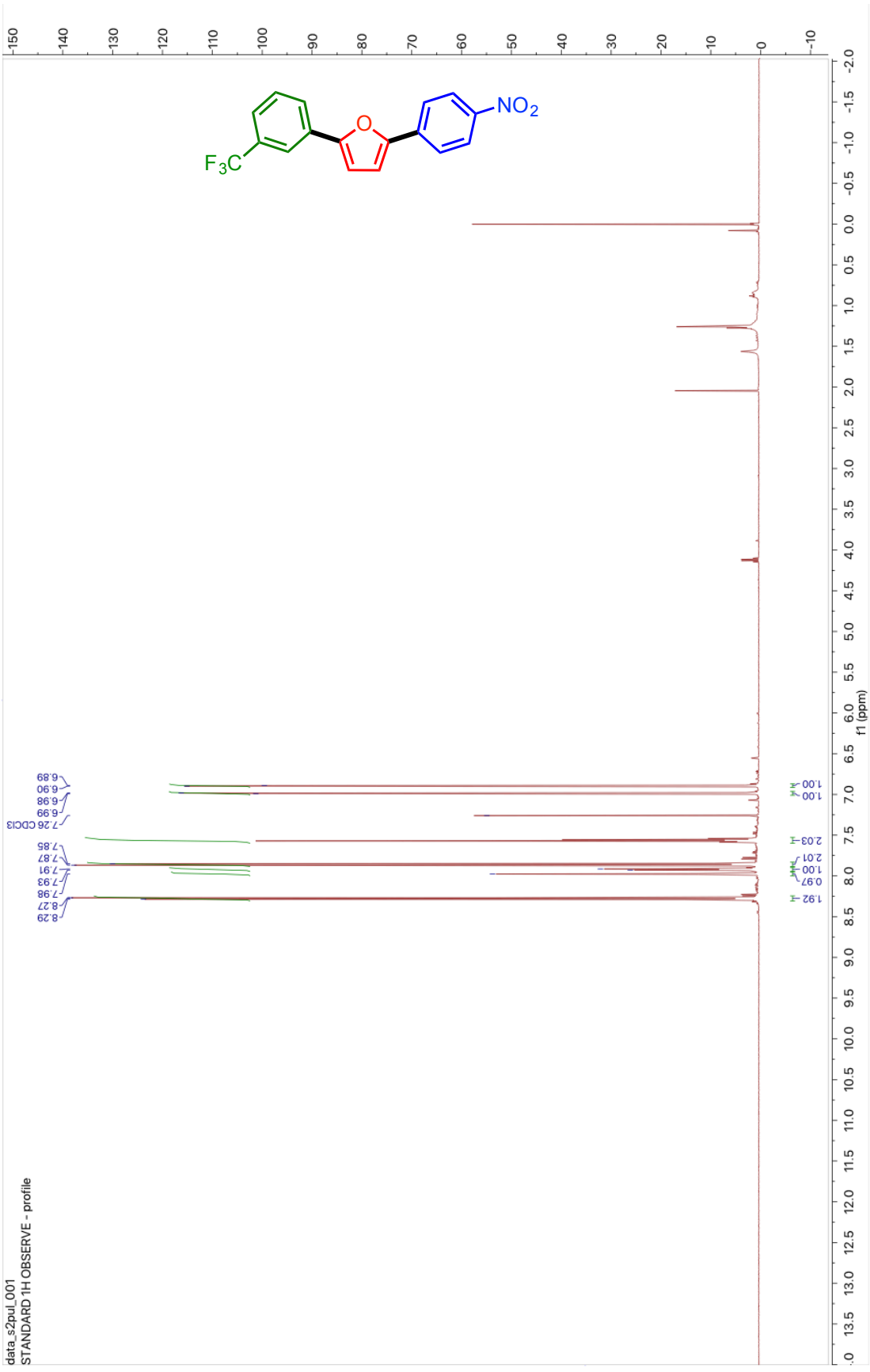
NO2
F3C
O
f1 (ppm)
data_s2pul_001
STANDARD 1H OBSERVE - profile

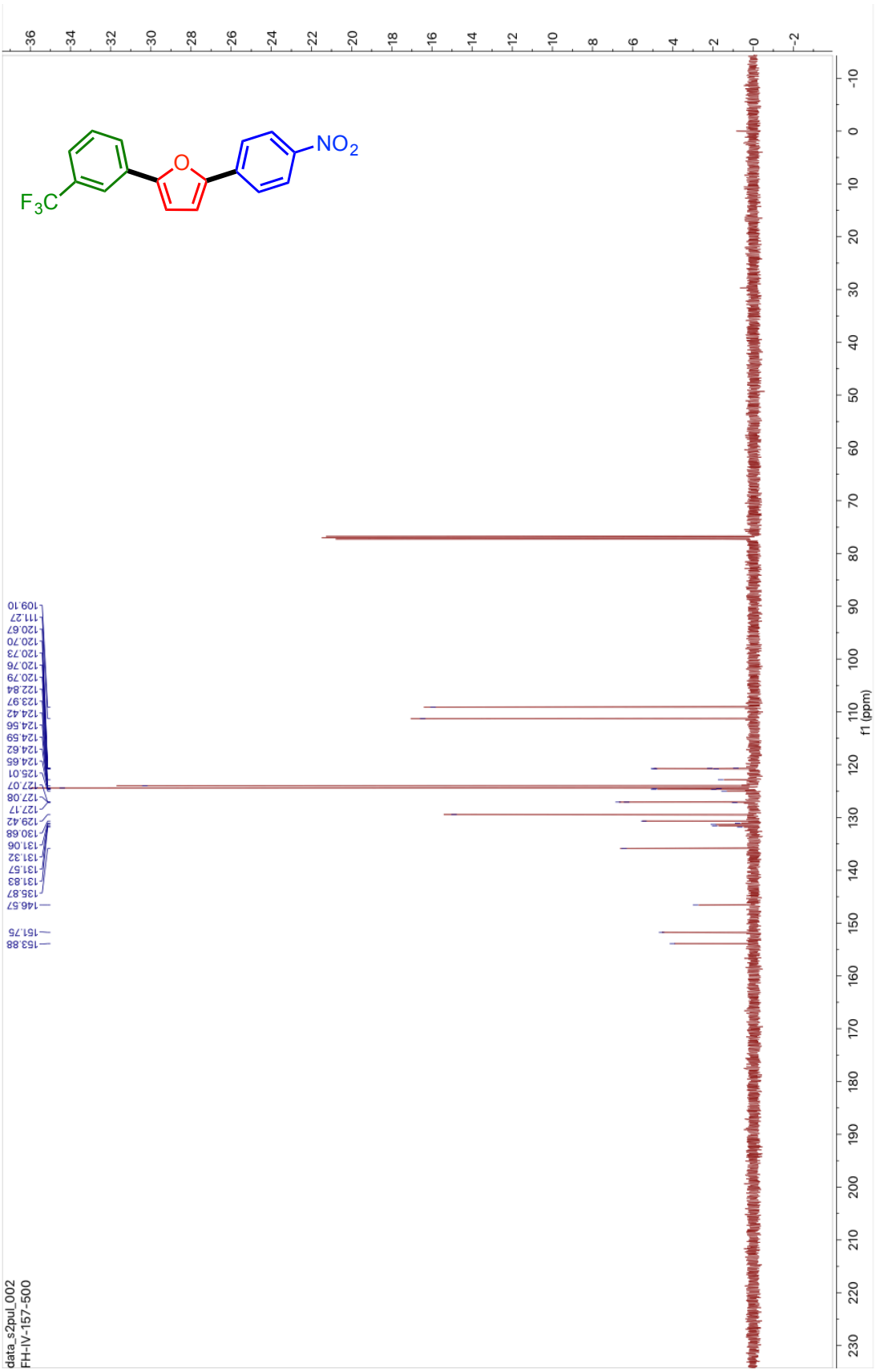
NO2
F3C
O
f1 (ppm)
data_s2pul_002
FH-IV-157-500

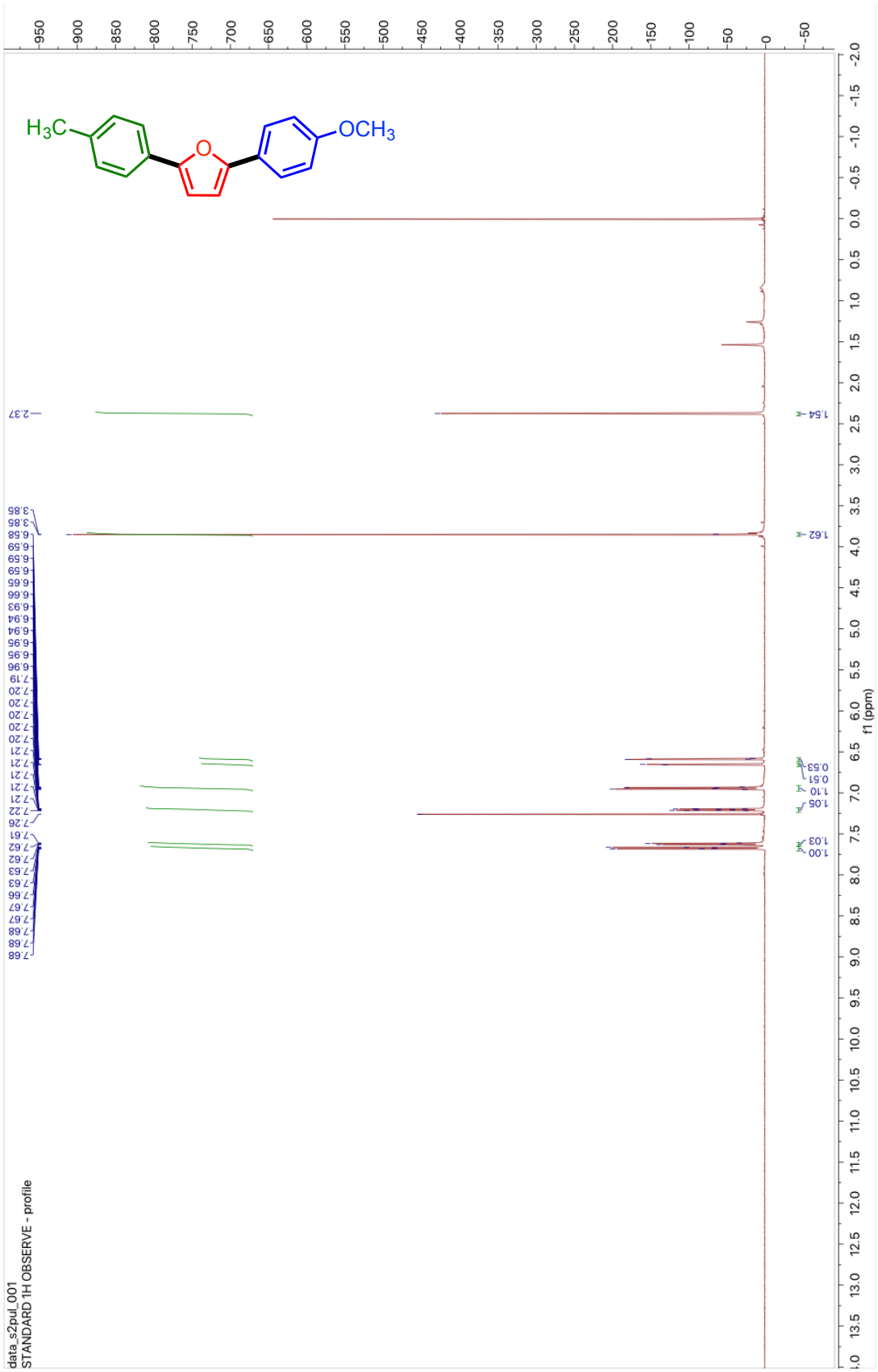
H3C
O
OCH3
data_s2pul_001
STANDARD 1H OBSERVE - profile
f1 (ppm)

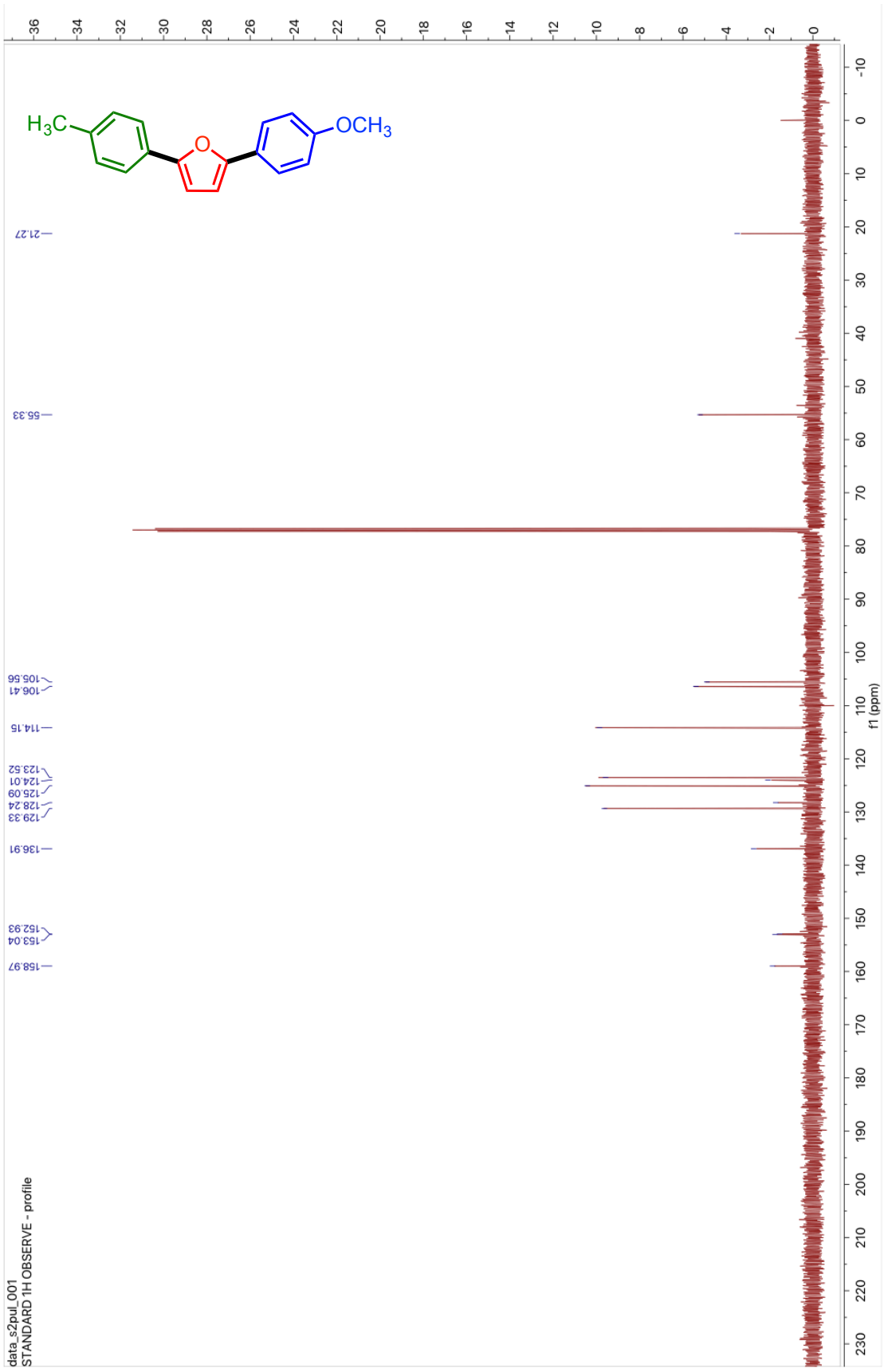
H3C
O
OCH3
21.27
55.33
105.56
106.41
114.15
123.52
124.01
125.09
128.24
129.33
136.91
152.93
153.04
158.97
f1 (ppm)
data_s2pul_001
STANDARD 1H OBSERVE - profile

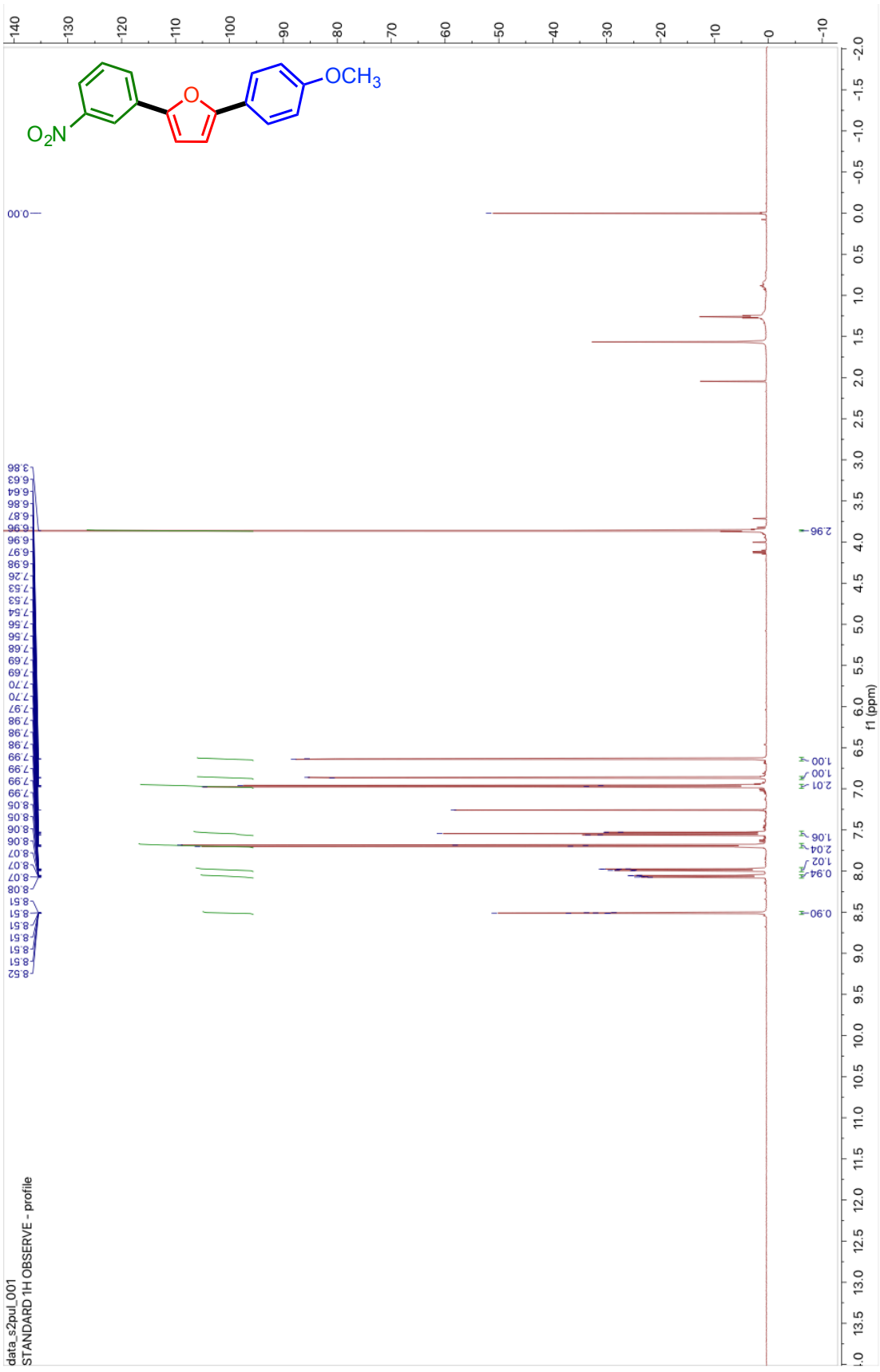
OCH3
O2N
O
data_s2pul_001
STANDARD 1H OBSERVE - profile
f1 (ppm)

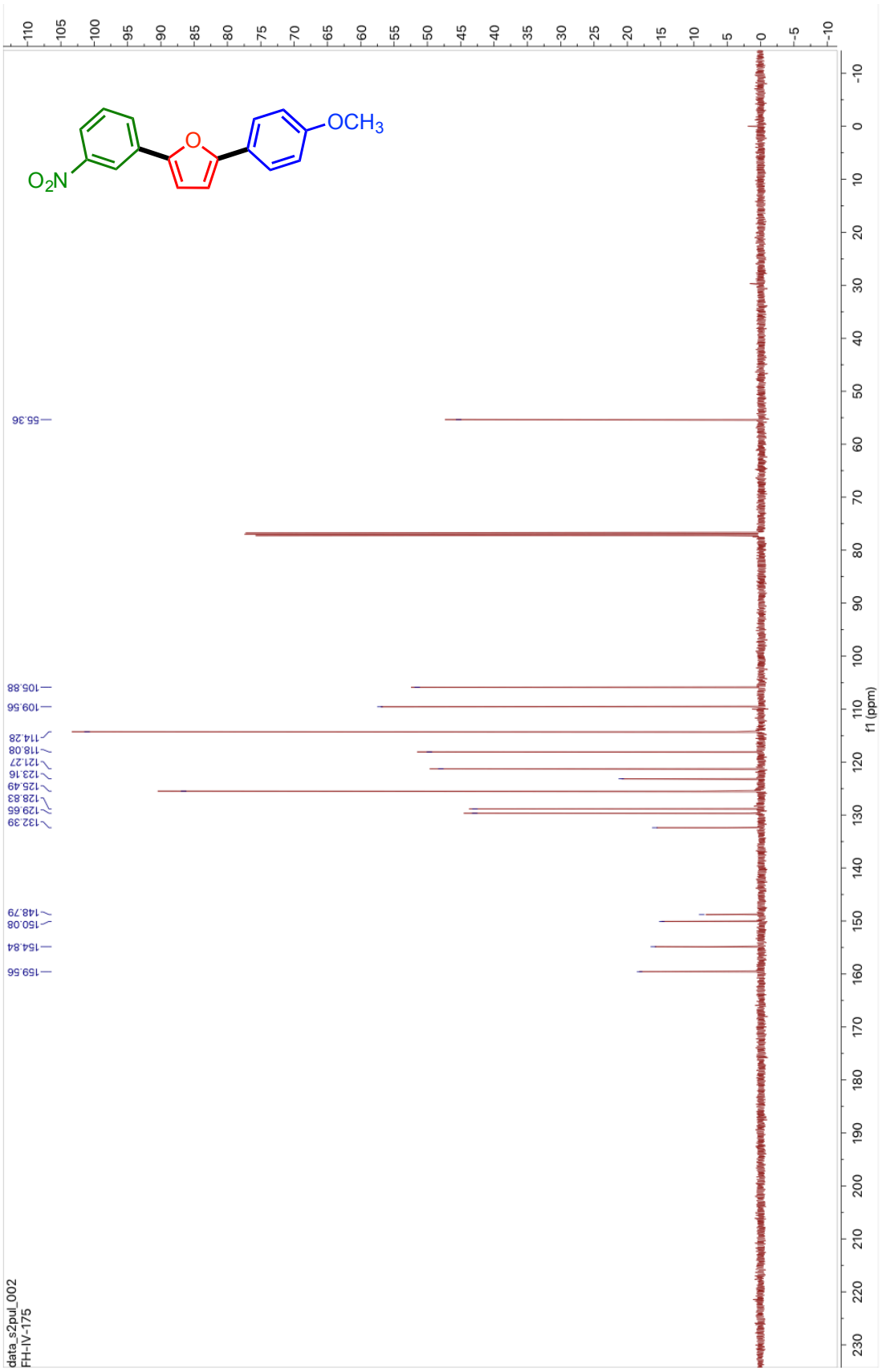
OCH3
O2N
O
55.36
105.88
109.56
114.28
118.08
121.27
123.16
125.49
128.83
129.65
132.39
148.79
150.08
154.84
159.56
f1 (ppm)
data_s2pul_002
FH-IV-175

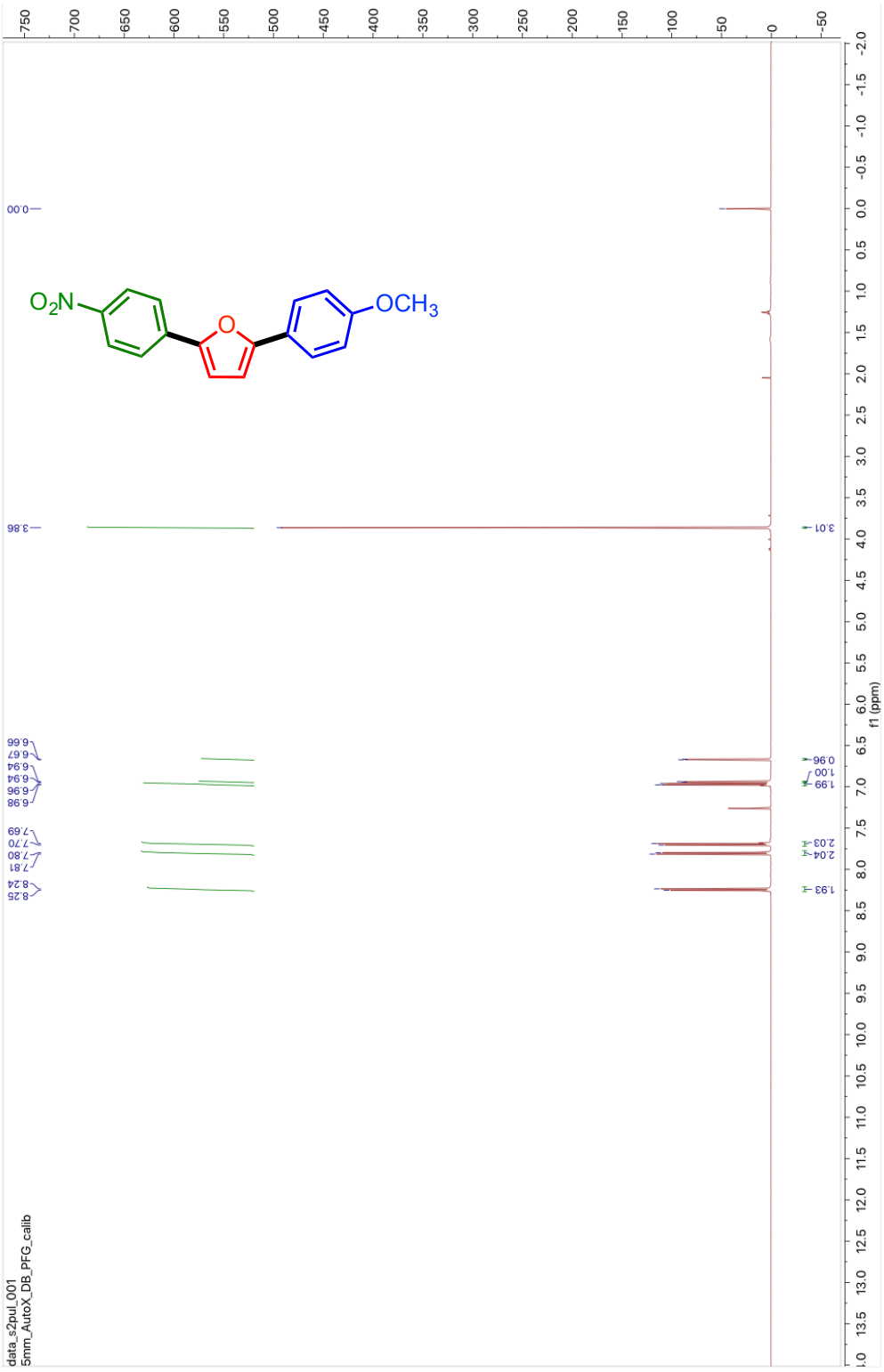
O2N
O
OCH3
f1 (ppm)
data_s2pul_001
5mm_AutoX_DB_PFG_calib

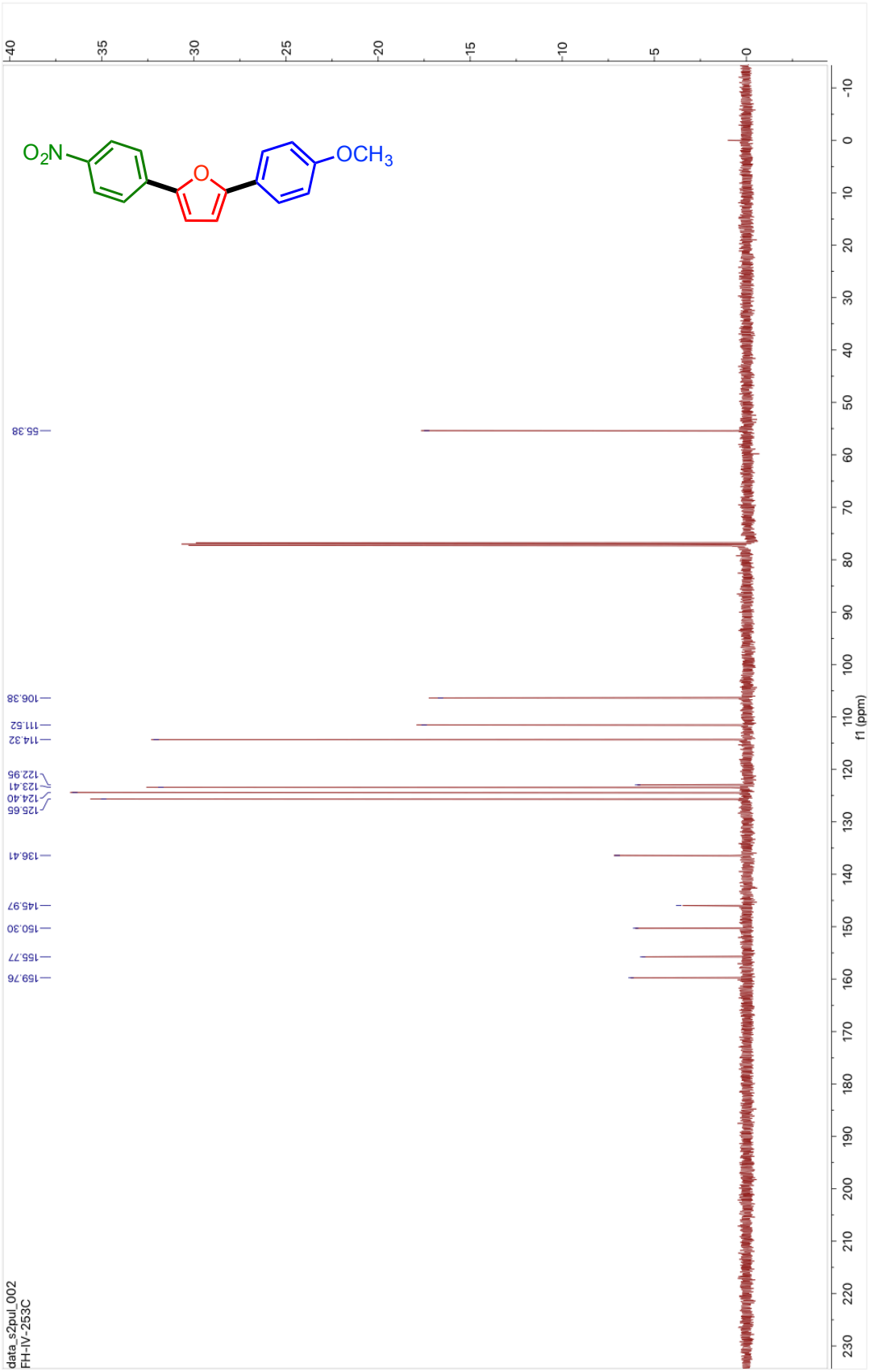
O2N
O
OCH3
55.38
106.38
111.52
114.32
122.95
123.41
124.40
125.65
136.41
145.97
150.30
155.77
159.76
f1 (ppm)
data_s2pul_002
FH-IV-253C

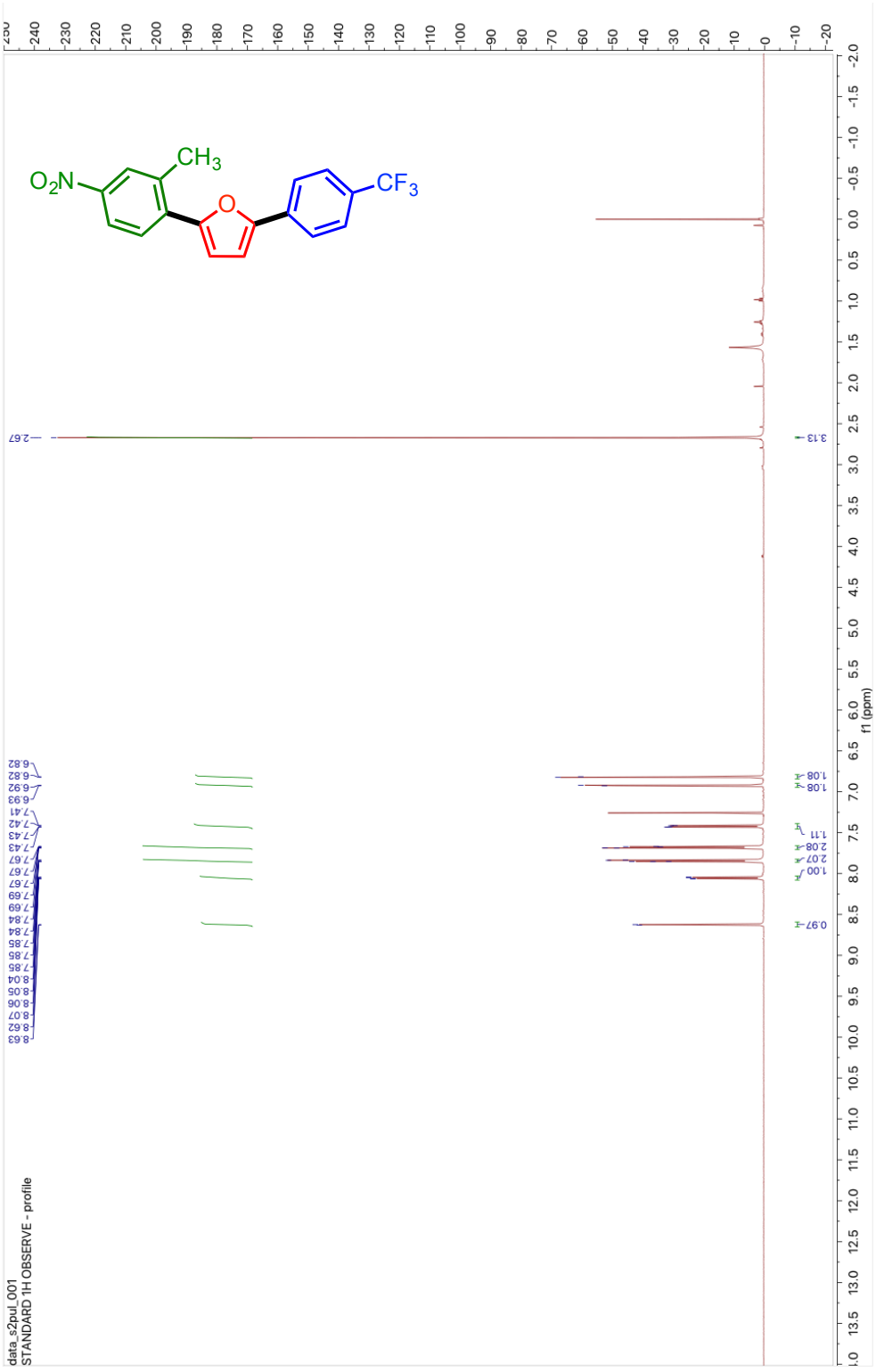
CH3
O2N
O
CF3
data_s2pul_001
STANDARD 1H OBSERVE - profile
f1 (ppm)

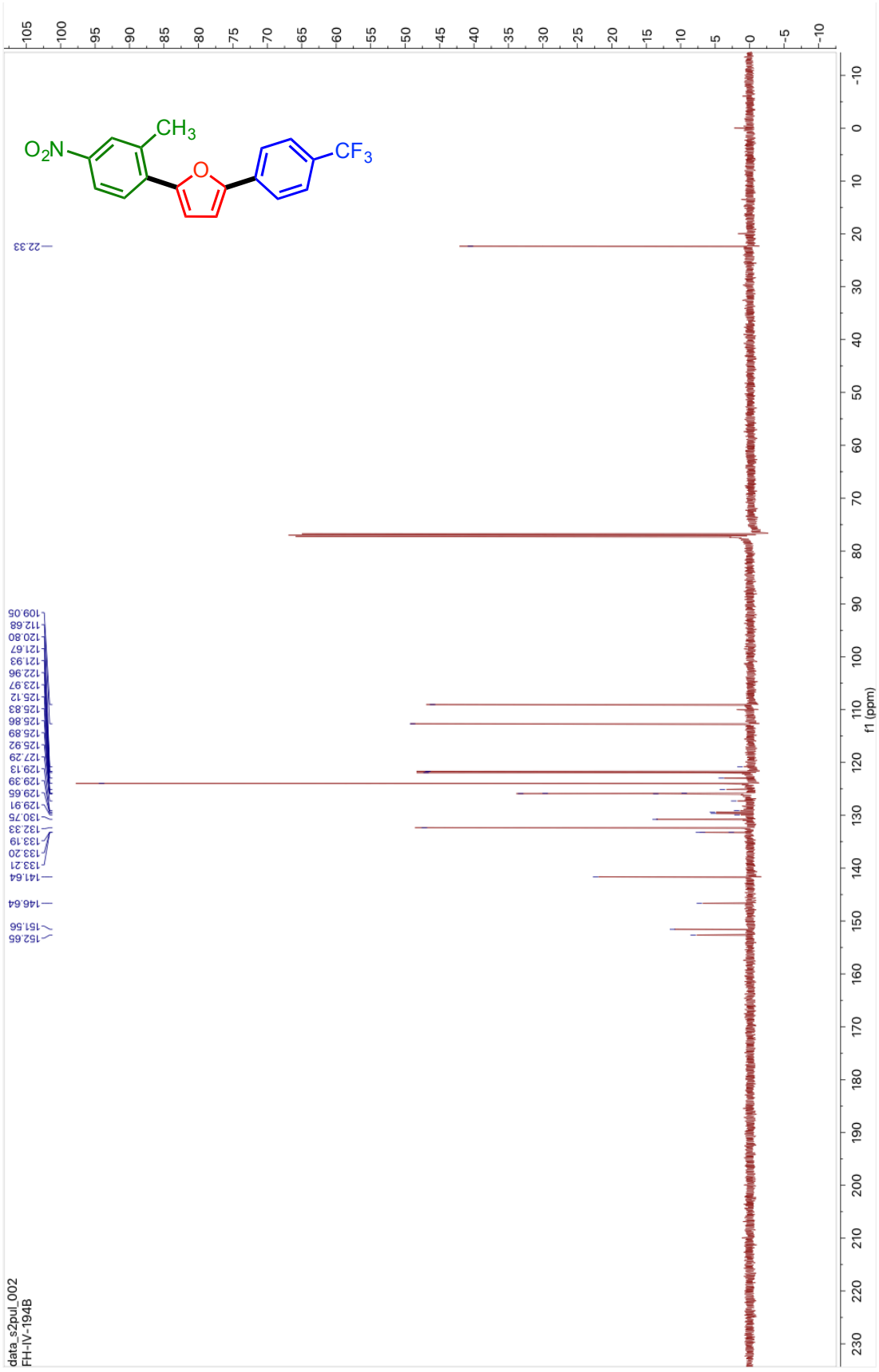
O2N
CH3
O
CF3
22.33
109.05
112.68
120.80
121.67
121.93
122.96
123.97
125.12
125.83
125.86
125.89
125.92
127.29
129.13
129.39
129.65
129.91
130.75
132.33
133.19
133.20
133.21
141.64
146.64
151.56
152.65
f1 (ppm)
data_s2pul_002
FH-IV-194B

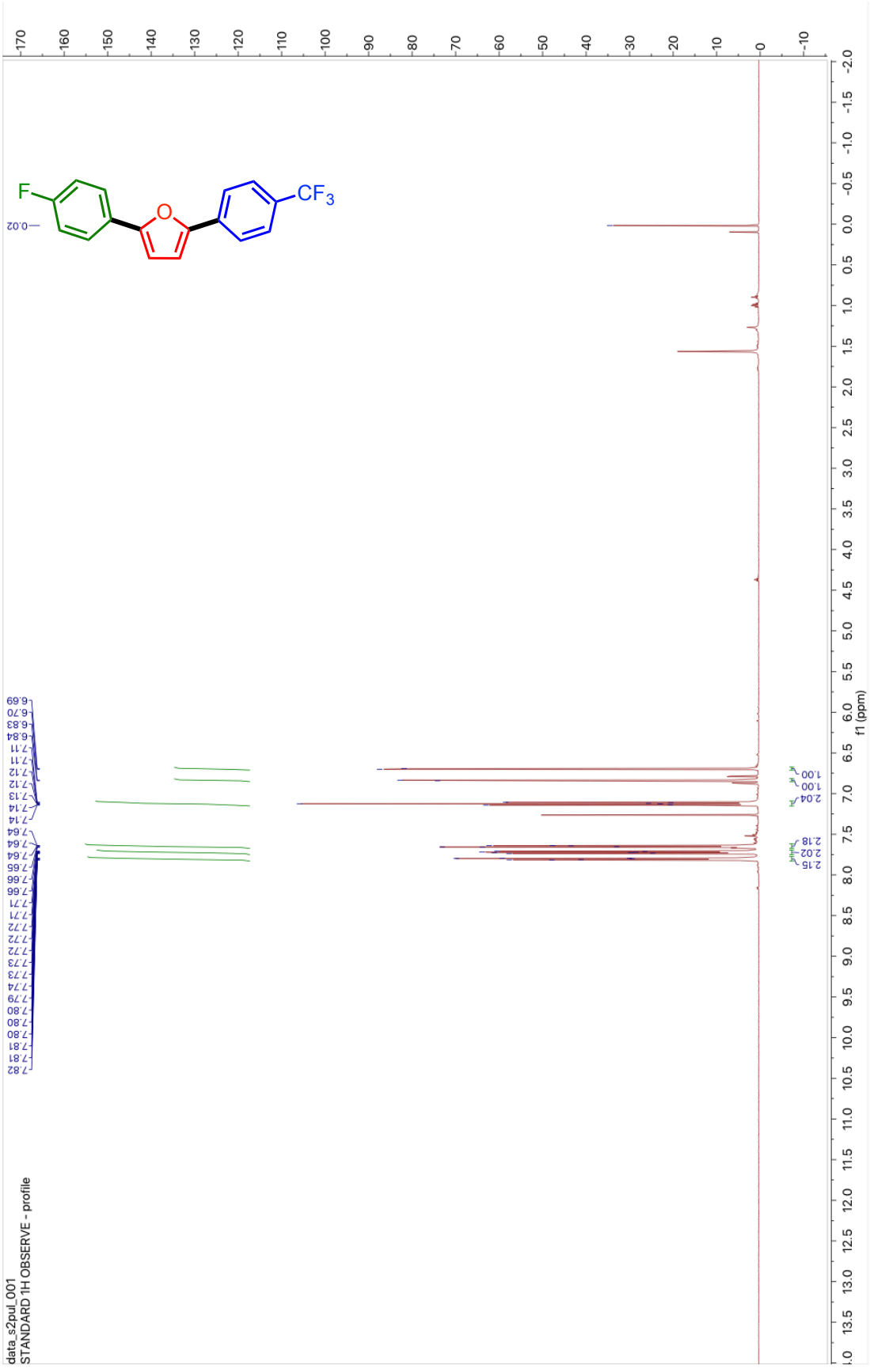
F
O
CF3
data_s2pul_001
STANDARD 1H OBSERVE - profile
f1 (ppm)

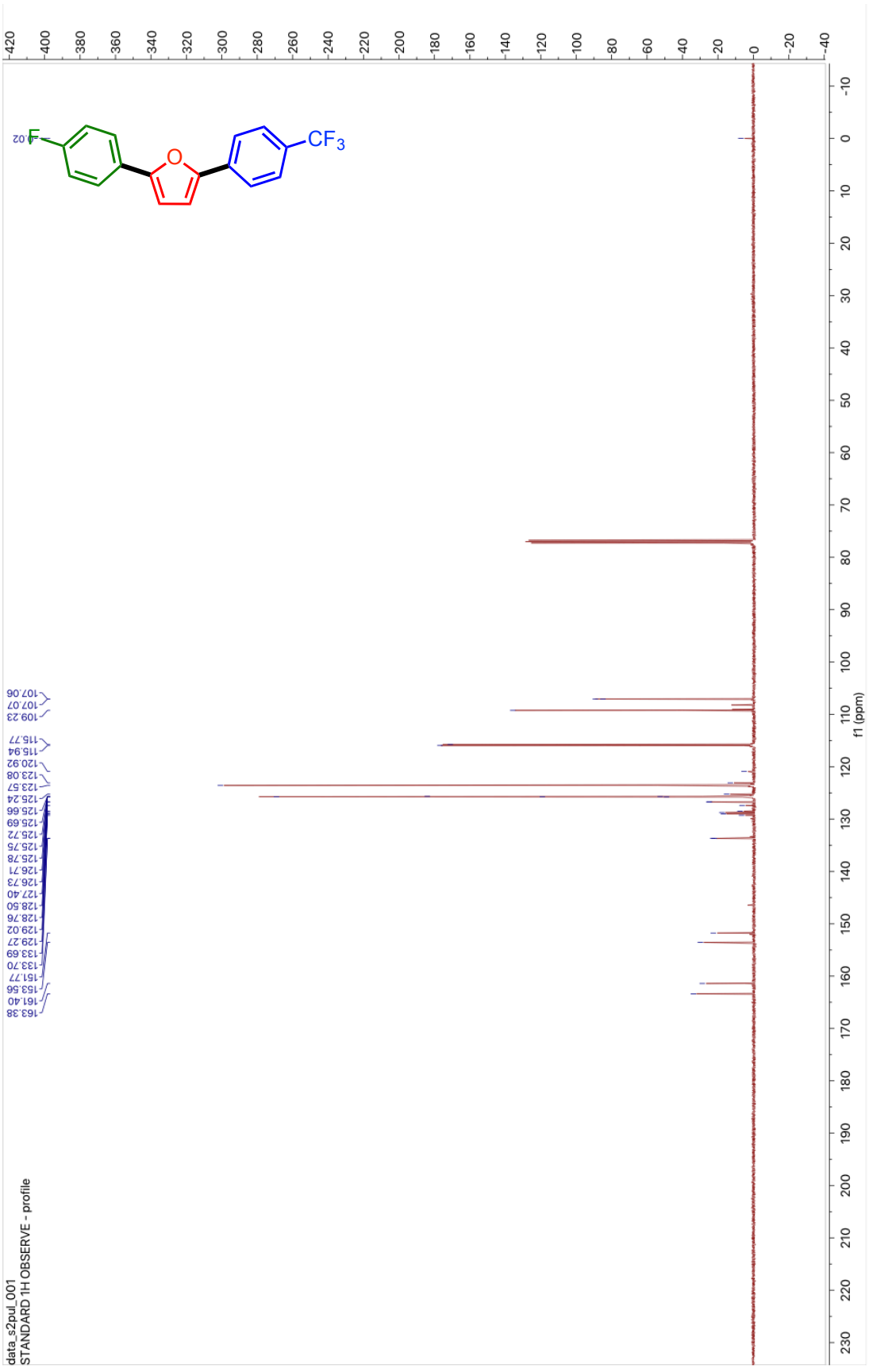
F
O
CF3
f1 (ppm)
data_s2pul_001
STANDARD 1H OBSERVE - profile

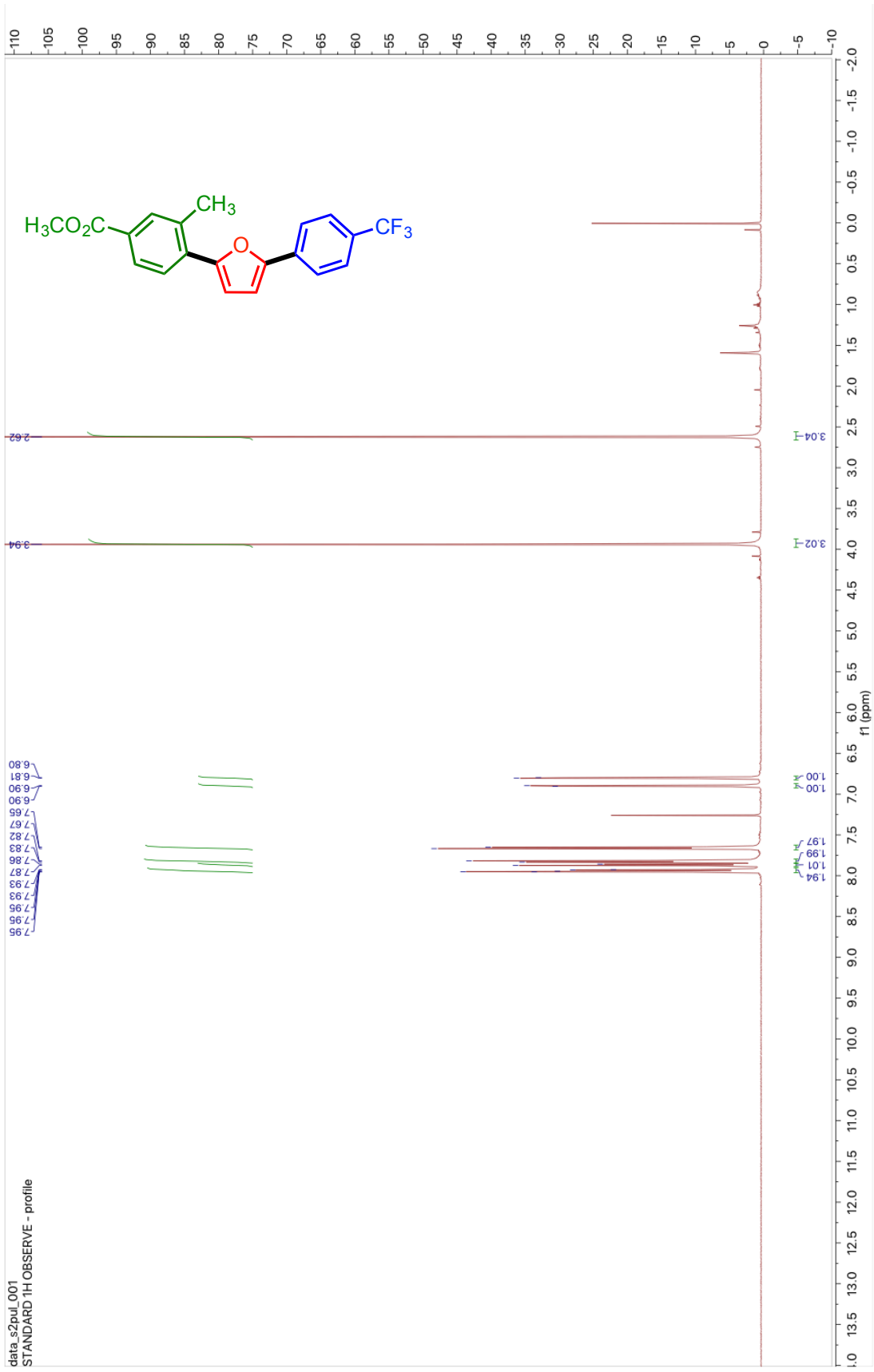
H3CO2C
CH3
O
CF3
f1 (ppm)
data_s2pul_001
STANDARD 1H OBSERVE - profile

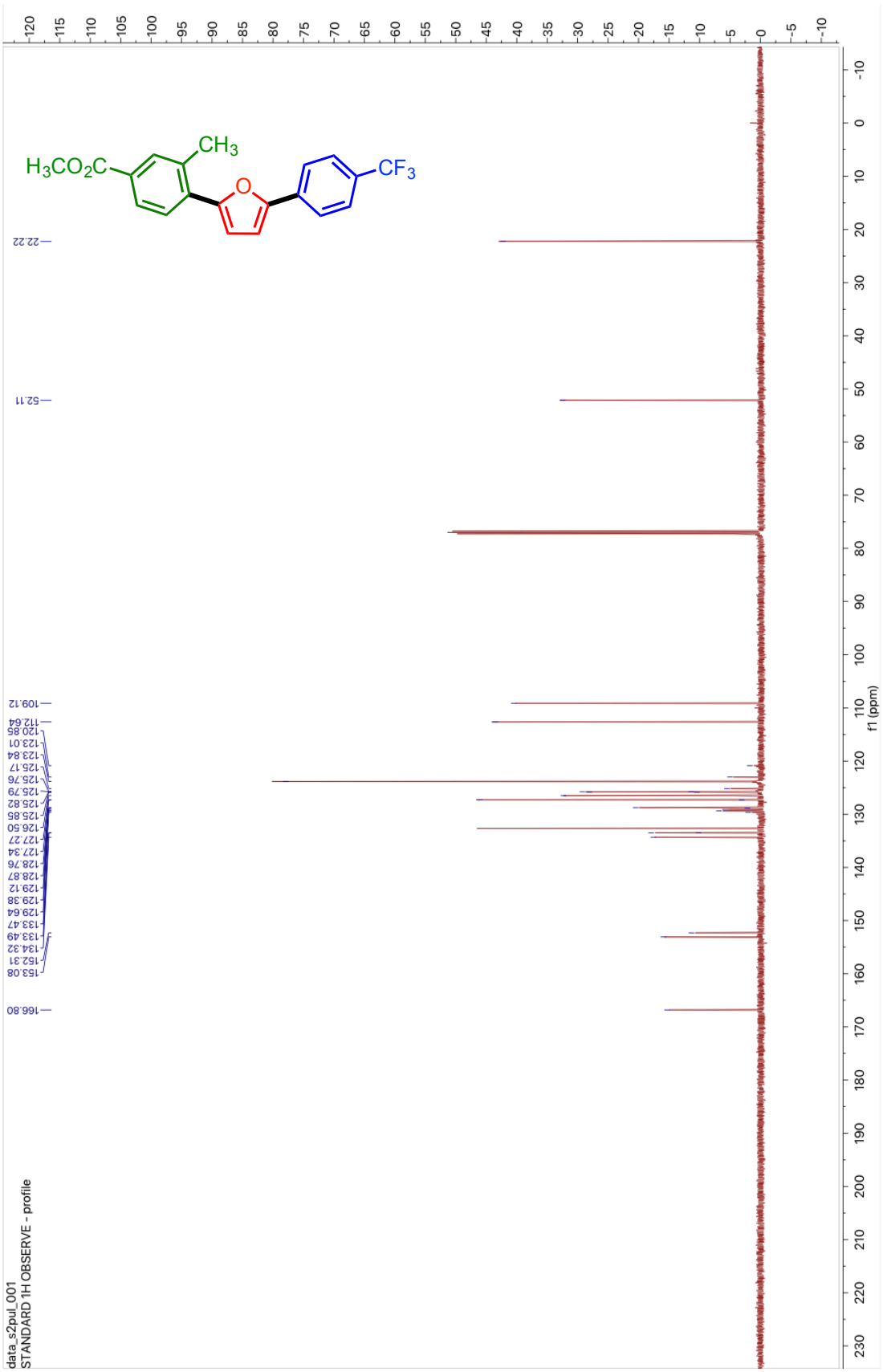
H3CO2C
CH3
O
CF3
22.22
52.11
109.12
112.64
120.85
123.01
123.84
125.17
125.76
125.79
125.82
125.86
126.50
127.27
127.34
128.76
128.87
129.12
129.38
129.64
133.47
133.49
134.32
152.31
153.08
166.80
f1 (ppm)
data_s2pul_001
STANDARD 1H OBSERVE - profile

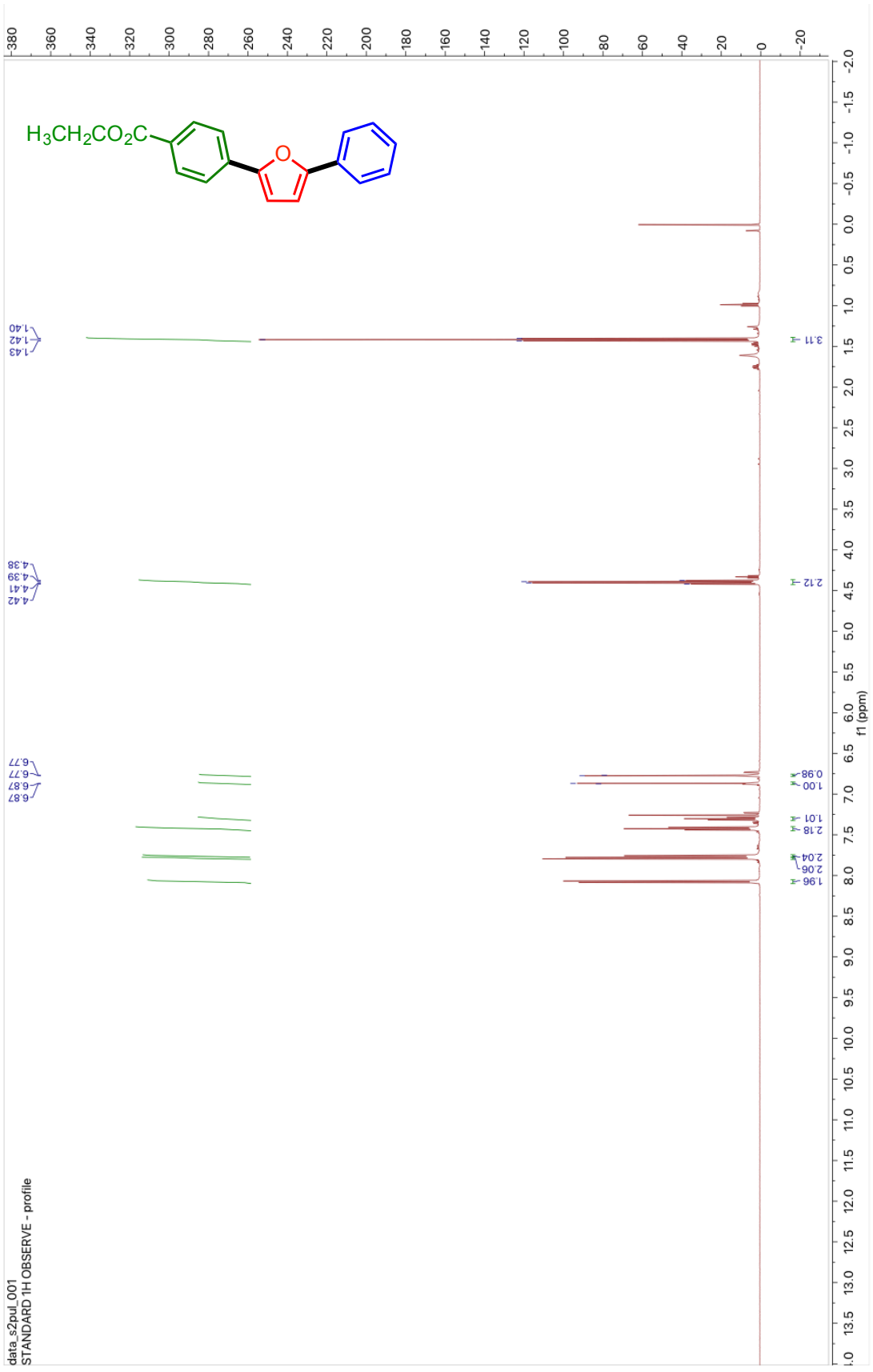
H3CH2CO2C
O
1.40
1.42
1.43
4.38
4.39
4.41
4.42
6.77
6.77
6.87
6.87
3.11
2.12
0.98
1.00
1.01
2.18
1.96
2.04
2.06
f1 (ppm)
data_s2pul_001
STANDARD 1H OBSERVE - profile

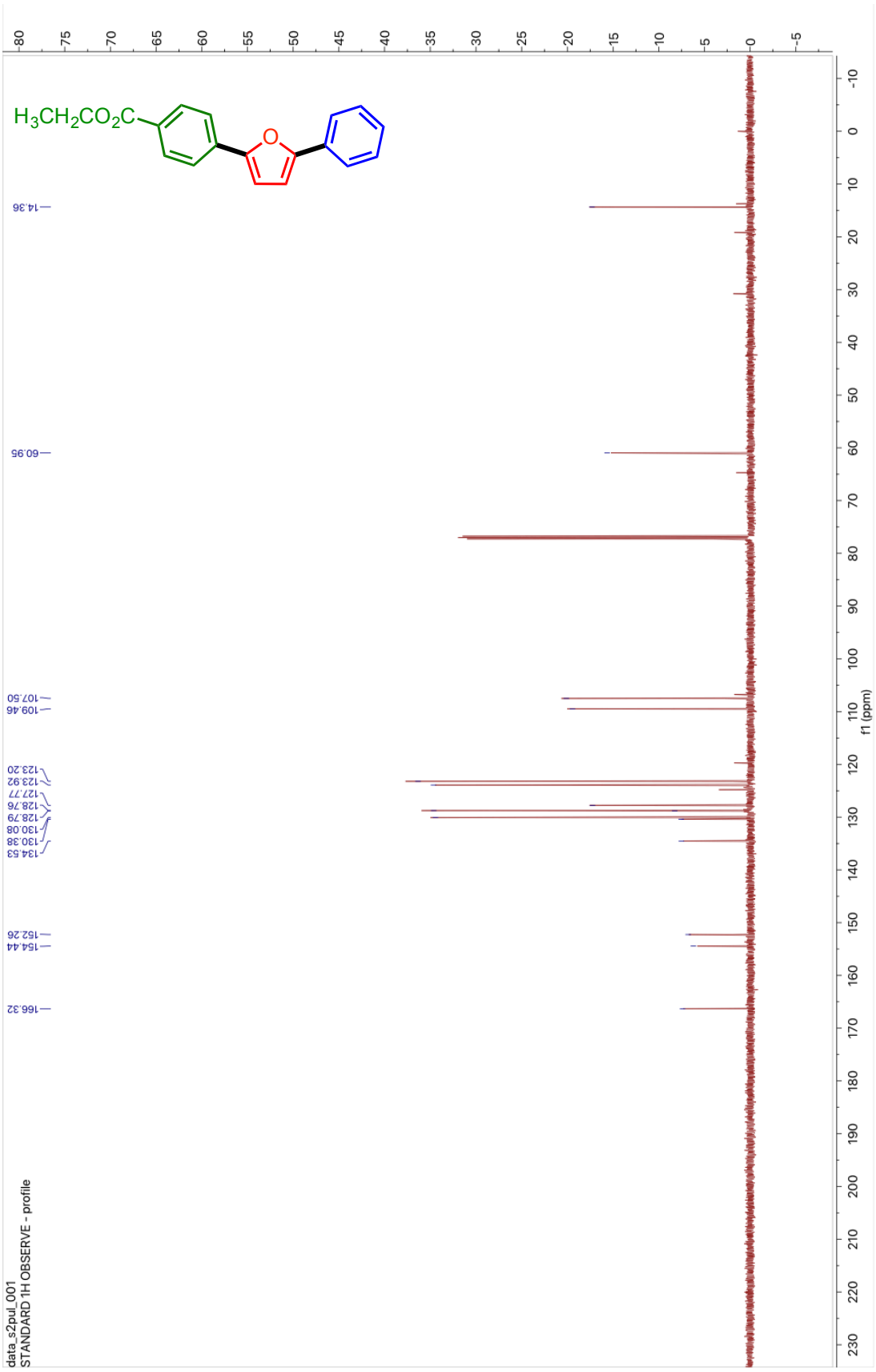
H3CH2CO2C
O
14.36
60.95
107.50
109.46
123.20
123.92
127.77
128.76
128.79
130.08
130.38
134.53
152.26
154.44
166.32
f1 (ppm)
data_s2pul_001
STANDARD 1H OBSERVE - profile

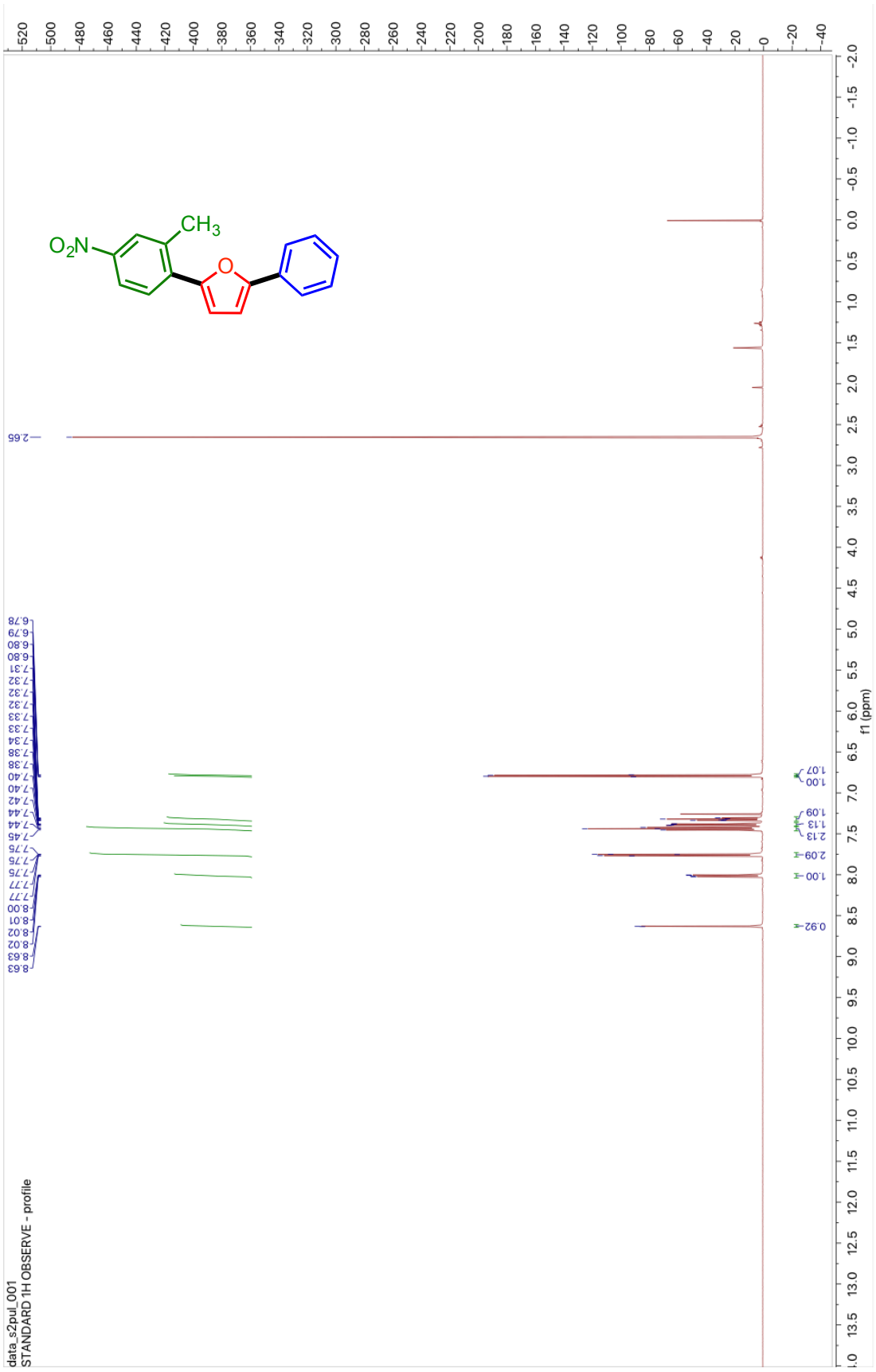
CH3
O2N
O
2.65
6.78
6.79
6.80
6.80
7.31
7.32
7.32
7.32
7.33
7.33
7.34
7.38
7.38
7.40
7.40
7.42
7.44
7.44
7.45
7.75
7.75
7.75
7.77
7.77
8.00
8.01
8.02
8.02
8.63
8.63
1.07
1.00
2.13
1.13
1.09
2.09
1.00
0.92
f1 (ppm)
data_s2pul_001
STANDARD 1H OBSERVE - profile

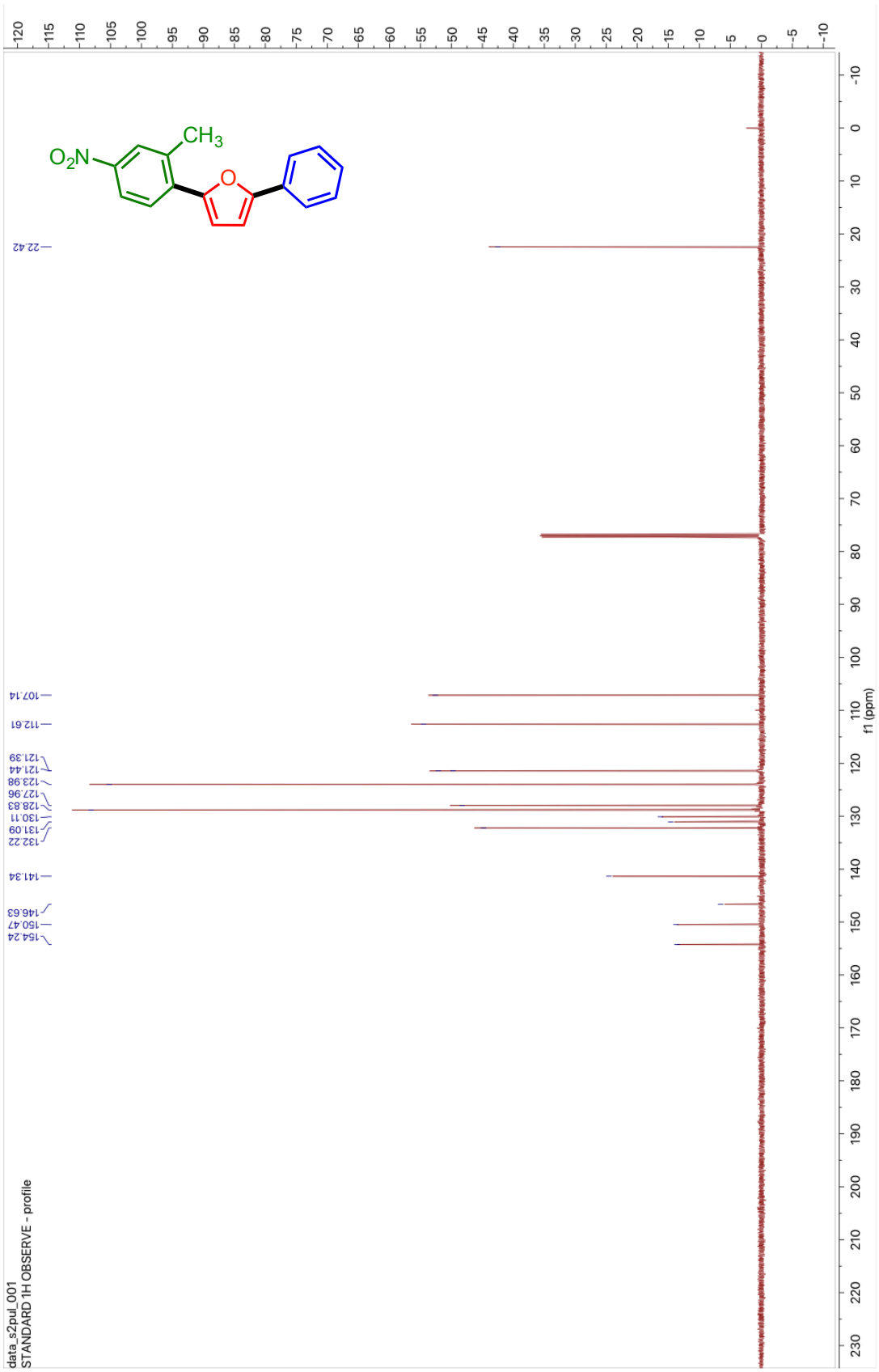
O2N
CH3
O
22.42
107.14
112.61
121.39
121.44
123.98
127.96
128.83
130.11
131.09
132.22
141.34
146.63
150.47
154.24
f1 (ppm)
data_s2pul_001
STANDARD 1H OBSERVE - profile

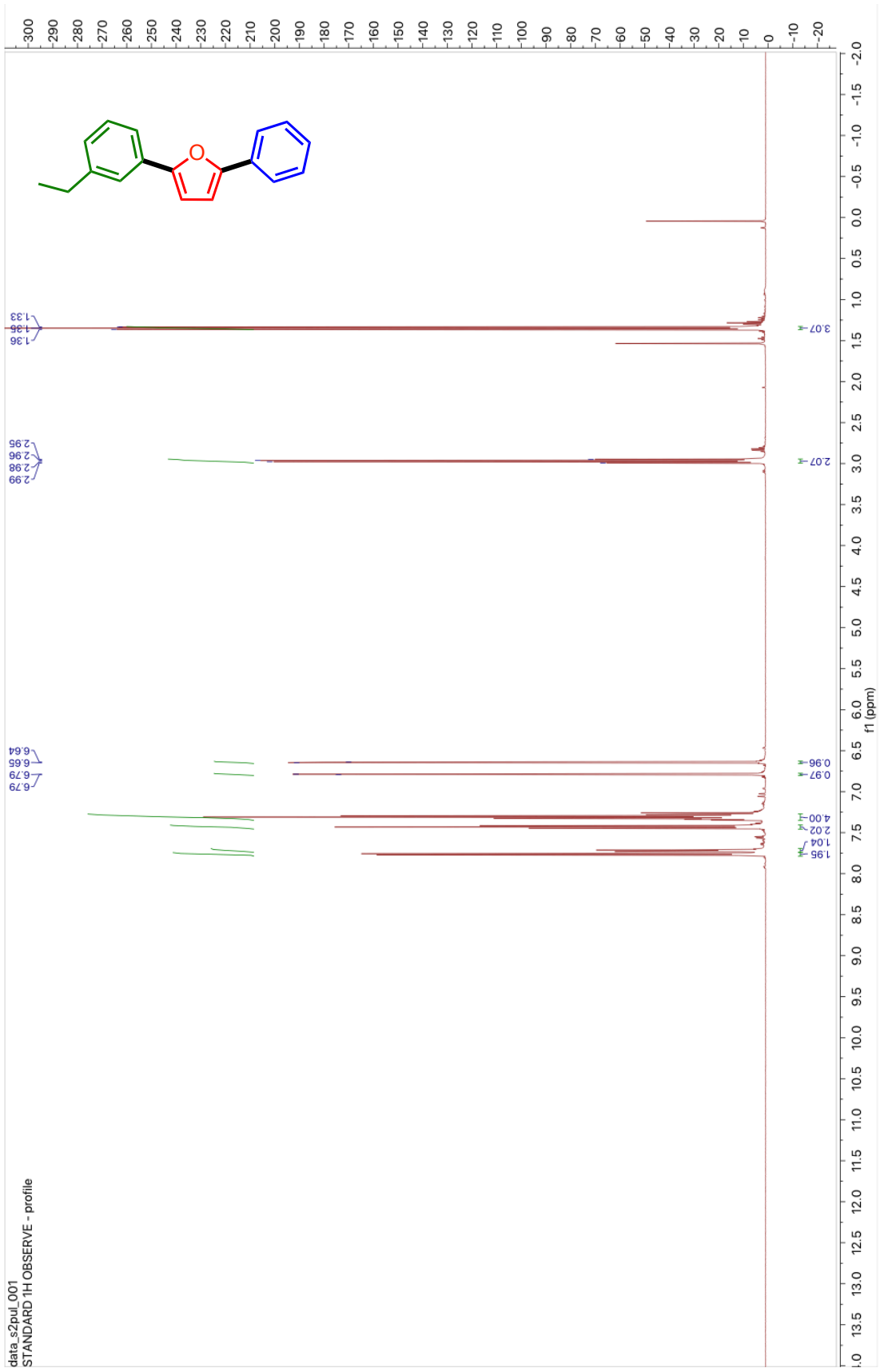
data_s2pul_001
STANDARD 1H OBSERVE - profile
f1 (ppm)
1.33
1.36
2.99
2.98
2.96
2.95
6.64
6.65
6.79
6.79
3.07
2.07
0.96
0.97
4.00
2.02
1.04
1.95

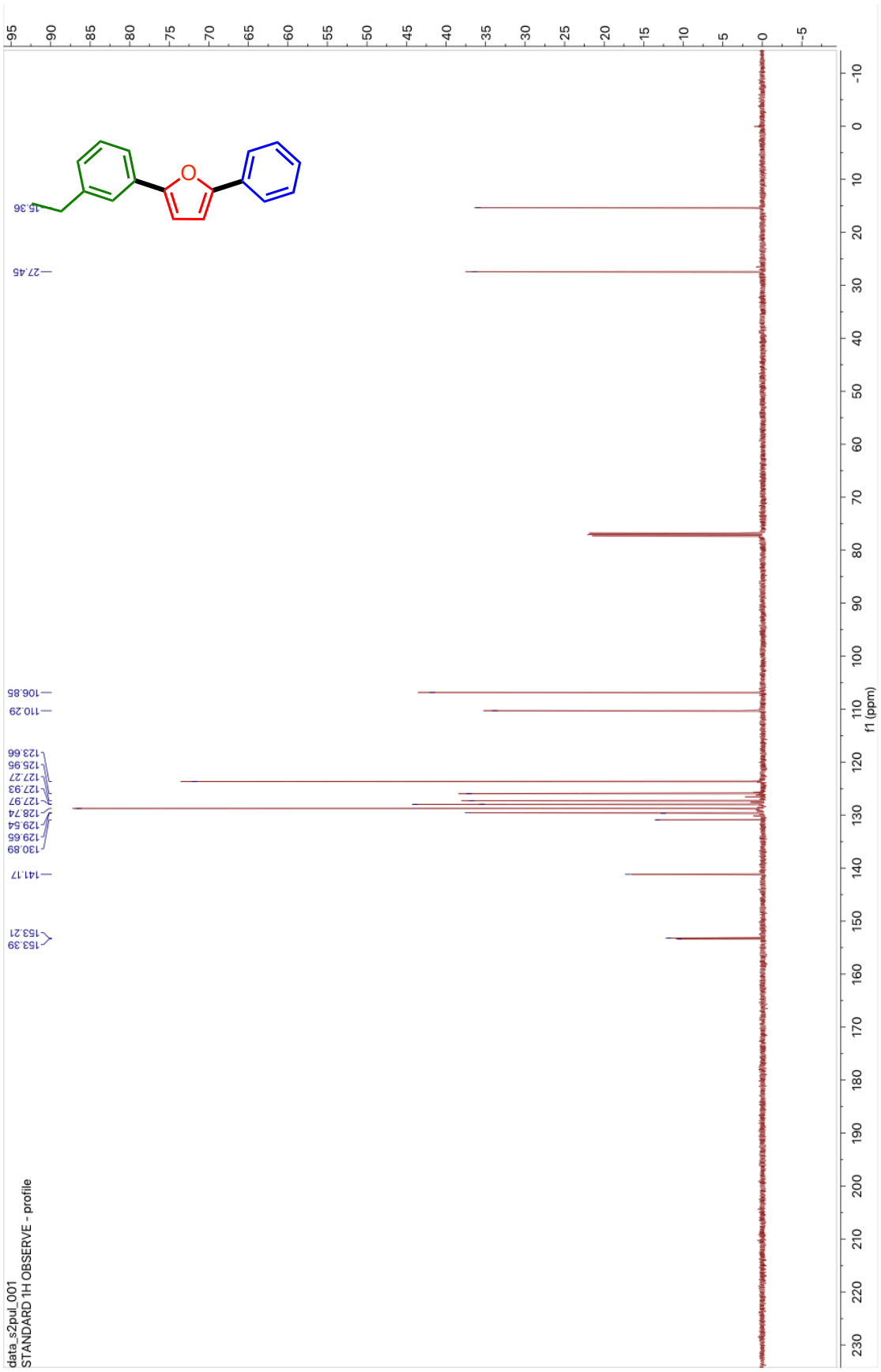
15.36
27.45
106.85
110.29
123.66
125.95
127.27
127.93
127.97
128.74
129.54
129.66
130.89
141.17
153.21
153.39
data_s2pul_001
STANDARD 1H OBSERVE - profile
f1 (ppm)

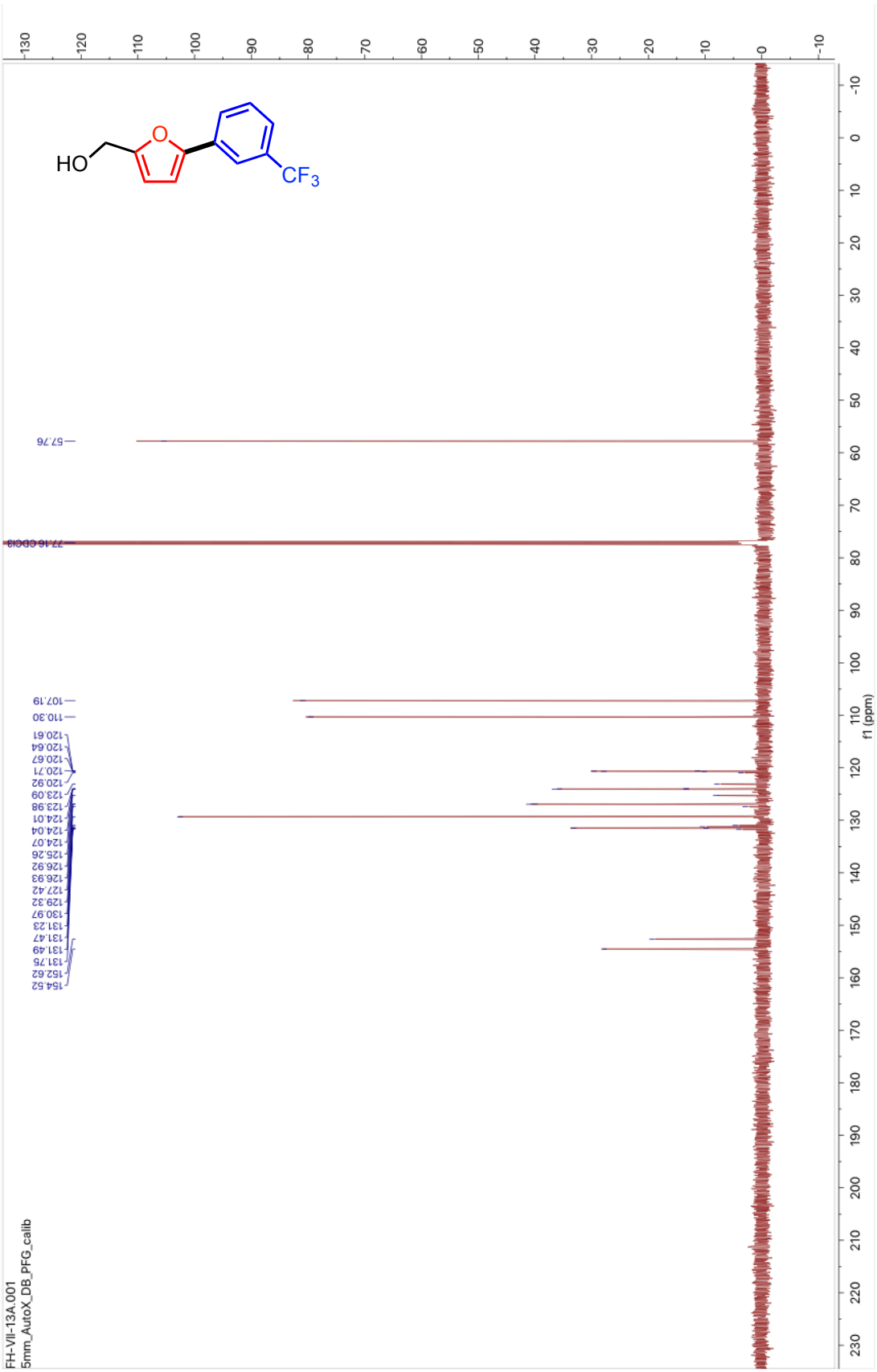
HO
O
CF3
57.76
77.16 CDCl3
107.19
110.30
120.61
120.64
120.67
120.71
120.92
123.09
123.98
124.01
124.04
124.07
125.26
126.92
126.93
127.42
129.32
130.97
131.23
131.47
131.49
131.75
152.62
154.52
FH-VII-13A.001
5mm_AutoX_DB_PFG_calib
f1 (ppm)

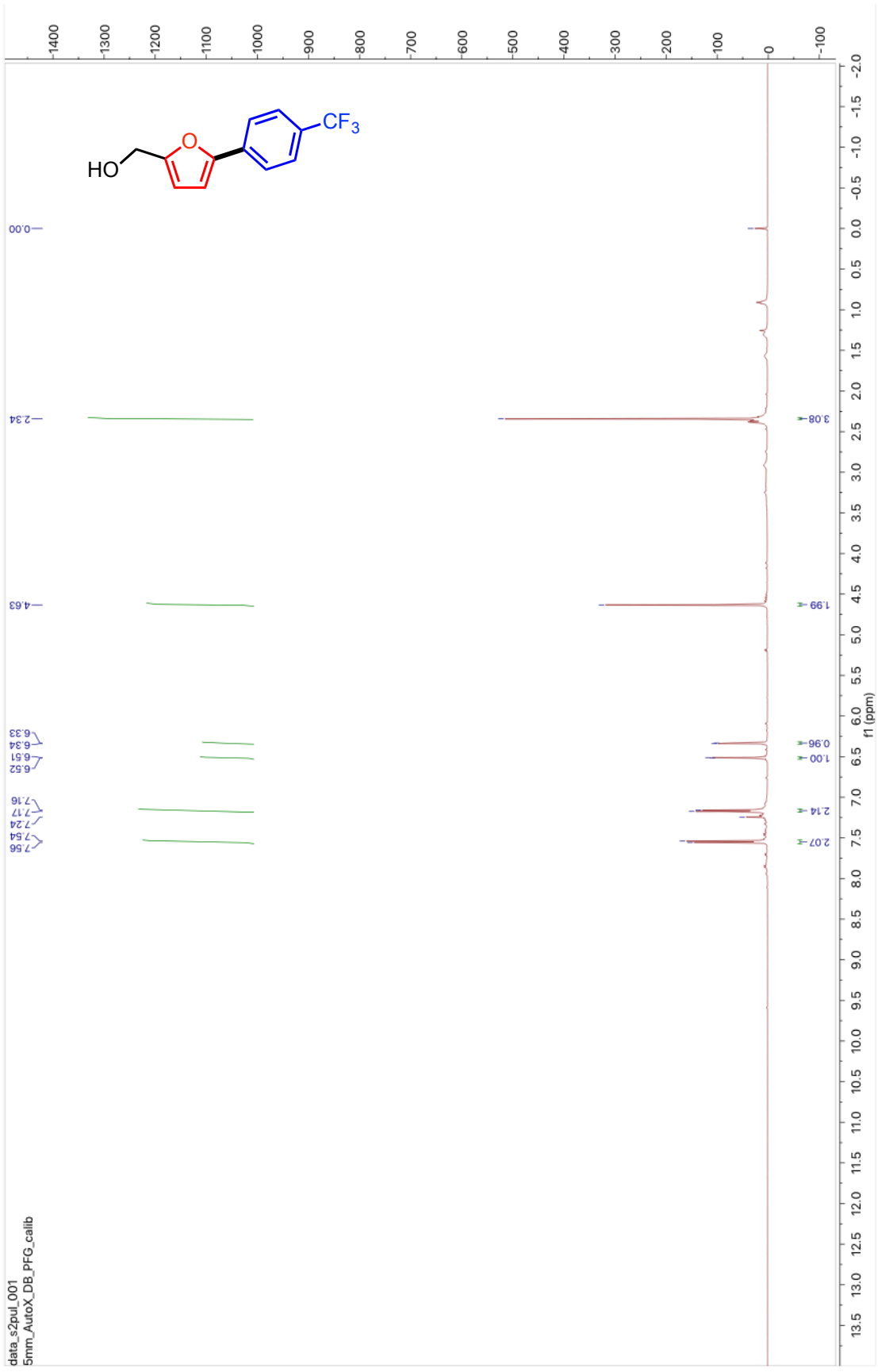
HO
O
CF3
0.00
2.34
4.63
6.33
6.34
6.51
6.52
7.16
7.17
7.24
7.54
7.56
3.08
1.99
0.96
1.00
2.14
2.07
f1 (ppm)
data_s2pul_001
5mm_AutoX_DB_PFG_calib

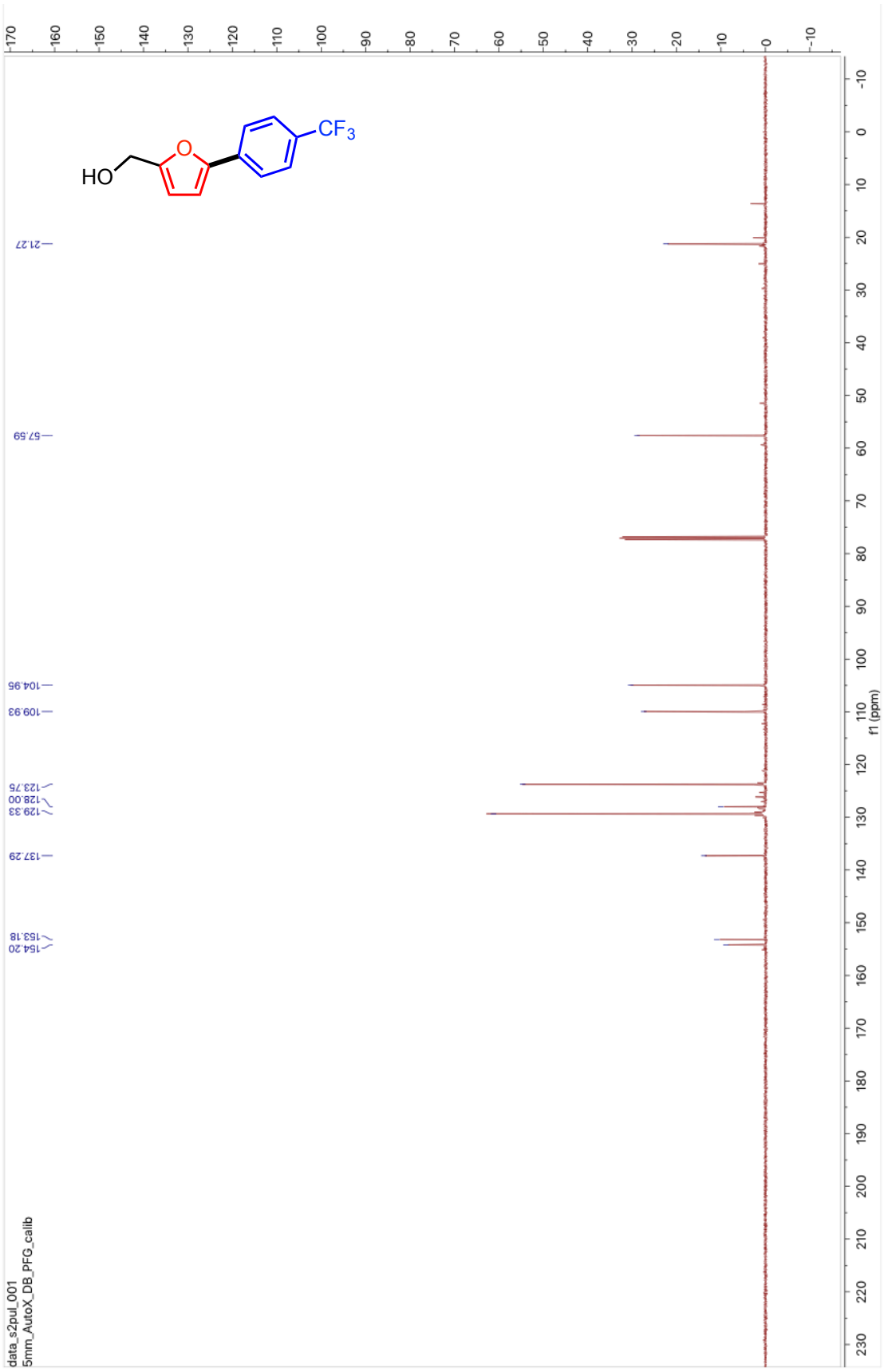
HO
O
CF3
21.27
57.59
104.95
109.93
123.75
128.00
129.33
137.29
153.18
154.20
f1 (ppm)
data_s2pul_001
5mm_AutoX_DB_PFG_calib

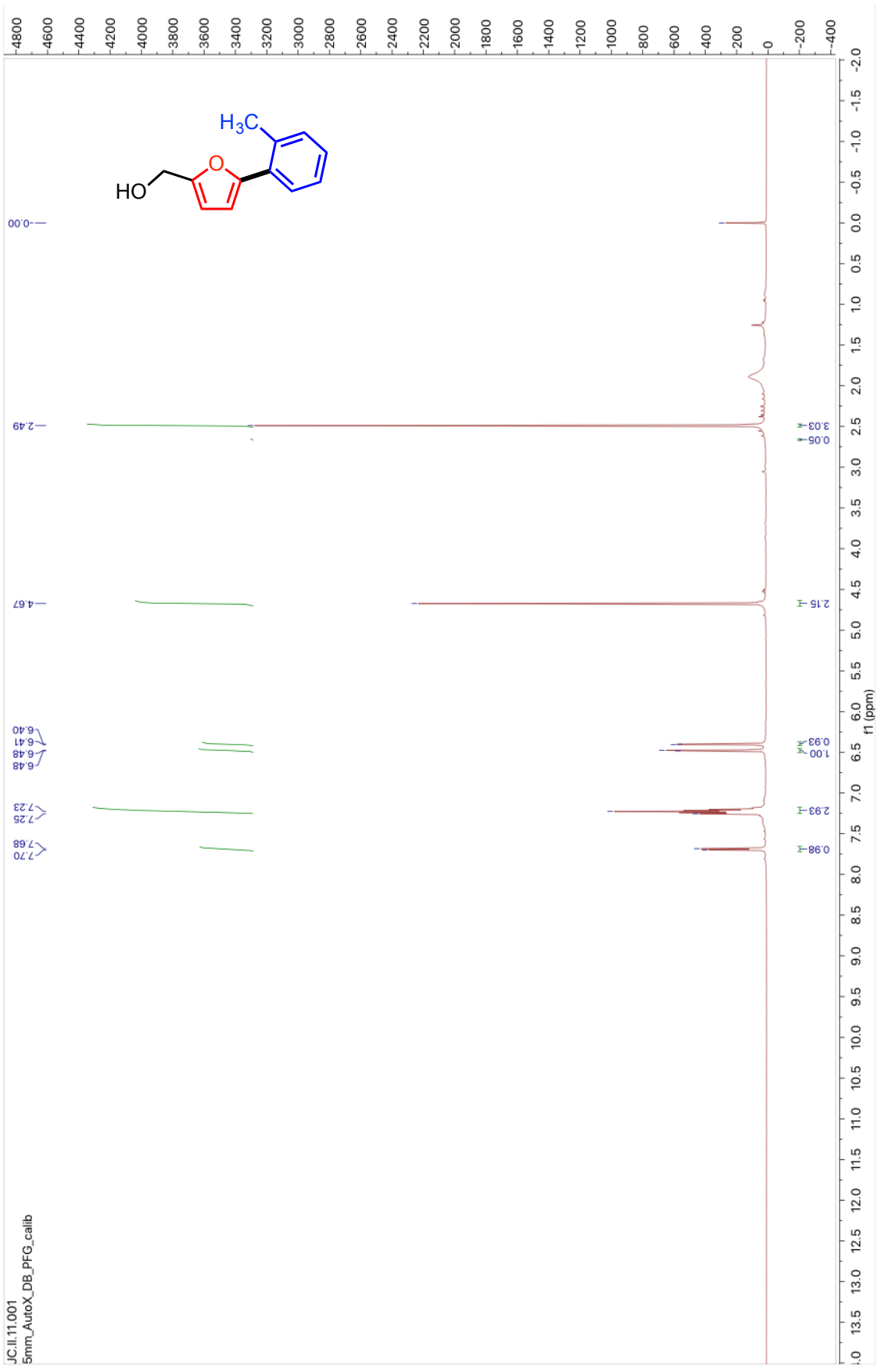
H3C
O
HO
JC.II.11.001
5mm_AutoX_DB_PFG_calib
f1 (ppm)

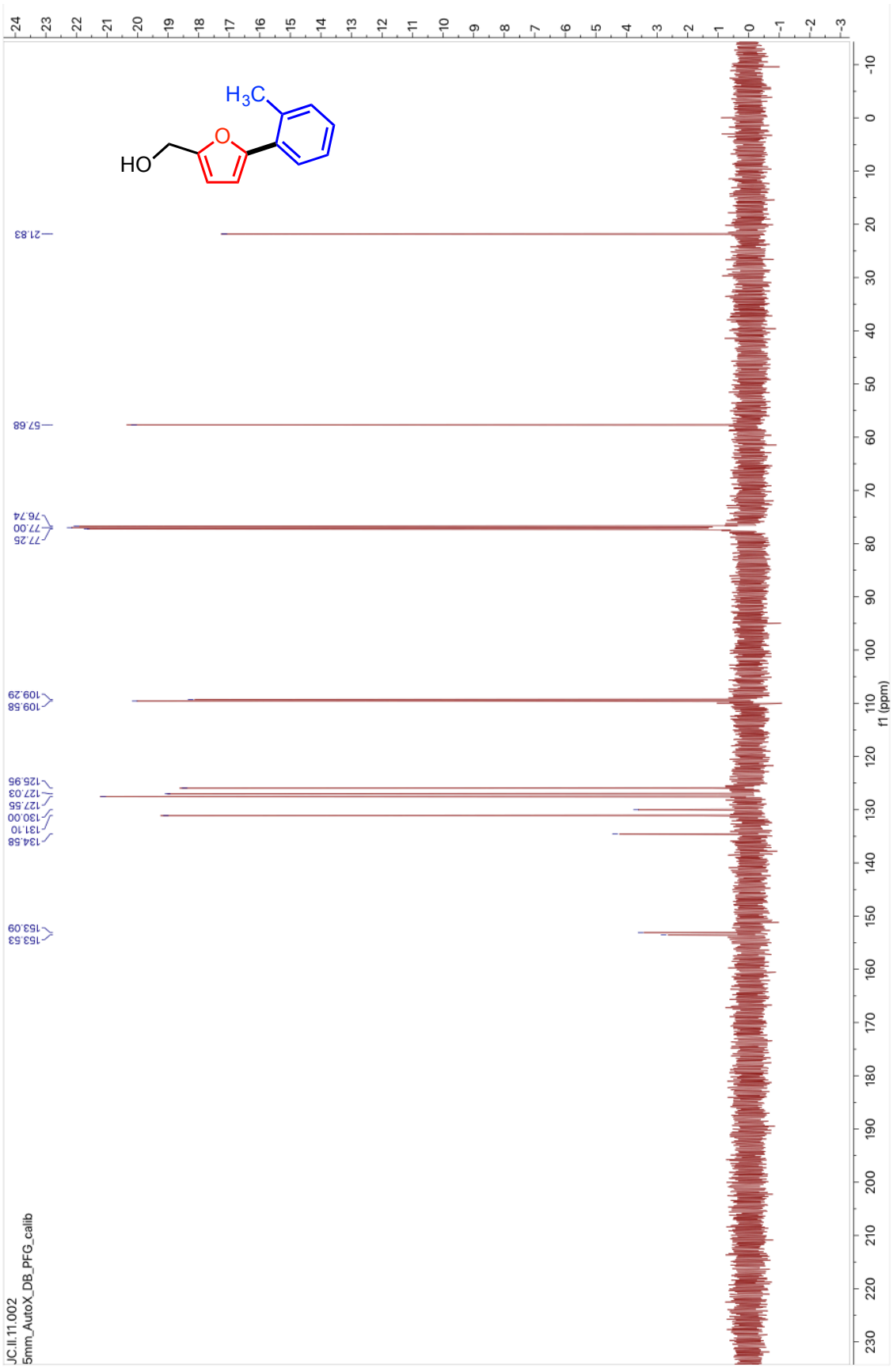
H3C
O
HO
21.83
57.68
76.74
77.00
77.25
109.29
109.58
125.96
127.03
127.55
130.00
131.10
134.58
153.09
153.53
f1 (ppm)
JC.II.11.002
5mm_AutoX_DB_PFG_calib

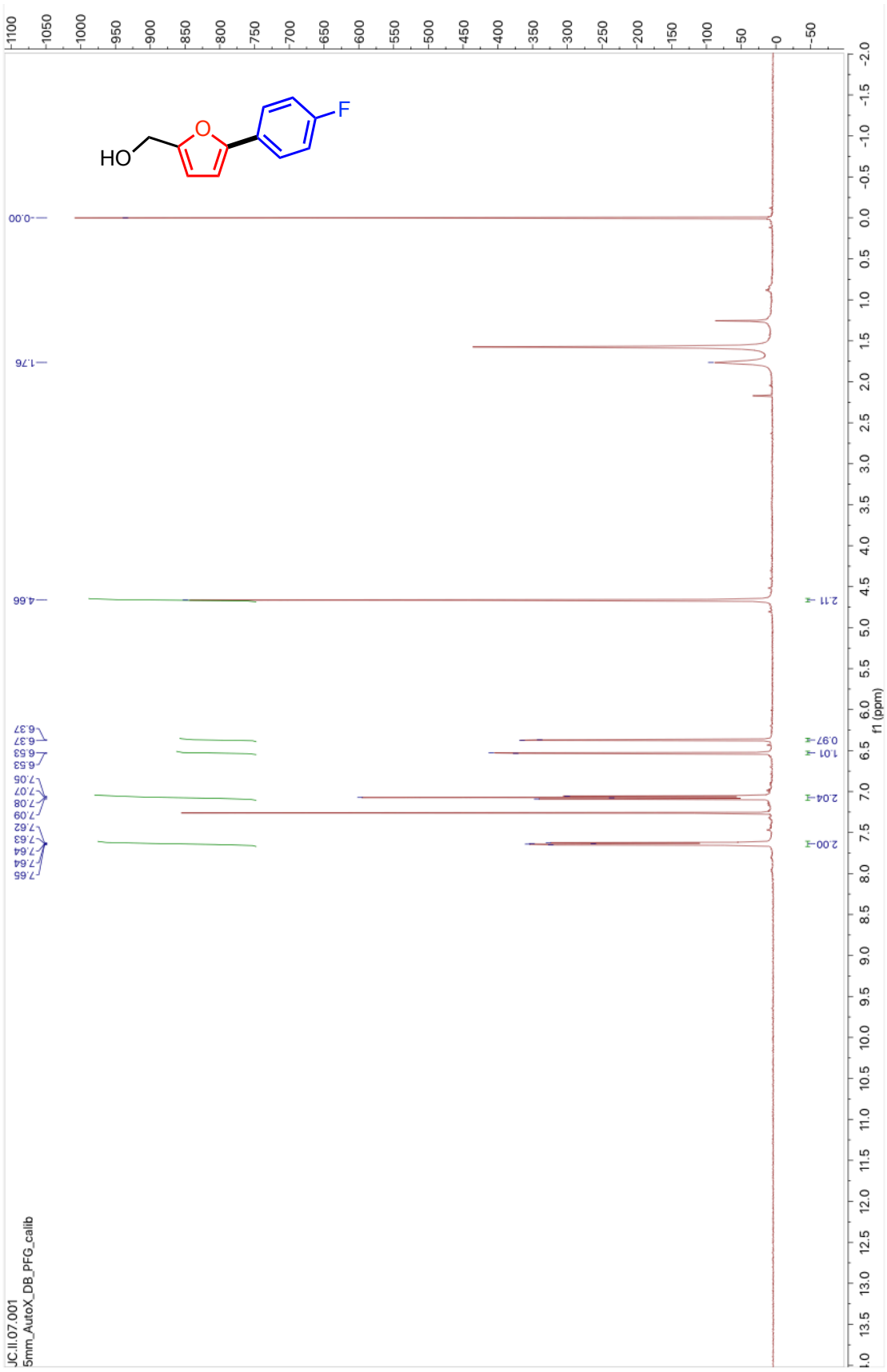
HO
O
F
JC.II.07.001
5mm_AutoX_DB_PFG_calib
f1 (ppm)

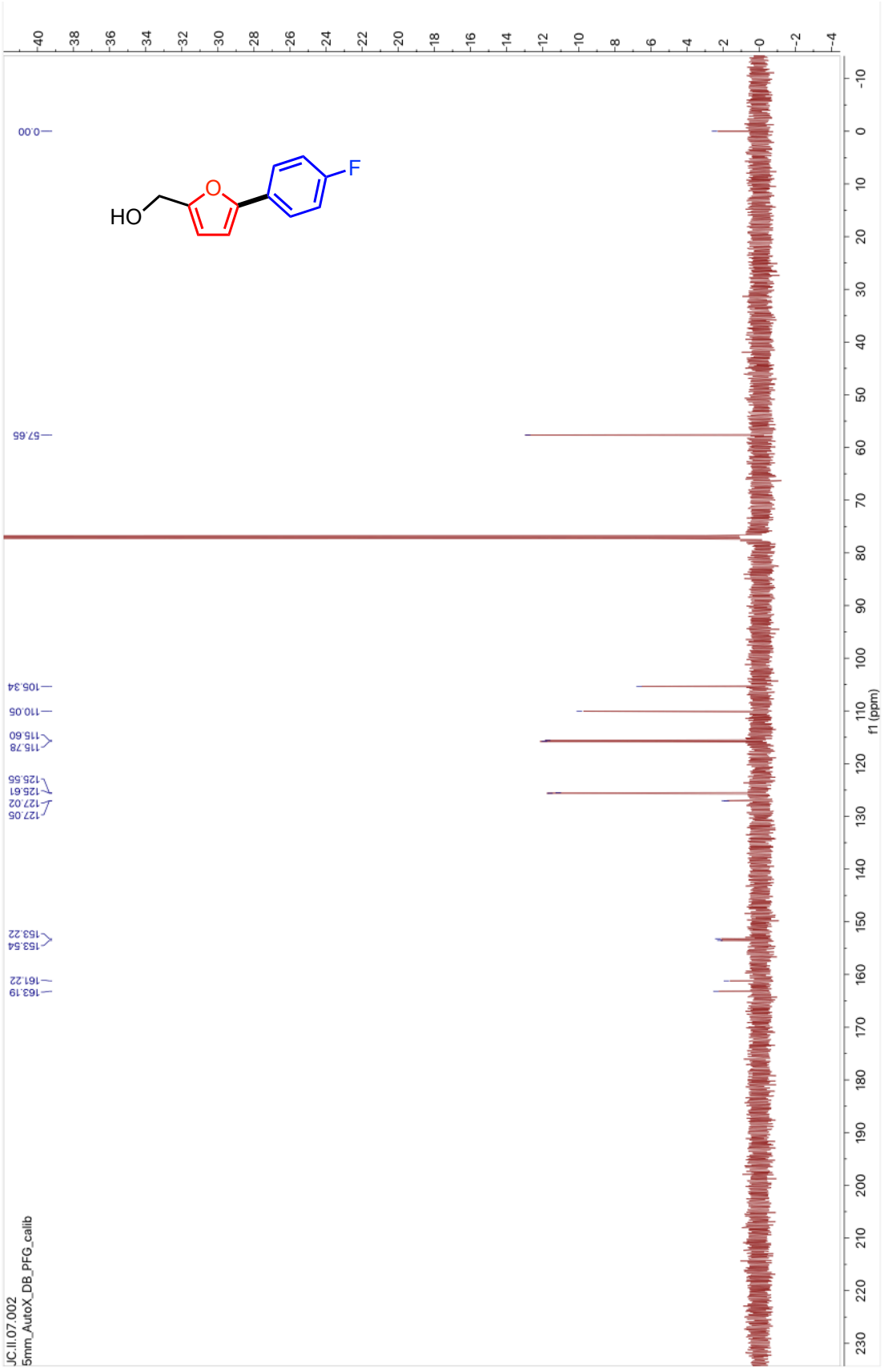
HO
O
F
0.00
57.65
105.34
110.05
115.78
115.60
125.55
125.61
127.02
127.05
153.54
153.22
163.19
161.22
f1 (ppm)
JC.II.07.002
5mm_AutoX_DB_PFG_calib

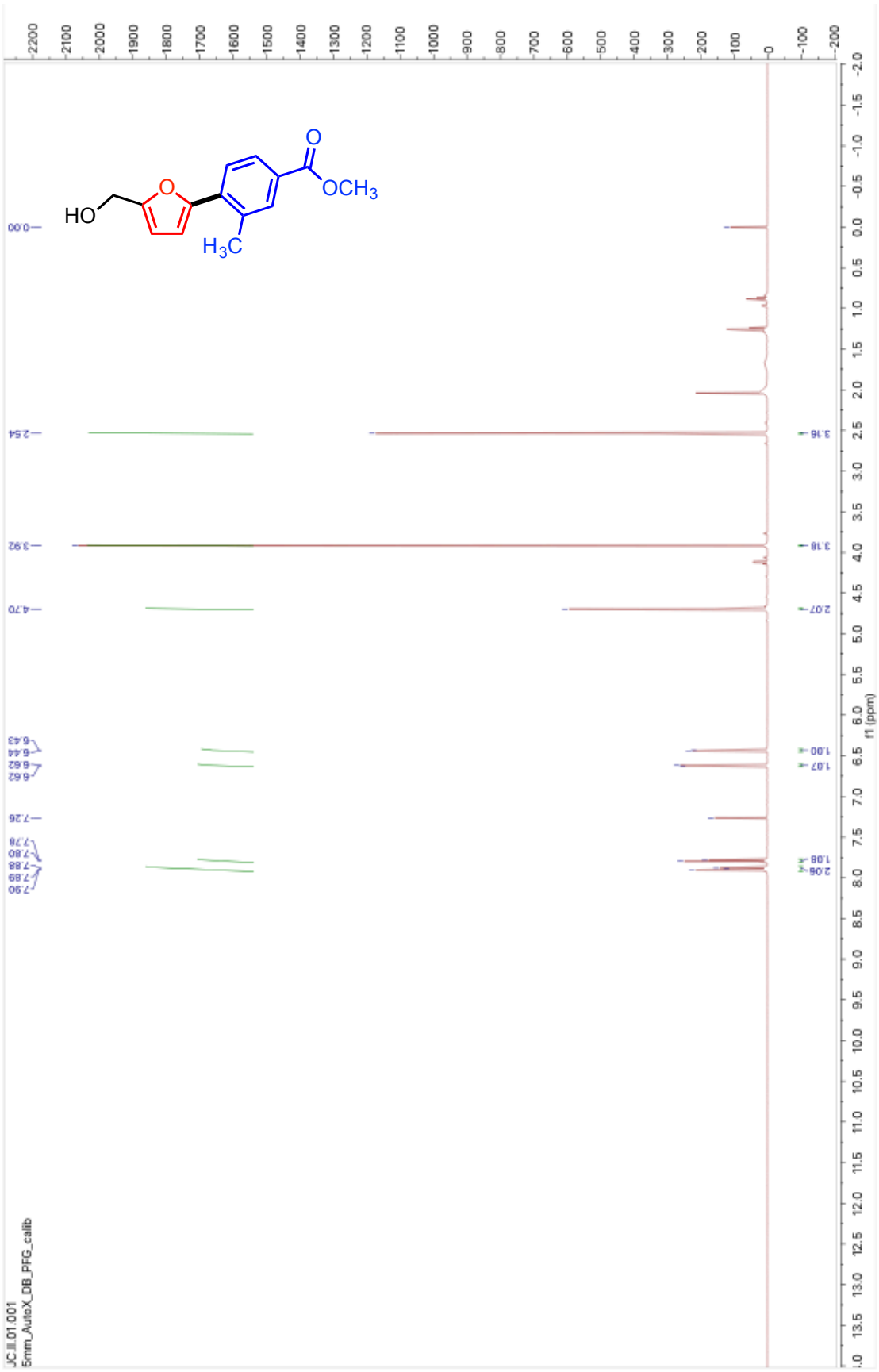
HO
O
O
OCH3
H3C
f1 (ppm)
JC.II.01.001
5mm_AutoX_DB_PFG_calib

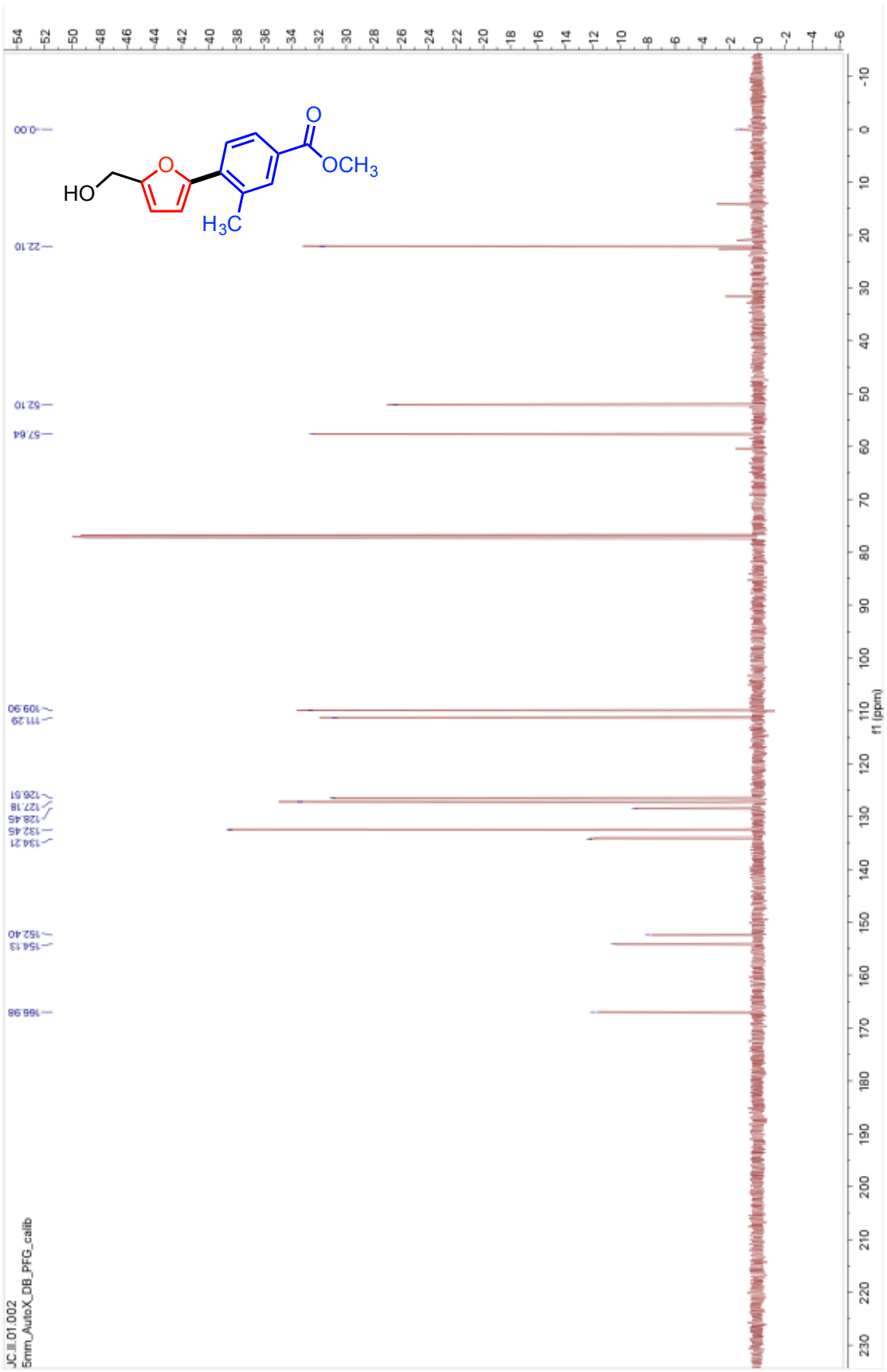
HO
O
O
OCH3
H3C
f1 (ppm)
JC.II.01.002
5mm_AutoX_DB_PFG_calib

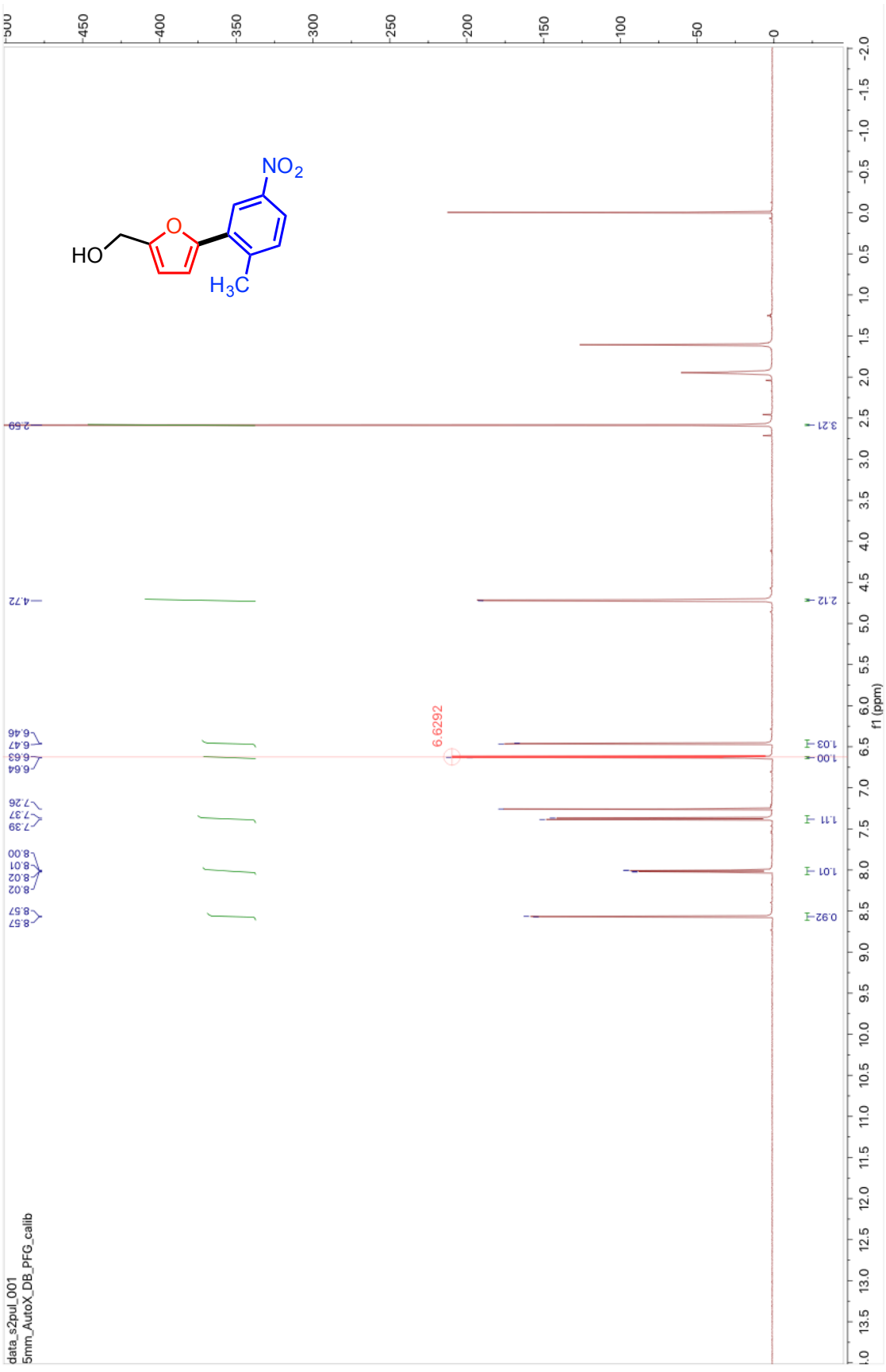
NO2
O
HO
H3C
f1 (ppm)
data_s2pul_001
5mm_AutoX_DB_PFG_calib

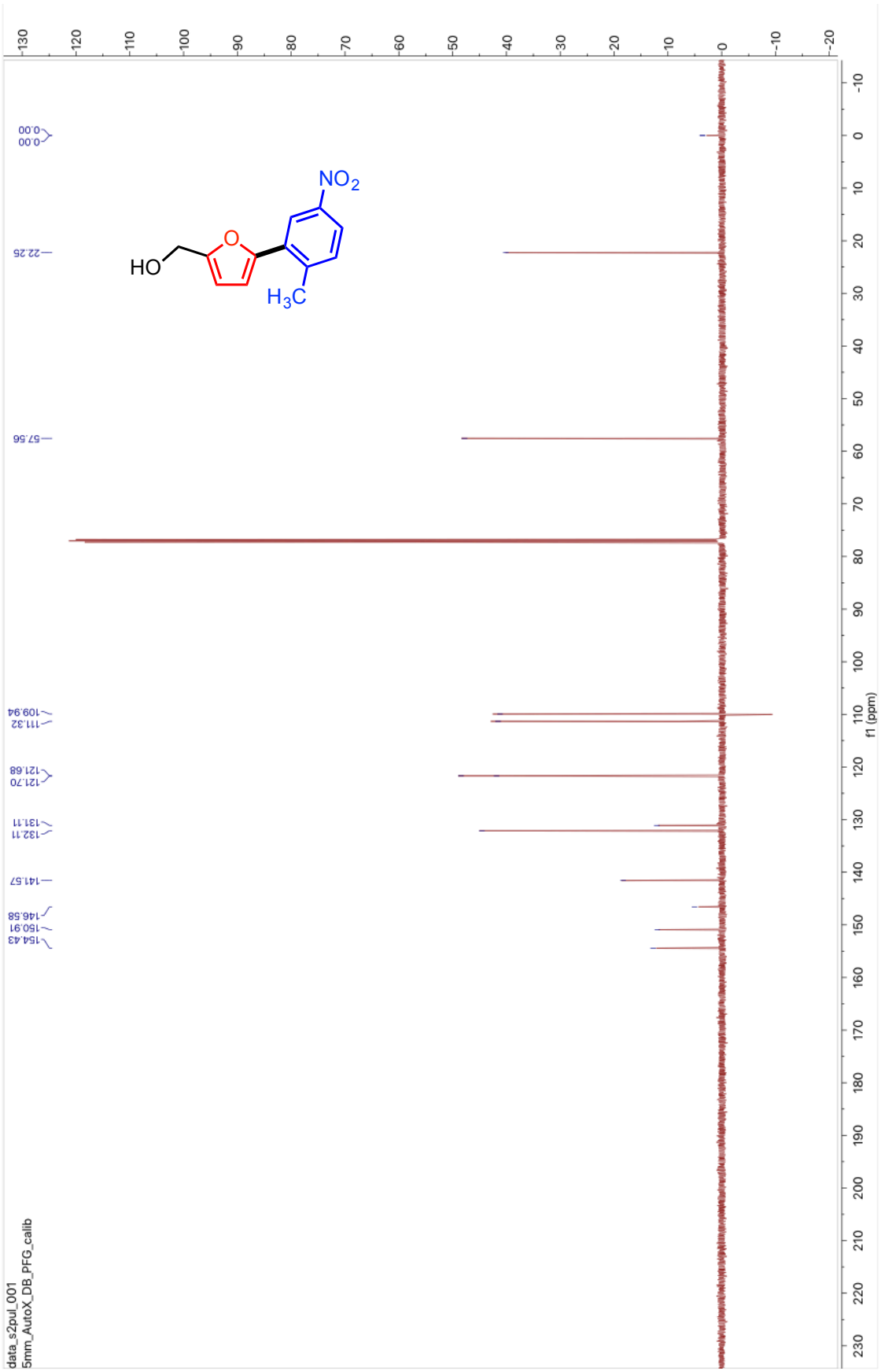
NO2
O
HO
H3C
0.00
22.25
57.56
109.94
111.32
121.68
121.70
131.11
132.11
141.57
146.58
150.91
154.43
f1 (ppm)
data_s2pul_001
5mm_AutoX_DB_PFG_calib

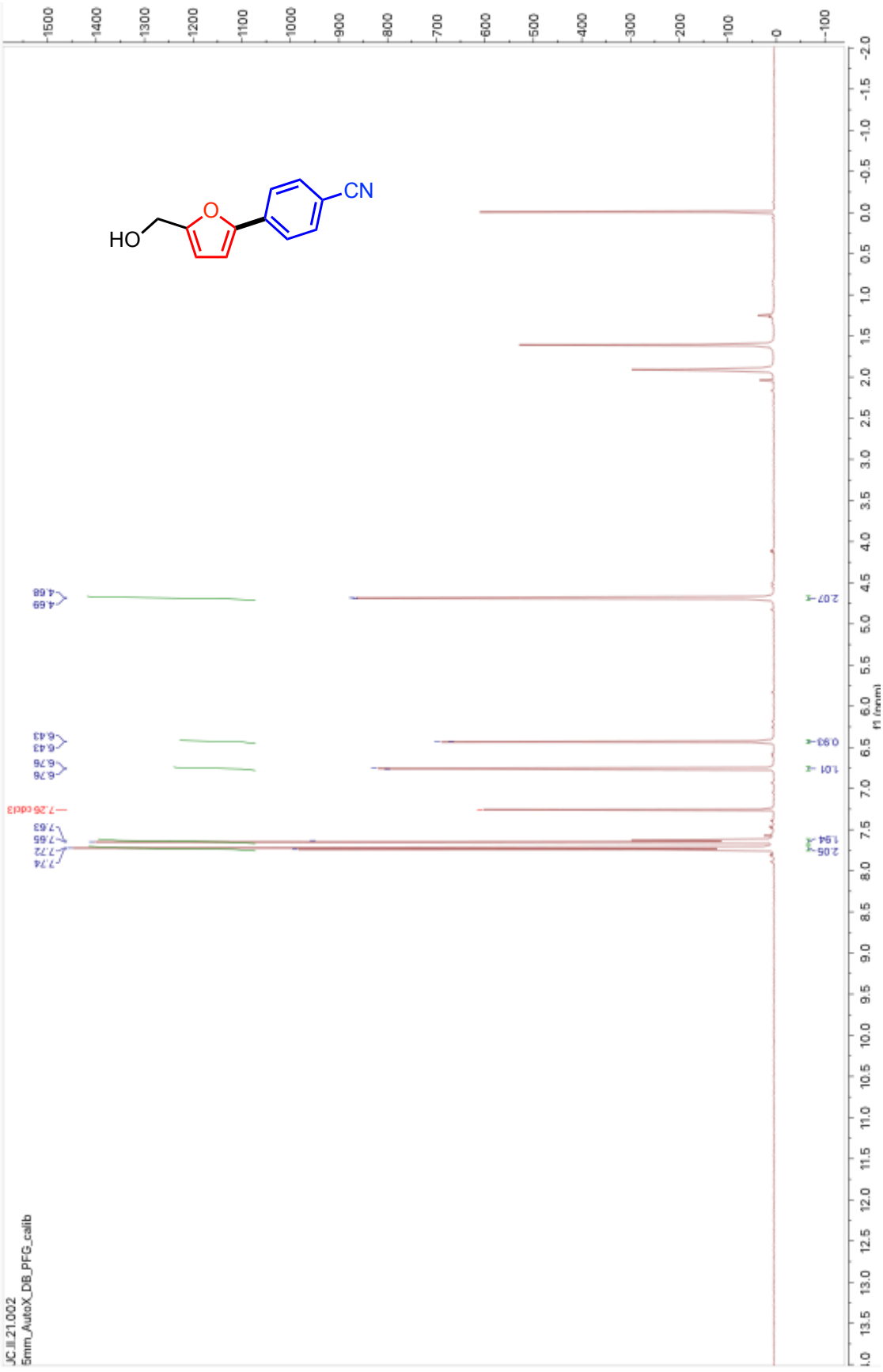
HO
O
CN
JC.III.21.002
5mm_AutoX_DB_PFG_calib
f1 (ppm)

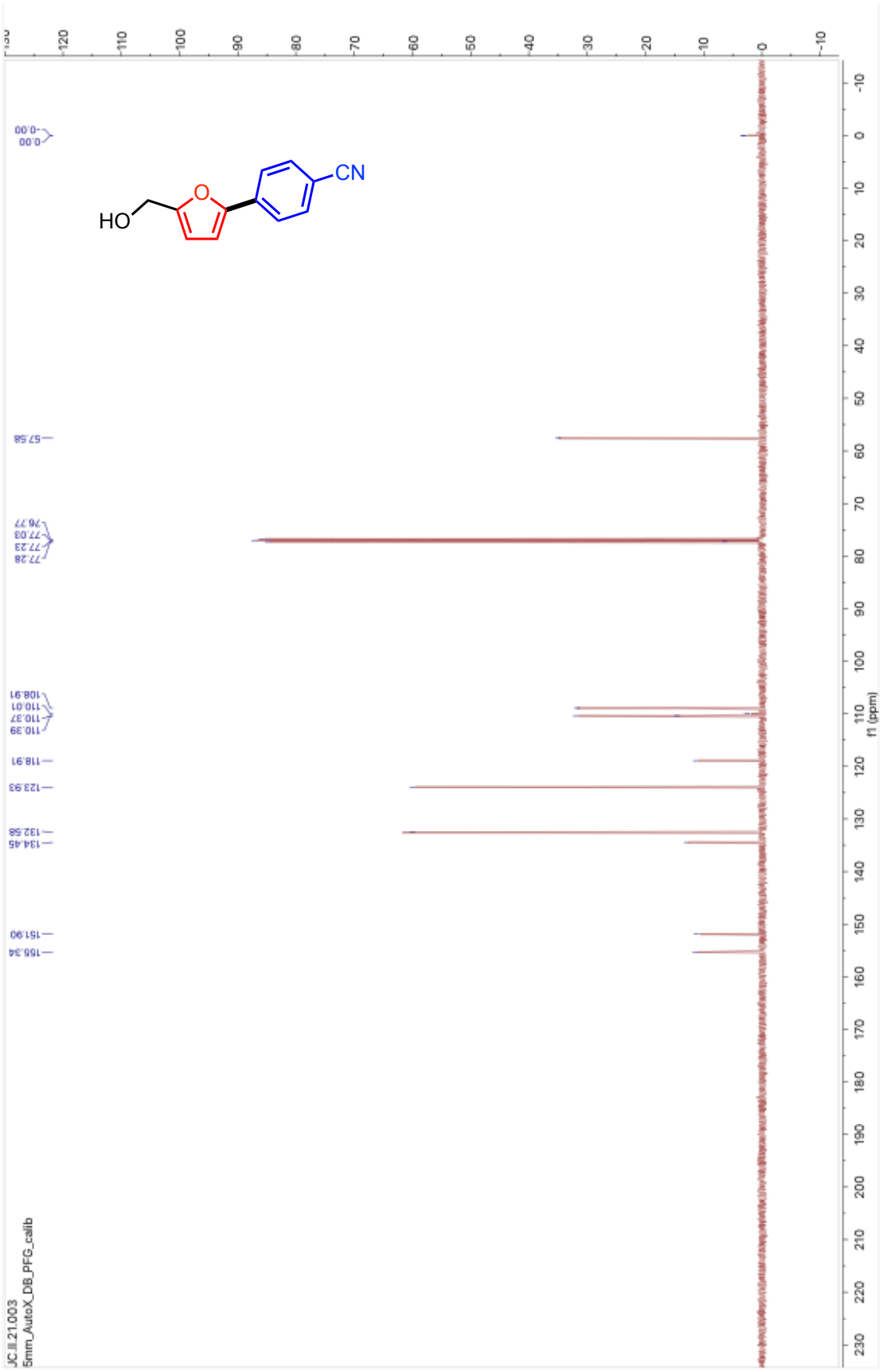
HO
O
CN
0.00
57.58
76.77
77.03
77.23
77.28
108.91
110.01
110.37
110.39
118.91
123.93
132.58
134.45
151.90
156.34
f1 (ppm)
JC.II.21.003
5mm_AutoX_DB_PFG_calib

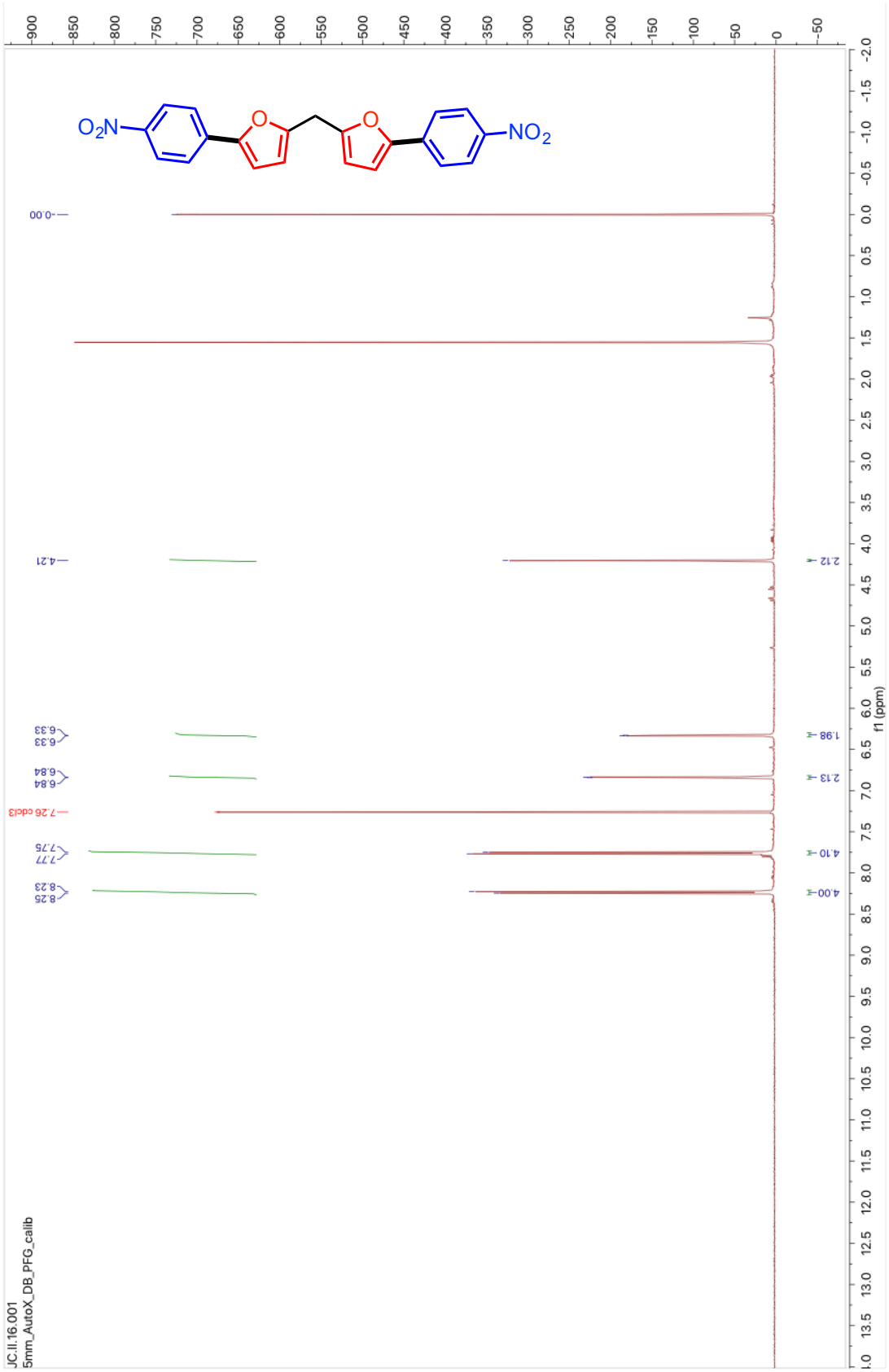
O2N
O
O
NO2
0.00
4.21
6.33
6.84
7.26
7.75
7.77
8.23
8.25
2.12
1.98
2.13
4.10
4.00
f1 (ppm)
JC.II.16.001
5mm_AutoX_DB_PFG_calib

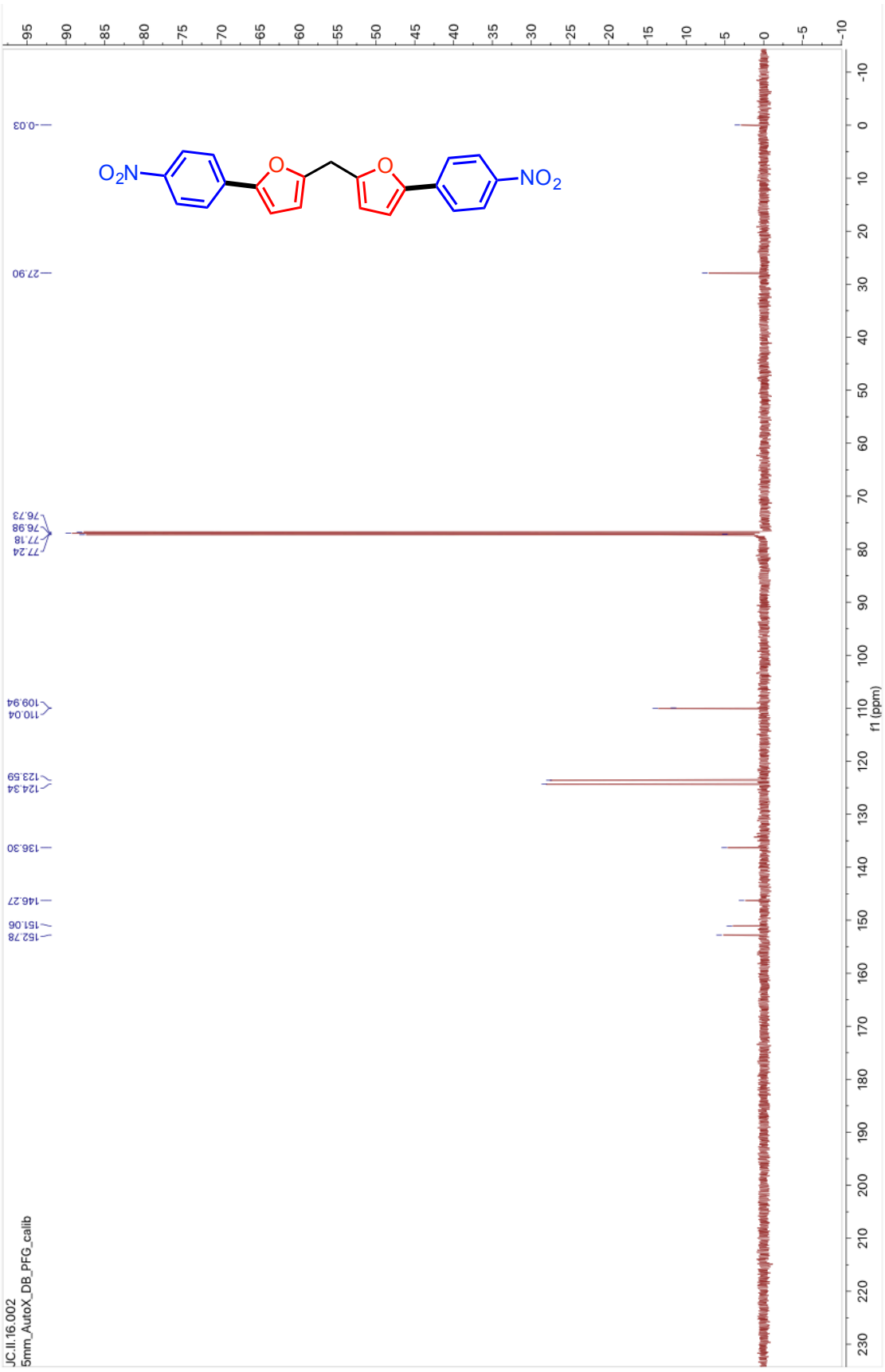
O2N
O
O
NO2
-0.03
27.90
76.73
76.98
77.18
77.24
109.94
110.04
123.59
124.34
136.30
146.27
151.06
152.78
f1 (ppm)
JC.II.16.002
5mm_AutoX_DB_PFG_calib

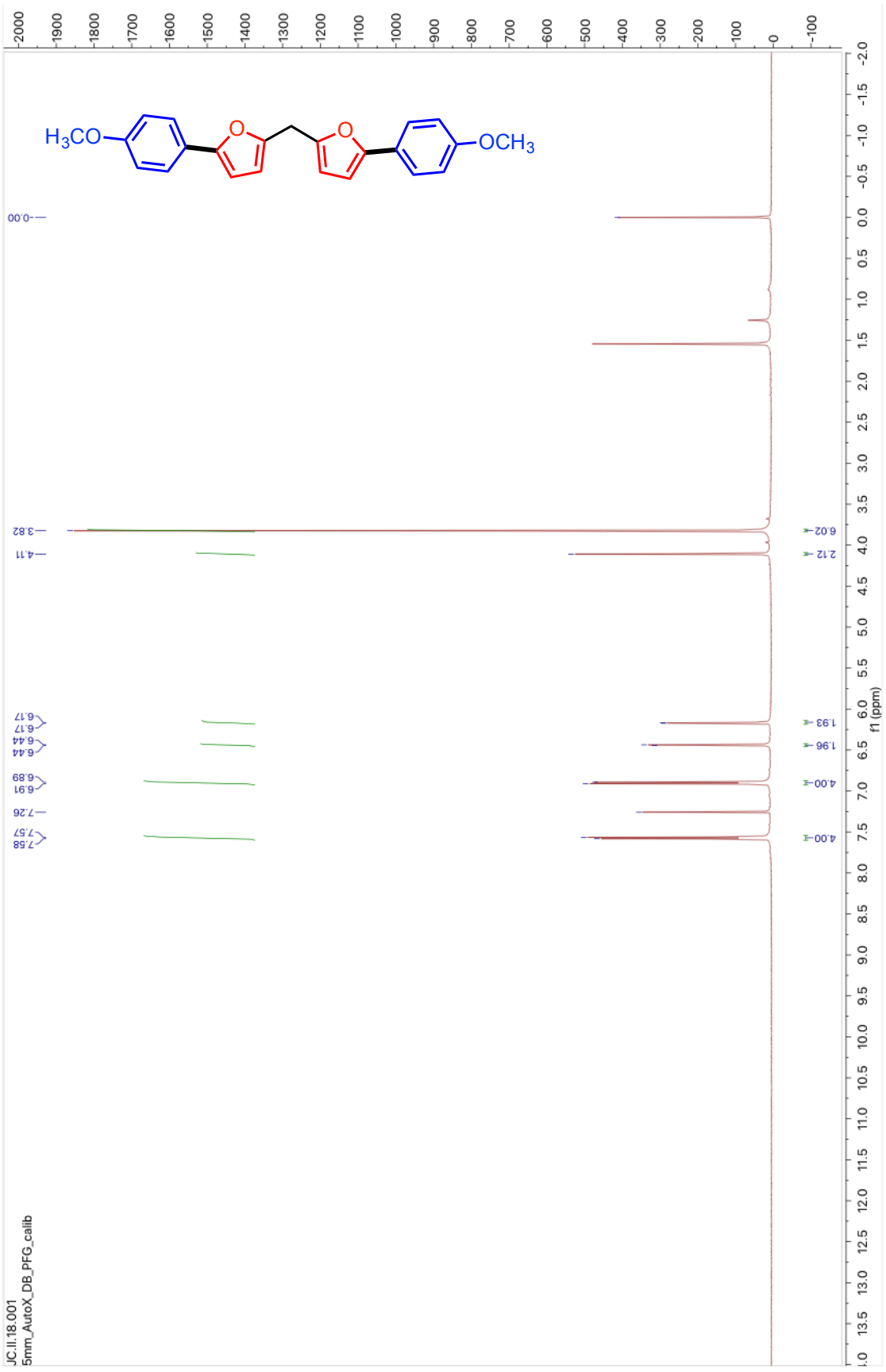
H3CO
O
O
OCH3
0.00
3.82
4.11
6.17
6.17
6.44
6.44
6.89
6.91
7.26
7.57
7.58
6.02
2.12
1.93
1.96
4.00
4.00
f1 (ppm)
JC.II.18.001
5mm_AutoX_DB_PFG_calib

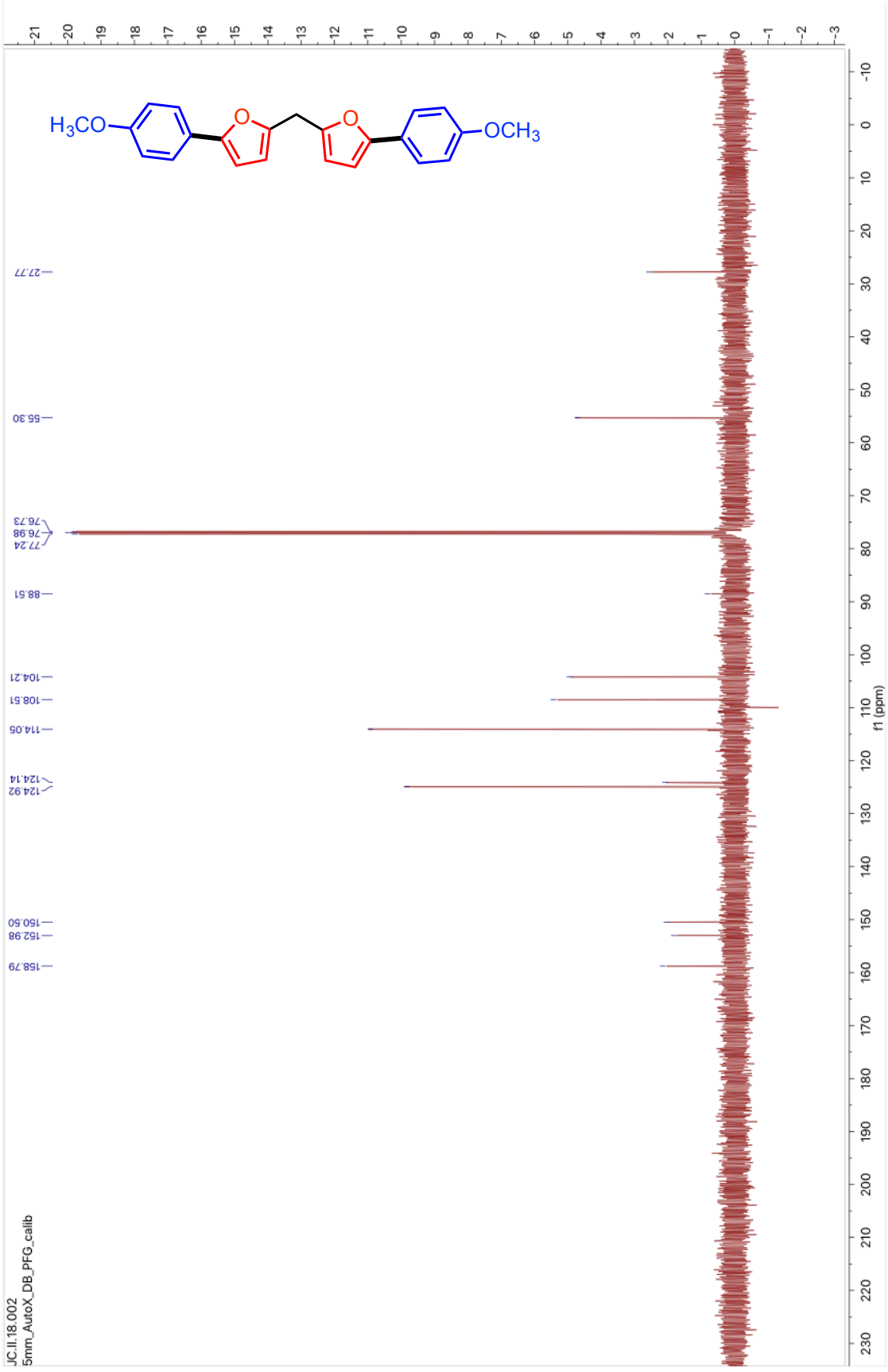
H3CO
O
O
OCH3
27.77
55.30
76.73
76.98
77.24
88.51
104.21
108.51
114.05
124.14
124.92
150.50
152.98
158.79
f1 (ppm)
JC.II.18.002
5mm_AutoX_DB_PFG_calib

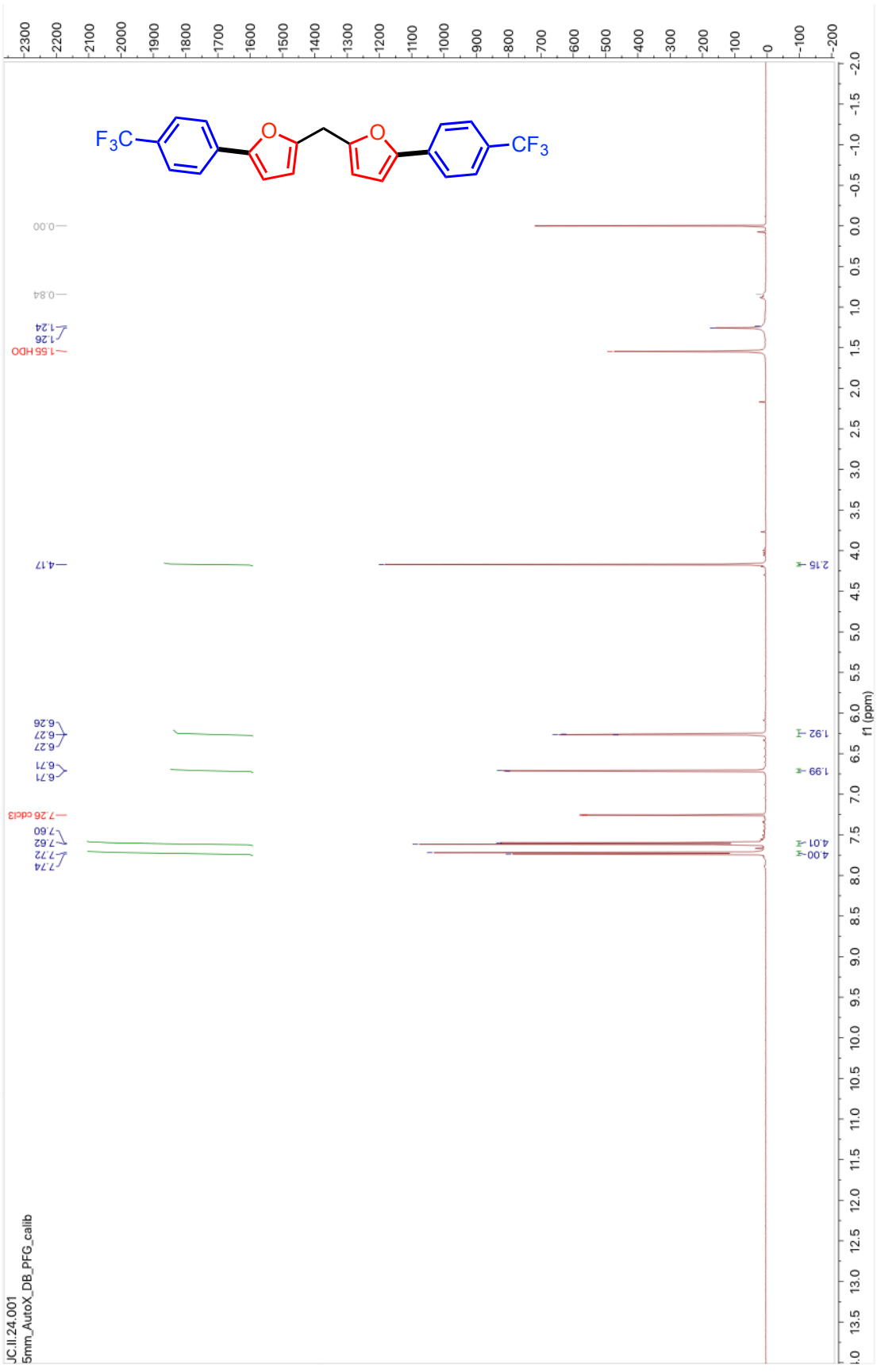
F3C
O
O
CF3
0.00
0.84
1.24
1.26
1.55 HDO
4.17
2.15
6.26
6.27
6.27
6.71
6.71
7.26 cdcl3
7.60
7.62
7.72
7.74
1.92
1.99
4.01
4.00
f1 (ppm)
JC.II.24.001
5mm_AutoX_DB_PFG_calib

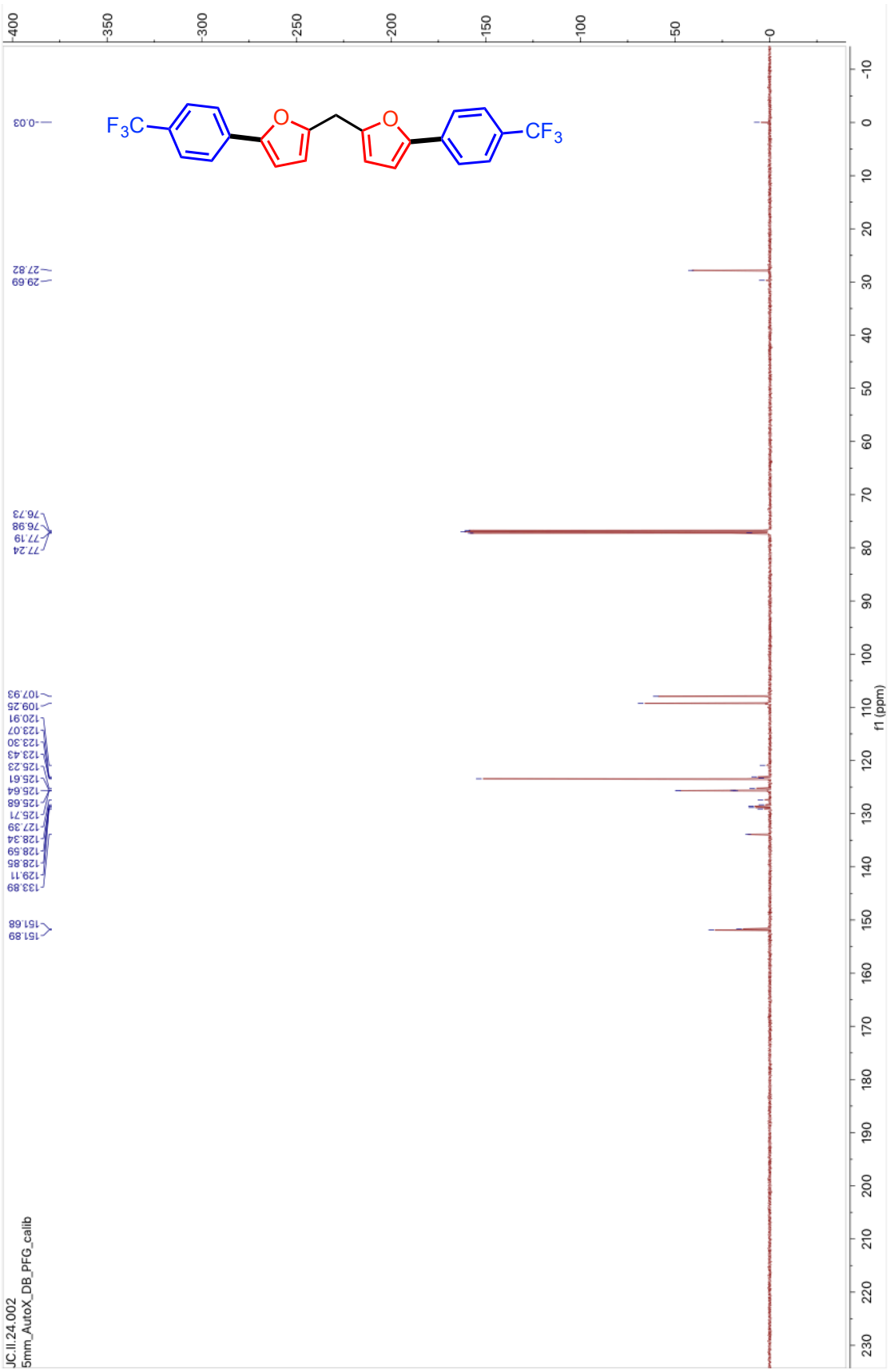
F3C
O
O
CF3
-0.03
27.82
29.69
76.73
76.98
77.19
77.24
107.93
109.25
120.91
123.07
123.30
123.43
125.23
125.61
125.64
125.68
125.71
127.39
128.34
128.59
128.85
129.11
133.89
151.68
151.89
f1 (ppm)
JC.II.24.002
5mm_AutoX_DB_PFG_calib

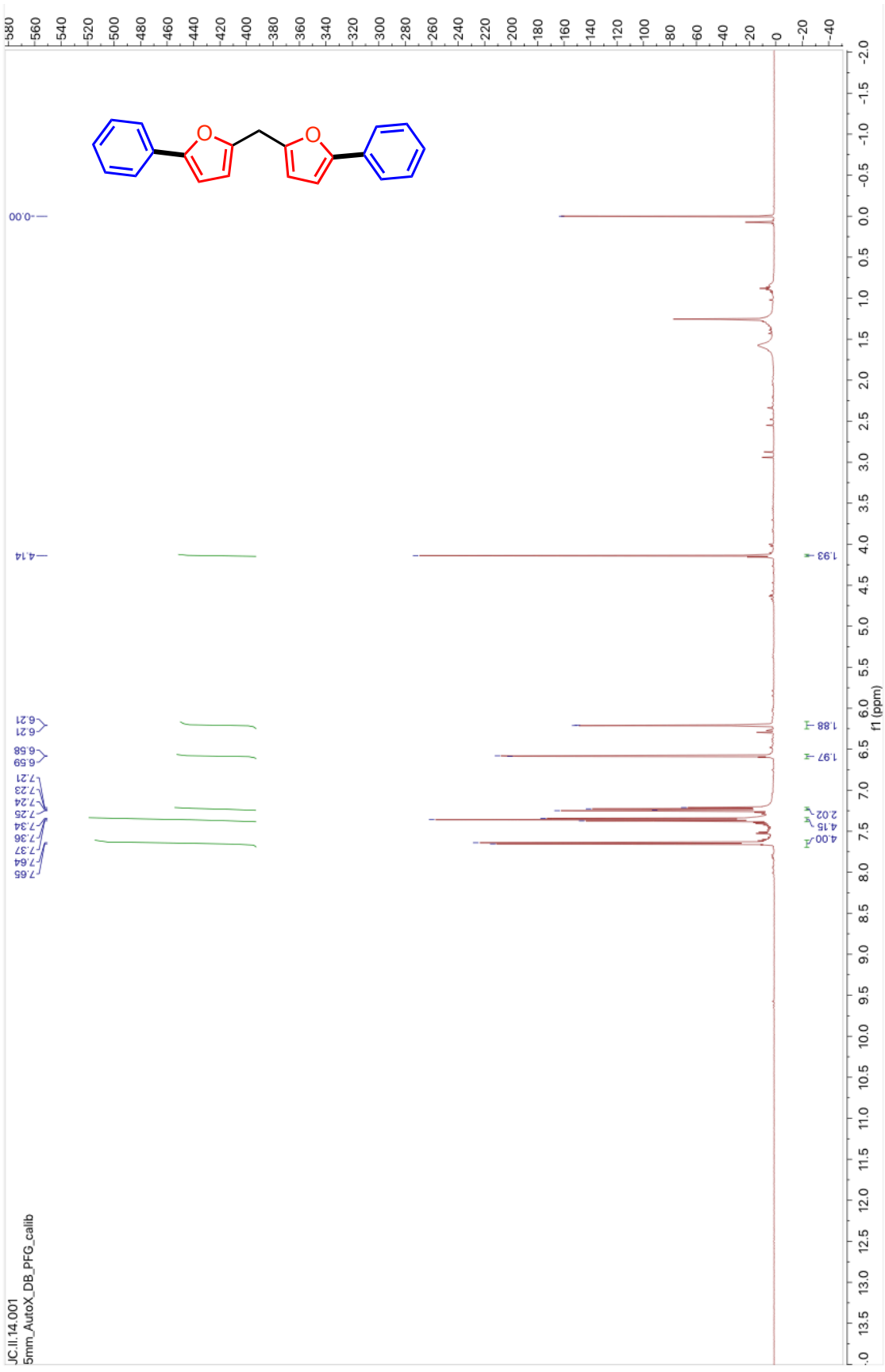
JC.II.14.001
5mm_AutoX_DB_PFG_calib
f1 (ppm)

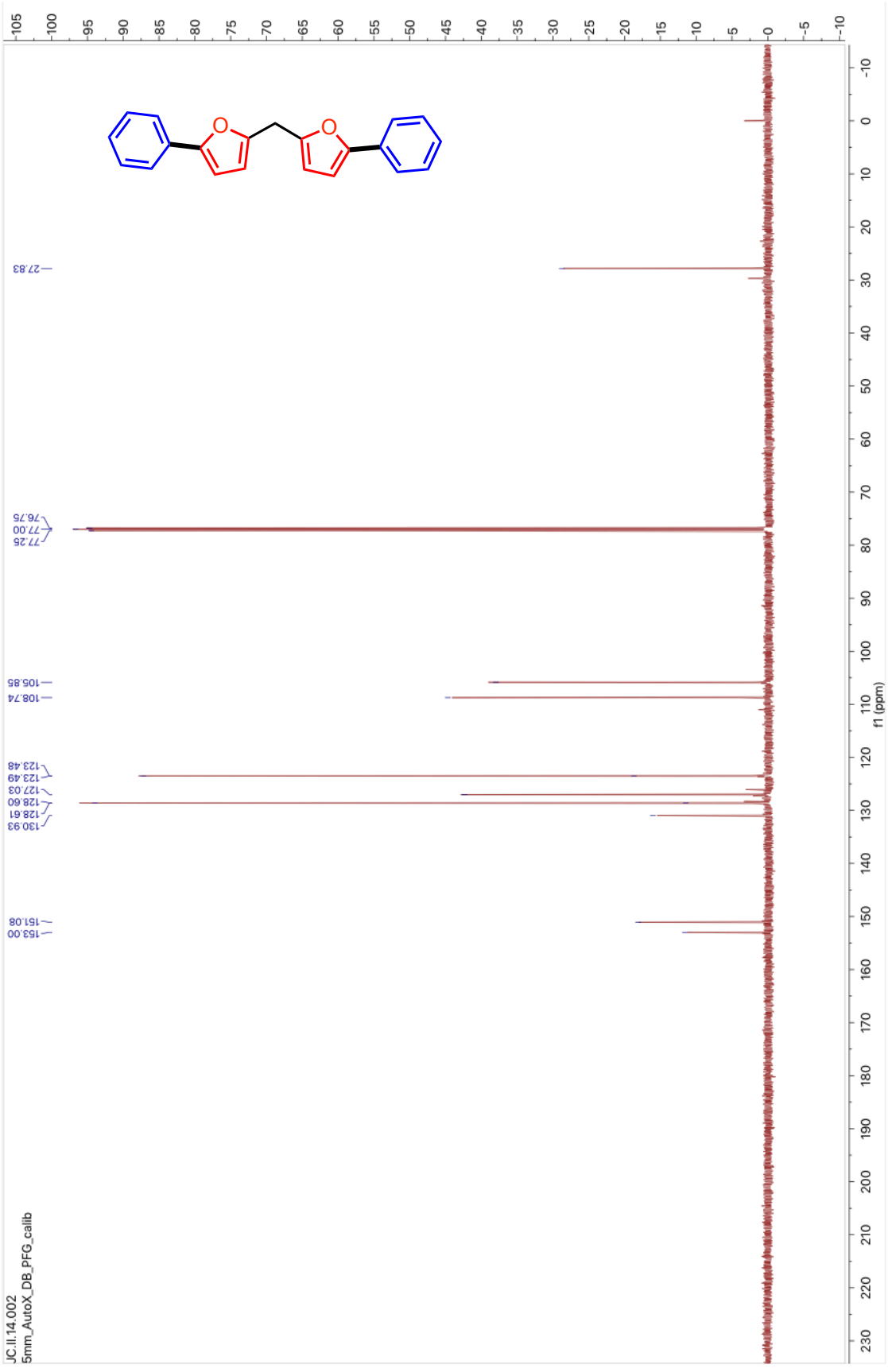
27.83
76.75
77.00
77.25
105.85
108.74
123.48
123.49
127.03
128.60
128.61
130.93
151.08
153.00
f1 (ppm)
JC.II.14.002
5mm_AutoX_DB_PFG_calib

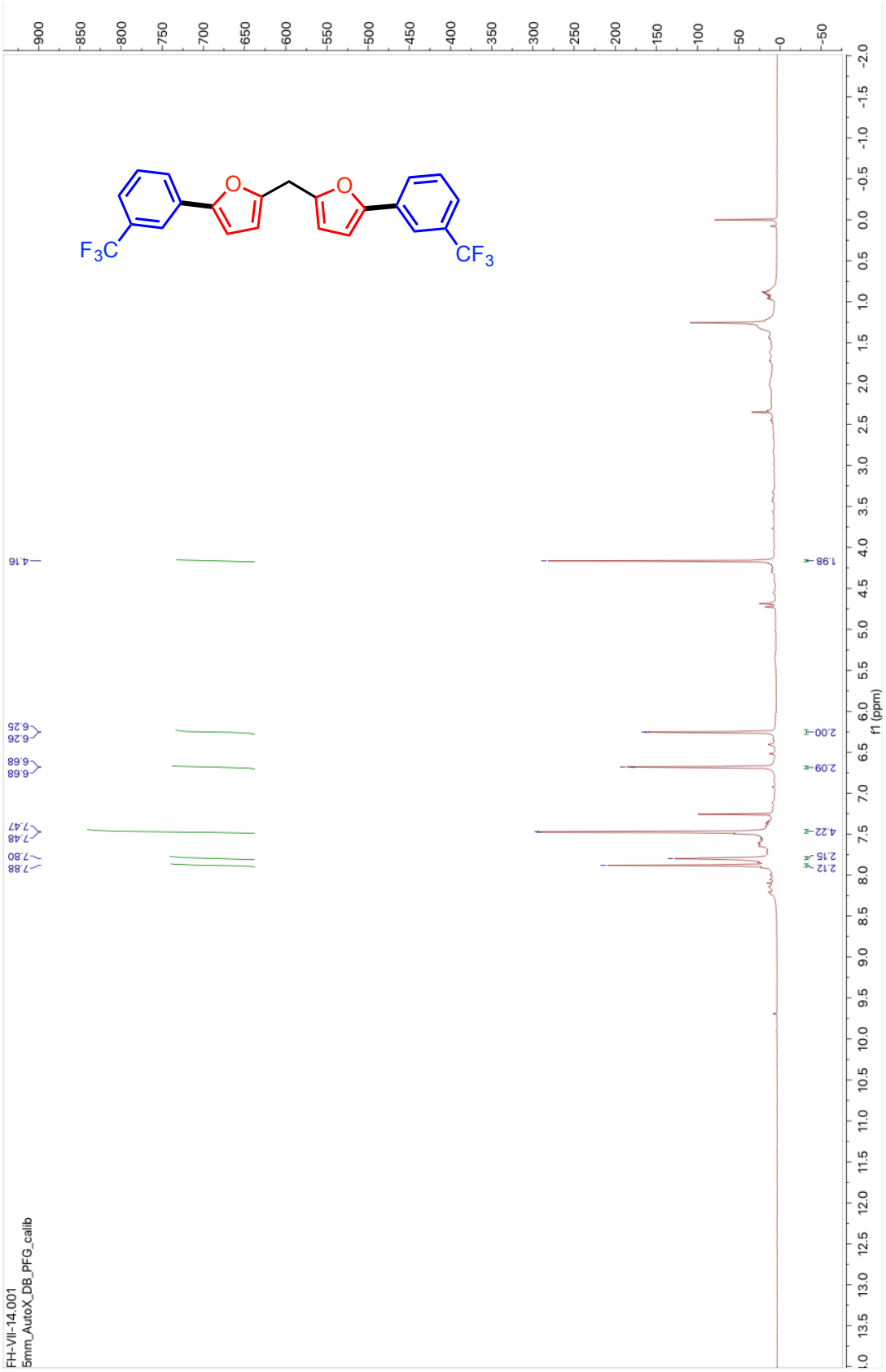
F3C
CF3
O
O
FH-VII-14.001
5mm_AutoX_DB_PFG_calib
f1 (ppm)

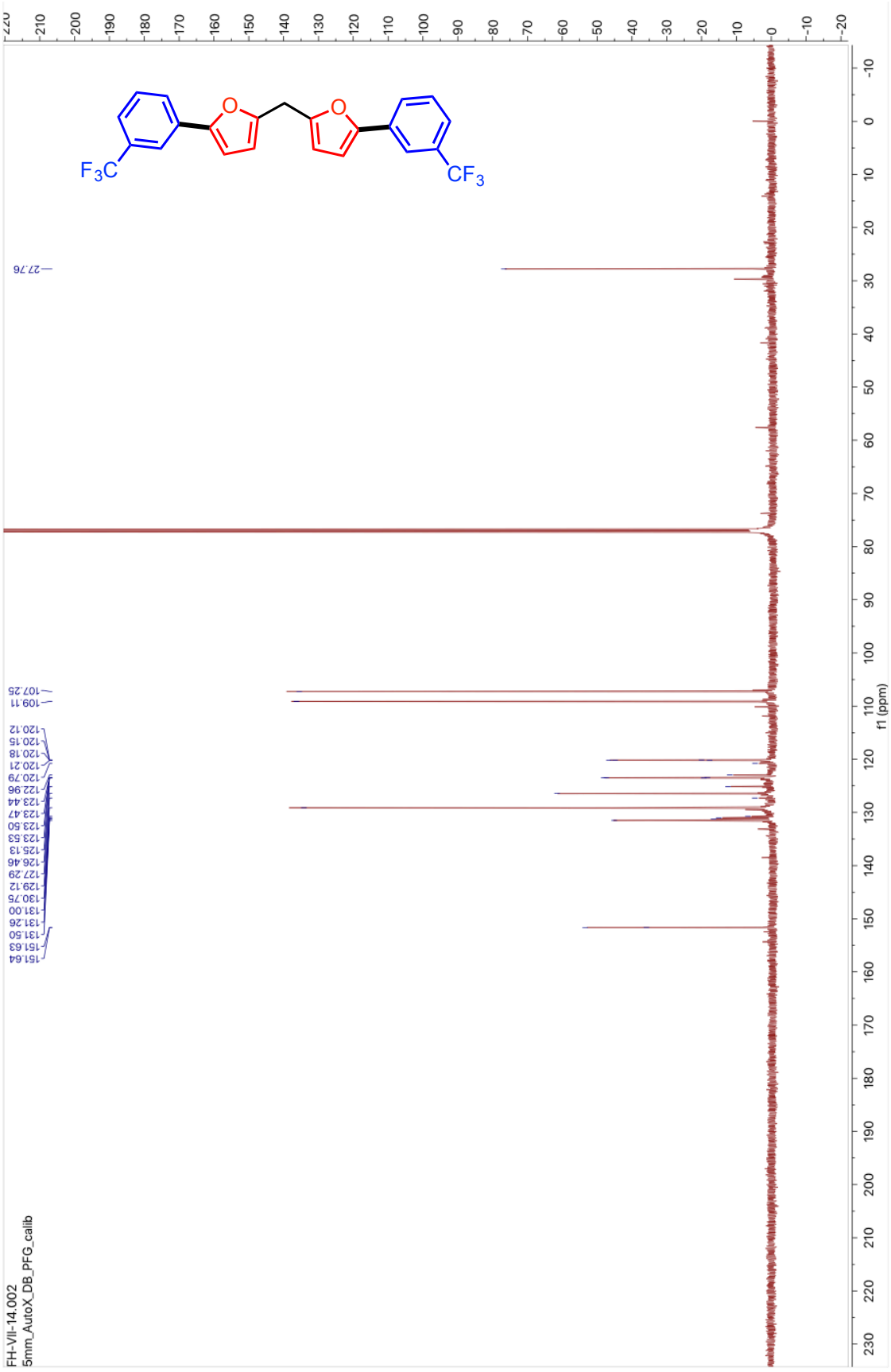
F3C
CF3
O
O
27.76
107.25
109.11
120.12
120.15
120.18
120.21
120.79
122.96
123.44
123.47
123.50
123.53
125.13
126.46
127.29
129.12
130.75
131.00
131.26
131.50
151.63
151.64
f1 (ppm)
FH-VII-14.002
5mm_AutoX_DB_PFG_calib

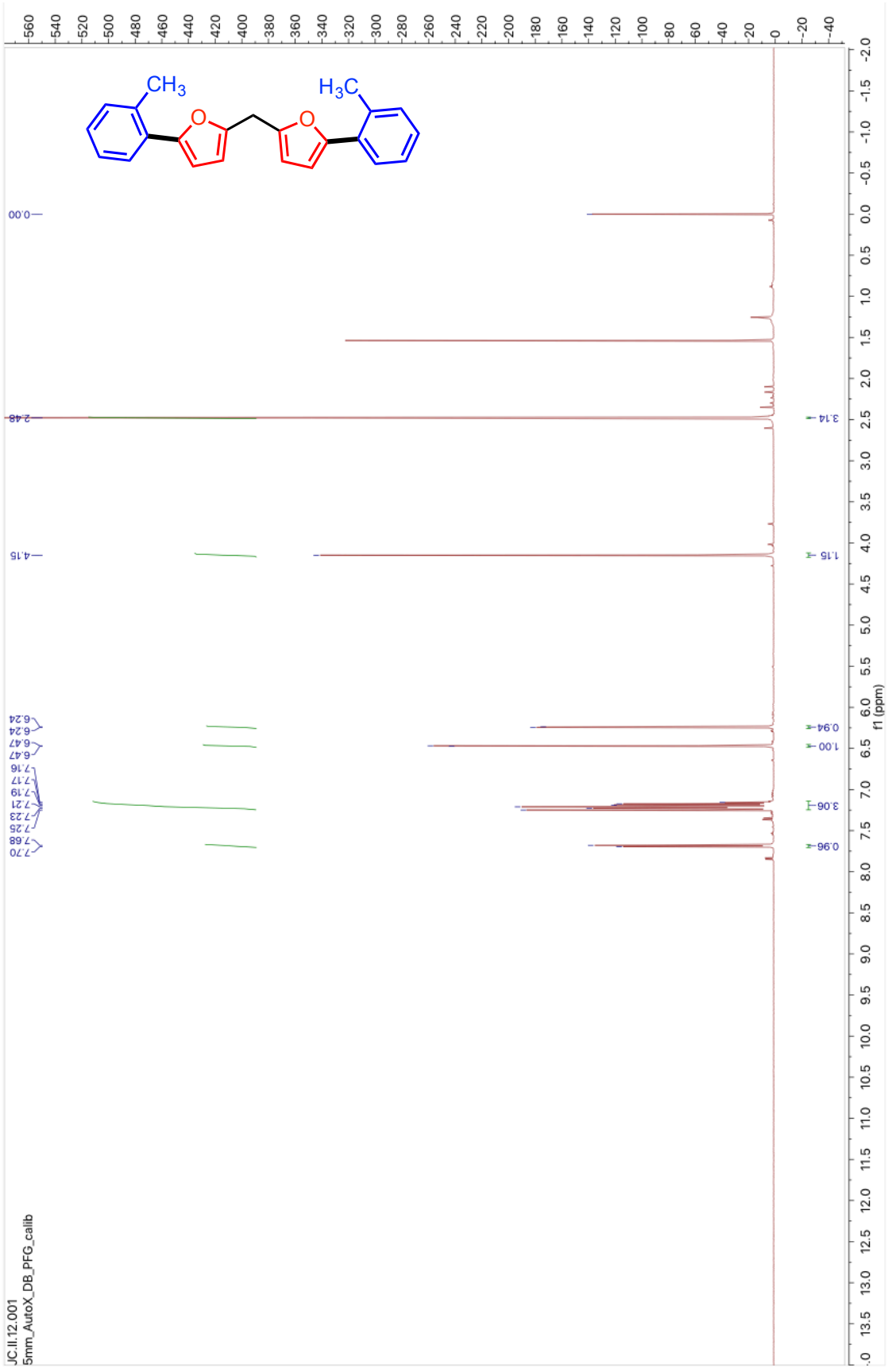
CH3
H3C
O
O
JC.II.12.001
5mm_AutoX_DB_PFG_calib
f1 (ppm)


CH3
H3C
O
O
21.91
27.76
108.37
109.44
125.91
126.75
127.15
130.24
131.08
134.30
150.71
152.57
f1 (ppm)
JC.II.12.002
JC_II_12_F3_3-4

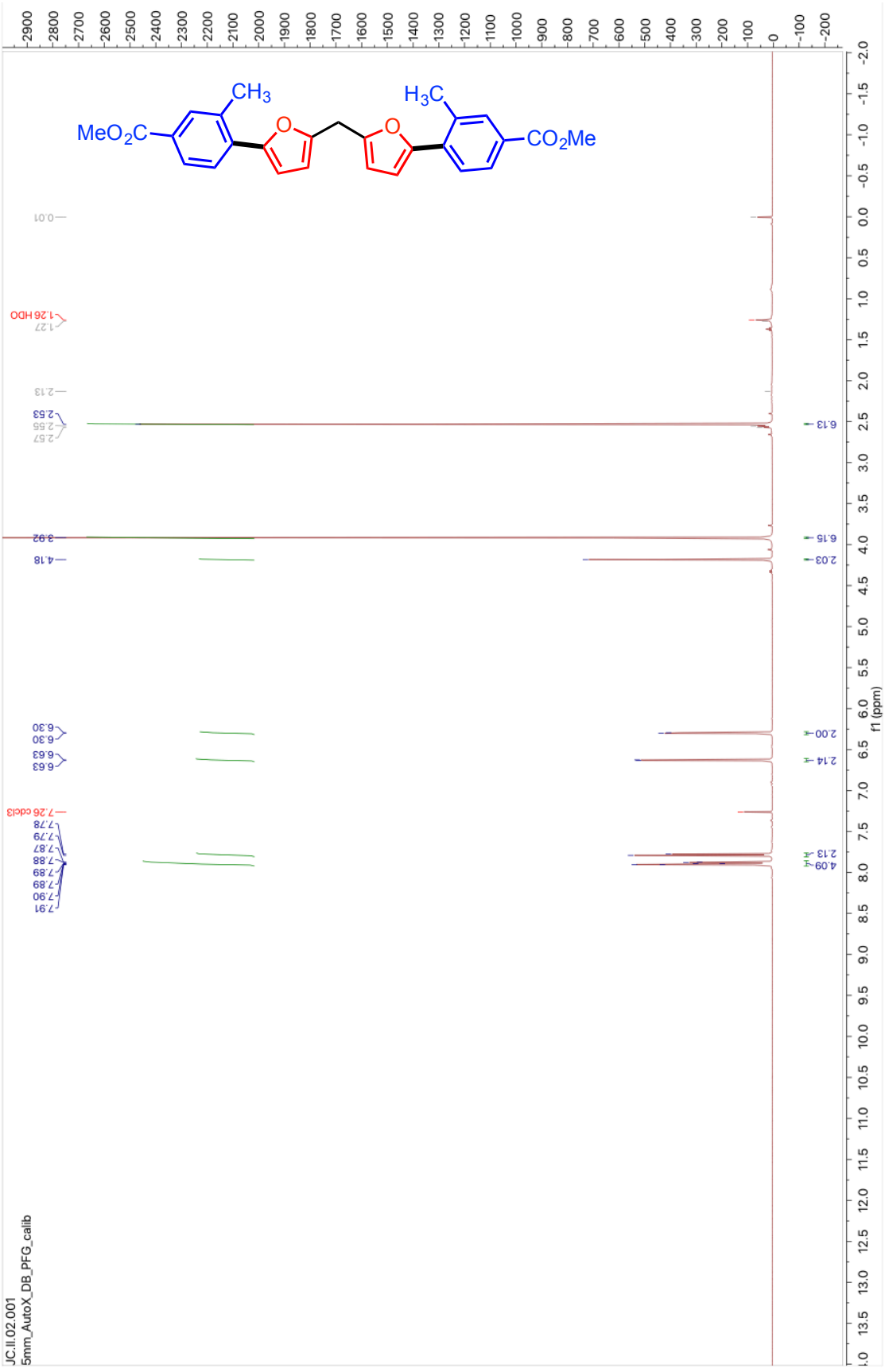
CH3
H3C
MeO2C
CO2Me
O
O
f1 (ppm)
JC.II.02.001
5mm_AutoX_DB_PFG_calib

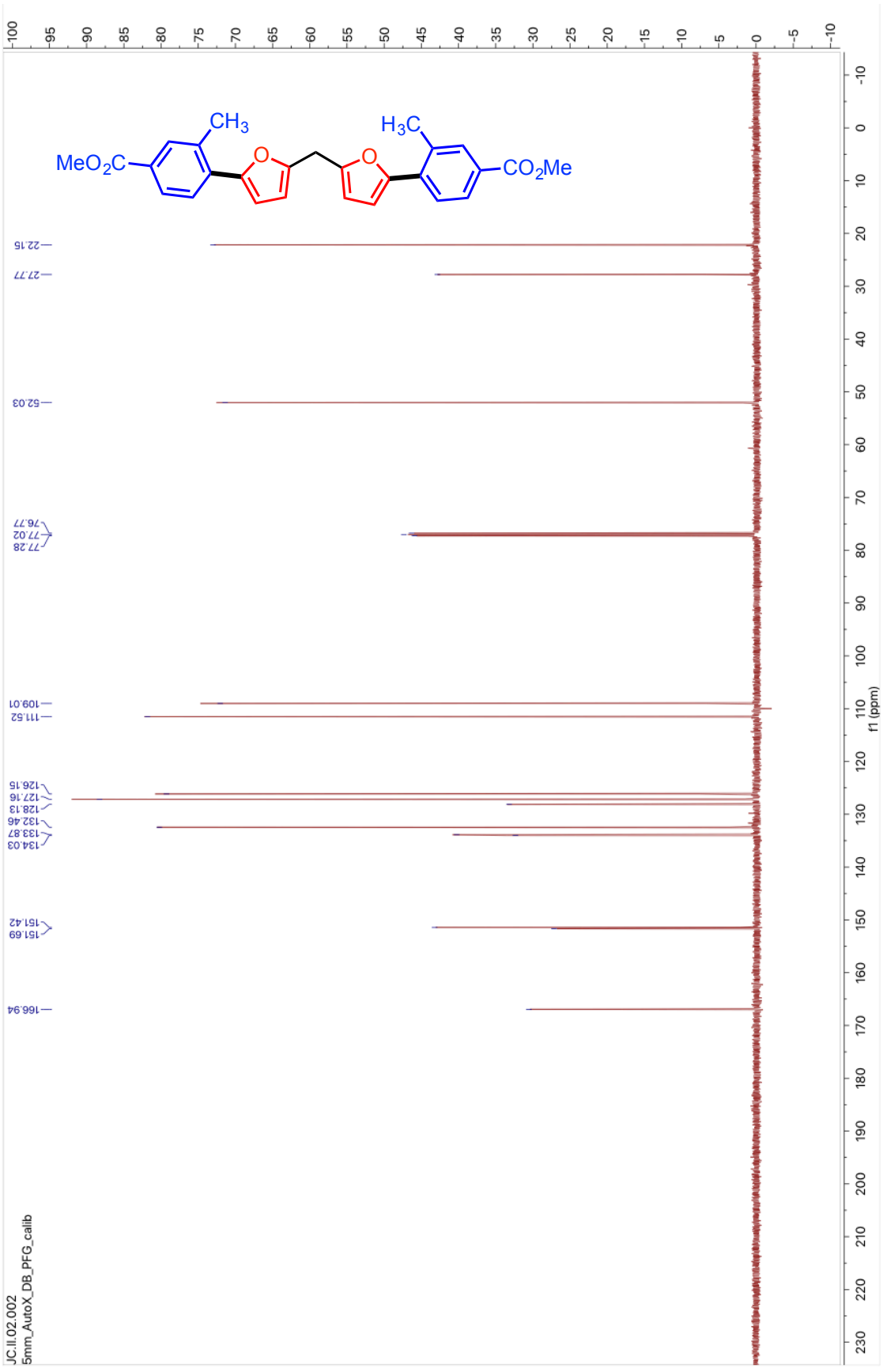
CH3
H3C
MeO2C
CO2Me
O
O
22.15
27.77
52.03
76.77
77.02
77.28
109.01
111.52
126.15
127.16
128.13
132.46
133.87
134.03
151.42
151.69
166.94
JC.II.02.002
5mm_AutoX_DB_PFG_calib
f1 (ppm)

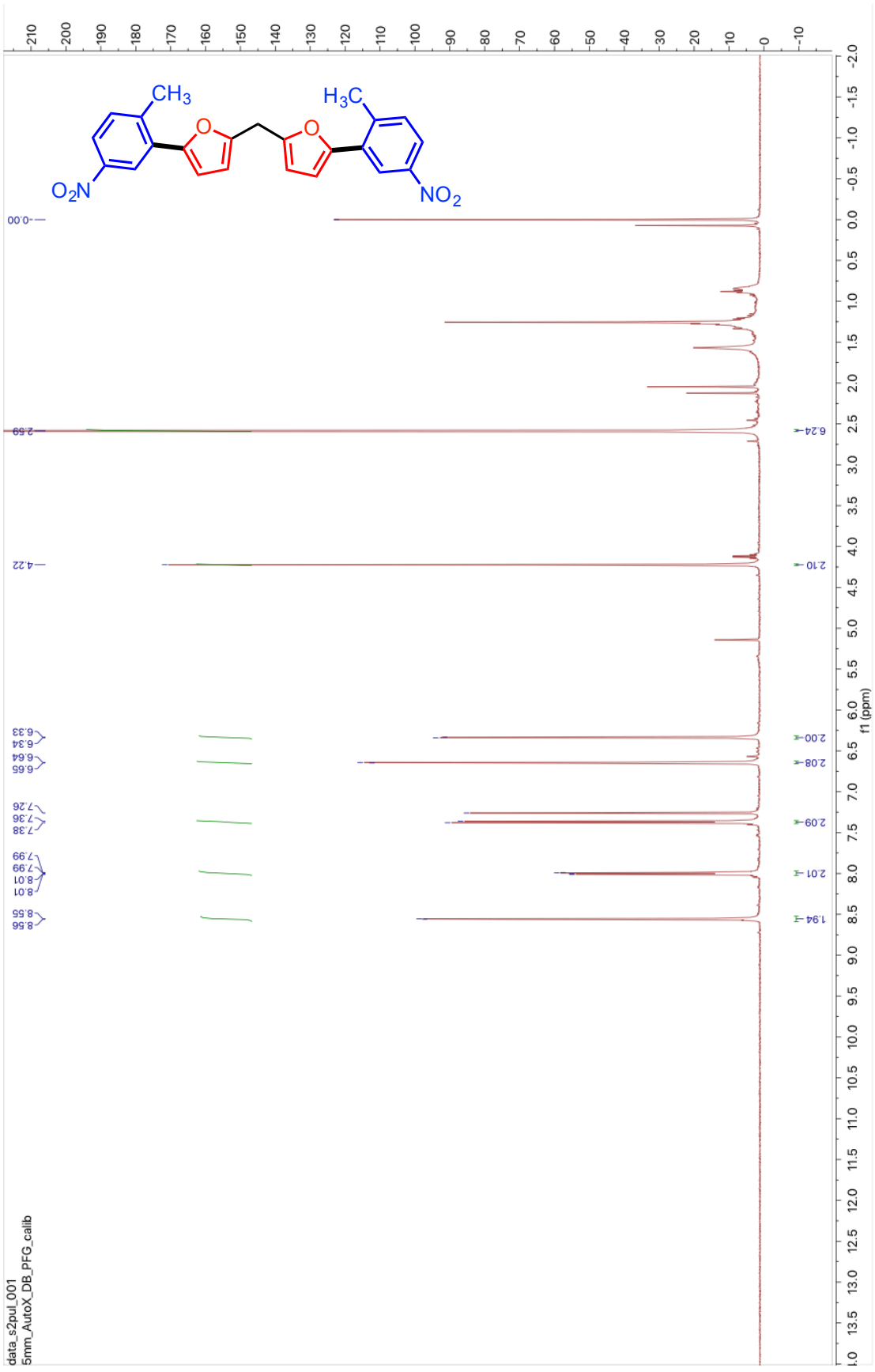
CH3
H3C
O2N
NO2
O
O
f1 (ppm)
data_s2pul_001
5mm_AutoX_DB_PFG_calib

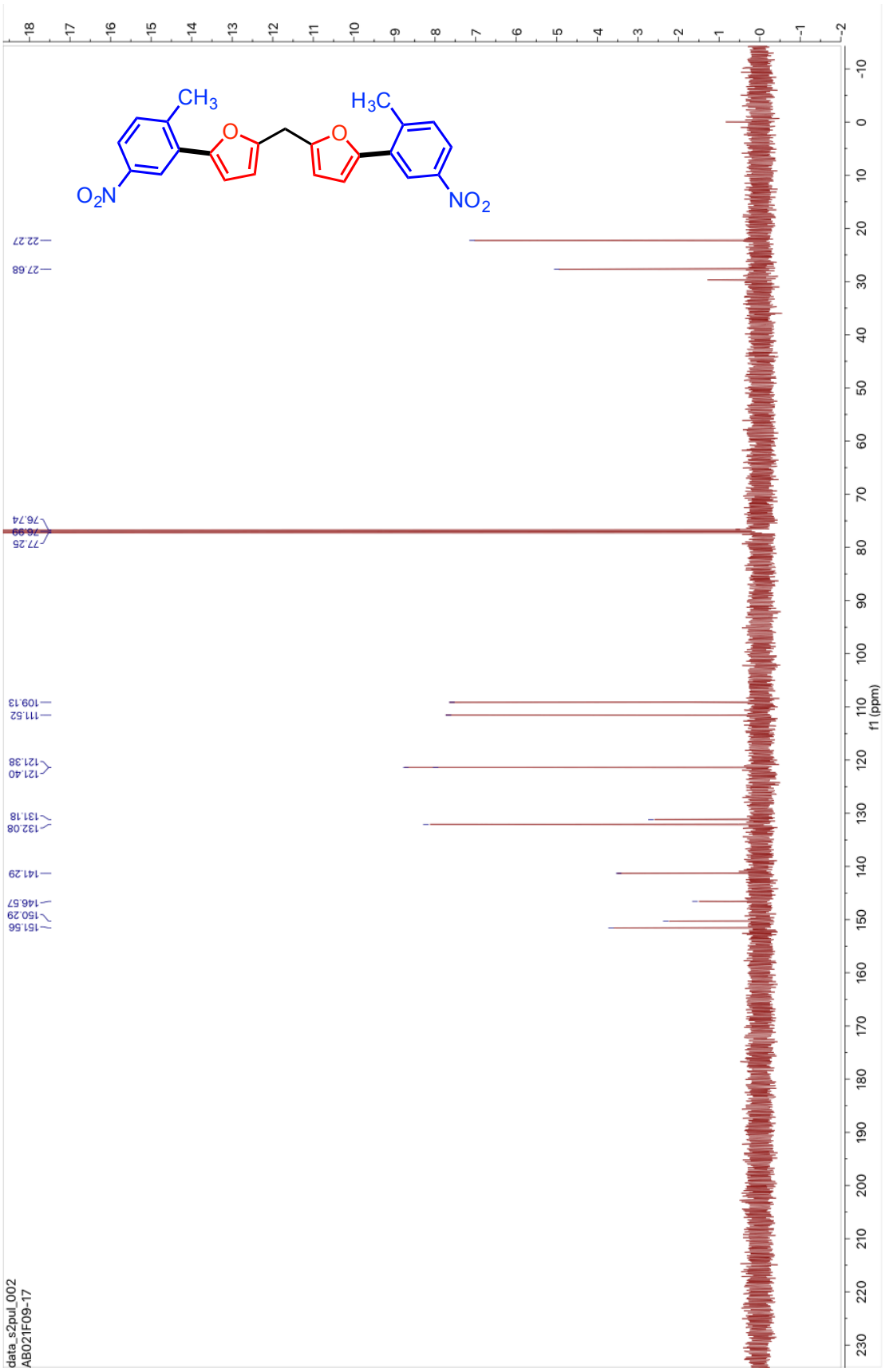
CH3
H3C
O
O
O2N
NO2
22.27
27.68
76.74
77.25
109.13
111.52
121.40
121.38
131.18
132.08
141.29
146.57
150.29
151.56
f1 (ppm)
data_s2pul_002
AB021F09-17

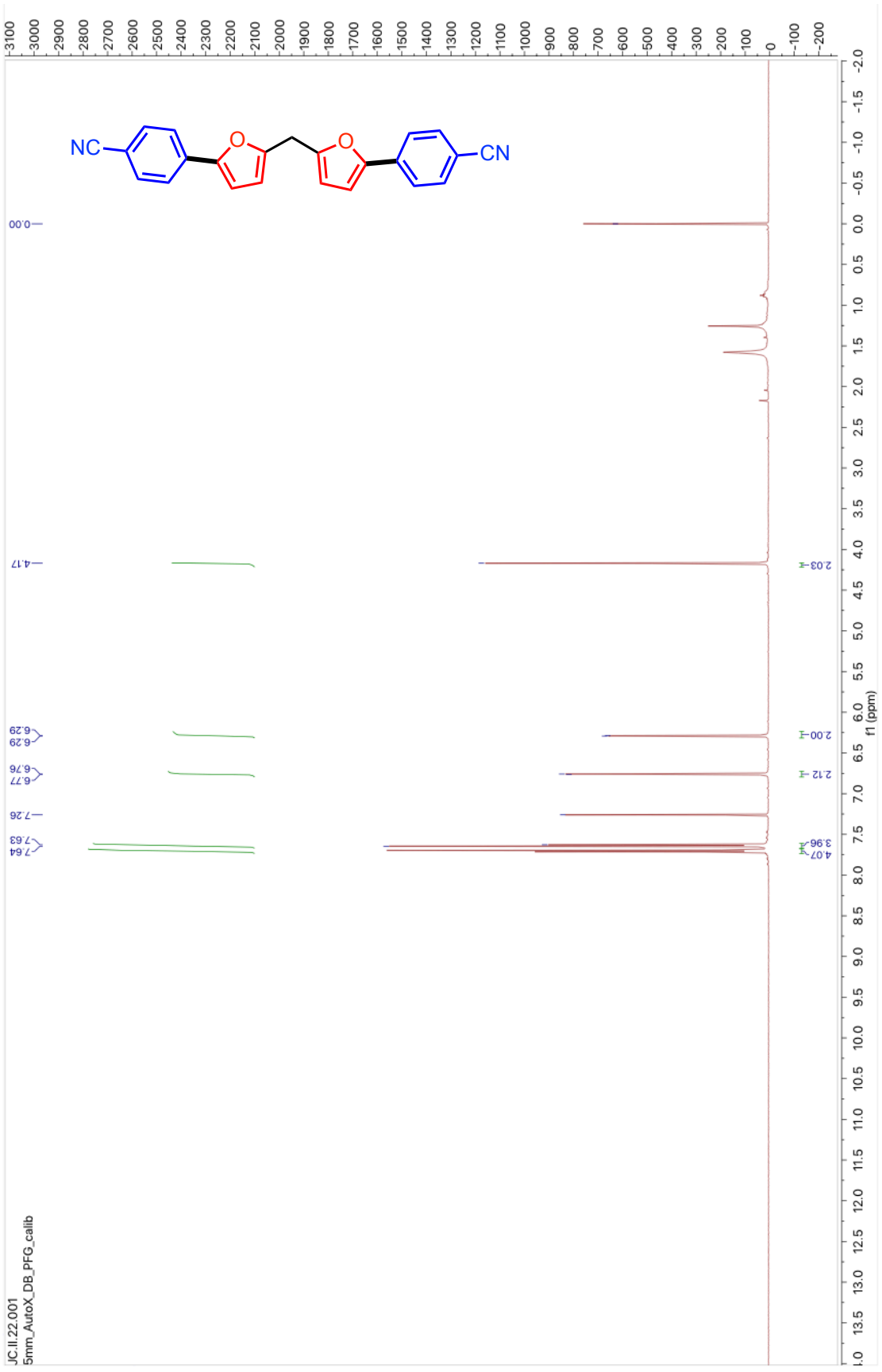
NC
O
O
CN
0.00
4.17
6.29
6.77
6.76
7.26
7.64
7.63
2.03
2.00
2.12
3.96
4.07
f1 (ppm)
JC.II.22.001
5mm_AutoX_DB_PFG_calib

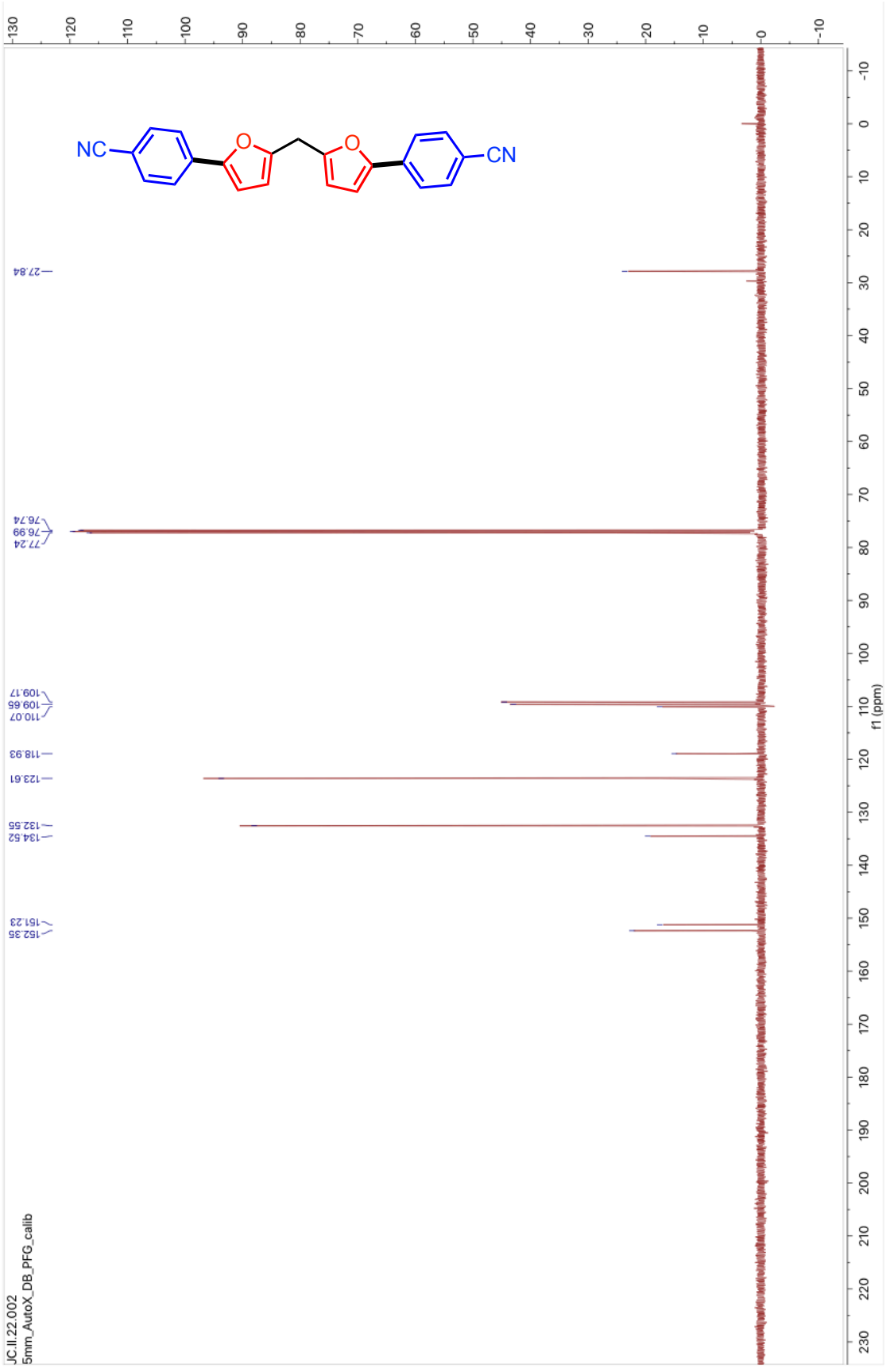
NC
O
O
CN
27.84
76.74
76.99
77.24
109.17
109.65
110.07
118.93
123.61
132.55
134.52
151.23
152.35
f1 (ppm)
JC.II.22.002
5mm_AutoX_DB_PFG_calib

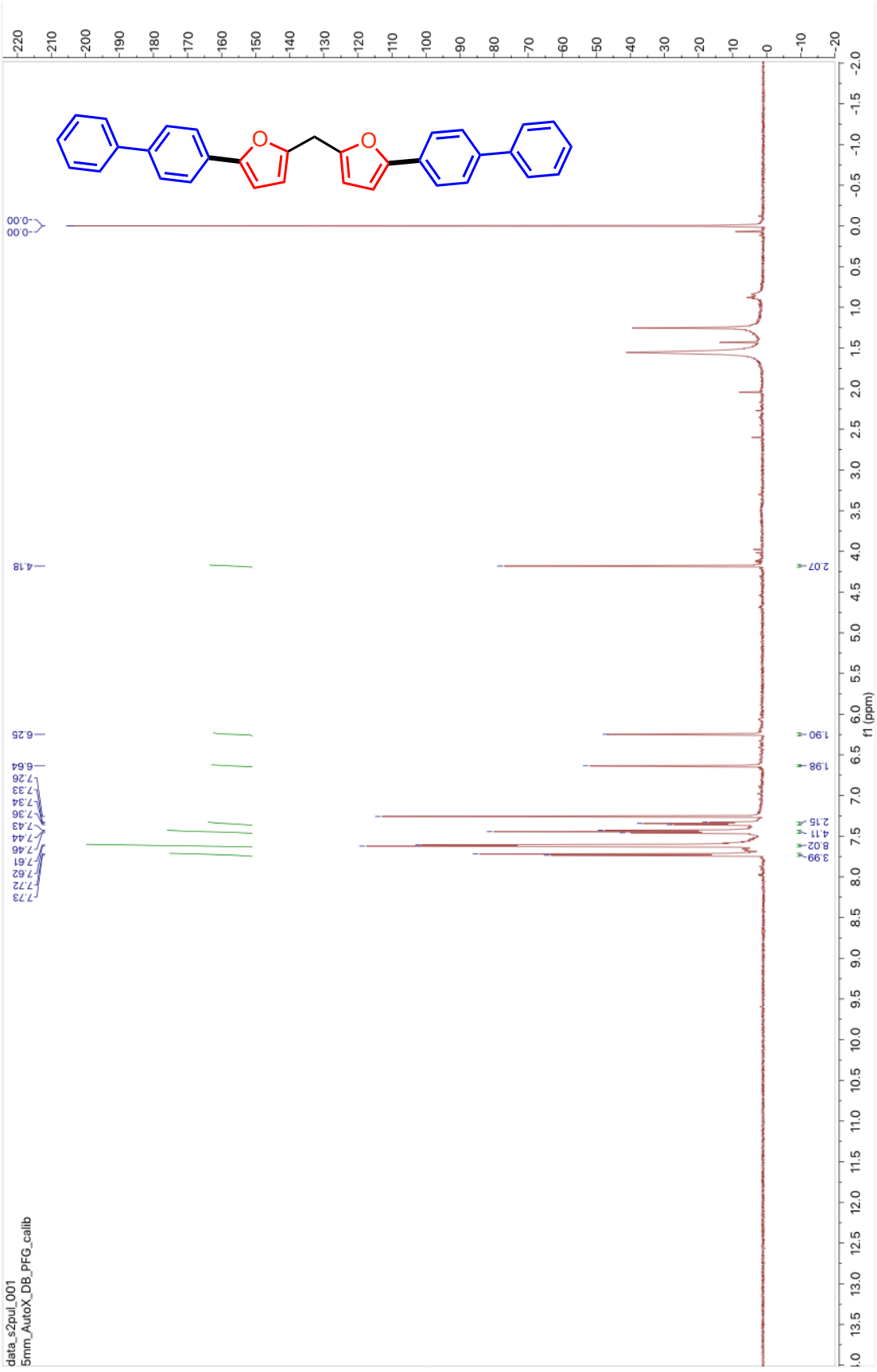
data_s2pul_001
5mm_AutoX_DB_PFG_calib
f1 (ppm)
O
O

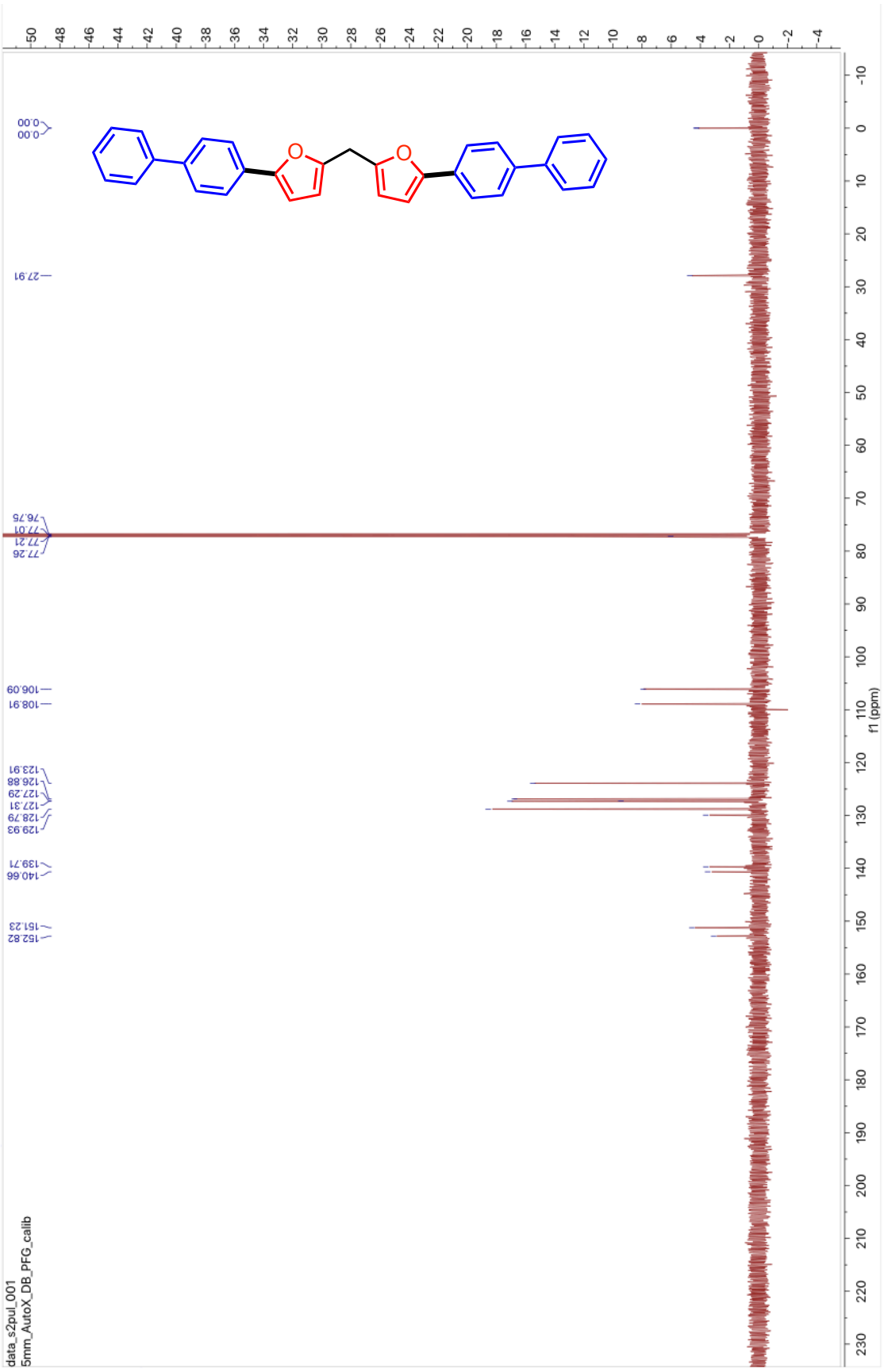
0.00
0.00
27.91
76.75
77.01
77.21
77.26
106.09
108.91
123.91
126.88
127.29
127.31
128.79
129.93
139.71
140.66
151.23
152.82
f1 (ppm)
data_s2pul_001
5mm_AutoX_DB_PFG_calib